CHARACTERIZATION OF ORGANIC ANION TRANSPORTING POLYPEPTIDE 1A1 (OATP1A1) IN THE BILE ACID HOMEOSTASIS OF MICE

by

Youcai Zhang

B.S., M.S., Chemistry, Nanjing University, Nanjing, China, 2005

Submitted to the graduate degree program in Pharmacology, Toxicology and Therapeutics and the Graduate Faculty of the University of Kansas in partial fulfillment of the requirements for the degree of Doctor of Philosophy

Dissertation Committee:

_____
Chariperson: Curtis D. Klaassen, Ph.D.

_____
Grace L. Guo, Ph.D.

_____
Bruno Hagenbuch, Ph.D.

_____
Partha Krishnamurthy, Ph.D.

_____
Glen K. Andrews, Ph.D.

Date defended: 2/28/2011

The Dissertation Committee for Youcai Zhang certifies that this is the approved version of the following dissertation:

CHARACTERIZATION OF ORGANIC ANION TRANSPORTING POLYPEPTIDE 1A1 (OATP1A1) IN THE BILE ACID HOMEOSTASIS OF MICE

Dissertation Committee:

_____
Chairperson: Curtis D. Klaassen, Ph.D.

Date approved: 2/28/2011

ABSTRACT

Organic anion transporting polypeptides (human: OATPs; all other species: Oatps; gene symbol: *SLCO/Slco*) are sodium-independent transport systems that mediate the transmembrane transport of a wide range of amphipathic endogenous and exogenous organic compounds. In mice, Oatp1a1, 1a4, and 1b2 are thought to account for the bulk of Na-independent bile acid (BA) uptake into liver during normal physiological conditions. The overall goal of this dissertation has focused on characterization of the *in vivo* role of mouse Oatp1a1 in BA homeostasis by using Oatp1a1-null mice. To achieve this overall goal, three specific aims were examined in the present dissertation.

In the first specific aim, a simple and sensitive UPLC-MS/MS method was established and validated for the simultaneous analysis of various BAs, and applied to investigate liver BA content in C57BL/6 mice fed 1% cholic acid (CA), 0.3% deoxycholic acid (DCA), 0.3% chenodeoxycholic acid (CDCA), 0.3% lithocholic acid (LCA), 3% ursodeoxycholic acid (UDCA), or 2% cholestyramine (resin). The purpose of this study was to understand the BA metabolic pathways in mice by using this newly developed BA-quantification method, and thus to provide tools and knowledge for the future study in Oatp1a1-null mice. Gender differences in liver BA composition were observed after feeding CA, DCA, CDCA, and LCA, but were not prominent after feeding UDCA. Sulfation of CA and CDCA was found at the 7-OH position, and increased by feeding CA or CDCA more in male than female mice. In contrast, sulfation of LCA and taurolithocholic acid (TLCA) was female predominant, and increased by feeding UDCA and LCA. The metabolic pathways of each BA *in vivo* are proposed, and can be used to interpret BA-mediated gene regulation and hepatotoxicity.

In the second specific aim, the hypothesis that Oatp1a1 is important in transporting unconjugated BAs was evaluated. The purpose of this study was to determine whether knockout of Oatp1a1 will alter BA metabolism in mice. To address this aim, the concentrations of individual BAs in serum, liver, and bile were compared between WT and Oatp1a1-null mice. The gender-divergent expression of Oatp1a1

was considered in the efforts to identify the endogenous BA substrates for Oatp1a1. In addition, DCA feeding and pharmacokinetic studies were conducted in WT and Oatp1a1-null mice to investigate the role of Oatp1a1 in the disposition of DCA. Data from this study show a critical role of Oatp1a1 in DCA metabolism of mice. Oatp1a1 in mouse liver does not appear to transport DCA, because knockout of Oatp1a1 does not prevent hepatic uptake and hepatotoxicity of DCA. Instead, knockout of Oatp1a1 increases the intestinal permeability and thus increases intestinal absorption of DCA. In addition, Knockout of Oatp1a1 markedly alters the composition and amount of intestinal bacteria. The alterations of intestinal bacteria in Oatp1a1-null mice result in marked changes of BA composition in the intestinal contents and feces, but have no effect on the total fecal BA excretion, due to the same billiary input of BAs in WT and Oatp1a1-null mice.

In the third specific aim, the hypothesis that knockout of Oatp1a1 decreases liver toxicity in mice during extrahepatic cholestasis was evaluated. The purpose of this study was to determine the *in vivo* role of Oatp1a1 in mice after bile duct ligation (BDL) by using Oatp1a1-null mice. Knockout of Oatp1a1 increased liver toxicity in mice after BDL, which may be due to the increase of secondary BAs in livers of mice. Knockout of Oatp1a1 resulted in an impaired cytoprotective response in mice during BDL-induced cholestasis. In addition, antibiotic treatment potentiated liver toxicity in Oatp1a1-null mice after BDL by increasing the intestinal absorption of BAs. Thus, Oatp1a1 plays a unique and essential protective role in the adaptive response to obstructive cholestasis liver injury.

Altogether, this dissertation demonstrates that: (1) A simple and sensitive UPLC-MS/MS method was established for the simultaneous analysis of various BAs and was applied to investigate the BA metabolism in mice fed CA, CDCA, DCA, LCA, UDCA, or resin; (2) Oatp1a1 does not mediate the hepatic uptake of DCA, but plays a critical role in the intestinal metabolism of DCA; (3) Knockout of Oatp1a1 increases intestinal bacteria and thus alters the urinary metabolomics in mice; and (4) Knockout of Oatp1a1 increases liver toxicity in mice after BDL, which may be due to the increase of secondary BAs in both serum and livers of mice.

Dedication

I would like to dedicate the work herein to my parents.

Acknowledgement

This work was supported by NIH grants ES009649, ES013714, ES009716, and RR021940. I would like to give my appreciation to all the United States Taxpayers whose tax revenues make basic science research possible.

I would like to express my deepest gratitude to my mentor, Dr. Curtis D. Klaassen. I enjoyed the four years working in your lab. It is not easy to take care of such a big department and such a big laboratory. I am so impressed that you are always available and ready to answer my questions, to discuss my project, to practice my presentation, and to review my manuscripts. You are a great mentor who shares both joys and pains. You taught me to be optimistic and not afraid to make mistakes. I have learned from you not only scientific method but also scientific philosophy. Thank you for all your time, your patience, your encouragement, and providing me with an excellent atmosphere for doing research. I look forward to your continued guidance and mentorship throughout my professional development.

Committee members: Drs. Bruno Hagenbuch, Grace L. Guo, Partha Krishnamurthy, and Glen K. Andrews, I thank each of you for your insightful suggestions and for being so generous with your time whenever I need to schedule a last-minute meeting. I enjoyed each time meeting with you to report my progress. I would never have been able to finish my dissertation without your guidance.

I would like to thank all the previous and current members in Dr. Klaassen's laboratory. I thank Drs. Ivan Csanaky, Xingguo Cheng, Pallavi Limaye, Rachel Chennault, Hong Lu, Lauren Aleksunes, and Yuji Tanaka for your help and contribution to my research. I thank Lucy, Andy, Cheryl, Helen, Jennifer, Jerry, and all graduate students in the lab. I enjoyed working with you all.

I would like to thank all the department faculty members and office staffs, especially Rosa Meagher, for your generous assistance during these years.

I want to especially thank my parents for their support at all times. Your love is always with me.

Table of Contents in Brief

Table of Contents Expanded

Chapter 1

Background and Significance

Chapter 2

Experimental Materials and Methods

Chapter 3

Bile Acid Metabolome in Mice: Effects of Feeding Bile Acid and A Bile Acid Sequestrant on Hepatic Bile Acid Metabolism in C57BL/6 Mice

Chapter 4

Characterization of Bile Acid Homeostasis in Oatp1a1-null Mice

Chapter 5

Characterization of Intestinal Bacteria and Bile Acids in Oatp1a1-null Mice

Chapter 6

The Critic Role of Mouse Oatp1a1 in Extrahepatic Cholestasis

List of Tables

List of Figures

List of Abbreviations

Abc: ATP-binding cassette

Acta2: actin alpha 2

ALT: alanine aminotransferase

ALP: alkaline phosphatase

alloLCA: allolithocholic acid, 3α-hydroxy-5α–cholan-24-oic acid

Asbt: apical sodium-dependent bile acid transporter

BA: bile acid

BAG: bile acid glucuronide

BAS: bile acid sulfate

Bcrp: breast cancer resistance protein

Bsep: bile salt export pump

CA: cholic acid, 3α,7α,12α–trihydroxy-5β–cholan-24-oic acid

CA3S: cholic acid 3-sulfate

CA7S: cholic acid 7-sulfate

CA12S: cholic acid 12-sulfate

Ccnd1: cyclin D1

CD1: cluster of differentiation 1

CDCA: chenodeoxycholic acid, 3α,7α-dihydroxy-5β–cholan-24-oic acid

CDCA3S: chenodeoxycholic acid 3-sulfate

CDCA7S: chenodeoxycholic acid 7-sulfate

Cdkn1a: cyclin-dependent kinase inhibitor 1A

Col1a1: collagen type I alpha 1

Ctgf: connective tissue growth factor

Cyp: Cytochrome P450

DCA: deoxycholic acid, 3α,12α-dihydroxy-5β–cholan-24-oic acid

3-DCA: 3-deoxycholic acid, 7α,12α-dihydroxy-5β–cholan-24-oic acid

DCA3S: deoxycholic acid 3-sulfate

DCA12S: deoxycholic acid 12-sulfate

3-dehydroCA: 7α,12α-dihydroxy-3-oxo-5β–cholan-24-oic acid

3-dehydroCDCA: 7α-dihydroxy-3-oxo-5β–cholan-24-oic acid

dehydroLCA: 3-oxo-5β-cholan-24-oic acid

Fgf15: fibroblast growth factor 15

FXR: farnesoid X receptor

Gadd45b: growth arrest and DNA-damage-inducible beta

Gapdh: Glyceraldehyde-3-phosphate dehydrogenase

GCA: glycocholic acid, 3α,7α,12α–trihydroxy-5β–cholan-24-oylglycine

GCDCA: glycochenodeoxycholic acid, 3α,7α-dihydroxy-5β–cholan-24-oylglycine

GCDCA3S: glycochenodeoxycholic acid 3-sulfate

GDCA: glycodeoxycholic acid, 3α,12α-dihydroxy-5β–cholan-24-oylglycine

GDCA3S: glycodeoxycholic acid 3-sulfate

GHDCA: glycohyodeoxycholic acid, 3α,6α-dihydroxy-5β–cholan-24-oylglycine

GLCA: glycolithocholic acid, 3α-hydroxy-5β–cholan-24-oylglycine

GLCAS: glycolithocholic acid sulfate

GUDCA: glycoursodeoxycholic acid, 3α,7β-dihydroxy-5β–cholan-24-oylglycine

HCA: hyocholic acid, 3α,6α,7α-trihydroxy-5β–cholan-24-oic acid

HDCA: hyodeoxycholic acid, 3α,6α-dihydroxy-5β–cholan-24-oic acid

HO-1: heme oxygenase 1

IL: interleukin

Mki67: antigen identified by monoclonal antibody Ki-67

Mrp: multidrug resistance-associated protein

Npc1l1: Niemann-Pick C1 Like 1

Ntcp: Na^+-taurocholate cotransporting polypeptide

IS: internal standard

isoDCA: iso-deoxycholic acid, 3β,12α-dihydroxy-5β–cholan-24-oic acid

isoLCA: iso-lithocholic acid, 3β-hydroxy-5β–cholan-24-oic acid

LCA: lithocholic acid, 3α-hydroxy-5β–cholan-24-oic acid

LCAS: lithocholic acid sulfate

LRH: liver receptor homolog 1

LXRα: liver X receptor α

αMCA: α-muricholic acid, 3α,6β,7α-trihydroxy-5β–cholan-24-oic acid

βMCA: β-muricholic acid, 3α,6β,7β-trihydroxy-5β–cholan-24-oic acid

ωMCA: ω-muricholic acid, 3α,6a,7β-trihydroxy-5β–cholan-24-oic acid

MDCA: murideoxycholic acid, 3α, 6β-dihydroxy-5β–cholan-24-oic acid

MRM: multiple reaction monitoring

m/z: mass to charge ratio

Oatp/OATP: organic anion transporting polypeptide

Ost: organic solute transporter

6-oxo-alloLCA: 3α-hydroxy-6-oxo-5α–cholan-24-oic acid

12-oxoCDCA: 3α,7α-dihydroxy-12-oxo-5β–cholan-24-oic acid

7-oxoDCA: 3α,12α-dihydroxy-7-oxo-5β–cholan-24-oic acid

7-oxoHDCA: 3α,6α-dihydroxy-7-oxo-5β–cholan-24-oic acid

6-oxoLCA: 3α-hydroxy-6-oxo-5β–cholan-24-oic acid

7-oxoLCA: 3α-hydroxy-7-oxo-5β–cholan-24-oic acid

12-oxoLCA: 3α-hydroxy-12-oxo-5β–cholan-24-oic acid

PCA: principle component analysis

Pcna: proliferating cell nuclear antigen

Pdgf: platelet-derived growth factor; TCA: tauro-cholic acid

RLU: relative light units

Rpl13a: ribosomal protein L13a

TCA: taurocholic acid, 3α,7α,12α–trihydroxy-5β–cholan-24-oyltaurine

TCA3S: taurocholic acid 3-sulfate

TCDCA: taurochenodeoxycholic acid, 3α,7α-dihydroxy-5β–cholan-24-oyltaurine

TCDCA3S: taurochenodeoxycholic acid 3-sulfate

TDCA: taurodeoxycholic acid, 3α,12α-dihydroxy-5β–cholan-24-oyltaurine

TDCA3S: taurodeoxycholic acid 3-sulfate

Tfg-β1: transforming growth factor beta 1

THDCA: taurohyodeoxycholic acid, 3α,6α-dihydroxy-5β–cholan-24-oyltaurine

TLCA: taurolithocholic acid, 3α-hydroxy-5β–cholan-24-oyltaurine

TLCAS: taurolithocholic acid sulfate

TNFα: tumor necrosis factor alpha

TαMCA: tauro-α-muricholic acid, 3α,6β,7α-trihydroxy-5β–cholan-24-oyltaurine

TβMCA: tauro-β-muricholic acid, 3α,6β,7β-trihydroxy-5β–cholan-24-oyltaurine

TωMCA: tauro-ω-muricholic acid, 3α,6a,7β-trihydroxy-5β–cholan-24-oyltaurine

THCA: taurohyocholic acid, 3α,6α,7α-trihydroxy-5β–cholan-24-oyltaurine

TMDCA: tauromurideoxycholic acid, 3α, 6β-dihydroxy-5β–cholan-24-oyltaurine

Top2α: topoisomerase II alpha

TUDCA: tauroursodeoxycholic acid, 3α,7β-dihydroxy-5β–cholan-24-oyltaurine

UDCA: ursodeoxycholic acid, 3α,7β-dihydroxy-5β–cholan-24-oic acid

UPLC-MS/MS: ultra performance liquid chromatography-tandem mass spectrometry

WT: wild-type

List of Appendices

CHARPTER I

BACKGROUND AND SIGNIFICANCE

I. The Enterohepatic Circulation of Bile Acids

A. Bile acid biosynthesis and metabolism.

Liver plays a central role in the maintenance of whole-body sterol balance and the regulation of plasma low-density lipoprotein (LDL)-cholesterol levels. This is partialy due to the unique ability of the liver to convert cholesterol to bile acids (BAs), the excretion of which represents a major route for the elimination of cholesterol from the body (Turley et al., 1988). BAs are synthesized from cholesterol in livers via two major pathways, namely the classic and alternative pathway (Chiang, 2002). Cyp7a1 is the rate-limiting enzyme in the classic pathway, which results in the formation of cholic acid (CA) and chenodeoxycholic acid (CDCA) (BA biosynthesis and metabolism shown in figure 1-1). The alternative pathway is initiated by mitochondrial Cyp27a1 and followed by Cyp7b1 to produce chenodeoxycholic acid (CDCA). Both CA and CDCA are primary BAs in humans and rodents. Rodent livers can hydroxylate CDCA at the 6β-position to form α-muricholic acid (αMCA), which can be further converted to βMCA by epimerization of its 7α-OH to 7β-OH (2). Therefore, α- and β-MCA are also primary BAs in rodents. BAs are conjugated with taurine or glycine in hepatocytes before excretion into bile.

The majority (95%) of BAs excreted into bile are reabsorbed from the intestine back to the liver, which is known as the enterohepatic circulation of BAs. Fecal loss of the remaining BAs (5%) represents the major route of cholesterol removal from the body (Turley et al., 1988). BAs are subject to multiple biotransformations during their enterohepatic circulation (Hofmann and Hagey, 2008). In liver, BAs undergo conjugation with taurine and glycine on the side chain, as well as conjugation with sulfate on the hydroxyl groups of the steroid nucleus (Hofmann et al., 1992; Deo and Bandiera, 2008). In the intestine, bacterial enzymes are capable of deconjugation, dehydroxylation at C-7, and epimerization of BAs.

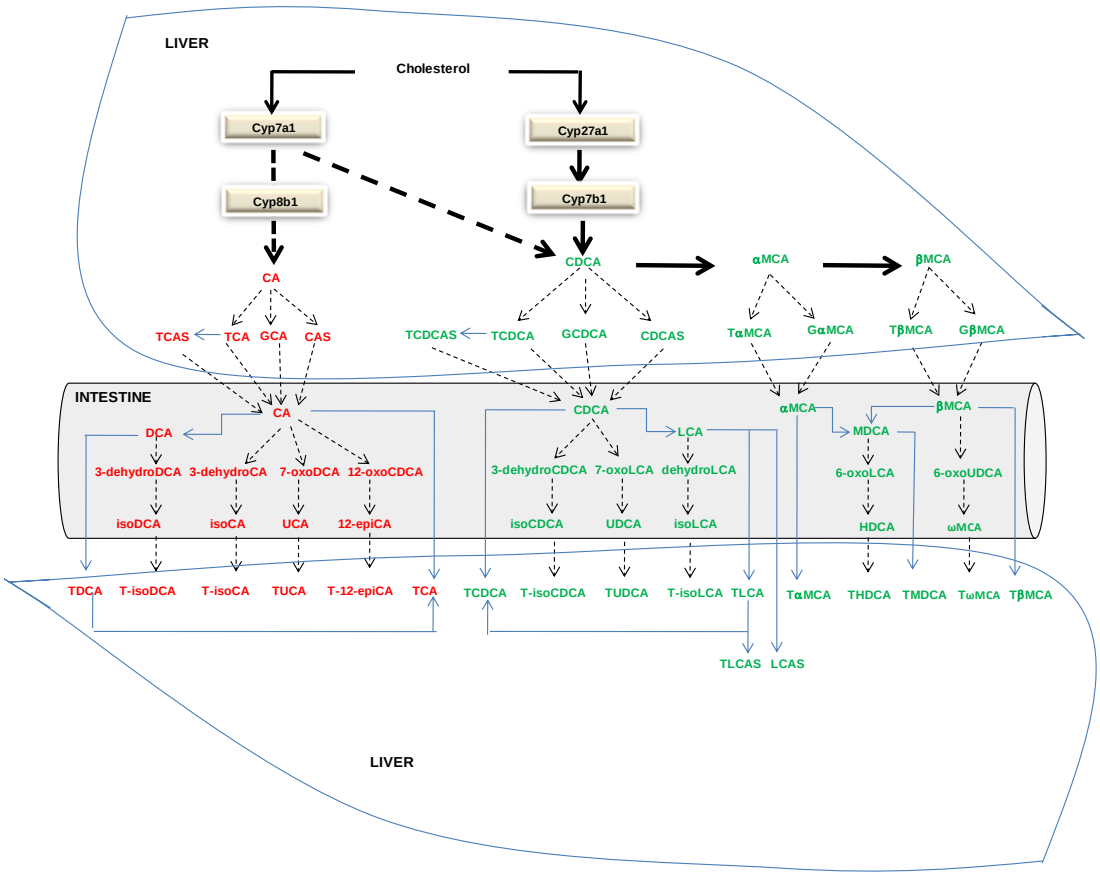

Figure 1-1. BA biosynthesis and metabolism in mice.

B. Bile acid transporters

Taurine- or glycine-conjugation of BAs lowers the pKa of BAs (which is about 5) to around 4 (Fini and Roda, 1987), resulting in almost full ionization of conjugated BAs at the physiological pH (Hofmann, 1994). The concentrations of BAs in liver and bile are higher than in plasma. For example, in C57BL/6 mice, BA concentrations in liver are about 300-fold higher than in plasma, and about 180-fold higher in bile than in liver (Alnouti et al., 2008). Both the hydrophilicity and concentration gradient of BAs necessitate an active transport system to complete the enterohepatic circulation of BAs. As shown in figure 1-2, several major transporters play critical roles in the BA circulation between liver and intestine. After BAs are synthesized and conjugated in hepatocytes, they are excreted into bile canaliculi by the

ATP-energized pump, namely, the bile salt export pump (BSEP/Bsep) (Gerloff et al., 1998). The importance of BSEP has been demonstrated in patients with progressive familial intrahepatic cholestasis type 2 (PFIC2), where several mutations in the BSEP gene have been identified that results in a decrease in the biliary excretion of BAs (Jansen et al., 1999).

The major site of BA absorption from the small intestine is the terminal ileum, where the apical bile salt transporter (ASBT/Asbt) mediates sodium-dependent cotransport of conjugated BAs. Basolateral transport out of the ileocytes into portal venous blood is mediated by a heterodimer of two proteins, OSTα/OSTβ (Dawson et al., 2005).

Uptake of BAs from blood into liver is mediated predominantly by NTCP/Ntcp and OATP/Oatps transporters. Ntcp in rat liver is thought to transport more than 80% of taurocholate, but less than 50% of cholate (Kullak-Ublick et al., 2004). OATP/Oatps mediate the Na^+-independent hepatocellular uptake of BAs and non-BA amphipathic compounds (Hagenbuch and Meier, 2003; Csanaky et al., 2010). In addition, conjugated BAs are transported from hepatocytes back into the sinusoidal blood by MRP4, a cotransporter of BAs and glutathione (Rius et al., 2006). Taken together, two transporters in the hepatocytes (Ntcp and Bsep) and two transporters in the ileocytes (Asbt and Ostα/β) are sufficient to explain the enterohepatic circulation of conjugated BAs.

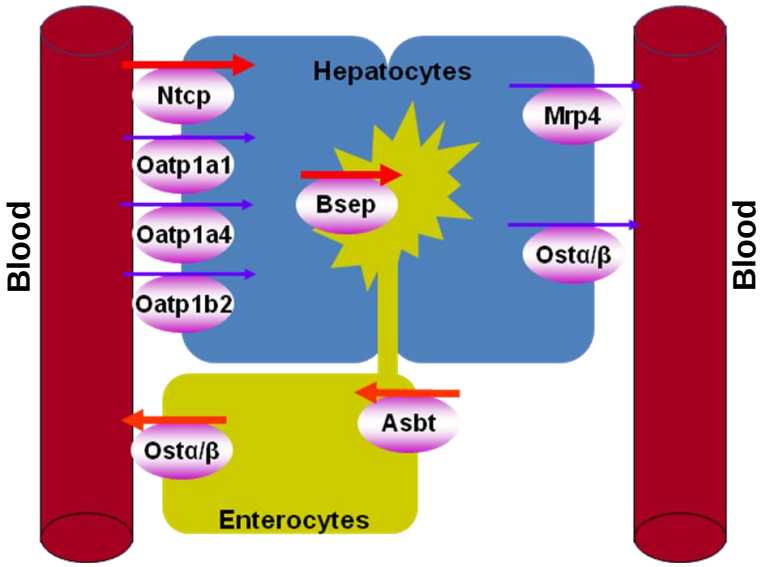

Figure 1-2. Major BA transporters for the enterohepatic circulation of BAs in mice.

C. Patho-physiological fuctions of bile acids

In addition to their role in cholesterol homeostasis, BAs are also functional steroidal detergents, which form micelles with lipids/fats/cholesterol to aid in the intestinal absorption of fat and fat-soluble vitamins (Gu et al., 1992). BAs have been recognized as signaling molecules, which regulate the expression of genes involved in cholesterol, lipid and energy homeostasis through nuclear receptors, such as the farnesoid-X-receptor (FXR) (Wang et al., 1999), pregnane-X-receptor (PXR) (Xie et al., 2001), liver-X-receptor-alpha receptor (Song et al., 2000), vitamin D receptor (VDR) (Makishima et al., 2002) and G-protein coupled receptor TGR5 (Sato et al., 2008). In addition, the amphipathic properties of BAs make them powerful solublizers of membrane lipids, and thus cause cytotoxicity. The increased intracellular BAs induce apoptosis and necrosis, probably by damage to mitochondria (Roberts et al., 1997). The elevated intraluminal concentration of BAs in the colon induces secretion of electrocytes and water, manifested clinically as diarrhea.

II. Intestinal Bacteria

A. Intestinal bacteria in humans and mice

In the human intestine, there are 10^{13} to 10^{14} microorganisms whose collective genome contains at least 100 times as many genes as the human genome. The vast majority of these microbes synthesize essential amino acids and vitamins, and process components of otherwise indigestible contributions to the diet, such as plant polysaccharides (Backhed et al, 2005). Recent research by using metagenomic analysis showed that the human gut microbiome are enriched for methanogenesis and isoprenoid biosynthesis (Gill et al., 2006). Historically, microbes have been studied in the laboratory as cultures of isolated species in a Petri dish, but only one percent of bacteria are able to grow in a Petri dish because their growth is dependent upon a specific natural environment which is often difficult to duplicate (Dubos et al., 1965). Recently, molecular methodologies relying on 16S rRNA gene sequences are commonly used for

the identification and classification of bacterial species within mixed microbial populations (Salzman et al., 2002).

Bacteroidetes and Firmicutes are two predominant bacterial divisions, which make up >99% of the identified phylogenetic types in the human gut microbiota (Ley et al., 2008). More than 95% of Firmicutes are members of the Clostridia class. The human large intestine harbors a high density of microbial flora, approximately 10^{12} bacteria/gram wet weight feces. The major bacterial classes in human large intestine include *Bacteroides, Eubacterium, Bifidobacterium, Ruminococcus, Peptostreptococcus, Propionibacterium, Clostridium, Lactobacillus, Escherichia, Streptococcus,* and *Methanobrevibacter*. In contrast, relatively low numbers and diversity of bacteria inhabit the human small intestine (duodenum ~10^3 bacteria/ml; jejunum ~10^4 bacteria/ml; ileum 10^6~10^8 bacteria/ml), due to a variety of suppressive mechanisms, including rapid transit times, antimicrobial peptides, proteolytic enzymes, and bile (Wilson, 2005). The major bacterial classes found in the human small intestine include *Lactobacillus, Streptococcus, Veillonella, Enterobacteria, Enterococcus, Bacteroides,* and *Clostridium*.

Traditional culturing methods of mouse microflora showed that both facultative anaerobes (*Lactobacillus* spp., *Enterococcus* spp., and *Enterobacillus* spp.) and obligate anaerobes (*Bacteroides* spp. and *Clostridium* spp.) inhabit the mouse intestine (Dubos et al., 1965; Schaedler et al., 1965). More recent analysis of 16s libraries of mouse gastrointestinal (GI) microflora revealed a large new group of mouse intestinal bacteria (Salzman et al., 2002). In mice, the amount and diversity of bacteria in the small intestine (*Bacillus mycoides, Lactobacillus acidophilus, Lcatobacillus reuteri, Lactobacillus murinus, Bacteroides distasonis, Desulfovibrio* sp., and *Ralstonia* sp.) are also far less than that in the large intestine (*Clostridium clostridiiformes, Ruminococcus schinkii, Clostridium celerecrescens,* Clostridium *fusiformis, Clostridium* sp. ASF502*, Clostridium polysaccharolyticum, Helicobacter* sp., *Lactobacillus* sp. ASF360*, Candidatus Xiphinematobacter, Bacteroides acidofaciens, Bacteroides* sp. ASF519*, Bacteroides vulgates, Bacteroides distasonis, Bacteroides forsythus, Porphyromonas* sp.,

Clostrodium sp., *Clostridium celerecrescens, Acetivibrio cellulosolvens, Ruminococcus gnavus,* and *Eubacterium desmolans*).

B. Role of intestinal bacteria in bile acid metabolism

During the enterohepatic circulation of BAs in humans, about 95% of BAs are reabsorbed in the small intestine, whereas 400-800 mg of BAs escape the enterohepatic circulation daily and are excreted into the feces. In the small intestine, BAs mainly undergo deconjugation and hydroxyl group oxidation. More BA biotransformations occur in the large intestine, including deconjugation, desulfation, 7-dehydroxylation, dehydrogenation, epimerization of 3- or 7-hydroxy groups, and isomerization of the A/B ring junction (Ridlon et al., 2006).

Deconjugation of BAs provides carbon, nitrogen, and sulfur for some bacteria species, which may enhance bacterial colonization in the lower GI tract. For example, taurine can serve as an energy source for bacteria under both aerobic and anaerobic conditions (Cook and Denger, 2002). Deconjugation of BAs is mediated by bile salt hydrolases (BSH), which have been cloned from *Bacteroides fragilis, Bacteroides vulgates, Clostridium perfringens, Lactobacillus plantarum, Lactobacillus johnsonii, Bifidobacterium Longum, Bifidobacterium bifidum, Bifidobacterium adolescentis,* and *Listeria monocytogenes*.

Hydroxysteroid dehydrogenases (HSDH) mediate the oxidation and epimerization of the 3-, 7-, and 12-hydroxy groups of BAs in the GI tract. Dehydrogenation of BAs may serve functions that are related to energy generation and to provide the proper composition of hydrophobic BAs for the intestinal bacteria. HSDHs have been cloned from *Clostridum perfringens, Clostridium* sp., *Clostridium absonum, Clostridium sordellii, Clostridium innocuum, Clostridium scindens, Clostridium bifermentans, Clostridium limosum, Clostridium leptum, Clostridium* group P strain, *Clostridium paraputrificum, Bacteroides fragilis, Bacteroides thetaiotaomicron, Peptostreptococcus productus, Escherichia coli, Eggerthella lenta,* and *Eubacterium aerofaciens.*

III. Organic Anion Transporting Polypeptides

A. History of OATP/Oatps

Organic anion transporting polypeptides (human: OATPs; all other species: Oatps; gene symbol: *SLCO/Slco*) are sodium-independent transport systems that mediate the transmembrane transport of a wide range of amphipathic endogenous and exogenous organic compounds (Hagenbuch and Meier, 2003; Hagenbuch and Meier, 2004). The first Oatp was cloned in 1994 from rat liver (Jacquemin et al., 1994). Since then, the superfamily of Oatps have expanded. A new nomenclature for the OATP/Oatp superfamily was introduced in 2004 (Hagenbuch and Meier, 2004). Basically, the OATP/Oatp superfamily is classified within the OATP/SLCO superfamily, which is subdivided into 6 families (more than 40% amino acid sequence identity, families OATP1/Oatp1 through OATP6/Oatp6), and each family, into subfamilies (more than 60% amino acid sequence identity, e.g., OATP1A/Oatp1a).

B. OATPs in the human liver

Human OATPs are expressed in various tissues as demonstrated by different techniques, such as RT-PCR. Human OATP1B1 and OATP1B3 are two liver-specific OATPs, which share 80% amino acid identity and are localized to the basolateral membrane of hepatocytes (Abe et al., 1999; Konig et al., 2000). In addition to its endogenous substrates, such as bilirubin and taurocholate (Briz et al., 2003; Kullak-Ublick et al., 2001), OATP1B1 also mediates the hepatic uptake of a wide range of drugs and toxins, including rifampicin, pravastatin, rosuvastatin, pitavastatin, and irinotecan (Hagenbuch and Gui, 2008). Although OATP1B3 shares many substrates with OATP1B1, it has its own specific substrates, such as cholecystokinin octapeptide (CCK-8) as well as the anticancer drugs paclitaxel and docetaxel (Ismair et al., 2001; Kullak-Ublick et al., 2001; Smith et al., 2005). In addition to OATP1B1 and OATP1B3, several other OATPs (OATP1A2, OATP2A1, OATP2B1, and OATP4A1) are also expressed in the human liver (Hagenbuch and Gui, 2008). Among them, OATP1A2 has been localized to

cholangiocytes (Lee et al., 2005), and OATP2A1 has been shown to regulate pericellular prostaglandin levels (Schuster, 2002).

C. Oatps in mouse liver

The constitutive mRNA expression of the 15 mouse Oatp genes have been quantified in 12 tissues (Cheng et al., 2005). Among them, Oatp1a1, 1a4, 1a6, 1b2, 2a1, and 2b1 have been detected in the mouse liver. As shown in figure 1-3, Oatp1a1, 1a4, and 2b1 are highly expressed in mouse liver. Oatp1b2 is predominantly, if not exclusively, expressed in liver. Recently, our lab showed that Oatp1b2-null mice are useful in elucidating the *in vivo* role of Oatp1b2, especially in the hepatic uptake and systemic disposition of mushroom toxins, such as phalloidin and microcystin-LR (Lu et al., 2008). Unlike Oatp1b2, rodent Oatp1a1 and 1a4 have no human orthologs, but their functions appear to be preserved in human OATP1B1 and 1B3. A gender difference in both Oatp1a1 and Oatp1a4 mRNA expression is observed in the mouse liver, with Oatp1a1 male-predominant and 1a4 female-predominant (Figure 1-3).

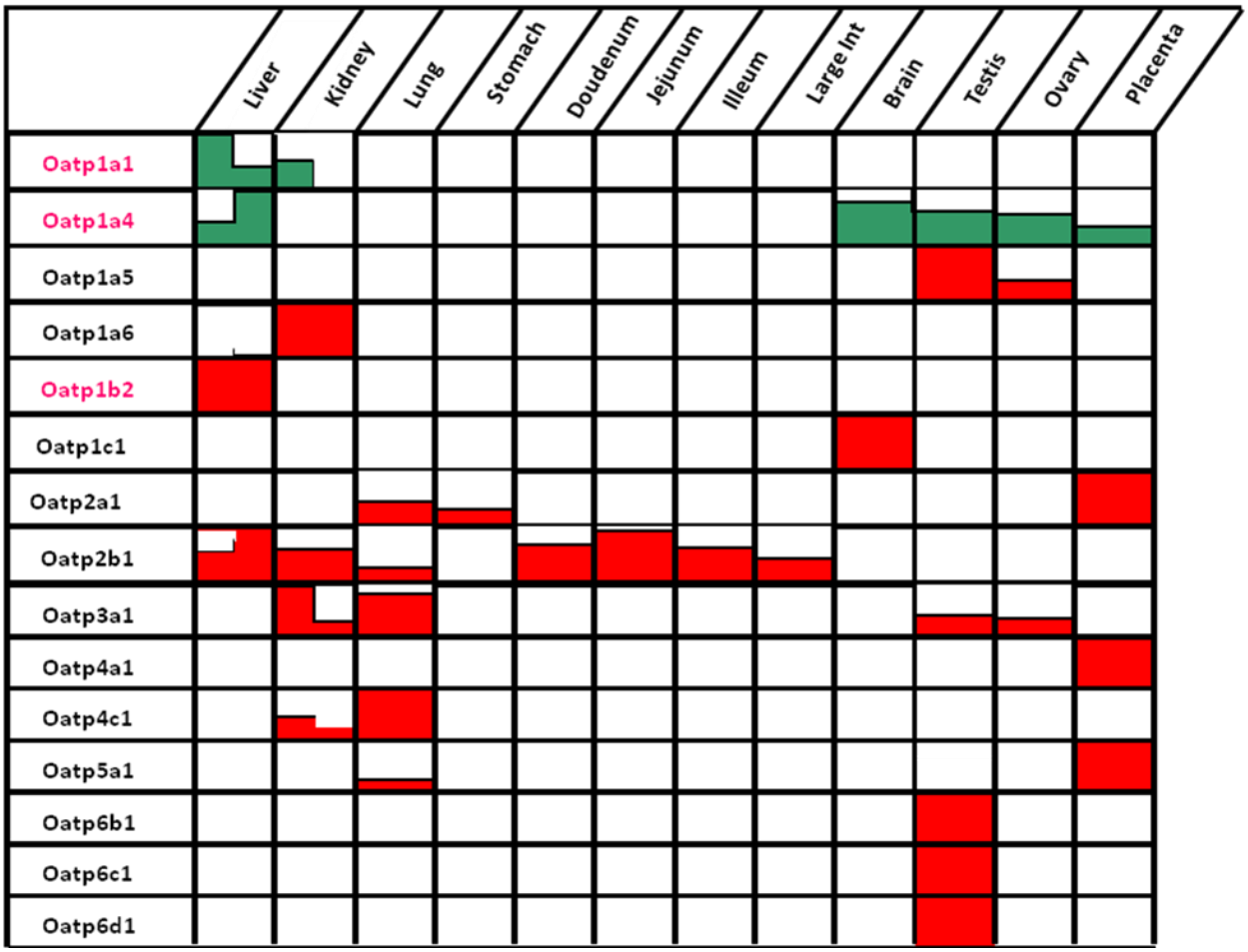

Figure 1-3. Tissue distribution of mouse Oatps (Cheng et al., 2005).

D. OATP/Oatps and bile acids

OATP/Oatps have been thought to mediate the Na^+-independent hepatocellular uptake of BAs. OATP1B1 polymorphism considerably affects the disposition of several endogenous BAs (especially UDCA and CDCA) and BA-synthesis in humans (Xiang et al., 2009). Knockout of Oatp1a/1b in mice dramatically increase the plasma levels of unconjugated BAs (Steeg et al., 2010). Recently, by using Oatp1b2-null mice, our lab showed that Oatp1b2 plays a major role in the hepatic uptake of unconjugated BAs, such as unconjugated cholic acid (Csanaky et al., 2010). However, little is known about the *in vivo* role of mouse Oatp1a1 and 1a4 in BA-transport. Rodent Oatp1a1 and 1a4 have overlapping specificities

to various BAs, but their localizations along liver sinusoids are different. Oatp1a1 has a homogeneous lobular distribution, but Oatp1a4 is predominantly expressed in perivenous hepatocytes (Zone 1) (Reichel et al.,1999; Kakyo et al., 1999). Such a difference in distribution is also observed in human OATP1B1 and 1B3. OATP1B1 is expressed in hepatocytes throughout the liver lobe, whereas OATP1B3 is highly expressed around the central vein (Konig et al., 2000). Because the major uptake of BAs occurs in periportal hepatocytes, Oatp1a1 is implicated in the uptake of BAs under normal conditions, whereas Oatp1a4 may assume a more important role in situations where Oatp1a1 is not able to remove most of the BAs (Aiso et al., 2000). Currently, it is generally accepted that Oatp1a1, 1a4, and 1b2 can account for the bulk of sodium-independent BA-uptake in the mouse liver under normal physiological conditions.

IV. Concluding Remarks for the Introduction

Since the term "bile acid" was first coined in 1838 by Dr. Demarcay, an enormous amount of careful and ingenious work has been done to obtain our current understanding of this acid fraction of bile (Duane, 2009). BAs interest both basic scientists and clinicians for their specific functions. First, BAs are the major excretion pathway for cholesterol. Second, BAs play a central role in absorption of dietary fat and solubilization of biliary cholesterol. Third, BAs serve to maintain bile flow and prevent cholestasis. Fourth, certain BAs have proven useful as therapeutic agents. Finally, BAs are signaling molecules which play a critical role at the cellular level.

Since the discovery of the first Oatp in 1994, many OATP/Oatps have been identified and their transport functions have been studied. The ability of OATP/Oatps to transport a wide range of structurally unrelated xenobiotics, including numerous drugs and toxins, suggests that potential drug-drug and drug-food interactions could occur at the transporter level. In addition to xenobiotics, OATP/Oatps have been shown to be important in transporting endogenous BAs, bilirubin, as well as hormones, such as thyroid hormones and eicosanoids.

Decades of study have yielded a relatively complete picture of the BA enterohepatic circulation, which is central to understanding the function of BAs. In liver, OATP/Oatps have been assigned to be responsible for Na^+-independent BA-uptake mechanisms. However, many questions remain to be clarified regarding the role of OATP/Oatps in the enterohepatic circulation of BAs: **1) Do individual OATP/Oatps play different *in vivo* roles in BA transport? 2) Which BAs are endogenous substrates for the individual OATP/Oatps? 3) How do OATP/Oatps transport BAs across hepatocytes? 4) How does the dysfunction of OATP/Oatps affect BA metabolism?** Although limited knowledge is available to answer these questions, emerging research has begun to reveal some answers to these questions.

V. SPECIFIC AIMS OF THIS DISSERTATION

Due to the lack of specific inhibitors, the physiological role of the OATP/Oatp family still remains to be clarified. The generation of Oatp-null mice facilitates the characterization of the *in vivo* functions of mouse Oatps. For example, Oatp1b2-null mice have been shown to be useful in elucidating the *in vivo* role of Oatp1b2 (Lu et al., 2008). In addition to Oatp1b2, mouse liver also has high expression of Oatp1a1 and Oatp1a4, which are thought to have similar functions as Oatp1b2. The lobular distribution of Oatp1a1 suggests that Oatp1a1 may be more important than Oatp1a4 in BA homeostasis. Thus, **the overall goal of my dissertation has focused on characterization of the *in vivo* role of mouse Oatp1a1 in BA homeostasis by using Oatp1a1-null mice**. The following three specific aims will be investigated to achieve the overall objective of this dissertation.

Specific aim 1 establishes **a LC-MS/MS method to study BA metabolism in C57BL/6 mice**. A simple and sensitive ultra performance liquid chromatography-tandem mass spectrometry (UPLC-MS/MS) method was established and validated for the simultaneous analysis of various BAs, and applied to investigate liver BA contents in C57BL/6 mice fed 1% cholic acid (CA), 0.3% deoxycholic acid (DCA), 0.3% chenodeoxycholic acid (CDCA), 0.3% lithocholic acid (LCA), 3% ursodeoxycholic acid (UDCA),

or 2% cholestyramine (resin). The purpose of this study was to understand the BA metabolic pathways in mice by using this newly developed BA-quantification method, and thus to provide tools and knowledge for the future study in Oatp1a1-null mice.

Specific aim 2 evaluates the hypothesis that **Oatp1a1 is important in transporting unconjugated BAs in mice**. To address this aim, the BA concentrations in serum, liver, bile, small intestinal contents, large intestinal contents, and feces were quantified and compared between WT and Oatp1a1-null mice. A diet supplemented with 0.3% DCA (w/w) was also fed to mice to investigate whether knockout of Oatp1a1 decreases the hepatic uptake of DCA. In addition, intestinal bacteria were quantified to explain the altered BA concentrations in the intestine of Oatp1a1-null mice. The purpose of this study was to determine the *in vivo* role of Oatp1a1 in the enterohepatic circulation of BAs and to reveal possible endogenous substrates for mouse Oatp1a1.

Specific aim 3 evaluates the hypothesis that **knockout of Oatp1a1 decreases liver toxicity in mice during extrahepatic cholestasis**. To address this aim, the impact of BDL on individual BA concentrations in serum and liver, as well as the mRNA expression of hepatic uptake transporters was investigated between 6 h and 14 days after BDL in male C57BL/6 mice. In addition, BDL was performed in WT and Oatp1a1-null mice to investigate whether knockout of Oatp1a1 decreases liver toxicity in mice after BDL. Furthermore, antibiotics were administered to WT and Oatp1a1-null mice to investigate whether antibiotic treatment decreased liver toxicity in Oatp1a1-null mice after BDL. The purpose of this study was to determine the *in vivo* role of mouse Oatp1a1 during extrahepatic cholestasis.

CHAPTER 2

EXPERIMENTAL MATERIALS AND METHODS

I. Chemicals and Reagents

In the present study, the BAs are named according to the previous literature (Hofmann et al., 1992; Hagio et al., 2009). The BA structures are shown as figure 2-1. Tauromurideoxycholic acid (TMDCA) and 7α-dihydroxy-3-oxo-5β–cholan-24-oic acid (3-dehydroCDCA) were kind gifts from Dr. Alan F. Hofmann (University of California, San Diego). Glycochenodeoxycholic-2,2,4,4-d_4 acid ($^2H_4$-GCDCA) and chenodeoxycholic-2,2,4,4-d_4 acid ($^2H_4$-CDCA) were purchased from C/D/N Isotopes, Inc. (Pointe-Claire, Quebec, Canada). Lithocholic acid (LCA), sodium taurolithocholate, lithocholic acid sulfate (LCAS) disodium salt hydrate, taurolithocholic acid sulfate (TLCAS) disodium salt, cholic acid (CA), glycocholic acid (GCA), deoxycholic acid (DCA), sodium glycodeoxycholate, sodium taurodeoxycholate hydrate, ursodeoxycholic acid (UDCA), sodium tauroursodeoxycholate, chenodeoxycholic acid (CDCA), sodium glycochenodeoxycholate, sodium taurochenodeoxycholate and cholestyramine (resin) were purchased from Sigma-Aldrich (St Louis, MO). Glycoursodeoxycholic acid (GUDCA), glycolithocholic acid (GLCA), hyodeoxycholic acid (HDCA), glycohyodeoxycholic acid (GHDCA), taurohyodeoxycholic acid (THDCA), taurocholic acid (TCA), 3α,12α-dihydroxy-7-oxo-5β–cholan-24-oic acid (7-oxoDCA), 3-oxo-5β–cholan-24-oic acid (dehydroLCA), α-muricholic acid (αMCA), tauro-α-muricholic acid (TαMCA), β-muricholic acid (βMCA), tauro-β-muricholic acid (TβMCA), hyocholic (HCA), tauro-hyocholic acid (THCA), murideoxycholic acid (MDCA), 3β,12α-dihydroxy-5β–cholan-24-oic acid (isoDCA), 7α,12α-dihydroxy-5β–cholan-24-oic acid (3-DCA), 3β-hydroxy-5β–cholan-24-oic acid (isoLCA), 3α-hydroxy-5α–cholan-24-oic acid (alloLCA), 3α-hydroxy-6-oxo-5α–cholan-24-oic acid (6-oxo-alloLCA), 3α-hydroxy-6-oxo-5β–cholan-24-oic acid (6-oxoLCA), 3α-hydroxy-7-oxo-5β–cholan-24-oic acid (7-oxoLCA), 3α-hydroxy-12-oxo-5β–cholan-24-oic acid (12-oxoLCA), 7α,12α-dihydroxy-3-oxo-5β–cholan-24-oic acid (3-dehydroCA), and 3α,7α-dihydroxy-12-oxo-5β–cholan-24-oic acid (12-oxoCDCA) were purchased from Steraloids, Inc. (Newport, Rhode Island).

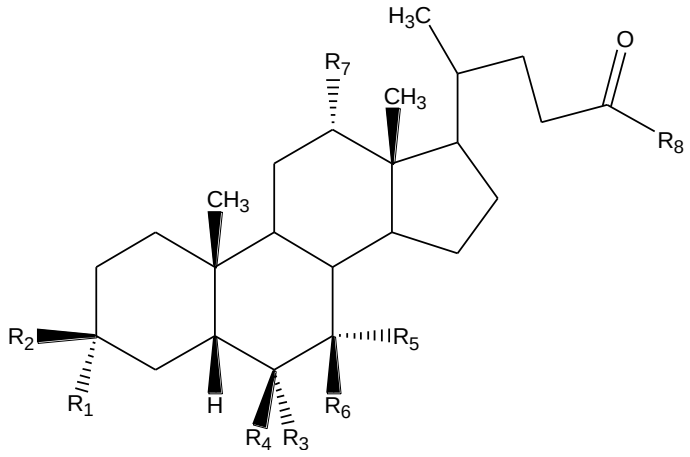

Bile acids	Abbreviation	R1	R2	R3	R4	R5	R6	R7
cholic acid	CA	OH	H	H	H	OH	H	OH
chenodeoxycholic acid	CDCA	OH	H	H	H	OH	H	H
deoxycholic acid	DCA	OH	H	H	H	H	H	OH
lithocholic acid	LCA	OH	H	H	H	H	H	H
hyodeoxycholic acid	HDCA	OH	H	OH	H	H	H	H
α-muricholic acid	αMCA	OH	H	H	OH	OH	H	H
β-muricholic acid	βMCA	OH	H	H	OH	H	OH	H
hyocholic acid	HCA	OH	H	OH	H	OH	H	H
ω-muricholic acid	ωMCA	OH	H	OH	H	H	OH	H
murideoxycholic acid	MDCA	OH	H	H	OH	H	H	H
ursodeoxycholic acid	UDCA	OH	H	H	H	H	OH	H
iso-lithocholic acid	isoLCA	H	OH	H	H	H	H	H
iso-deoxycholic acid	isoDCA	H	OH	H	H	H	H	OH
3-deoxycholic acid	3-DCA	H	H	H	H	OH	H	OH

Bile acids	R1	R5	R7	R8
unconjugate				OH
taurine conjugate				NH(CH2)2SO3H
glycine conjugate				NHCH2COOH
BA 3-sulfate	OSO3H			
BA 7-sulfate		OSO3H		
BA 12-sulfate			OSO3H	

Figure 2-1. Backbone and side chain structures of the BAs.

CDCA-3-glucuronide, CDCA-24-glucuronide, CA-24-glucuronide, LCA-3-glucuronide, LCA-24-glucuronide, DCA-3-glucuronide, HDCA-6-glucuronide, and HDCA-24-glucuronide were kindly provided by Dr. Oliver Barbier (Laval University, Québec, Canada). 3α,12α-Diol-7-oxo-5β–cholan-24-oic acid (7-oxoDCA) was a hydrolysis product of methyl 7-oxo-3α,12α-diol-5β-cholan-24-oate, which was an intermediate during CA7S and CA12S synthesis. TωMCA was synthesized by conjugation of taurine with ωMCA according to a previous method (Tserng et al., 1977c). All other chemicals, unless indicated, were purchased from Sigma-Aldrich (St. Louis, MO). Oasis HLB SPE cartridges were purchased from Waters (Milford, MA).

II. **Synthesis of Reference BA Sulfates**

7,12-Diformylcholic acid, 7-formylchenodeoxycholic acid, and 12-formyldeoxycholic acid were synthesized according to a previous method (Tserng and Klein, 1977a) with minor modifications. Briefly, 2.5 g of CA, CDCA, or DCA was dissolved in 10 ml of 90% formic acid containing 2 drops of 70% perchloric acid. After stirring at 55^{o}C for 1.5 hr, the mixture was allowed to cool to about 40^{o}C. Approximately 8 ml of acetic anhydride was added dropwise at a rate that maintained the temperature between 55-60^{o}C until a large quantity of bubbles appeared. The mixture was then cooled to room temperature and poured into 100 ml of water. The precipitate was collected, washed with water, and dried under vacuum. The products were then dissolved in boiling ethanol (25 ml), diluted with 25 ml of boiling water, and recrystallized as white needles (formylated BA). A suspension of formylated BA (formylated CA: 2.46 g; formylated CDCA and DCA: 2.24 g) in 25 ml of acetone to which 50 ml of 0.2 N NaOH was added dropwise for 30 min, and then maintained at room temperature for 1 hr. The solution was acidified with 2.5 ml of dilute acetic acid (1.3 g glacial acetic acid in 10 ml water), and then extracted with 50 ml of ethyl acetate (AcOEt). The organic layer was washed with water 3 times, dried over anhydrous Na_2SO_4, and evaporated.

The 3-monohydroxy formylated compounds (7,12-diformylcholic acid, 7-formylchenodeoxycholic acid, and 12-formyldeoxycholic acid) were thus obtained and used for preparation of 3-sulfates according to a previous method (Tserng and Klein, 1978) with minor modifications. To a solution of 3-monohydroxy formylated compound (2 mmol) in 4 ml of dimethylformamide (DMF), sulfur trioxide-triethylamine complex (2.02 mmol), synthesized according to a previous method (Tserng and Klein, 1977b), was added. After 30 min at room temperature, the reaction mixture was extracted with AcOEt, evaporated, and dried under vacuum. The product was dissolved with 20 ml of 0.5 N NaOH in a 30-ml centrifuge tube and heated in a steam bath for 10 min. After cooling to room temperature, the solution was acidified to pH 5-6 with dilute HCl. Four ml of 1 M *p*-toluidine hydrocholoride was added and stirred vigorously. The oily suspension that formed was centrifuged and washed with ice-cold water (1 ml). The final syrup-like product was dissolved in 20 ml of 0.2 N methanolic NaOH, and poured into 50 ml of ether. The precipitate (BA 3-sulfate) was collected, washed with ether, and dried under vacuum.

The taurine-conjugated BA 3-sulfates were synthesized by the following method. In a 30-ml centrifuge tube, BA 3-sulfate (0.2 mmol), EEDQ (CA and CDCA 3-sulfate: 0.28 mmol; DCA 3-sulfate: 0.54 mmol), taurine (0.22 mmol), and triethylamine (40 µl) were dissolved in 1 ml of DMF, stirred in a 90^{o}C bath for 1 hr, and maintained at room temperature for another 1 hr. The solution was added to 10 ml of ice-cold ether and centrifuged to collect the oily product. After washing with another 10 ml of ether, the oily product was dissolved in 2 ml of 0.5 N NaOH, heated on a steam bath for 5 min, and cooled to room temperature. After adjusting the pH to 7 with dilute HCl, 2 ml of 1 M *p*-toluidine hydrochloride was added. The suspension was centrifuged and the lower syrupy layer was dissolved in 2 ml of 0.2 N methanolic NaOH. The solution was diluted with 10 ml of ether and centrifuged again. The precipitate (taurine-conjugated BA 3-sulfate) was collected, washed with ether, and dried under vacuum.

The glyine-conjugated BA 3-sulfates were synthesized by the following method. A suspension of 3-monohydroxy formylated BA (2 mmol), ethyl glycinate HCl (2.8 mmol), 2-ethoxy-1-ethoxycarbonyl-

1,2-dihydroquinoline (EEDQ, 2.8 mmol), and triethylamine (400 µl) in 30 ml of AcOEt was refluxed for 4 hr. After cooling to room temperature, the mixture was washed successively with 0.5 N NaOH (10 ml), 0.5 N HCl (10 ml x3), and water (20 ml x2). The organic layer was dried over anhydrous $MgSO_4$, evaporated, and dried under vacuum. The solid product so obtained was transferred into a 30-ml centrifuge tube, dissolved in 4 ml of DMF, and sulfur trioxide-triethylamine (3.2 mmol) was added and maintained at room temperature for 30 min. After adding 30 ml of ether, the suspension was centrifuged. The lower oily product was washed with ether, dried under vacuum, and hydrolyzed, precipitated as a *p*-toluidinium salt, and converted to the disodium salt (glycine-conjugated BA sulfate) as described for taurine-conjugated BA 3-sulfates. The BA 3-sulfates synthesized using this method include cholic acid 3-sulfate (CA3S), chenodeoxycholic acid 3-sulfate (CDCA3S), deoxycholic acid 3-sulfate (DCA3S), taurocholic acid 3-sulfate (TCA3S), tauro- or glyco-chenodeoxycholic acid 3-sulfate (TCDCA3S, GCDCA3S), tauro- or glyco-deoxycholic acid 3-sulfate (TDCA3S, GDCA3S), as well as glyco-lithocholic acid 3-sulfate (GLCAS). Cholic acid 7-sulfate (CA7S) and cholic acid 12-sulfate (CA12S) were synthesized according to a previous method (Tserng and Klein, 1979). The final products were characterized and verified by their mass and NMR spectra (typical NMR spectra for CA7S shown in figure 2-2, other NMR results are not shown).

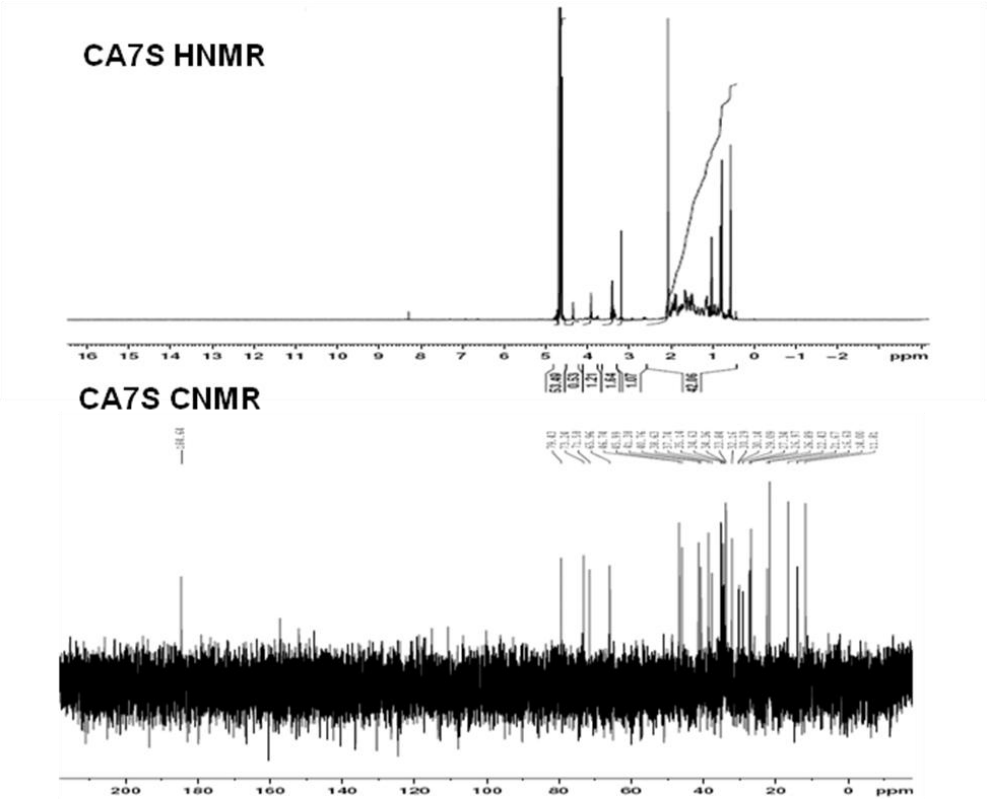

Figure 2-2. Typical ^{1}HNMR and ^{13}CNMR spectra of CA7S.

III. Liquid Chromatographic and Mass Spectrometric Conditions

A Waters ACQUITY ultra performance LC system (Waters, Milford, MA) was used for BA quantification. Chromatographic separations were performed on an ACQUITY UPLC BEH C18 column (1.7 µm, 100 x 2.1 mm I.D.) heated to 45 ^{o}C in the column compartment, using a gradient elution of mobile phase A (10 mM ammonium acetate in 20% acetonitrile) and mobile phase B (10 mM ammonium acetate in 80% acetonitrile) as follows: 5% B (0-5 min), 5-14% B (5-14 min), 14-25% B (14-14.5 min), 25% B (14.5-17.5 min), 25-50% B (17.5-18 min), 50% B (18-22 min), 50-80% B (22-22.5 min), 80% B (22.5-24.5 min), 80-5% B (24.5-25 min), and 5% B (25-28 min). All BAs were well separated (Figure 2-3). The injection volume was 5 µl, and the flow rate set at 0.4 ml/min. The sample manager system temperature was maintained at 4 ^{o}C.

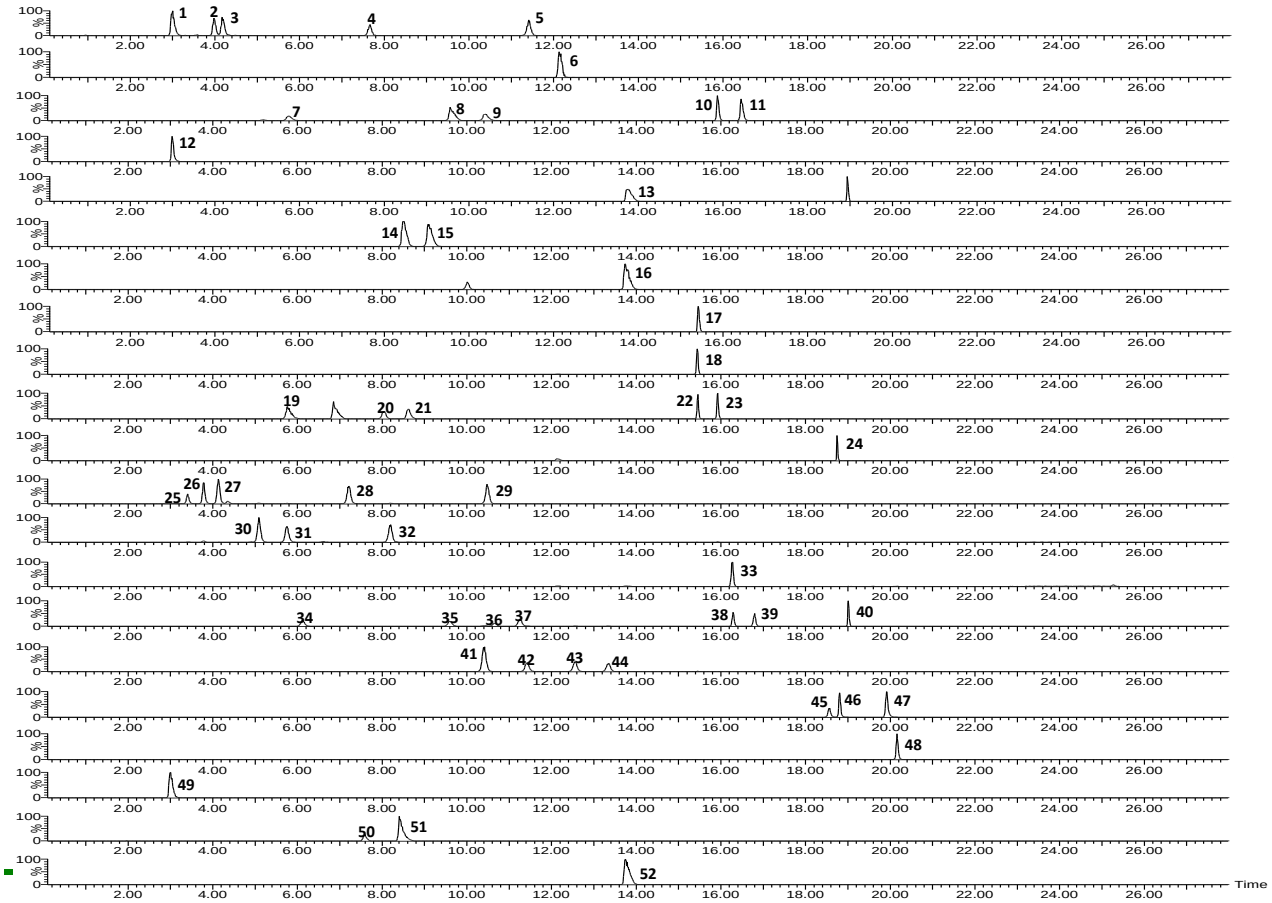

Figure 2-3. Representative UPLC-MS/MS chromatograms of various BAs under the final chromatography and detection conditions. 1, TωMCA; 2, TαMCA; 3, TβMCA; 4, THCA; 5, TCA; 6, GLCAS; 7, TMDCA; 8, TUDCA; 9, THDCA; 10, TCDCA; 11, TDCA; 12, CA3S; 13, TLCA; 14, CDCA3S; 15, DCA3S; 16, GCA; 17, LCAS; 18, $^{2}H_{4}$-GCDCA; 19, GMDCA; 20, GUDCA; 21, GHDCA; 22, GCDCA; 23, GDCA; 24, GLCA; 25, ωMCA; 26, αMCA; 27, βMCA; 28, HCA; 29, CA; 30, 7-oxoDCA; 31, 12-oxoCDCA; 32, 3-dehydroCA; 33, $^{2}H_{4}$-CDCA; 34, MDCA; 35, UDCA; 36, HDCA; 37, isoDCA; 38, CDCA; 39, DCA; 40, 3-DCA; 41, 6-oxoDCA; 42, 6-oxo-alloLCA; 43, 7-oxoLCA; 44, 12-oxoLCA; 45, alloLCA; 46, isoLCA; 47, LCA; 48, dehydroLCA; 49, TCA3S; 50, TCDCA3S; 51, TDCA3S; 52, TLCAS.

The mass spectrometer used was a Waters Quattro Premier XE triple quadrupole instrument with an ESI source (Waters, Milford, MA). The entire LC-MS system was controlled by MassLynx 4.1 software. All BAs were detected in the negative mode. The source and desolvation temperatures were set at 120 and 350^{o}C, respectively. The capillary, extractor, and RF voltages were set at 3 kV, 4 V, and 0

V, respectively. The source, desolvation, and collision gas were set at 650 L/h, 75 L/h, and 0.15 mL/min, respectively. The multiple reaction monitoring (MRM) transitions for all BAs are shown in table 2-1. The inter-channel delay, inter-scan delay, and dwell time were 5, 5, and 20 ms, respectively.

IV. Preparation of Standard Solutions and Calibration Curves

$^{2}H_4$-GCDCA (40 µg/ml) and $^{2}H_4$-CDCA (20 µg/ml) were used as internal standards (ISs). Ten mg/ml stock solutions of BAs and ISs were individually prepared in MeOH. Liver, bile, plasma, and urine were collected and each pooled from 5 untreated mice. Livers were homogenized in deionized water (1:5 w/v). Aliquots of liver homogenates, plasma, bile, and urine were incubated with 100 mg/ml activated charcoal for 1 hr to strip these matrices of endogenous BAs. Mixtures were centrifuged at 13,000 g for 10 min, and the supernatants were filtered. The matrices for kidney, intestinal tissue, and feces were prepared similarly as liver. The filtrates of these stripped matrices were used to construct the calibration curves, each in the corresponding biological matrix to be analyzed. Fixed volumes of these stripped matrices were spiked with 20 µl of the appropriate standard solution containing ISs to construct a calibration curve with the range of 0.04-100, 0.02-50, 0.01-25 µg/ml for T-BAs, unconjugated BAs, and G-BAs, respectively. All standard curves were constructed using a 1/concentration^2 weighted quadratic regression.

Table 2-1. Mass spectrometer conditions for quantification of various BAs.

Name	Precursor (m/z)	Product (m/z)	Cone (V)	Collision (eV)
TLCAS	280.3	464.2	35	25
Tauro-dihydroxy BAS	288.7	480.3	40	25
TCA3S	296.7	496.3	40	25
DehydroLCA	373.4	373.4	65	15
Monohydroxy BA	375.4	375.4	65	20
oxoLCA	389.4	389.4	70	15
Dihydroxy BA	391.4	391.4	65	15
^{2}H4-CDCA	395.3	395.3	60	18
DehydroCA	405.4	405.4	70	15
Trihydroxy BA	407.4	407.4	65	15
GLCA	432	432	60	15
Glyco-dihydroxy BA	448	448	60	15
^{2}H4-GCDCA	452.1	452.1	60	18
LCAS	454.8	96.8	60	42
GCA	464	464	60	15
Dihydroxy BAS	470.8	96.8	60	45
TLCA	482.1	80	90	70
Trihydroxy BAS	486.8	96.8	60	45
Tauro-dihydroxy BA	498.1	79.9	90	70
GLCAS	511.7	432	50	32
Tauro-trihydroxy BA	514.1	79.9	90	70
Glyco-dihydroxy BAS	528	448.3	50	30
Glyco-trihydroxy BAS	544.3	464.3	50	30
Monohydroxy BAG	551.5	375.5	35	40
Dihydroxy BAG	567.1	391.5	45	40
Trihydroxy BAG	583.1	407.2	46	36

BAS: BA sulfate; BAG: BA glucuronide

V. Animal Breeding

Oatp1a1-null mice, which were originally generated by Deltagen Inc. (San Carlos, CA), were obtained from Bristol-Myers Squibb Co. (Princeton, NJ). For the present experiments, homozygous null mice were backcrossed on the C57BL/6N background (Charles River, Raleigh NC), and homozygous null mice representing those obtained after at least 10 generations of backcrossing on the C57BL/6N background were used. Small segments of null mouse tails were sent to Jackson Lab (Bar Harbor, ME) for congenic genotyping, showing >99% congenicity with the C57BL/6 strain. Age-matched C57BL/6 mice were purchased from Charles River Laboratories (Wilmington, MA). All animals were maintained in a temperature-controlled facility with a 12 h light/dark cycle and allowed *ad libitum* access to water and a Teklad Rodent Diet #8604 (Harlan Laboratories, Madison, WI), according to the American Animal Association Laboratory Animal Care guidance. All studies were approved by the University of Kansas Medical Center Institutional Animal Care and Use Committee.

VI. Genotyping Analysis

Purified DNA (tail snips) were used for PCR analysis (REDExtract-N-Amp™ Tissue PCR kit; Sigma, St. Louis, MO). The primers for wild-type (WT) Oatp1a1 were 5'–AGAATGAGGACATAGTGGC ATACAG-3' and 5'- AAAAGGGACTGTCTCATGCTATATG -3', and the knockout allele was detected with the neo-specific primer 5'- GGGCCAGCTCATTCCTCCCACTCAT-3'. This strategy yielded fragments of 521 and 273 bp for the WT and null alleles, respectively. Multiplex PCR was performed on the digested, neutralized genomic DNA with 500 nM of each primer for the Oatp1a1 gene. The amplification conditions were: 95°C for 7 min (Taq DNA polymerase activation) and 35 cycles of 96°C for 10 sec (denaturing), 60°C for 30 sec (annealing) and 68°C for 1 min 30 sec (extension) followed by 7 min (68°C) at the end of the run. Amplification products were resolved on 1.4% agarose gels with ethidium bromide (40 min at 100V).

VII. Western Blot Analysis

Liver (approximately 75-100 mg) was minced in 800 µl of ice-cold homogenizing buffer (0.25 M sucrose, 10 mM Tris-HCl at pH 7.5, containing 25 µg/ml leupeptin, 50 µg/ml aprotinin, 40 µg/ml phenylmethanesulphonylfluoride [PMSF], 0.5 µg/ml pepstatin, and 50 µg/ml antipatin), then homogenized on ice, and subjected to centrifugation at 100,000 g for 1 h at 4^{o}C. The resulting membrane pellet was resuspended in 0.25 M sucrose, containing 10 mM HEPES, and 40 µg/ml PMFS. Protein concentrations were quantified with the Bradford protein assay (Sigma) with bovine serum albumin as standard. For electrophoretic separation, membrane proteins were mixed with sample loading buffer (75 µg protein/lane), separated on a 4-20% precast polyacrylamide gel (Beckman, Brea, CA), and transferred to a nitrocellulose membrane (1 h at 100 V at 4^{o}C). Membranes were blocked for 1 h at room temperature with 5% nonfat dry milk in Tris-buffered saline containing 0.1% Tween-20 (TBS-T) prior to incubation with Oatp antibodies. The Oatp1a1 antibody was raised in rabbits against the mouse Oatp1a1-specific peptide (NH2-CRKFHFPGDIHSPDTE-COOH) by Covance Research Products, Inc. (Berkeley, CA), and a polyclonal rabbit anti-mouse Oatp1a4 was purchased from Santa-Cruz Biotechnology, Inc. (Santa-Cruz, CA). Primary antibodies were diluted 1:200 with 5% non-fat milk in TBS-T and blots were incubated overnight at 4^{o}C. After washing, blots were incubated with goat anti-rabbit IgG horseradish peroxidase-linked secondary antibody (1:2000 dilution with 5% non-fat milk in TBS-T) for 1 h. Immunoreactive bands were detected with an enhanced chemical luminescence kit (Pierce Biotechnology Inc., Rockford, IL), and Oatp1a1 and 1a4 protein bands were visualized by exposure to Fuji Medical X-Ray film**.**

VIII. Bile Acid Feeding

The control diet was prepared by grinding Harlan Teklad Rodent Diet #8064 (Harlan Laboratories, Madison, WI). To prepare BA-supplemented diets, BAs were first ground with a small

amount of control diet using a mortar and pestle, and then mixed with a large amount of control diet in a Hobart food mixer (Hobart Corporation, Troy, Ohio). Cholestyramine-supplemented diet (2% resin, by weight of diet) was prepared using the same method as BA-supplemented diets. During a preliminary study, C57BL/6 mice were fed diets supplemented with different concentrations (0.01%, 0.1%, 0.3%, and 3%, by weight of diet) of individual BAs. Concentrations that were non-lethal were selected for the present study (Song and Klaassen, to be submitted). Individually housed C57BL/6 mice (n=5/gender/group) were fed a control diet or a diet supplemented with 1% CA, 0.3% DCA, 0.3% CDCA, 0.3% LCA, 3% UDCA, or 2% resin for 7 days. Mice were anesthetized between 8:00 AM and 12:00 AM on day 7, and gallbladders were carefully removed. Livers were then harvested with gallbladders removed, washed, frozen in liquid nitrogen, and stored at -80^{o}C until time of analysis.

In another experiment, individually housed C57/BL6 and Oatp1a1-null mice (n=5/gender/group) were fed a diet supplemented with 0.3% DCA. After 7 days, mice were anesthetized, blood was taken by orbital bleeding and centrifuged at 6,000 g for 15 min to collect serum. Gallbladders were carefully collected and stored at -80^{o}C until time of analysis. Livers were harvested from the same animals, washed, frozen in liquid nitrogen, and stored at -80^{o}C until time of analysis. The three small intestine segments, namely duodenum, jejunum, and ileum, as well as cecum and large intestine tissues, were divided, cut open, contents removed, and stored separately at -80^{o}C.

IX. Sample Preparation for Bile Acid Analysis

Mice (n=6/group) were anesthetized i.p. using ketamine (100 mg/kg)/midazolam (5 mg/kg). Body temperature of the mice was maintained at 37^{o}C with a heating pad. The common bile duct was cannulated with 30-gauge needle attached to PE-10 tubing. Bile was collected from the cannula for 2 hr at 15-min intervals.

Another set of mice (n=5/group) were anesthetized, blood collected by orbital bleeding into heparanized tubes, and serum obtained after centrifuging the blood at 6,000 g for 15 min. Livers, with gallbladders removed, were washed, frozen in liquid nitrogen, and stored at -80^{o}C until time of analysis. Small intestine, cecum and large intestine were divided, cut open, and vortexed in 3 ml of saline, respectively. Intestinal contents were collected and stored at -80^{o}C. The three small intestine segments, namely duodenum, jejunum, and ileum, as well as cecum and large intestine tissues, were stored separately at -80^{o}C. To collect urine and feces, a set of mice (n=9/group) were placed separately in metabolic cages. The collection of urine and feces was maintained at ice-cold temperature.

X. Bile Acid Extraction from Plasma, Bile, Urine, and Gallbladders

For plasma samples, simple protein precipitation using ice-cold MeOH was used. Accurately, 100 µl of serum was spiked with 20 µl of ISs. After equilibrating on ice for 10 min, 1 ml of ice-cold MeOH was added to the mixture, vortexed, and centrifuged at 12,000 g for 10 min. The supernatant was aspirated, and the pellet was re-extracted with 500 µl of ice-cold MeOH. The pooled supernatants were evaporated under vacuum, and reconstituted in 100 µl of 50% MeOH.

For bile samples, Oasis-HLB SPE cartridges were used for sample extraction. Bile samples were diluted 50 fold with deionized water, 200 µl of diluted bile samples were spiked with 20 µl of ISs, vortexed, and loaded onto SPE cartridges, which were pre-conditioned with 1 ml of MeOH and followed by 1 ml of H_2O. Loaded cartridges were washed with 2 ml of H_2O, and eluted with 2 ml of MeOH. The eluate was evaporated under vacuum and reconstituted in 200 µl of 50% MeOH. Urine samples (200 µl) were spiked with 20 µl of ISs and prepared similarly as bile samples.

To extract BA from gallbladders, 1 ml of methanol was added to each gallbladder pre-mixed with 100 µl of ISs. The mixture was vortexed vigorously, sonicated for 10 min, centrifuged at 16,000 g for 10

min, and the supernatant collected. The pellet was extracted with another 2 ml of methanol. The two supernatants were combined, evaporated under vacuum, and reconstituted in 1 ml of 50% MeOH.

Extraction recoveries were determined for each quality control (QC) point in each matrix as the ratio of the analyte peak area in samples spiked before extraction compared to the corresponding peak area in untreated samples prepared in neat solution.

XI. Bile Acid Extraction from Intestinal Contents and Feces.

To extract BAs from mouse intestinal contents and feces, preliminary experiments were performed to optimize BA extraction. Briefly, intestinal contents were mixed with 100 µl of ISs and centrifuged at 12,000 g for 10 min to collect the supernatant. The pellet was extracted with 3 ml of methanol twice. The mixture was centrifuged at 12,000 g for 20 min to collect the supernatants. The three supernatants were pooled, evaporated under vacuum, and reconstituted in 1 ml of 50% methanol.

Mouse feces were dried under vacuum and grounded well using a mortar and pestle. One hundred mg of feces were mixed with 50 µl of ISs and 3 ml of methanol was added. After shaking for 1 hr at room temperature, the mixture was centrifuged at 12,000 g for 10 min to collect the supernatant. The pellet was extracted with another 2 ml of methanol. The pooled supernatants were evaporated under vacuum, and reconstituted in 500 µl of 50% methanol.

XII. Bile Acid Extraction from Liver

Approximately 120 mg of liver was homogenized in 5 volumes of H_2O. Six hundred µl of liver homogenate was spiked with 20 µl of ISs, mixed, and equilibrated on ice for 10 min. Three ml of ice-cold alkaline acetonitrile (5% ammonia in acetonitrile) was added to the homogenate, which was then

vortexed vigorously and shaken continuously for 1 hr at room temperature. The mixture was centrifuged at 12,000 g for 10 min, and the supernatant collected. The pellet was resuspended in 2 ml of methanol, sonicated for 5 min, and centrifuged at 15,000 g for 30 min. The two supernatants so obtained were combined, evaporated under vacuum, and reconstituted in 200 µl of 50% methanol. The suspension was transferred into a 0.2 µm Costar Spin-X HPLC microcentrifuge filter (Corning Inc., Corning, NY), and centrifuged at 12,000 g for 10 min. The filtrate was centrifuged again at 20,000 g for 10 min before injection.

XIII. Bacterial DNA Extraction

Small and large intestinal luminal contents from WT and Oatp1a1-null mice (n=6/group) were collected in ice-cold PBS containing 10 mM DTT. After the contents were centrifuged at 20,000 *g* for 30 min at 4°C, the supernants were carefully discarded and the pellets were weighed. Total genomic bacterial DNA was extracted from the pellets using QIAmp DNA® stool kit (Qiagen, Valencia, CA) following the manufacturer's instructions. The integrity, concentration, and quality of the total DNA were assessed by agarose gel electrophoresis, and determination of absorption at A_{260}, and A_{260} to A_{280} ratio, respectively. DNA solutions were stored at -20ºC till further analysis.

XIV. Bacteria Quantification

The bacteria qunantified in this study were based on previous data indicating the microflora that reside in the intestine of mice (Salzman et al 2002). To compare the composition of intestinal microbiota of WT and Oatp1a1-null mice, a strategy based on quantification of the 16s rRNA gene by branched DNA (bDNA) assay was utilized. The 16s rRNA gene assay was performed using the Quantigene 2.0 Reagent System (Panomics/Affymetrix, Fremont, CA), as described in the manufacturer's protocol.

Briefly, the oligonucleotide probes targeted against the 16s rRNA gene sequence of various bacteria were custom manufactured. Accession numbers for the 16s rRNA genes of the corresponding bacteria are given in Table 2-2. Because the majority of the bacteria residing in the intestine are unculturable, the bacterial sequences are defined as the closest known relative in the phylogenic tree (Salzman et al. 2002). Total bacterial DNA (1 ng/μl, 20 μl) was added to each well preloaded with 80 μl of lysis buffer containing blocking reagent and each probe set. Sample DNA was allowed to hybridize to each probe overnight at 55°C. Subsequently, the plate was washed with washing buffer thrice. Samples were hybridized with the amplification reagent (100 μl/well) in the amplifier/label probe buffer for 1 h at 55°C. The plate was washed with wash buffer thrice. Label probe diluted in amplifier/label probe buffer was added to each well (100 μl/well), and the alkaline phosphatase-conjugated label probe was allowed to hybridize to the bDNA-DNA complex for 1 h at 50°C. The plate was washed with wash buffer thrice. The enzyme reaction was triggered by the addition of substrate (100 μl/well) and incubated for 5 min. The resulting luminescence was quantified using a luminometer with an integration time of 0.2 sec.

Table 2-2. Gene accession numbers of the 16s rRNA genes assessed in the present study and the corresponding closest relative bacteria.

Bacterial Species	NCBI accession number
Acetibibrio cellulosolvens	AJ418058
Bacillus mycoides	AJ308388
Bacteroides distasonis (i)	AJ400243
Bacteroides distasonis (ii)	AJ400242
Bacteroides distasonis (iii)	AJ400241
Bacteroides distasonis (iv)	AJ400234
Bacteroides forsythus (i)	AJ400249
Bacteroides forsythus (ii)	AJ400236
Bacteroides vulgatus	AJ400246
Bacteroides distasonis (v)	AJ400254
Bacteroides acidofaciens	AJ400252
Bacteroides sp. ASF519	AJ400245
Bifidobacterium animalis	AB027536
Candidatus xiphinematobactor	AJ400275
Clostridium absonum	X77842
Clostridium celerecrescence (i)	AJ400265
Clostridium celerecrescence (ii)	AJ400256
Clostridium clostridiiformes	AJ400247
Clostridium fusiformis	AJ400260
Clostridium methylpentosum	AJ400237
Clostridium perfringens	FJ384389
Clostridium polysaccharolyticum	AJ400272
Clostridium scindens	AY878326
Clostridium sp	AJ400251
Clostridium sp. ASF502 (i)	AJ400255
Clostridium sp. ASF502 (ii)	AJ308396
Clostridium sp. ASF502 (iii)	AJ400261
Desulfovibrio sp.	AJ308394
Eubacterium desmolans	AJ400270
Eubacterium limosum	AB298910
Helicobactor sp.	AJ308389
Klebsiella granulomatis	EU333881
Lactobacillus acidophilus (i)	AJ400238
Lactobacillus murinus	AJ308393
Lactobacillus reuteri	AJ308392
Lactobacillus salivarius	FJ378897
Lactobacillus sp. ASF519	AJ308390
Lactobaciluus acidophilus (ii)	AJ300391
Lactococcus lactis	FJ378886
Porphyromonas sp. (i)	AJ400264
Porphyromonas sp. (ii)	AJ400235
Prevotella sp. (i)	AJ400267
Prevotella sp. (ii)	AJ400266
Ralstonia sp.	AJ308395
Ruminococcus gnavus	AJ308386
Ruminococcus schinkii	AJ400250
Segmented Filamentous Bacteria (SFB)	AJ308387
Streptococcus gordnii	EU156758
TM7 phylum sp	AJ400239

XV. Kinetics of DCA (i.v.) in Mice

Age-matched WT and Oatp1a1-null mice (n=6) were anesthetized i.p. with ketamine (100 mg/kg)-midazolam (5 mg/kg) and body temperature was maintained at 37^{o}C with a heating pad. Subsequently, the right carotid artery was cannulated with PE-10 tubing, and the common bile duct was cannulated with the shaft of 30-gauge needle attached to PE-10 tubing. To avoid possible renal elimination of BAs, the renal pedicles were ligated through a median abdominal incision. After stabilizing bile flow with a 10-min bile collection, each mouse was injected i.v. with sodium deoxycholate (50 μmol/kg in pathogen-free water). Blood samples (about 30-40 μL) were collected at 0, 2, 5, 11, 21, 31, and 41 min after DCA administration into heparinized tubes.

The plasma concentration (Cp) for DCA was found to fit an open 2-compartment pharmacokinetic model described by the biexponential equation:

$$C_p = Ae^{-\alpha t} + Be^{-\beta t}$$

where A and α hybrid constants are the y intercept and elimination rate constant of the distributive phase, whereas B and β hybrid constants describe the y intercept and elimination rate constant of the terminal phase of the 2 components of the curve. The data were fitted to the exponential components of the equation by a method of least squares with the coefficient of correlation used as the indicator of data fit. This curve fitting was made by Sigma plot 10.0 (Systat Software Inc., San Jose, CA). The model described the distribution of DCA between a central compartment, V_{cent} (plasma and plasma-like tissue), and a peripheral compartment, V_{perif} (all other tissues that behave kinetically differently from plasma). The distribution half-life time ($T_{1/2\ dist}$), elimination half-life time ($T_{1/2\ el}$), apparent volume of distribution at steady state (V_{app}) for the central compartment (V_{cent}) and peripheral compartment (V_{perif}), total body clearance (Cl) were calculated based on the following equations:

$$T_{1/2\ dist} = \frac{0.693}{\alpha}$$

$$T_{1/2\ el} = \frac{0.693}{\beta}$$

$$V_{d\ cent} = \frac{D}{A + B}$$

$$V_{d\ perif} = \frac{D}{B}$$

$$V_{d\ app} = \frac{D}{A/\alpha + B/\beta}$$

$$Cl = V_{d\ app} \frac{0.693}{T_{1/2\ el}}$$

XVI. Bile Duct Ligation

Adult male mice (WT, Oatp1a1-null, Oatp1a4-null, and Oatp1b2-null mice, n=5/group) were individually housed in mouse cages. All surgical tools were autoclaved and maintained in 70% alcohol. For induction of anesthesia, mice were placed into a closed-circuit chamber with an inflow of 3% isoflurane and an oxygen flow rate of 1 L/min. After induction of anesthesia, the head of each mouse was positioned into a face mask connected to an anesthesia machine with an inflow of 1% isoflurane and an oxygen flow rate of 1 L/min. Depth of anesthesia was monitored by pinching the footpad of the mice before and throughout surgery. Heart rate and respiratory rate were monitored throughout surgery. Body temperatures were maintained at 37^{o}C by means of heating pads. The abdomen of each mouse was shaved and swabbed with Betadine and 70% alcohol. Surgical silk thread (7-0) was placed around the common bile duct using a micro-dissection forcep. The common bile duct was ligated doubly, close to the beginning of its intrapancreatic portion, with the gallbladder removed. Sham surgeries were performed without BDL by the same method. The abdominal cavity was closed with an interlocking running stitch with 5-0 silk. The skin was then be reapproximated with 5-0 nylon suture. After closing the

abdomen, the incision was again wiped with Betadine. All surgeries were performed between 8:30 AM and 1:30 PM. Twenty-four hr after surgery, mice were anesthetized with 4% isoflurane, blood was collected by orbital bleeding into heparanized tubes, and serum was obtained by centrifuging blood at 6,000 g for 15 min. Livers were washed with saline, frozen in liquid nitrogen, and stored at -80^{o}C until time of analysis. The contents of the small intestine, cecum, and large intestine were collected in ice-cold PBS containing 10 mM DTT. The intestinal tissues were divided, and stored at -80^{o}C till further analysis.

XVII. Antibiotic Treatment

Cephalothin and neomycin combination treatment have been shown to result in nearly complete suppression of microbial populations in the gut (Goris et al., 1986). Age-matched WT and Oatp1a1-null mice (n=5/group) were individually housed in mouse cages. Cephalothin (2 g/L) and neomycin (2 g/L) were dissolved in drinking water and given to mice. Drinking water was changed daily with fresh antibiotics. On day 10, sham and BDL surgeries were conducted on both WT and Oatp1a1-null mice with the same fresh antibiotic-treated drinking water. Twenty-four hr after surgery, mice were sacrificed and tissues collected as described previously.

XVIII. Intestinal Permeability Test

Mice were acclimatized in wire-bottomed metabolic cages for 3 days with free access to food and water. Feed was removed overnight before the mice were administrated 13.3 mg lactulose and 10.1 mg mannitol p.o. (Sigma-Aldrich, St. Louis, MO). Urine was collected the next 20 h in 10 µl of 1% NaN3. Urinary lactulose and mannitol were quantified by LC-MS/MS. Two hundred µl of urine was loaded onto Oasis-HLB SPE cartridges pre-conditioned with 1 ml of MeOH, followed by 1 ml of H_2O. Loaded cartridges were eluted with 2 ml of H_2O. The eluate was evaporated under vacuum and reconstituted in 200 µl of H_2O.

A Waters ACQUITY ultra performance LC system (Waters, Milford, MA) was used for lactulose and mannitol quantification. Chromatographic separations were performed on an ACQUITY UPLC BEH C18 column (1.7 µm, 100 x 2.1 mm I.D.) heated to 45^{o}C in the column compartment, using a gradient elution of mobile phase A (10 mM ammonium acetate in 20% acetonitrile) and mobile phase B (10 mM ammonium acetate in 80% acetonitrile) as follows: 20% B (0-3 min), 20-80% B (3-3.2 min), 80% B (3.2-4 min), 80-20% B (4-4.2 min), and 20% B (4.2-7 min). The sample manager system temperature was maintained at 4^{o}C.

The mass spectrometer was a Waters Quattro Premier XE triple quadrupole instrument with an ESI source (Waters, Milford, MA). The entire LC-MS system was controlled by MassLynx 4.1 software. Sugars were detected in the negative mode. The source and desolvation temperatures were set at 120 and 350^{o}C, respectively. The capillary, extractor, and RF voltages were set at 4 kV, 7 V, and 1 V, respectively. The source, desolvation, and collision gases were set at 650 L/h, 75 L/h, and 0.15 mL/min, respectively. The multiple reaction monitoring (MRM) transitions for lactulose and mannitol were 340.8>160.7 and 180.8>88.9, respectively. The cone voltages were 35 and 26 V for lactulose and mannitol, respectively. The collision energies were 10 and 16 eV for lactulose and mannitol, respectively. The inter-channel delay, inter-scan delay, and dwell time were 20, 20, and 5 ms, respectively.

XIX. Serum Biochemistry

Analytical kits for serum total bilirubin, conjugated bilirubin, triglycerides, and glucose were obtained from Pointe Scientific Inc. (Canton, MI). Analytical kits for serum free cholesterol were purchased from Wako Chemicals (Richmond, VA).

XX. H&E Staining

Liver samples were formalin-fixed, embedded in paraffin, sectioned (5 μm), and stained with hematoxylin-eosin. Sections were visualized under a microscope and the hepatocellular damage was analyzed by a board-certified pathologist (Fang Fan, MD, PhD, Kansas University Hospital, Kansas City, KS).

XXI. Metabonomics Study by UPLC-TOF-MS

Urinary samples were prepared by mixing 40 μl of urine with 160 μl of 50% acetonitrile and centrifuged at 20,000 g for 10 min. Serum samples were prepared by mixing 75 μl of serum with 75 μl of acetonitrile, followed by vortexing and centrifugation at 15,000 g for 10 min. A 100 mm × 2.1 mm (Acquity 1.7 μm) UPLC BEH C18 column (Waters) was used for metabolite separation. The flow rate of the mobile phase was 0.3 ml/min with a gradient ranging from 2 to 98% aqueous acetonitrile containing 0.1% formic acid in a 10-min run. TOFMS was operated in both positive and negative modes with electrospray ionization. The source temperature and desolvation temperature were set at 120 and 350°C, respectively. Nitrogen was applied as the cone gas (10 L/h) and desolvation gas (700 L/h), and argon as the collision gas. TOFMS was calibrated with [Glu1]-fibrinopeptide and monitored by the intermittent injection of lock mass leucine enkephalin in real time. The capillary voltage and the cone voltage were set at 3.5 kV and 35 V in the positive ion mode. Screening and identification of major metabolites were performed by using MarkerLynx software (Waters) based on accurate mass measurement (mass errors less than 10 ppm).

Mass chromatograms and mass spectra were acquired by MassLynx software in centroid format from 50 to 1000 m/z. Centroid and integrated mass chromatographic data were processed by MarkerLynx software to generate a multivariate data matrix. Principal component analysis (PCA) and orthogonal projection to latent structures-discriminant analysis (OPLS-DA) were conducted on Pareto-scaled data.

The corresponding data matrices were then exported into SIMCA-P+ (version 12; Umetrics, Kinnelon, NJ) for multivariate data analysis.

XXII. Total RNA Isolation

Total RNA was isolated using RNA-Bee reagent (Tel-Test Inc., Friendswood, TX) according to the manufacturer's protocol. Total RNA concentrations were quantified spectrophotometrically at 260 nm. One microgram per microliter solutions were prepared from the stock RNA solution by dilution in diethyl pyrocarbonate-treated deionized water. Integrity of RNA samples was determined by formaldehyde-agarose gel electrophoresis with visualization by ethidium bromide fluorescence under ultraviolet light.

XXIII. mRNA Quantification by RT-PCR

The primer sequences for each gene are shown in table 2-3. Briefly, total RNA (1 µg) was reversely transcribed into cDNA in a total of 50 µl of reaction buffer by adding 2.5 U of Moloney murine leukemia virus reverse transcriptase (M-MLVRT) and 0.66 ng of random hexamers (Invitrogen, Carlsbad, CA). The samples were incubated in a Thermo Cycler at 42^{o}C for 15 min, and followed by 95^{o}C for 15 min. The cDNA thus obtained was diluted 10 fold with water and subjected to real-time PCR. Using Primer Express 2.0 (Applied Biosystems, Foster City, CA), the primers and probes were designed to cross introns to ensure that only cDNA but not genomic DNA was amplified. The PCR reaction mix contained per reaction: 12.5 µl of Applied Biosystems SYBR® green PCR master mix, 2.5 µl of 3 µM forward and reverse primer mix, 5 µl of RNAse-free H_2O, and 5 µl of 2 ng/µl cDNA. Reactions were seeded in a 384-well optical reaction plate (Applied Biosystems) and fluorescence was quantified in real time using Applied Biosystems 7300 Real Time PCR System (Foster City, CA) under the following conditions: 50°C for 2 min, 95°C for 10 min, (95°C for 15 sec, 60°C for 1 min) X 40 cycles, dissociation stage: 95°C for 15

sec, 60°C for 30 sec, and 95°C for 15 sec. Relative standard curves were generated for each target gene to determine the relative amount of transcript present in the sample. Relative amounts of gene transcript were then normalized to the housekeeping transcript Gapdh or β-actin.

Table 2-3. Mouse real time-PCR primer sequence (5'-3')

Gene	GenBank Number	Position	Forward	Reverse
Gapdh	M32599	306-835	aggccggtgctgagtatgtc	tgcctgcttcaccaccttct
β-actin	V01217	2371-2445	tgaccgagcgtggctacag	gggcaacatagcacagcttct
Asbt	NM_011388	835-951	tggaatgcagaacactcagc	gcaaagacgagctggaaaac
Mrp3	NM_029600	3120-3222	tggtcatgctgtcagctttc	aaggactgaggggaacgaat
Mrp4	BC150822	1257-1395	gcaaagcccatgtaccatct	accacggctaacaactcacc
Ostα	NM_145932	49-196	ttgtgatcaaccgcatttgt	ttgtgatcaaccgcatttgt
Ostβ	NM_178933	226-369	atcctggcaaacagaaatcg	ggccaagtctggtttctctg
AhR	NM_013464	2951-3064	accagaactgtgagggttgg	ctcccatcgtatagggagca
CAR	NM_009803	122-271	ctcaaggaaagcagggtcag	agttcctcggcccatattct
FxR	NM_009108	357-503	tgggtaccagggagagactg	gtgagcgcgttgtagtggta
LDLR	NM_010700	3741-3884	gaactcagggcctctgtctg	agcaggctggatgtctctgt
FGF15	NM_020013	254-261	ctgggggtctaccaagcata	atcctccctgatctccaggt
Nrf2	BC026943	1645-1723	cgagatatacgcaggagaggtaaga	gctcgacaatgttctccagctt
PXR	AF031814	223-339	cccatcaacgtagaggagga	tctgaaaaacccccttgcatc
SHP	NM_011850	699-820	ctcatggcctctaccctcaa	ggtcacctcagcaaaagcat
Cyp1a2	NM_009993	1055-1137	gacatggcctaacgtgcag	ggtcagaaagccgtggttg
Cyp2b10	AF128849	829-975	aaggagaagtccaaccagca	ctctgcaacatgggggtact
Cyp3a11	NM_007818	65-148	acaaacaagcagggatggac	ggtagaggagcaccaagctg
Cyp4a14	NM_010011	1048-1165	cacaccctgatcaccaacag	tccttgatgcacattgtggt
HO-1	M33203	F-R	cctcactggcaggaaatcatc	cctcgtggagacgctttacata
IL-6	J03783	13-90	gcccaccaagaacgatagtca	gaaggcaactggatggaagtct
Npc1L1	NM_207242	725-854	ctggctcaacttccaaggag	attgcagggtgtgatcttcc
TGF-β	M13177	1323-1399	gaccctgcccctatatttgga	gcccgggttgtgttggt
Pcna	NM_011045	600-727	ccacattggagatgctgttg	ccgcctcctcttctttatcc
Ibabp	NM_008375	192-326	caccattggcaaagaatgtg	aacttgtcacccacgacctc

XXIV. Multiplex Suspension Array

Messenger RNA was quantified by mutiplex suspension array (Panomics-Affymetrix, Inc., Fremont, CA). Individual gene accession numbers can be accessed at www.panomics.com (sets #21021 and #21151). Samples were analyzed using a Bio-Plex 200 System Array reader with Luminex 100

xMAP, and the data were acquired using Bio-Plex Data Manager version 5.0 (Bio-Rad, Hercules, CA). Assays were performed according to each manufactures' protocol. During preliminary experiments, the mRNA of three housekeeping genes, namely ribosomal protein 13a (Rpl13a), glyceraldehyde 3-phosphate dehydrogenase (Gapdh), and beta-actin (β-actin) were quantified and compared. For the BDL experiments, BDL did not alter Rpl13a or Gapdh, but increased β-actin in mouse livers. Therefore, RNA data in the BDL study are presented as relative light units (RLU) normalized to either Rpl13a or Gapdh mRNA.

XXV. Data Analysis

Data are represented as Mean ± SEM (n=5-6). Differences between mean values were tested for statistical significance ($P<0.05$) by the two tailed Student's t-test.

CHAPTER 3

BILE ACID METABOLOME IN MICE: EFFECTS OF FEEDING BILE ACIDS AND A BILE ACID SEQUESTRANT ON HEPATIC BILE ACID METABOLISM IN C57BL/6 MICE

Specific Aim and Hypothesis

Chapter 3 will address specific aim 1 which will develop **a LC-MS/MS method to investigate bile acid metabolism in both male and female C57BL/6 mice**. A simple, direct, and valid method is a prerequisite to investigate BA metabolism. The purpose of this study is **to improve a previous LC-MS/MS method developed in our laboratory, and to investigate BA metabolism in mice by challenging both male and female C57BL/6N mice with various BA-supplemented diets and a resin that binds BAs**.

I. Introduction

Bile acids (BAs) are synthesized from cholesterol in livers via two major pathways (Figure 1-1), namely the classic and alternative pathway (Chiang, 2002). Cyp7a1 is the rate-limiting enzyme in the classic pathway, which results in the formation of cholic acid (CA) and chenodeoxycholic acid (CDCA). The alternative pathway is initiated by mitochondrial Cyp27a1 and followed by Cyp7b1 to produce chenodeoxycholic acid (CDCA). Both CA and CDCA are primary BAs in humans and rodents. Rodent livers can hydroxylate CDCA at the 6β-position to form α-muricholic acid (αMCA), which can be further converted to βMCA by epimerization of its 7α-OH to 7β-OH (Botham and Boyd, 1983). Therefore, α- and β-MCA are also primary BAs in rodents.

BAs are subject to multiple biotransformations during their enterohepatic circulation, resulting in various BAs (Hofmann and Hagey, 2008). In liver, BAs can undergo conjugation with taurine, glycine, sulfate, and glucuronic acid, as well as P450-mediated oxidations (Deo and Bandiera, 2008). In the intestine, bacterial enzymes are capable of deconjugation, dehydroxylation, epimerization, and oxidization of BAs. Deoxycholic acid (DCA) and lithocholic acid (LCA) are major secondary BAs, because they are formed from 7-dehydroxylation of CA and CDCA, respectively, by intestinal bacteria. ωMCA is formed from βMCA by intestinal bacterial enzymes, which epimerize its 6β-OH to 6α-OH. Hyodeoxycholic acid (HDCA) is formed either by dehydroxylation of ωMCA at its 7β-OH, or directly from βMCA via intestinal bacteria (Eyssen et al., 1999). Ursodeoxycholic acid (UDCA) is formed from CDCA by epimerization of its 7α-OH to 7β-OH (Macdonald et al., 1982). Further oxidative biotransformation of BAs leads to the formation of oxo-BAs, which are constituents of human feces, and are increased in the urine during liver cirrhosis (Lepage et al., 1978; Amuro et al., 1981).

Gender differences in BA metabolism and toxicity have been reported in several species. The smaller BA pool in women suggests a possible mechanism for the higher prevalence of gallstones among females (Bennion et al., 1978). The relatively higher capacity of the male rat liver to convert the more toxic CDCA to the less toxic βMCA may explain the gender difference of rats to CDCA hepatotoxicity (Yousef et al., 1973). In contrast, more DCA is converted to taurocholic acid (TCA) in isolated perfused livers of female than male rats (Fisher et al., 1974). Hepatic metabolism of LCA might also be different between male and female mice, because female mice have a much higher capacity to sulfate LCA than male mice (Kitada et al., 2003).

It is known that individual BAs vary markedly in their pathological and physiological responses in vivo, such as activation of nuclear receptors, hepatotoxicity, and tumor promoting activities (Reddy et al., 1977; Yousef et al., 1981; Parks et al., 1999). Therefore, the nature and extent of these activities are affected by both the concentration and composition of the BA pool. For example, LCA is the most toxic BA and a potent PXR ligand (Staudinger et al., 2001), whereas CDCA is less cytotoxic and a FXR ligand

(Parks et al., 1999). Enzymatic methods using BA hydroxysteroid dehydrogenase have been widely applied for routine analysis of BAs in physiological fluids due to their simplicity. However, those methods determine the concentration of total 3-OH BAs, but not the concentrations of individual BAs. The presence of isomeric forms and relatively low concentrations in biological samples make chromatographic techniques the ideal methods to quantify BA profiles. For example, GC and GC-MS have been applied in BA analysis for decades (Klaassen, 1971; Alme et al., 1977; Setchell and Worthington, 1982; Stellaard et al., 1989). However, the GC technique requires complex sample preparation, derivatization, and hydrolysis of conjugated BAs, which makes the high-performance liquid chromatography (HPLC) techniques more desirable for BA analysis. For example, HPLC-UV and LC-MS/MS assays have been developed and successfully applied to satisfy certain purposes, for example, to quantify sulfated BAs (Goto et al., 1978). However, most methods were limited by complex sample extraction, lack of validation, long run times, and/or designed to quantify limited BAs only in plasma. Ultra performance liquid chromatography (UPLC) allows shortening of the analysis time as well as improved resolution and sensitivity compared to conventional HPLC, due to its small particle size and high working pressure. By taking advantage of UPLC, our lab has developed a simple, sensitive, direct, and valided method to quantify BAs in serum, liver, bile, and urine of mice (Alnouti et al., 2008). However, both LC-MS/MS conditions and sample preparation were designed to quantify only several major BAs. Therefore, we improved the LC-MS/MS method by optimizing the LC-MS conditions and sample preparation so that it can simultaneously quantify non-oxo BAs, oxo-BAs, as well as BA sulfates and glucuronides in both physiological fluids and tissues of mice.

The purpose of this study is to investigate BA metabolism and synthesis, along with potential gender differences in C57BL/6N mice. To achieve this purpose, the changes of BA profiles were determined in livers of both male and female C57BL/6 mice, which were subjected to a diet containing either a primary BA (CA or CDCA), a secondary BA (DCA or LCA), a therapeutic BA (UDCA), or a BA binding resin (cholestyramine). The design of the present study is based on three considerations. First,

the present study will provide valuable guidance and information for BA feeding experiments in mice. Various BA-supplemented diets have been fed to rodents to investigate hepatic gene regulation, BA hepatotoxicity, as well as the potential therapeutic use of BAs (Alpini et al., 1999; Hofmann, 1999; Goodwin and Kliewer, 2002). For example, because CDCA was shown to be a potent ligand for FXR, a number of studies fed mice CDCA to investigate FXR activation pathways in mouse livers. Unfortunately, little is known about how CDCA is metabolized in mice. Thus, it is not possible to determine whether the effects of CDCA feeding are direct or indirect. Second, several BA-metabolic pathways, which are minor under normal conditions, can be manifested by feeding BAs to mice. Although BAs undergo various biotransformations during their enterohepatic circulation, the metabolites of some pathways, such as sulfation, glucuronidation, and oxidation, are difficult to be detected under normal conditions. Feeding BAs will increase the amount of exogenous BAs in mice and thus magnify BA biotransformations in mice. By comparing BA profiles before and after feeding BAs, the metabolic pathways of BAs may be more readily elucidated. Finally, the present study will provide valuable information regarding the species differences between humans and mice. BAs have been used therapeutically in humans for a long time. For example, UDCA has been used to dissolve gallstone, to treat cholestasis of pregnancy, and to prevent cirrhosis in cystic fibrosis. Primary BAs have been used to treat patients with inborn errors of BA synthesis. For example, CA is administered to patients with defects in BA steroid nucleus maturation, whereas CDCA is prescribed to patients with *Cerebrotendinous Xanthomatosis* (Bonnot et al., 2010). Recently, several BA derivatives, namely INT-747 and INT-777, have been developed to selectively activate FXR and TGR5, respectively (Fiorucci et al., 2005; Pellicciari et al., 2009). The metabolic pathways of BAs elucidated in the present study will help to predict the difference between humans and mice, and thus aid in the interpretation of drug development and toxicity.

Taken together, **the overall goal for specific aim 1 is to provide the necessary tools (BA quantification) and knowledge (BA metabolic pathways) for the future study in Oatp1a1-null mice.**

II. Results

2. 1 Extraction of BAs from Mouse Livers

During preliminary experiments, different BA extraction methods were compared. In previous BA analyses, livers were either homogenized in 50% methanol (Alnouti et al., 2008) or ground as frozen tissue (Hagio et al., 2009). In the present study, livers were homogenized in 5 volumes of water to obtain a homogenate that was easily transferred with a pipet. To optimize BA extraction, liver homogenates were divided into small portions, each of which was spiked with or without a mixture of ISs and BA standards. BAs were then extracted with various solvents (ethanol, methanol, and acetonitrile) at various temperatures (25^{o}C, 37^{o}C, 60^{o}C, and 100^{o}C) and pHs (7, 9, 11, and 12). The extraction recoveries were determined by the ratio of the peak area of recovered BAs compared to the corresponding peak area of BA standards in neat solution (50% methanol). Finally, a two-step extraction using a combination of alkaline acetonitrile and methanol was found to be sufficient for maximum recovery of the BAs. The optimized extraction resulted in better recovery, especially for unconjugated BAs (Figure 3-1). BA standards (unconjugated BAs, oxo-BAs, taurine-, glycine-, and sulfate-conjugated BAs) were stable during this extraction procedure. The recovery ratios of the exogenous standards calculated from each raw peak area were from 75 to 90%. The recovery ratios of two ISs were from 75 to 85%. The recovery extent of BA standards and the ISs was consistent and reproducible.

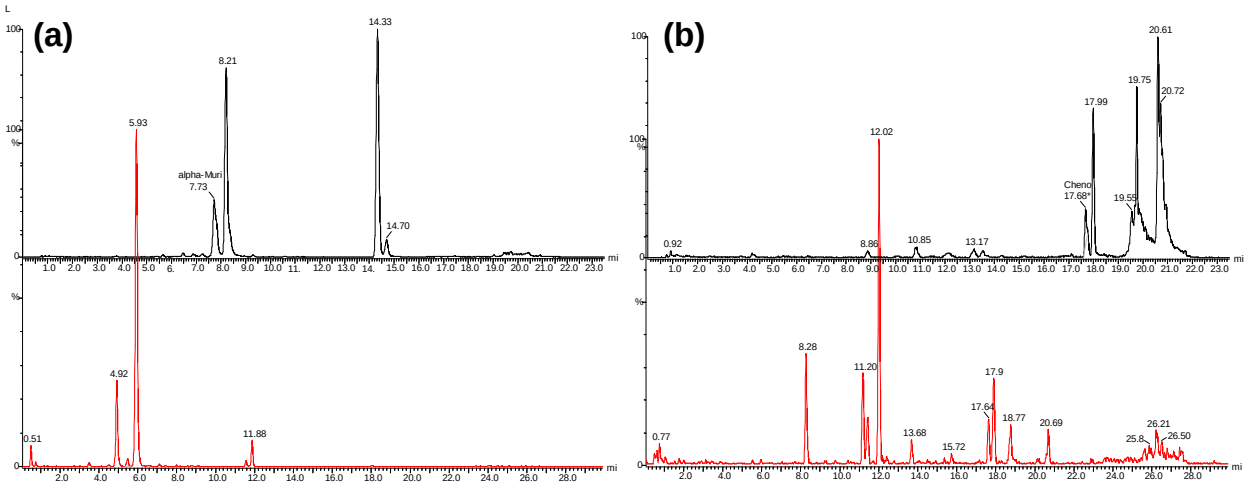

Figure 3-1. Enhanced recovery of unconjugated BAs from mouse liver after optimization of sample extraction. BAs were extracted using either the original method or the optimized method from the liver of the same mouse. The chromatographs were compared between the original LC-MS method (Black) and the optimized LC-MS method (Red). (a) The chromatograph window for unconjugated tri-hydroxy BAs. (b) The chromatograph window for unconjugated di-hydroxy BAs.

2.2 Validation of BA Quantification

To optimize the chromatographic conditions, we compared the methods used by Alnouti et al. (2008) with that by Hagio et al. (2009). The Hagio method resulted in a better separation between ω-, α-, and βMCA, whereas the signal intensity was only about 50% of the Alnouti method. Compared to the Alnouti method, more peaks were found in the chromatograph window for CDCA using the Hagio method. Therefore, chromatographic conditions similar to Hagio's with small modifications were used in the present study to separate all BA standards in less than 28 min. The new method resulted in better separation and peak intensity than Alnouti's method (Figure 3-2). The intra-day and inter-day accuracy and precision were determined according to the previous method (Alnouti et al., 2008), and their relative standard deviations were below 15% for all BA standards (data not shown). All standard curves were constructed using a 1/concentration^2 weighted quadratic regression, and the correlation coefficient (r^2) for

all BAs was above 0.99 (the standard curves for TαMCA and αMCA shown in figure 3-3). The limit of detection (signal/noise ratio=3) for the various BAs was in the range of 5-10 ng/ml.

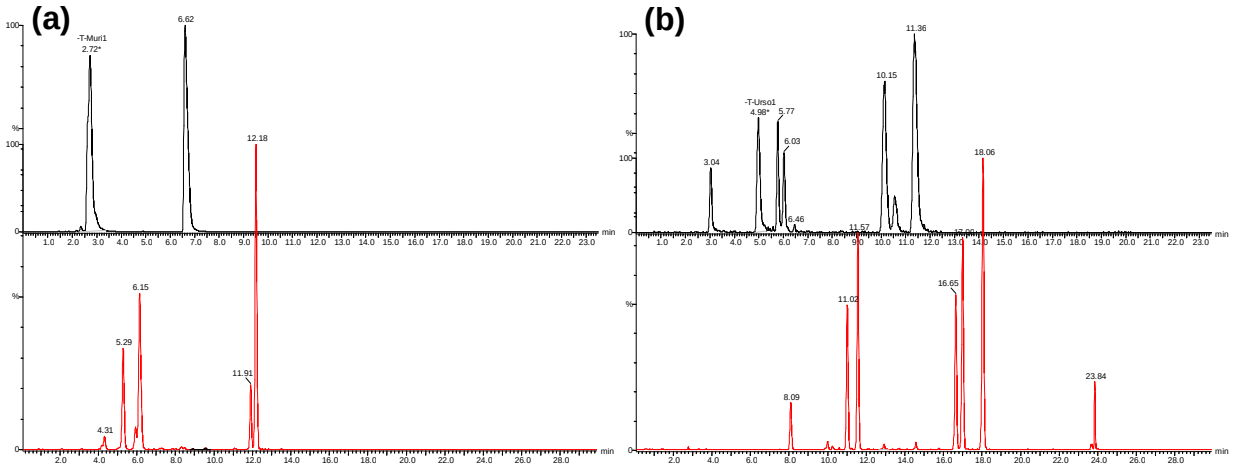

Figure 3-2. Enhanced separation of BAs from mouse liver after optimization of LC-MS conditions. BAs were extracted using the newly optimized method from liver and subjected to analysis under either the original or optimized LC-MS conditions. The chromatographs were compared between the original LC-MS method (Black) and the optimized LC-MS method (Red). (a) The chromatograph window for tauro-tri-hydroxy BAs. (b) The chromatograph window for tauro-di-hydroxy BAs.

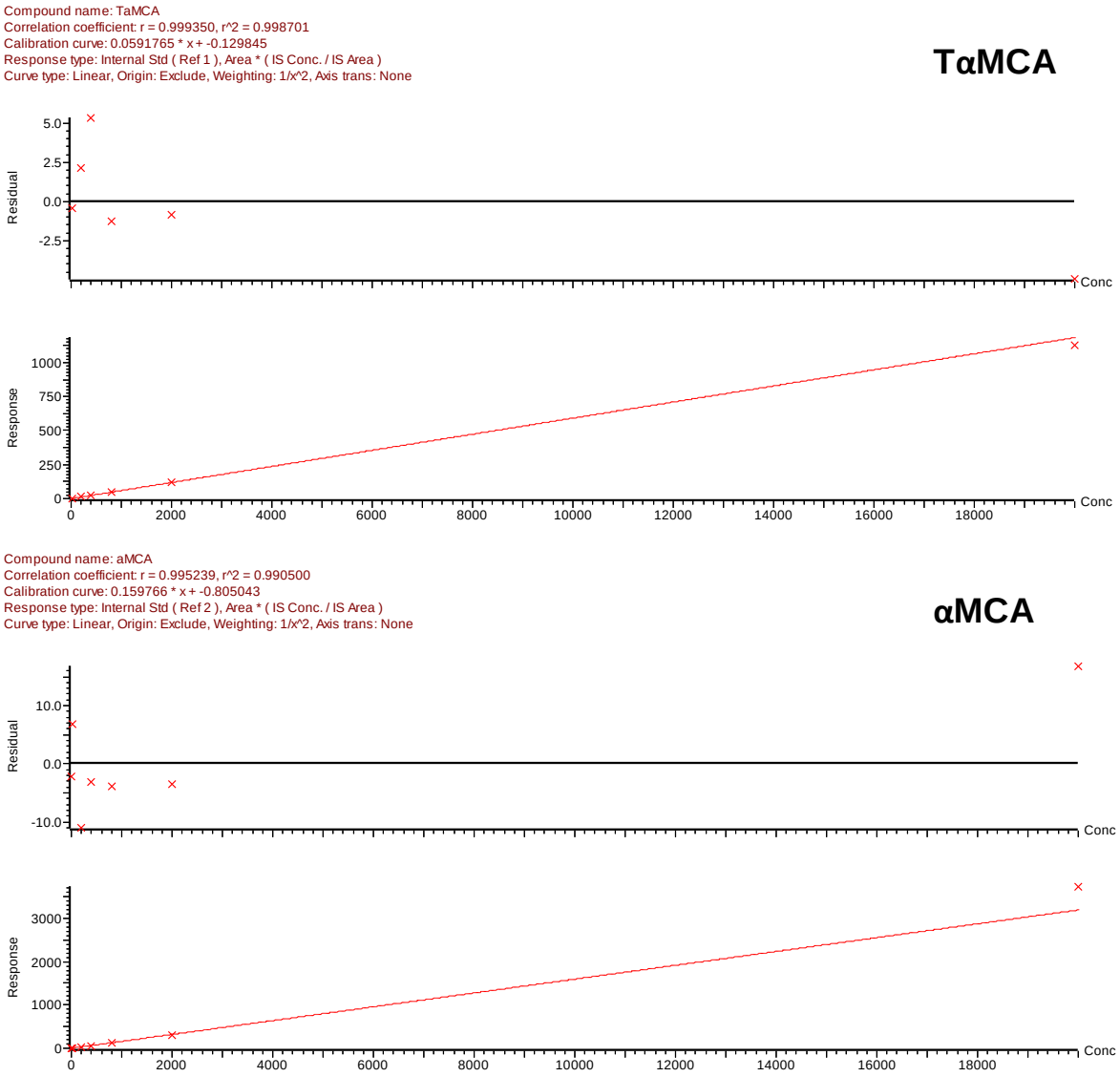

Figure 3-3. Standard curvers for TαMCA and αMCA. The standard curves were constructed using a 1/concentration^2 weighted quadratic regression, and the correlation coefficient (r^2) for both TαMCA and αMCA was above 0.99.

2.3 Sulfation Position of BAs in Mice

In the present study, sulfates of GCDCA, GDCA, and GLCA were not detected in any group of mouse livers (data not shown). CA can theoretically be sulfated at the 3-, 7-, and 12-OH positions to form CA3S, CA7S, and CA12S, respectively. In control livers of male and female mice, one peak was found in the chromatograph window of CA3S, but with a different retention time than the CA3S standard. This peak was also found at high concentrations in the intestinal contents (data not shown). By comparing the retention time and mass spectra with CA7S and CA12S standards, this peak was identified as CA7S (Figure 3-4a). To further confirm the position of CA sulfation, liver samples were mixed with one of the CA sulfate standards and separated on UPLC. Only one peak was found when liver samples were mixed with CA7S, but not when mixed with CA3S or CA12S (data not shown). One peak was found in the chromatograph window of TCA3S, with a similar retention time as TCA3S (Figure 3-4b). Because CA was sulfated at the 7-position, it was likely that sulfation of TCA was also at the 7-position (TCA7S), which might not separate from TCA3S under the current chromatographic conditions. DCA can be theoretically sulfated at the 3-OH and 12-OH positions. No peaks were observed in the chromatograph windows for DCAS or TDCAS in the livers of mice fed DCA, indicating that sulfation is not a detoxification pathway of DCA in mice (Figure 3-5).

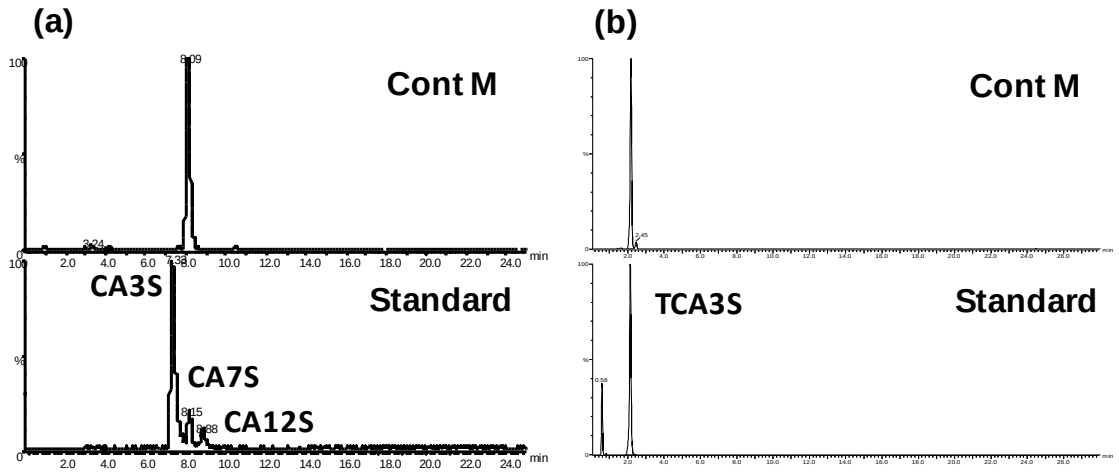

Figure 3-4. UPLC-MS/MS chromatograms of liver samples from control male mice. (a) The peaks at m/z 486.8>96.8 from liver samples of control mice and the CAS standards. Standard CA7S eluted at the same time as the sample peak. (b) The peaks at m/z 296.7>496.3 from liver samples eluted at the same time as the standard TCA3S.

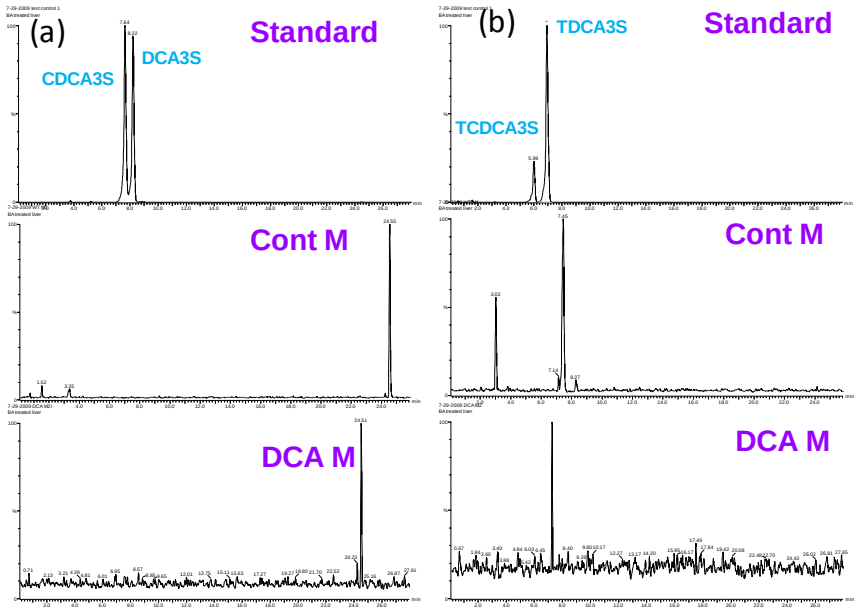

Figure 3-5. UPLC-MS/MS chromatograms of liver samples from control and DCA-fed male mice. (a) The standard peaks, which were CDCA3S and DCA3s, were not observed in liver samples from either control or DCA-fed mice. (b) The standard peaks for TCDCA3S and TDCA3S were not observed in liver samples from either control or DCA-fed mice.

CDCA can theoretically be sulfated at its 3-OH and 7-OH positions. One peak was found in the chromatograph window of TCDCA3S and TDCA3S. This peak increased markedly in livers of mice fed CDCA, whereas it was almost non-detectable in livers of mice fed DCA or UDCA. This suggests the peak is a sulfate of TCDCA. One peak in the chromatograph window of CDCA3S and DCA3S was found in livers of mice fed CDCA, but not other BAs (Figure 3-6). This suggests the peak is a sulfate of CDCA. In addition, these two peaks have different retention times than TCDCA3S and CDCA3S. Because CDCA can only be sulfated at either the 3-OH or 7-OH position, these two peaks are TCDCA7S and CDCA7S, respectively. Overall, CDCA is sulfated at the 7-OH in livers of mice.

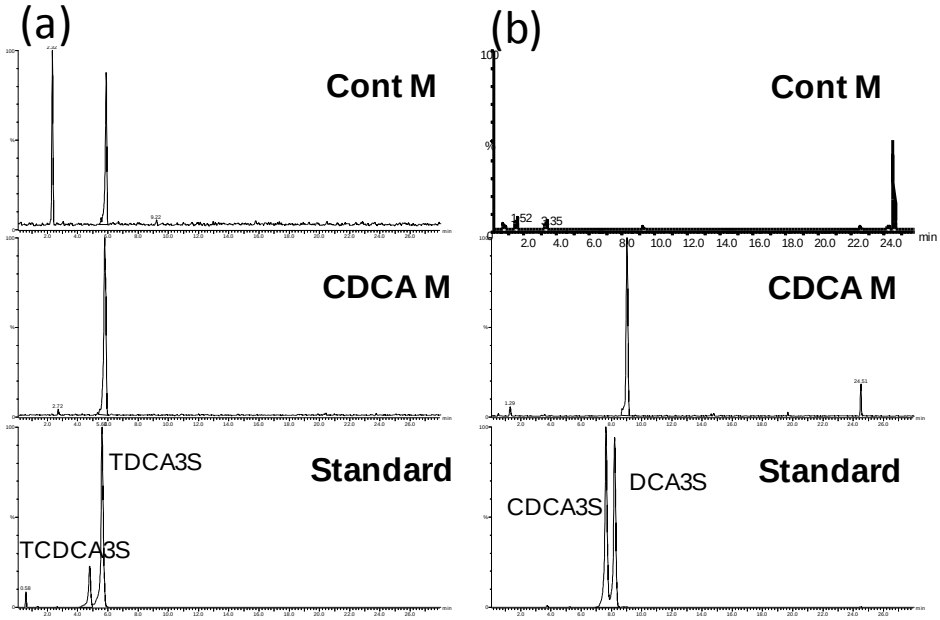

Figure 3-6. UPLC-MS/MS chromatograms of liver samples from control and CDCA-fed male mice. (a) The peak from livers of CDCA-fed mice was larger than that from control mice, and eluted at a different time than TCDCA3S and TDCA3S standards. (b) The peaks from livers of CDCA-fed mice eluted at a different time than CDCA3S and DCA3S standards.

LCA sulfates could not be detected in livers of either male or female control livers, indicating LCA sulfation is not a major pathway for LCA metabolism in normal mouse livers. Feeding LCA

increased TLCAS, but not LCAS in female mouse livers. In contrast, neither TLCAS or LCAS was observed in livers of male mice after feeding LCA. This suggests that sulfation is female predominant, and more favorable toward TLCA than LCA in mouse livers. Because feeding a high dose of UDCA (3%) dramatically increased both TLCA and LCA in mouse liver, both TLCAS and LCAS were increased in livers of female mice (Figure 3-7). The possible enzyme responsible for LCA sulfation is Sult2a1, which is predominantly expressed in livers of female mice (Alnouti and Klaassen, 2006). Taken together, LCA sulfation is female predominant in livers of mice, and can be manifested by feeding LCA and its precursor UDCA to mice.

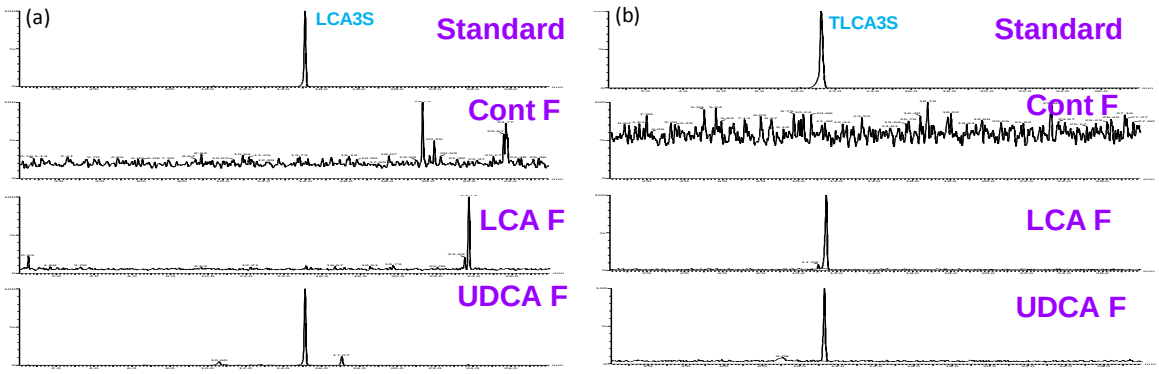

Figure 3-7. UPLC-MS/MS chromatograms of liver samples from control, LCA-, and UDCA-fed female mice. (a) The peak from livers of UDCA-fed mice was eluted at the same time as LCAS, whereas no peaks were detected in livers of control and LCA-fed mice. (b) The peaks from livers of LCA- and UDCA-fed mice eluted at the same time as TLCAS.

2.4. BA Concentrations in Livers of Mice Fed 2% Resin.

To determine the effect of resin on liver BA concentrations, both male and female C57BL/6 mice were fed a diet supplemented with 2% resin for 7 days. Tauro-conjugated BA concentrations were similar in livers of male and female control mice (Figure 3-8a). Feeding the resin decreased TωMCA (M 98%; F 95%), TβMCA (M 96%; F 91%), THCA (M 92%; F 68%), TUDCA (M 86%; F 77%), and THDCA (M 94%; F 76%) in both male and female mice. Feeding the resin decreased TαMCA in male (65%), but not significantly in female mice. In contrast, feeding the resin increased TCDCA (150%) and TLCA (504%) in female, but not significantly in male mice. Feeding the resin did not affect TDCA, but tended to decrease TCA in both male and female mouse livers. In general, feeding the resin had little effect on liver glycine-conjugated BAs, except that it decreased GDCA about 60% in male mice. In mice fed the control-chow diet, unconjugated BAs, such as ωMCA (40%), αMCA (52%), CDCA (56%), and LCA (37%) were lower in female than male mouse livers (Figure 3-8b). Feeding the resin decreased ωMCA (M 98%; F 96%), βMCA (M 96%; F 93%), and HDCA (M 92%; F 75%) in both male and female mice. Moreover, feeding the resin decreased αMCA (63%) and UDCA (82%) in male, whereas it decreased CA (55%) in female mouse livers. In contrast, CDCA (136%) and LCA (405%) were increased in female, but not in male mouse livers. Oxo-BAs, such as 7-oxoDCA (300%), 7-oxoLCA (490%), and 12-oxoLCA (340%), were higher in livers of male than female control mice (Figure 3-8b). Feeding the resin decreased 7-oxoDCA (M 77%; F 78%) and 12-oxoCDCA (M 96%; F 95%). Moreover, feeding the resin decreased 6-oxoLCA in male (82%), but not significantly in female mice.

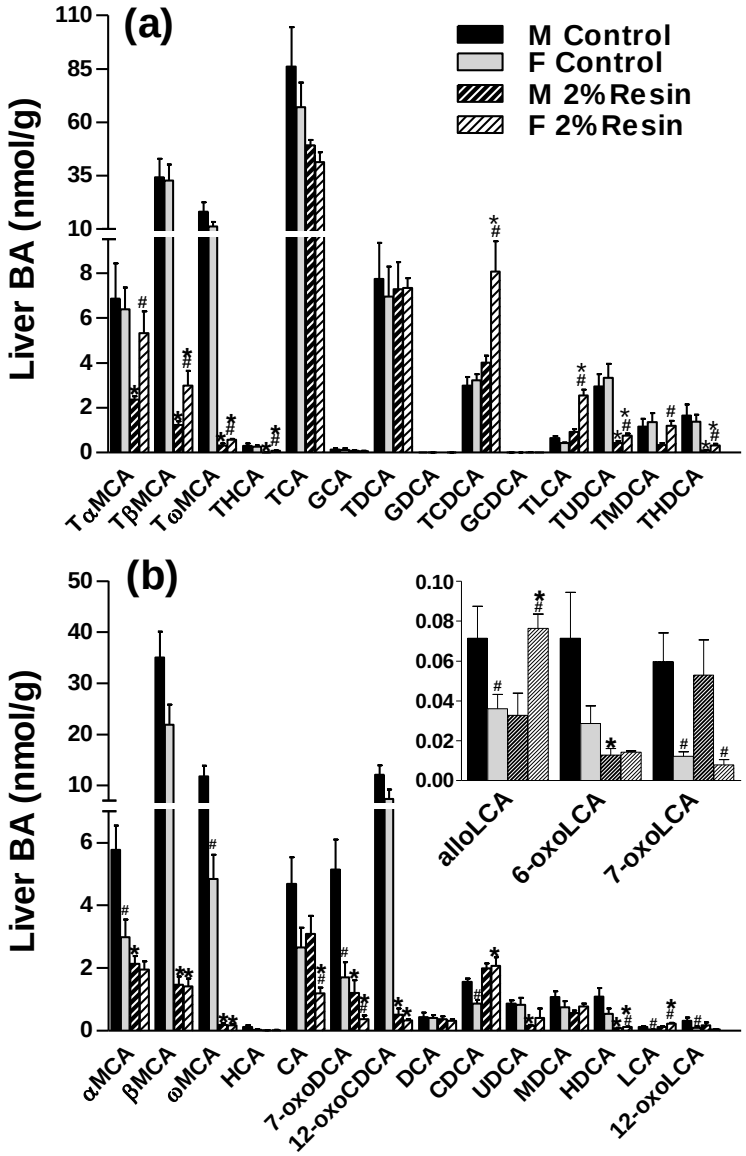

Figure 3-8. Conjugated (a) and unconjugated (b) BA concentrations in livers of mice fed 2% resin for 7 days. All BA data are expressed as mean ± S.E. of five mice in each group. *, statistically significant difference between the same gender of control and resin-fed groups ($p<0.05$). #, statistically significant difference between male and female mouse livers in the same group ($p<0.05$).

2.5. BA Concentrations in Livers of Mice Fed 1% CA.

In the present study, mice were fed a diet supplemented with 1% CA for 7 days to investigate the effect of CA on liver BA concentrations. As shown in figure 3-9a, feeding CA decreased TωMCA (M 97%; F 96%), TαMCA (M 70%; F 67%), TβMCA (M 92%; F 92%), THCA (M 76%; F 79%), TUDCA (M 70%; F 77%), THDCA (M 91%; F 84%), TCDCA (M 47%; F 55%), and TLCA (M 63%; F 46%). Feeding CA decreased TMDCA in male (82%), but not significantly in female mice. In contrast, feeding CA increased TCA (M 247%; F 227%) and TDCA (M 397%; F 426%). Regarding liver glycine-conjugated BAs, feeding CA increased GCA (M 233%; F 191%) and GDCA (M 371%; F 420%). As shown in figure 3-9b, feeding CA decreased ωMCA (M 97%; F 98%), αMCA (M 84%; F 91%), βMCA (M 94%; F 96%), MDCA (M 80%; F 85%), UDCA (M 67%; F 88%), HDCA (M 93%; F 98%), and CDCA (M 67%; F 82%). Feeding CA decreased alloLCA (53%) and LCA (54%) in male, but not significantly in female mouse livers. In contrast, feeding CA increased CA (300%) in male, but not significantly in female mice. IsoDCA and DCA were increased by feeding CA to male (1830% and 1080%, respectively) more than to female mice (460% and 340%, respectively). Furthermore, feeding CA decreased 7-oxoDCA (M 76%; F 93%) and 12-oxoCDCA (M 92%; F 96%) in mouse livers. In contrast, feeding CA markedly increased 12-oxoLCA in male (278%), but not significantly in female mice.

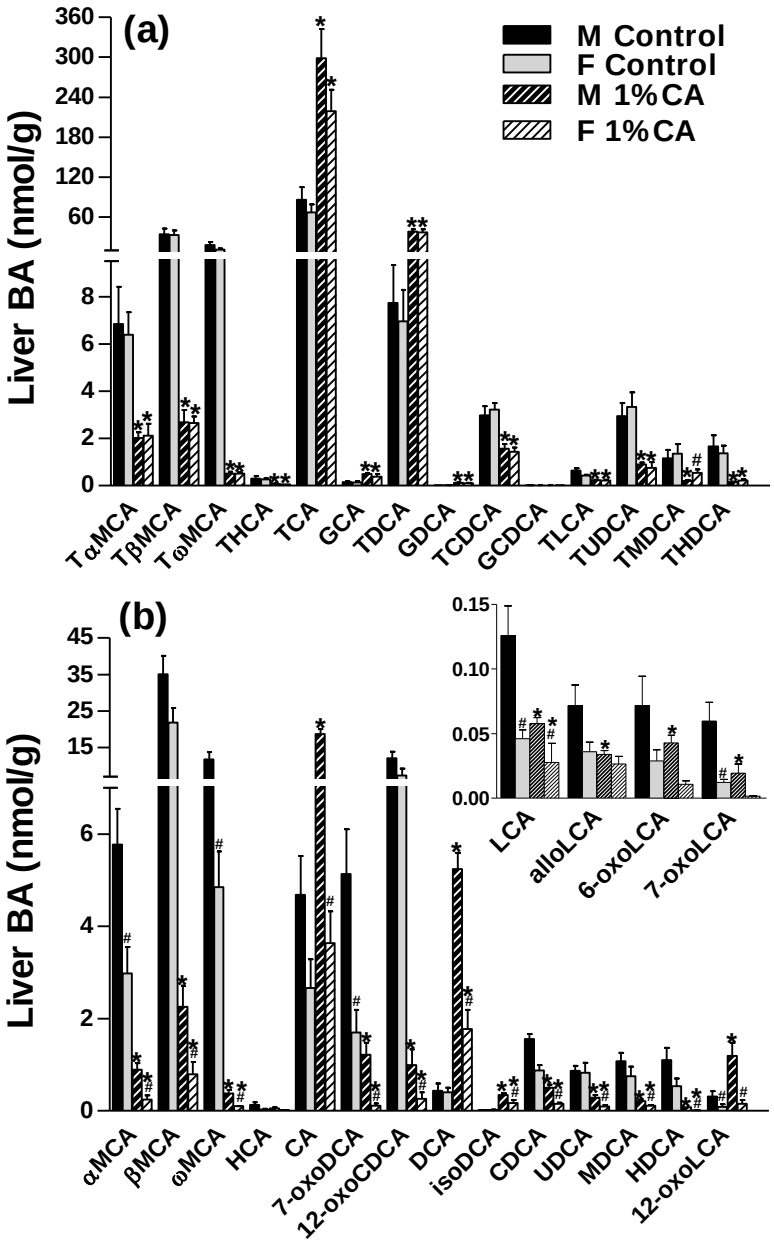

Figure 3-9. Conjugated (a) and unconjugated (b) BA concentrations in livers of mice fed 1% CA for 7 days. All BA data are expressed as mean ± S.E. of five mice in each group. *, statistically significant difference between the same gender of control and resin-fed groups ($p<0.05$). #, statistically significant difference between male and female mouse livers in the same group ($p<0.05$).

2.6. BA Concentrations in Livers of Mice Fed 0.3% DCA.

DCA is formed from CA by bacterial enzymes in the intestine, and is one of the major secondary BAs in mice. To investigate the effect of DCA on mouse liver BA concentrations, both male and female mice were fed a diet supplemented with 0.3% DCA for 7 days. As shown in figure 3-10a**,** feeding DCA decreased TωMCA (M 94%; F 86%), TαMCA (M 60%; F 69%), TβMCA (M 885; F 84%), THCA (M 89%; F 71%), TUDCA (M 79%; F 73%), TCDCA (M 54%; F 59%), and TLCA (M 60%; F 38%). Feeding DCA decreased TMDCA (69%) and THDCA (73%) in female, but not significantly in male mice. Feeding DCA increased TDCA more in livers of male (639%) than female mice (356%). Similarly, feeding DCA increased GDCA more in male (520%) than in female (240%) mouse livers (Fig 9c). As shown in figure 3-10b, feeding DCA decreased ωMCA (M 96%; F 89%), αMCA (M 91%; F 87%), βMCA (M 94%; F 88%), MDCA (M 76%; F 74%), HDCA (M 86%; F 75%), and CDCA (M 85%; F 76%). Feeding DCA decreased UDCA and LCA in male (89% and 80%, respectively), but not significantly in female mice. In contrast, feeding DCA increased DCA and isoDCA more in male (1050% and 2530%, respectively) than in female mice (219% and 272%, respectively). Feeding DCA decreased oxo-BAs, such as 7-oxoDCA (M 80%; F 76%) and 12-oxoCDCA (M 91%; F 90%). Moreover, feeding DCA decreased 6-oxoLCA (76%) and 7-oxoLCA (86%) in male, but not significantly in female mice. In contrast, feeding DCA increased 12-oxoLCA in male (202%), but not significantly in female mice.

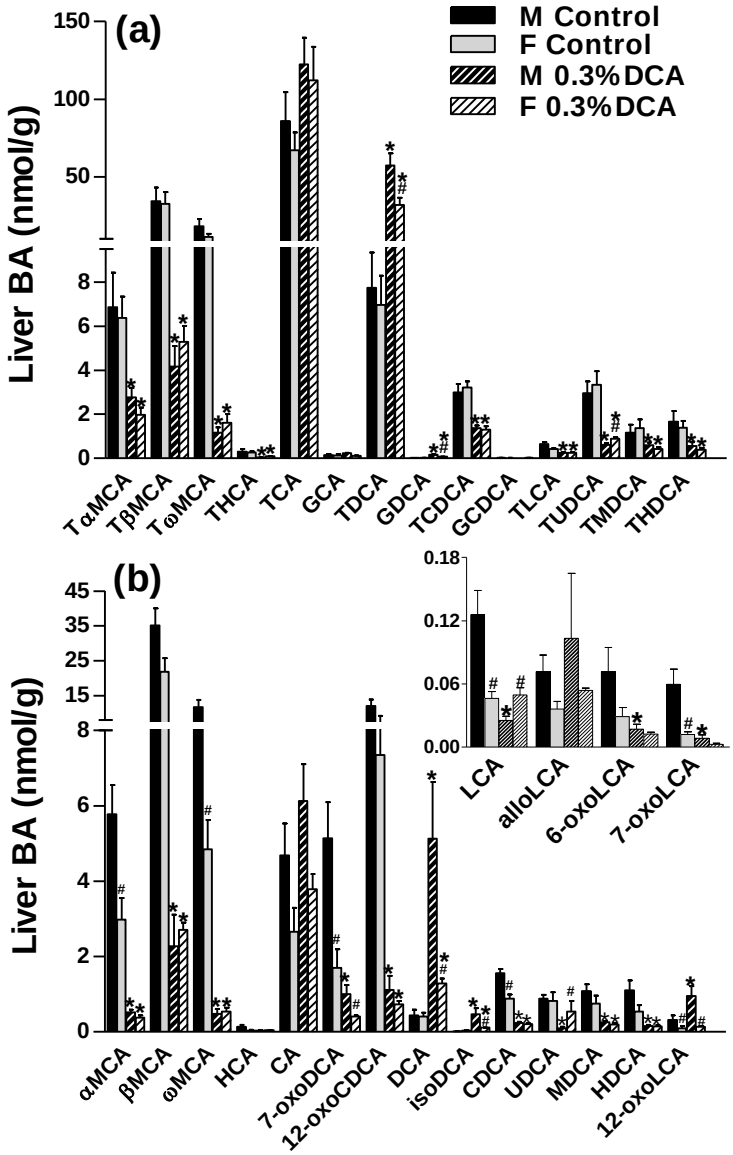

Figure 3-10. Conjugated (a) and unconjugated (b) BA concentrations in livers of mice fed 0.3 % DCA for 7 days. All BA data are expressed as mean ± S.E. of five mice in each group. *, statistically significant difference between the same gender of control and resin-fed groups ($p<0.05$). #, statistically significant difference between male and female mouse livers in the same group ($p<0.05$).

2.7. BA Concentrations in Livers of Mice Fed 0.3% CDCA.

To determine the effect of CDCA on liver BA metabolism, both male and female mice were fed a diet supplemented with 0.3% CDCA for 7days. As shown in figure 3-11a, feeding CDCA decreased TωMCA (M 83%; F 68%), TCA (M 93%; F 90%), and TDCA (M 73%; F 74%). Feeding CDCA decreased TβMCA in male (64%), but not significantly in female mice. In contrast, feeding CDCA increased TαMCA (M 363%; F 399%), THCA (M 650%; F 584%), TMDCA (M 249%; F 266%), TUDCA (M 318%; F 287%), TCDCA (M 1340%; F 954%), and TLCA (M 859%; F 960%). Regarding liver glycine-conjugated BAs (Fig 10c), feeding CDCA decreased GCA (M 92%; F 90%), whereas it increased GCDCA (M 935%; F 1170%). As shown in figure 3-11b, feeding CDCA decreased ωMCA (M 80%; F 64%) and CA (M 94%; F 94%) in mouse livers. Feeding CDCA also decreased βMCA in livers of male (63%), but not significantly in female mice. In contrast, feeding CDCA decreased DCA in livers of female (73%), but not significantly in male mice. Feeding CDCA increased αMCA (M 429%; F 528%), HCA (M 696%; F 762%), MDCA (M 286%; F 333%), UDCA (M 663%; F 476%), CDCA (M 2210%; F 1500%), isoLCA (M 431%; F 849%), and LCA (M 742%; F 670%). Feeding CDCA increased CDCA and LCA more in livers of male than female mice. In contrast, feeding CDCA increased HDCA in livers of female (107%), but not significantly in male mice. Feeding CDCA also increased oxo-BAs, such as 7-oxoDCA (M 82%; F 115%), 6-oxoLCA (M 138%; F 152%), and 7-oxoLCA (M 2030%; F 1960%). However, feeding CDCA markedly decreased 12-oxoCDCA (M 48%; F 56%) and 12-oxoLCA (M 81%; F 84%).

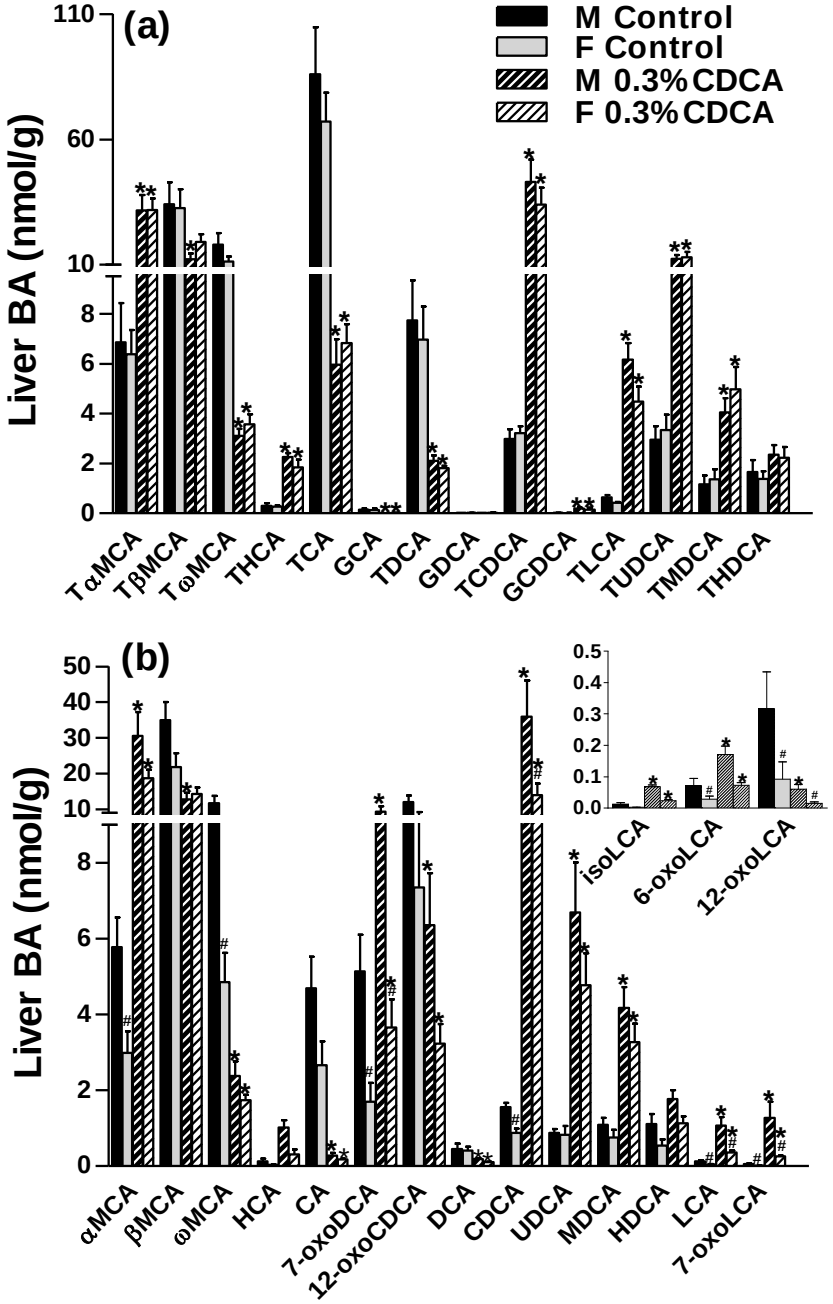

Figure 3-11. Conjugated (a) and unconjugated (b) BA concentrations in livers of mice fed 0.3 % CDCA for 7 days. All BA data are expressed as mean ± S.E. of five mice in each group. *, statistically significant difference between the same gender of control and resin-fed groups ($p<0.05$). #, statistically significant difference between male and female mouse livers in the same group ($p<0.05$).

2.8. BA Concentrations in Livers of Mice Fed 0.3% LCA.

LCA is formed by 7-dehydroxylation of CDCA via intestinal bacteria. In the present study, both male and female mice were fed a 0.3% LCA-supplemented diet for 7 days. As shown in figure 3-12a, feeding LCA increased TαMCA (M 191%; F 187%), THCA (M 168%; F 251%), TMDCA (M 3240%; F 1160%), THDCA (M 539%; F 411%), TCDCA (M 659%; F 394%), and TLCA (M 3780%; F 2160%). Feeding LCA increased TUDCA in male (88%), but not significantly in female mice. In contrast, feeding LCA decreased TCA in male (66%), but not significantly in female mice. Regarding liver glycine-conjugated BAs, feeding LCA tended to, but not significantly, decrease GCA and increase GCDCA in mouse livers. Feeding LCA decreased GDCA in male (60%), but not in female mice. As shown in figure 3-12b, feeding LCA decreased ωMCA (M 83%; F 64%), βMCA (M 78%; F 68%), and CA (M 83%; F 72%) in livers of mice. In contrast, feeding LCA increased MDCA (M 1980%; F 1670%), HDCA (M 447%; F 668%), CDCA (M 327%; F 668%), isoLCA (M 1700%; F 17000%), and LCA (M 2390%; F 5640%) in mouse livers. Feeding LCA decreased 7-oxoDCA (M 65%; F 62%) and 12-oxoCDCA (M 70%; F 61%), but increased 6-oxoLCA (M 858%; F 751%) and 7-oxoLCA (M 205%; F 244%) in mouse livers. DehydroLCA, which was not detected in control mouse livers, was increased markedly by feeding LCA to female mice more than to male mice.

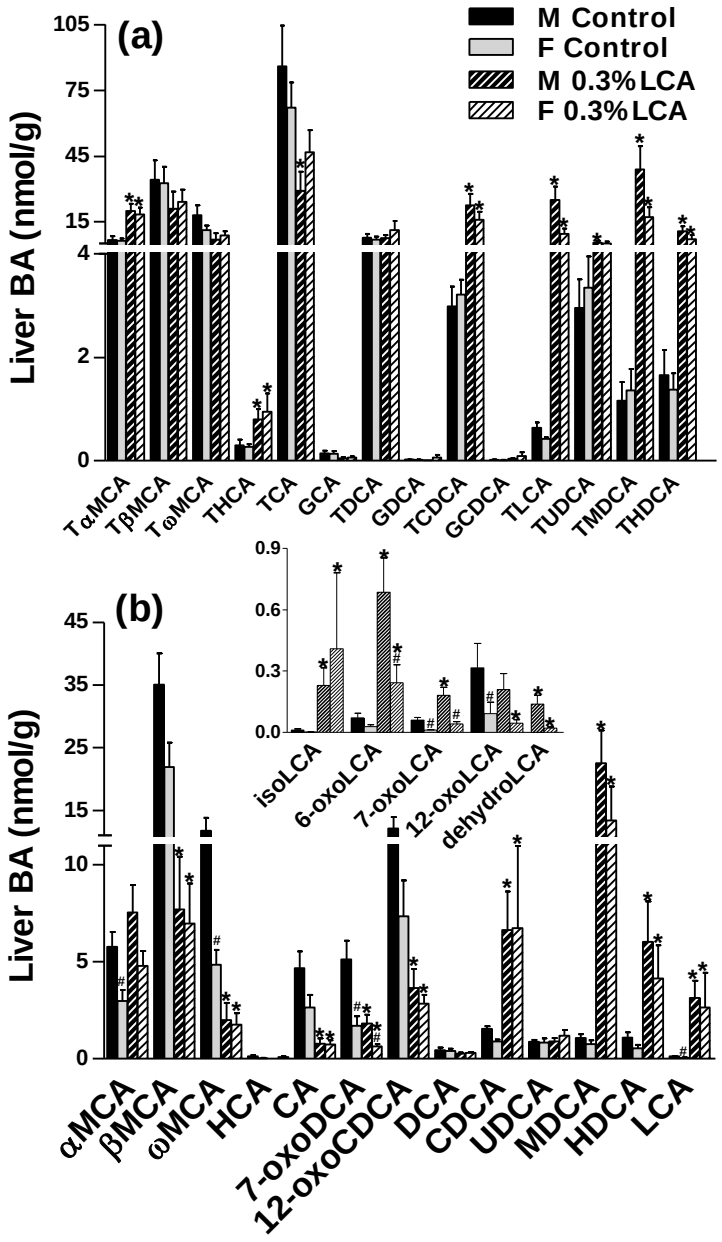

Figure 3-12. Conjugated (a) and unconjugated (b) BA concentrations in livers of mice fed 0.3 % LCA for 7 days. All BA data are expressed as mean ± S.E. of five mice in each group. *, statistically significant difference between the same gender of control and resin-fed groups ($p<0.05$). #, statistically significant difference between male and female mouse livers in the same group ($p<0.05$).

2.9. BA Concentrations in Livers of Mice Fed 3% UDCA.

UDCA is prescribed for patients with various liver diseases. In the present study, both male and female mice were fed a 3% UDCA-supplemented diet for 7 days to investigate the effect of UDCA on liver BA metabolism. Figure 3-13a shows the liver concentrations of taurine-conjugated BAs. THDCA peaks in the chromatogram were very small in livers of mice fed UDCA and could not be separated from the large TUDCA peaks (data not shown). Therefore, THDCA was not considered in the present study. Feeding UDCA decreased TωMCA (M 97%; F 96%), TαMCA (M 63%; F 73%), TβMCA (M 82%; F 79%), THCA (M 80%; F 86%), TCA (M 98%; F 98%), and TDCA (M 88%; F 99%) in mouse livers. In contrast, feeding UDCA increased TMDCA (M 500%; F 409%), TUDCA (M 6750%; F 6570%), TCDCA (M 163%; F 107%), and TLCA (M 1620%; F: 3790%) in mouse livers. Regarding liver glycine-conjugated BAs, feeding UDCA decreased GCA (M 88%; F 86%), but increased GCDCA (M 1430%; F 1300%). GUDCA and GLCA were not detected in control mouse livers, whereas they were increased markedly by feeding UDCA. As shown in figure 3-13b, feeding UDCA increased ωMCA, αMCA, βMCA and HCA in livers of female mice (1870%, 221%, 201%, and 359%, respectively), but not significantly in male mouse livers. Feeding mice UDCA decreased CA (M 81%; F 74%), but increased MDCA (M 2910%; F 3010%), UDCA (M 99,800%; F 125,000%), CDCA (M 1160%; F 1400%), isoLCA (M 19,200%; F 54,900%), and LCA (M 37,600%; F: 94,400%) in livers. Feeding UDCA decreased 7-oxoDCA (M 91%; F 91%) and 12-oxoCDCA (M 89%; F 89%), whereas it increased 7-oxoLCA (M 3980%; F 5010%) in mouse livers. In addition, feeding UDCA markedly increased dehydroLCA, which was not detected in control mouse livers.

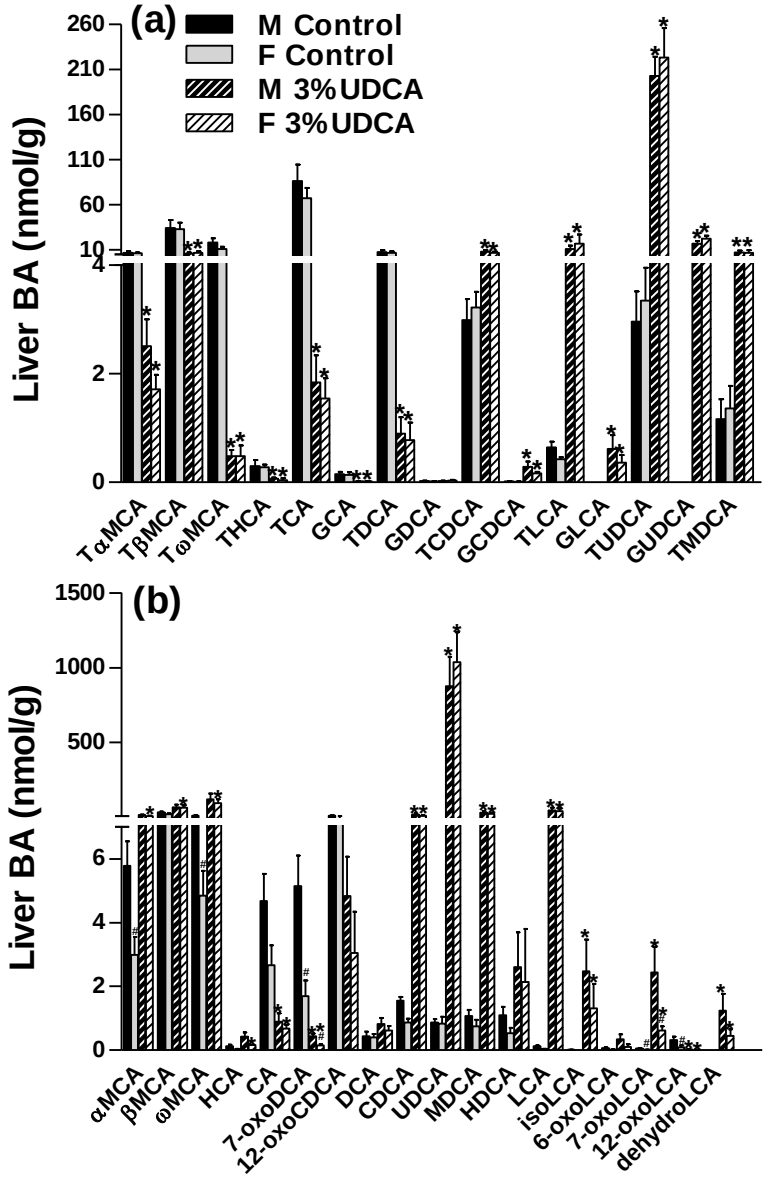

Figure 3-13. Conjugated (a) and unconjugated (b) BA concentrations in livers of mice fed 3 % UDCA for 7 days. All BA data are expressed as mean ± S.E. of five mice in each group. *, statistically significant difference between the same gender of control and resin-fed groups ($p<0.05$). #, statistically significant difference between male and female mouse livers in the same group ($p<0.05$).

2.10. Conjugated, Unconjugated, and Total BAs in Livers of Mice.

To determine the effect of various BAs on liver BA homeostasis, the total conjugated, total unconjugated, and total BAs in livers of mice fed various BA-supplemented diets were calculated (Figure 3-14). Feeding CA increased conjugated BAs (M 112%; F 99%), whereas it decreased unconjugated BAs (M 54%; F 80%) in mouse livers. As a result, total BAs in mouse livers tended to, but not significantly, increase by feeding CA. Feeding DCA did not increase conjugated BAs, whereas it markedly decreased unconjugated BAs (M 75%; F 72%). Overall, the total BAs in liver were not altered by feeding DCA. Feeding CDCA and LCA did not alter conjugated BAs, unconjugated BAs, or total BAs in either male or female mouse livers. In contrast, feeding UDCA increased both conjugated BAs (M 66%; F 127%) and unconjugated BAs (M 1790%; F 3490%) in mouse livers. As a result, the total BAs (M 505%; F 790%) were increased markedly by feeding UDCA. Feeding the resin decreased both conjugated (M 59%; F 47%) and unconjugated BAs (M 84%; F 75%) in mouse livers. As a result, feeding the resin decreased total BAs in both male (68%) and female (55%) livers.

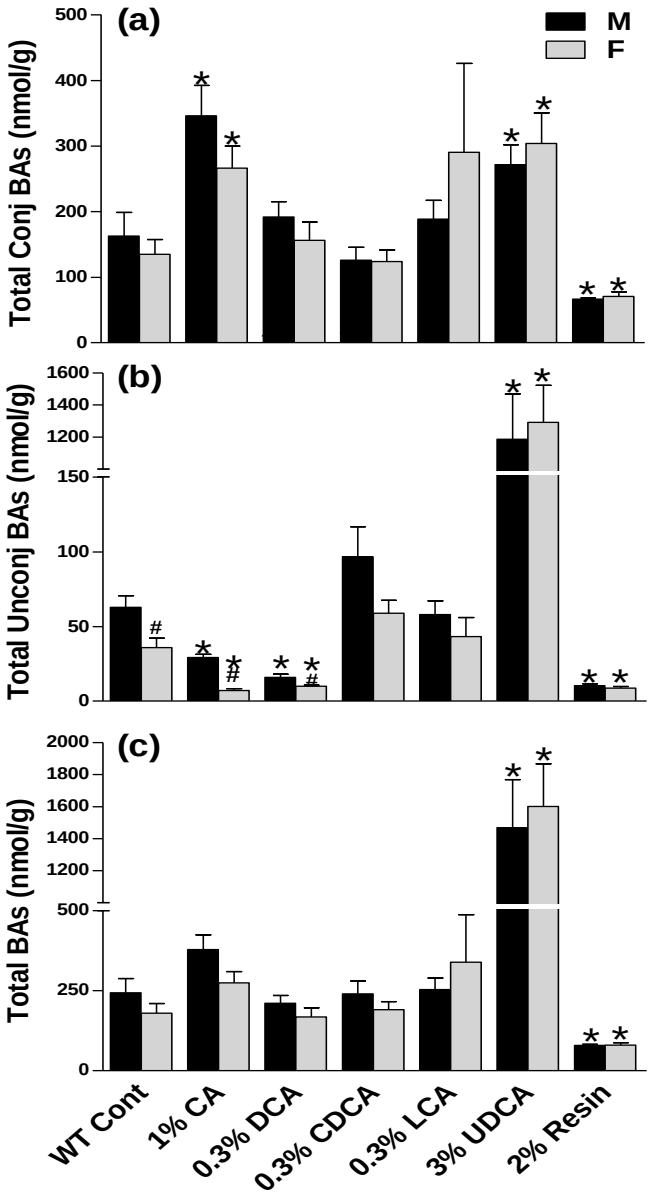

Figure 3-14. Conjugated BAs, unconjugated BAs, and total BAs in livers of mice fed BAs and resin. All BA data are expressed as mean ± S.E. of five mice in each group. *, statistically significant difference between the same gender of control and BA-fed groups ($p<0.05$). #, statistically significant difference between male and female mouse livers in the same group ($p<0.05$).

2.11. BA Sulfates in Livers of Mice.

In the present study, due to the lack of pure standards, the peak areas of BA sulfates were normalized with those of internal standards to quantify their concentrations in livers of mice fed various BA-supplemented diets. As shown in figure 3-15a, TCA7S was higher in control male than control female mouse livers. Feeding the resin increased TCA7S (M 69%; F 47%), whereas feeding CDCA decreased TCA7S (M 95%; F 96%). Feeding CA increased TCA7S about 92% in livers of male mice, but not significantly in females. In contrast, feeding LCA suppressed TCA7S in livers of female (58%), but not significantly in male mice. Interestingly, TCA7S could not be detected in livers of mice fed UDCA. Similar to TCA7S, CA7S was also higher in control male than control female mouse livers (Figure 3-15b). Feeding CA increased CA7S about 234% in male, but not significantly in female mouse livers. In contrast, feeding CDCA and UDCA markedly suppressed CA7S in mouse livers. TCDCA7S was also higher in control male than control female mouse livers (Figure 3-15c). Feeding the resin markedly increased TCDCA7S (M 90%; F 358%). Feeding either CA or DCA suppressed TCDCA7S in male, but not in female mouse livers. In contrast, feeding CDCA (M 1650%; F 1030%) and LCA (M 760%; F 578%) markedly increased TCDCA7S in mouse livers. Similar to TCA7S and CA7S, TCDCA7S was almost non-detectable in livers of mice fed UDCA.

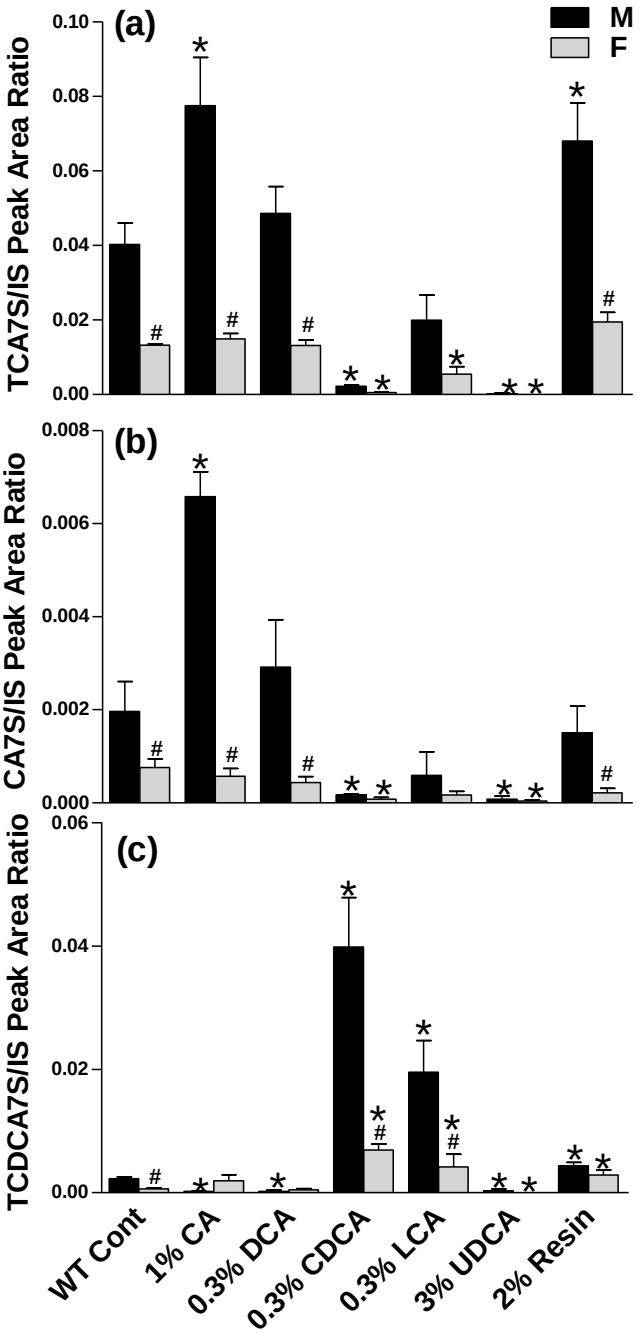

Figure 3-15. TCA7S (a), CA7S (b), and TCDCA7S (c) in livers of mice fed BAs and resin. The peak areas of TCA7S, TCDCA7S and CA7S were normalized to that of GCDCA-d_4. The data are expressed as the mean ± S.E of five mice in each group. *, statistically significant difference between the same gender of control and BA-fed groups ($p<0.05$). #, statistically significant difference between male and female mouse livers in the same group ($p<0.05$).

2.12. BA-synthetic Genes in Livers of Mice.

To investigate the effects of various BAs on liver BA synthesis, mRNA levels of BA synthetic enzymes, such as Cyp7a1, 8b1, 27a1, and 7b1 were quantified. Cyp7a1, which is the rate-limiting enzyme in the classic pathway of BA synthesis, tended to be higher in control male than control female mouse livers (Figure 3-16). The mRNA expression of Cyp7a1 was increased by feeding the resin (M 197%; F 1650%), whereas it was decreased by feeding CA (M 92%; F 85%), CDCA (M 95%; F 83%), DCA (M 92%; F 64%), and UDCA (M 99%; F 99%). Cyp8b1, which is an essential enzyme for CA formation, was higher in control male than control female mouse livers. Such a gender difference was not observed in livers of mice fed CA, DCA, LCA, or the resin. Cyp8b1 mRNA was increased by feeding the resin (M 92%; F 177%), whereas it was decreased by feeding CA (M 99%; F 99%), CDCA (M 50%; F 77%), DCA (M 98%; F 98%), and UDCA (M 99%; F 94%). Cyp8b1 mRNA was higher in livers of male than female mice fed CDCA, whereas it was higher in livers of female than male mice fed UDCA. In addition, feeding LCA decreased Cyp8b1 mRNA in male (44%), but not female mice. Cyp27a1 mRNA was increased by feeding the resin to female (27%), but not to male mice. In contrast, Cyp27a1 mRNA was decreased by feeding CA (M 27%; F 23%) and UDCA (M 54%; F 63%). Moreover, Cyp27a1 mRNA was decreased by feeding CDCA (22%) and DCA (27%) in male, but not female mice. Control male mice have much higher Cyp7b1 than females. Feeding the resin, DCA, CDCA, or LCA did not affect Cyp7b1 mRNA, whereas feeding CA decreased Cyp7b1 mRNA in male (38%), but not female mice. Feeding UDCA markedly decreased Cyp7b1 mRNA (M 85%; F 64%) in both male and female mouse livers.

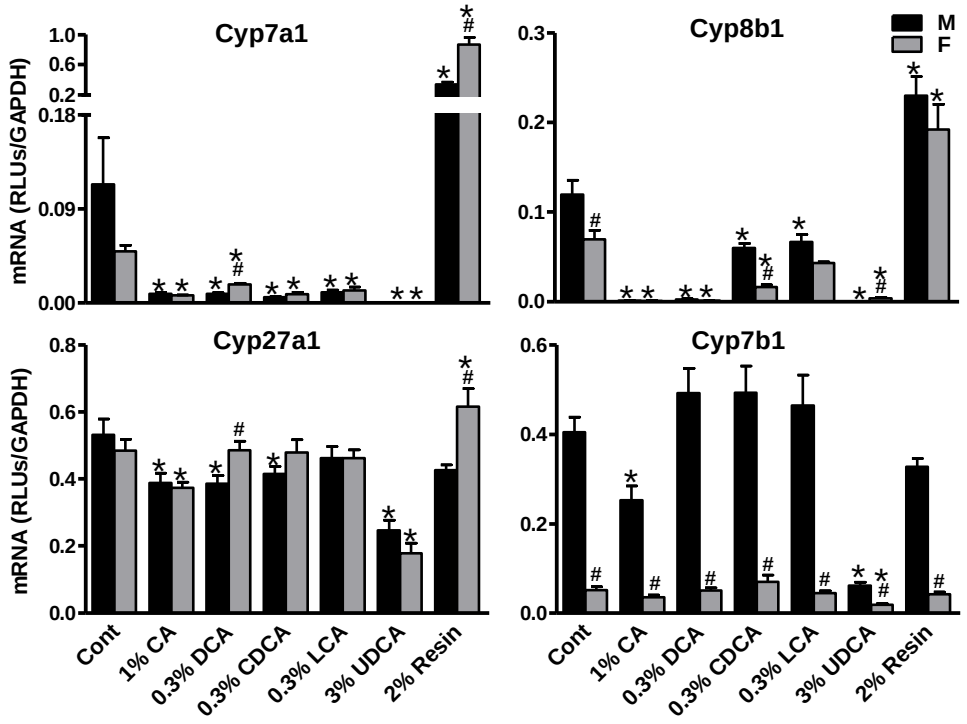

Figure 3-16. The mRNA levels of BA synthetic genes in livers of mice fed BAs and resin. Total RNA from livers of control and BA-fed mice (n=5/gender/group) were analyzed by mutiplex suspension array. The mRNA level of each gene was normalized to GAPDH. All data are expressed as mean ± S.E. of five mice in each group. *, statistically significant difference between the same gender of control and BA-fed groups ($p<0.05$). #, statistically significant difference between male and female mouse livers in the same group ($p<0.05$).

2.13. BA-uptake Transporters in Livers of Mice.

To investigate the effects of various BAs on hepatic uptake of BAs, mRNA levels of BA-uptake transporters, such as Ntcp, Oatp1a1, Oatp1a4, and Oatp1b2 were quantified (Figure 3-17). Feeding CA (M 35%; F 30%), CDCA (M 14%; F 13%), DCA (M 40%; F 20%), and UDCA (M 41%; F 45%) decreased Ntcp mRNA in livers of both male and female mice. Feeding the resin decreased Ntcp mRNA in male (21%) but not female mice. As a result, the gender difference of Ntcp, which is higher in female

than male mice, was maintained in mice fed CDCA, DCA, and resin, but not in mice fed CA and UDCA. Interestingly, feeding LCA had no effect on Ntcp mRNA in either male or female mice. Feeding CA decreased Oatp1a1 mRNA in male (50%) but not female mice, whereas feeding DCA increased Oatp1a1 mRNA in female (170%) but not male mice. Feeding CDCA and LCA had no effect on Oatp1a1 mRNA, whereas feeding UDCA and resin decreased Oatp1a1 mRNA in both male and female mice. As a result, the male-predominant expression of Oatp1a1 in control mice was maintained in mice fed CA, CDCA, LCA, and resin, but disappeared in mice fed DCA and UDCA. Feeding CA increased Oatp1a4 mRNA in female (55%) but not male mice, whereas feeding UDCA increased Oatp1a4 mRNA in male (290%) but not female mice. As a result, no gender difference of Oatp1a4 mRNA, which is female-predominant in control mice, was observed in mice fed UDCA. Interestingly, feeding CDCA, DCA, LCA and resin had little effect on the mRNA of Oatp1a4. Oatp1b2 mRNA was decreased by feeding CA (25%), CDCA (16%), and resin (24%) in male but not female mice. Feeding UDCA decreased Oatp1b2 mRNA in both male (49%) and female (45%) mice, whereas feeding DCA and LCA had no effect on Oatp1b2 mRNA. Taken together, feeding CA, UDCA, and resin had more prominent effects on BA-uptake transporters in livers, when compared with feeding CDCA, DCA, and LCA to mice.

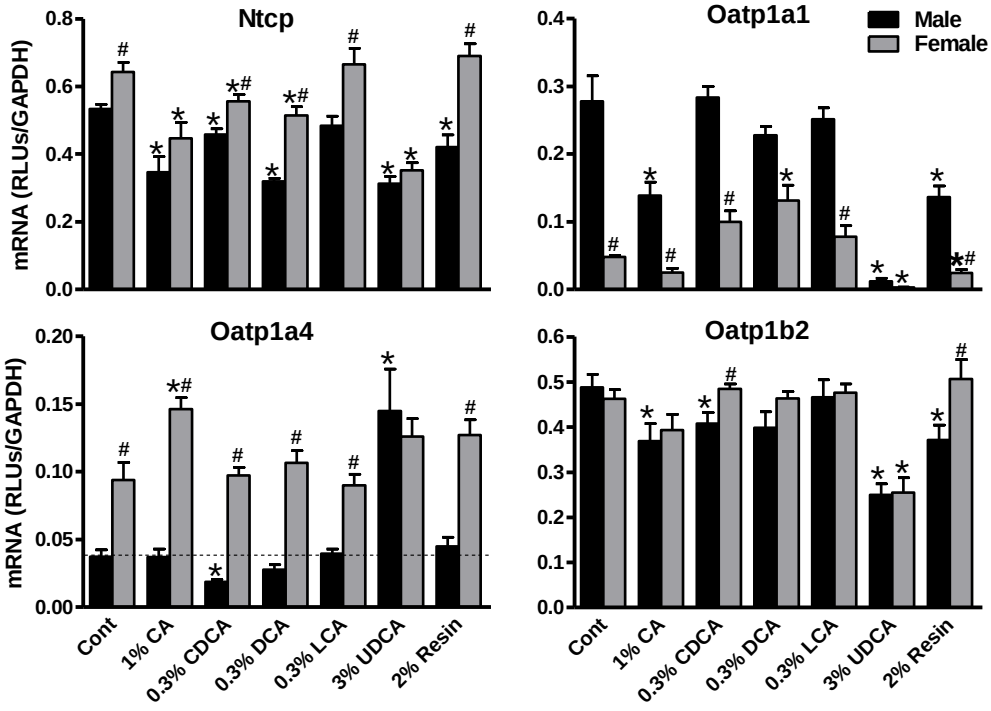

Figure 3-17. The mRNA levels of BA-uptake transporters in livers of mice fed BAs and resin. Total RNA from livers of control and BA-fed mice (n=5/gender/group) were analyzed by mutiplex suspension array. The mRNA level of each gene was normalized to GAPDH. All data are expressed as mean ± S.E. of five mice in each group. *, statistically significant difference between the same gender of control and BA-fed groups ($p<0.05$). #, statistically significant difference between male and female mouse livers in the same group ($p<0.05$).

2.14. BA-efflux Transporters in Livers of Mice.

To investigate the effects of various BAs on hepatic efflux of BAs, mRNA levels of basolateral BA-efflux transporters (Mrp3 and Mrp4) and canalicular BA-efflux transporters (Bsep and Mrp2) were quantified (Figure 3-18). Feeding BAs had little effect on Mrp3 mRNA, except that feeding UDCA slightly decreased Mrp3 mRNA in female (35%) but not male mice. In contrast, feeding resin decreased Mrp3 mRNA in both male (40%) and female (45%) mice. Feeding CA (30%) and DCA (70%) increased Mrp4 mRNA in female but not male mice, whereas feeding UDCA increased Mrp4 about 270% in both

male and female mice. In contrast, feeding CDCA, LCA, and resin had little effect on Mrp4 mRNA. Feeding CA (40%) and DCA (46%) increased Bsep mRNA in both male and female mice, whereas feeding UDCA (40%) and resin (35%) decreased Bsep mRNA in both male and female mice. In contrast, feeding CDCA and LCA had little effect on Bsep mRNA. Feeding BAs and BA-binding resin had little effect on Mrp2 mRNA, except that feeding CA increased Mrp2 mRNA about 24% in female mice and feeding the resin decreased Mrp2 mRNA about 30% in male mice. Taken together, during BA and resin feedings, Bsep was more ready to be regulated than other BA efflux transporters, such as Mrp2, Mrp3, and Mrp4.

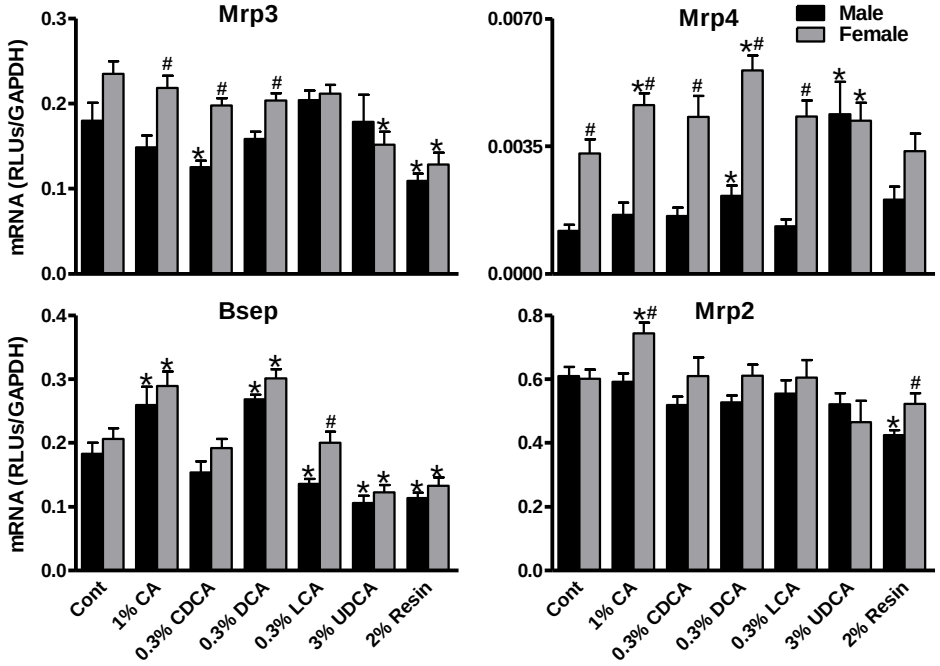

Figure 3-18. The mRNA levels of BA-efflux transporters in livers of mice fed BAs and resin. Total RNA from livers of control and BA-fed mice (n=5/gender/group) were analyzed by mutiplex suspension array. The mRNA level of each gene was normalized to GAPDH. All data are expressed as mean ± S.E. of five mice in each group. *, statistically significant difference between the same gender of control and BA-fed groups ($p<0.05$). #, statistically significant difference between male and female mouse livers in the same group ($p<0.05$).

2.15. Liver Proliferation and Fibrosis.

To investigate the hepatotoxicity of BAs, the mRNA of several proliferation and fibrosis markers, such as Mki67, Pcna, c-Myc, Tgf-β, Col1a1, Acta2, CD1, Top2α, and Gadd45β, were quantified in livers of both male and female mice (Figure 3-19). Among them, Mki67, Pcna, and c-Myc are three proliferation markers. Feeding CA and DCA increased Mki67 mRNA in both male and female mice, whereas feeding LCA and UDCA increased Mki67 mRNA in male but not female mice. Interestingly, feeding the resin decreased Mki67 mRNA in female but not male mice. As a result, the gender-difference of Mki67, which was higher in female than male mice, was maintained in mice fed CA, CDA, DCA, and LCA, but not in mice fed UDCA and resin. Pcna mRNA expression was somewhat higher in female than male mice. Feeding CA, DCA, and UDCA increased Pcna mRNA in male mice more than in female mice, resulting in a similar expression of Pcna in male and female mice. In contrast, feeding CDCA, LCA, and resin had no effect on Pcna mRNA. Feeding CA, DCA, LCA and resin had little effect on c-Myc mRNA. Feeding CDCA increased c-Myc mRNA in male but not female mice, whereas feeding UDCA increased c-Myc mRNA in both male and female mice. As a result, c-Myc mRNA was higher in male than female mice fed CA and UDCA.

Tgf-β, Col1a1 and Acta2 are the markers for liver fibrosis. Feeding CA increased Tgf-β mRNA in male but not female mice, whereas feeding DCA increased Tgf-β mRNA in both male and female mice. In contrast, feeding CDCA, LCA, UDCA, and resin had little effect on Tgf-β mRNA. Feeding CA and DCA increased Col1a1 mRNA in both male and female mice, whereas feeding CDCA, LCA, UDCA, and resin had no effect on Col1a1 mRNA. Feeding BAs and resin had little effect on Acta2 mRNA, except that feeding UDCA increased Acta2 mRNA in male but not female mice.

CD1, Top2α, and Gadd45β are involved in the regulation of the cell cycle. The mRNA expression of CD1 was higher in female than male mice. Feeding CA and CDCA increased CD1 mRNA in both male and female mice, whereas feeding CDCA and LCA increased CD1 mRNA in female but not male mice. In contrast, feeding resin had no effect on CD1 mRNA. Similar as CD1, the mRNA

expression of Top2α was also higher in female than male mice. Feeding CA and DCA increased Top2α mRNA in both male and female mice. As a result, Top2α mRNA showed no gender difference in mice fed DCA. Feeding CDCA, LCA and UDCA had little effect on Top2α mRNA, whereas feeding resin decreased Top2α mRNA in female but not male mice. Feeding CA and DCA increased Gadd45β mRNA in female but not male mice, whereas feeding UDCA increased Gadd45β mRNA markedly in both male and female mice. In contrast, feeding CDCA, LCA, and resin had little effect on Gadd45β mRNA.

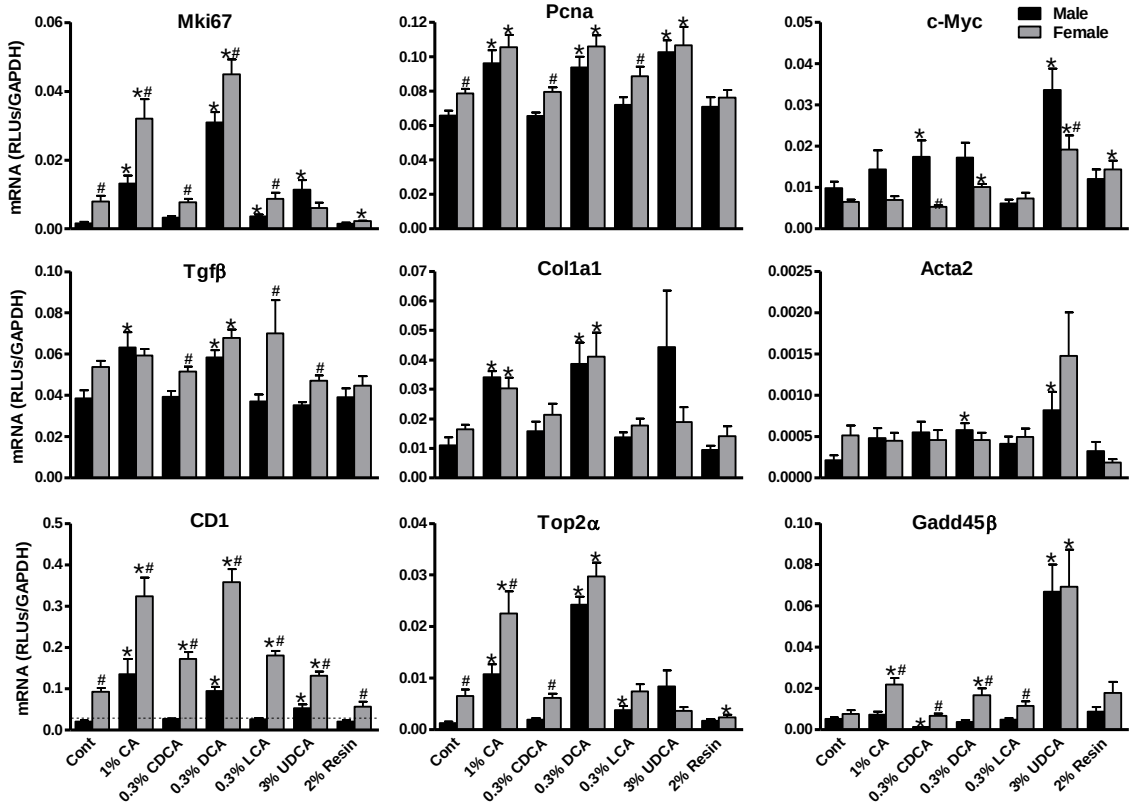

Figure 3-19. The mRNA levels of marker genes for liver proliferation (Mki67, Pcna, and c-Myc), liver fibrosis (Tgf-β, Col1a1, and Acta2), and cell cycle regulation (CD1, Top2α, and Gadd45β) in livers of mice fed BAs and resin. Total RNA from livers of control and BA-fed mice (n=5/gender/group) were analyzed by mutiplex suspension array. The mRNA level of each gene was normalized to GAPDH. All data are expressed as mean ± S.E. for five mice in each group. *, statistically significant difference between the same gender of control and BA-fed groups ($p<0.05$). #, statistically significant difference between male and female mouse livers in the same group ($p<0.05$).

III. Discussion

To understand the effects of BA feedings on hepatic gene regulation and hepatotoxicity, it is important to know the changes of liver BA concentrations and composition after BA feeding. The data from the present study shows that mouse liver has a remarkable ability to maintain total BA concentrations during BA feedings. The liver BA concentration is determined by rates of BA hepatic uptake and canalicular secretion, BA biosynthesis, and BA biotransformation. The purpose of the present study was to investigate BA biotransformation in mice fed various BAs.

BA sulfation and glucuronidation are thought to be important pathways to detoxify and eliminate BAs (Trottier et al., 2006; Alnouti, 2009). The present study shows that BA glucuronidation is a minor BA metabolic pathway in mice. BA glucuronidation was only detected in livers of mice fed UDCA (Figure 3-20), which may be because the massive dose of UDCA (3%) may have overloaded the capacity of enzymes that conjugate BAs with amino acids (taurine or glycine). Hofmann (2007) has summarized the reasons why glucuronidation is not a major metabolic pathway for BAs. There are conflicting data regarding the sulfation position on the steroid nucleus of BAs. Raedsch et al. (1981) reported that in urine of patients with varying degrees of cholestasis, BAs are sulfated at either the 3-OH position (about two thirds) or the 7-OH position (about one third). However, Almé et al. (1977) reported that monosulfates of BAs in human urine were sulfated at the 3-OH position. In mouse feces, only monosulfates at the 7-OH position of BAs were detected (Eyssen et al., 1976). In the present study, CA and CDCA are found to be sulfated at the 7-OH position. This sulfation is likely specific to the 7α-OH position, because feeding DCA or UDCA did not result in an increase of DCA or UDCA sulfates (data not shown).

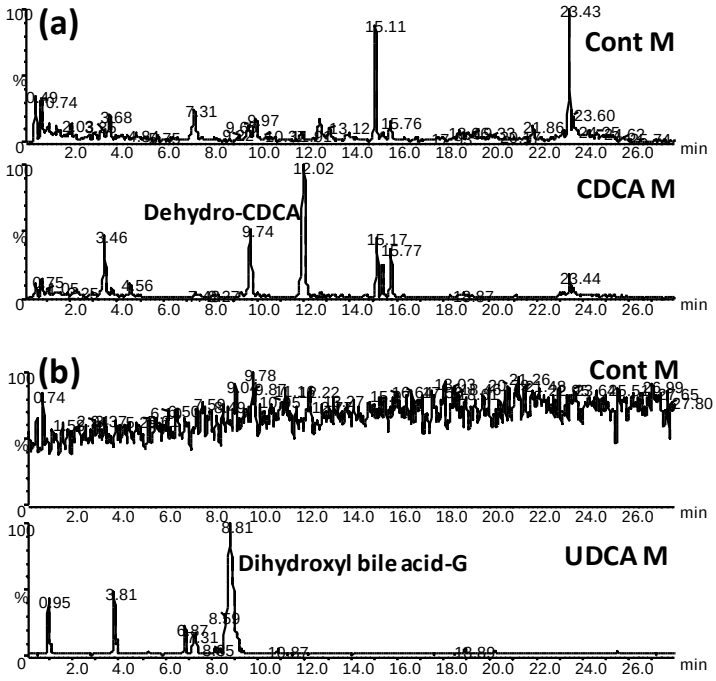

Figure 3-20. UPLC-MS/MS chromatograms of liver samples from control, CDCA-fed, and UDCA-fed male mice. (a) Three major peaks at m/z 389.4>389.4 were increased markedly in livers of mice fed CDCA. (b) No peaks at m/z 567.1>391.5 were detected in livers of control male mice, whereas five peaks appeared in livers of mice fed UDCA.

Sulfation is an important detoxification pathway of LCA in man, chimpanzee, and rodents (Hofmann, 2004). However, in the present study, LCAS was only detected in female mice fed UDCA, and TLCAS was detected in female mice fed LCA or UDCA. The reason why LCAS was only detected in mice fed UDCA is that feeding the high dose of UDCA markedly increased LCA and TLCA, whereas feeding LCA only increased TLCA. Sulfation activity is known to be gender-dependent in rodents (Klaassen et al., 1998; Alnouti and Klaassen, 2006). For example, in germfree rats, the percentage of BA sulfates was about 10-fold higher in female than male cecal contents (Eyssen et al., 1977). The female-

predominant sulfation of LCA is likely due to Sult2a, which is predominantly expressed in female mouse livers but essentially absent from male mouse livers (Alnouti and Klaassen, 2008). Unlike sulfation of LCA, sulfation of CA and CDCA is male-predominant in mouse liver. CA or CDCA can suppress each other's sulfation, indicating that CA and CDCA are sulfated by the same enzyme.

Based on the increased BAs in male mouse livers after BA feeding, metabolic schemes are proposed for each BA in mice. During CA feeding, the fed CA can be metabolized to its secondary BA (DCA) by intestinal bacteria (Figure 3-21). Both CA and DCA are absorbed from the intestine, travel to the liver, where the majority is taken up and conjugated with taurine. Therefore, feeding CA markedly increased hepatic TCA and TDCA. Only a small fraction of CA and DCA were conjugated with glycine in mouse liver, because mouse BA CoA:amino acid *N*-acyltransferase is specific for taurine (Falany et al., 1997). IsoDCA is a possible product of DCA epimerization by intestinal bacteria, and 12-oxoLCA is a possible product of DCA oxidation by mouse livers. Both of these BAs are minor metabolites during CA feeding. A previous study showed that incubation of CA with human liver microsomes produced 3-dehydroCA as the only metabolite (Deo and Bandiera, 2008). In the present study, 3-dehydroCA was not detected in livers of mice fed CA. Interestingly, feeding CA decreased most BAs in livers, especially the muricholic acids (>70%). This is consistent with the previous report that the percentage of TβMCA in hepatic bile was markedly decreased in mice fed CA and DCA for 7 days (Wang et al., 2003). The decrease in liver BAs, other than the metabolites of the fed BA, may be due to their dilution, enhanced excretion, biotransformation, or suppressed biosynthesis. Feeding CA markedly inhibited the mRNA expression of BA-synthetic enzymes (Cyp7a1, 27a1, 8b1, and 7b1), which may partially contribute to the suppression of liver BAs in mice.

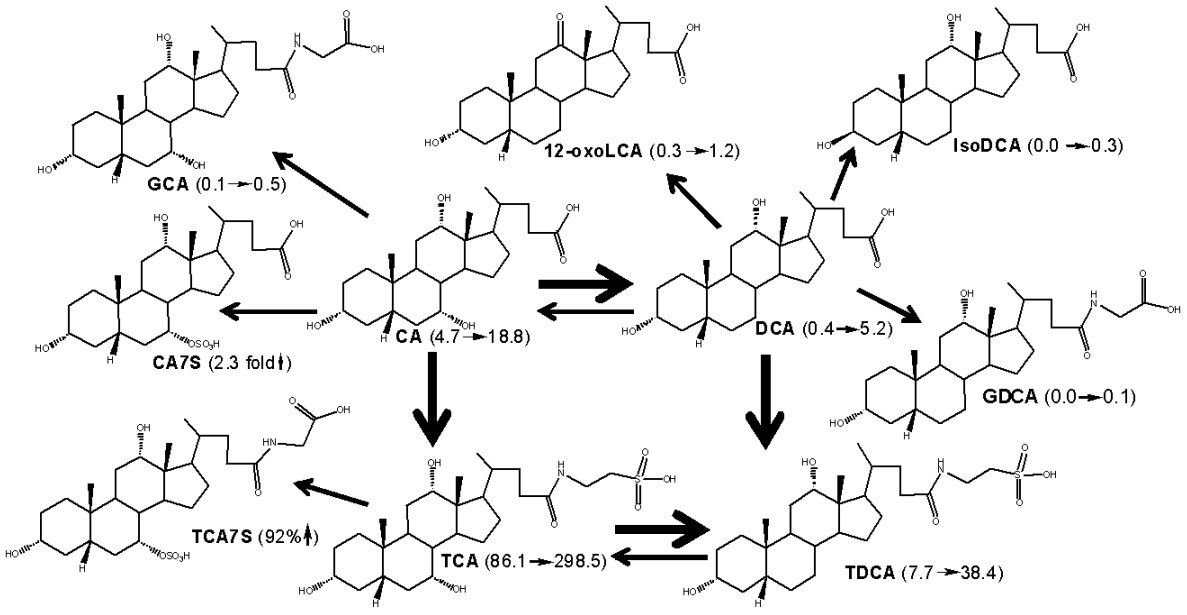

Figure 3-21. Proposed metabolic pathways for CA in mice. The dark arrows indicate the major metabolic pathway. The number in the parenthesis indicates the average concentration of individual BAs in mouse livers. For example, CA (4.7→18.8) means that CA was increased from 4.7 to 18.8 nmol/g in livers of male mice fed CA. TCA7S (92%↑) means that TCA7S was increased 92% in livers of male mice fed CA.

The concentrations of various BAs in mouse liver after feeding DCA were changed similarly to that after CA feeding (Figure 3-22). The majority of DCA fed was conjugated with taurine in mouse liver. DCA feeding tended to increase hepatic TCA and CA, which was statistically significant when mice were fed a higher concentration of DCA (data not shown). Therefore, DCA and TDCA can be rehydroxylated to CA and TCA in mouse liver, a process known as BA "repair" (Hofmann and Hagey, 2008). IsoDCA and 12-oxoDCA were minor metabolites during DCA feeding. DCA can undergo hepatic 3α-dehydrogenation to form 3-dehydroDCA in the guinea-pig (Cantafora et al., 1986). In mice, 3-dehydroDCA is also a possible intermediate between DCA and isoDCA. However, due to lack of a standard, we did not quantify 3-dehydroDCA in the present study. Shefer et al. (1982) showed that iso-BAs can undergo hepatic transformation to their corresponding 3α-hydroxy epimers in rats. Therefore,

the DCA metabolite isoDCA could be converted back to DCA in mouse liver. Similar to feeding CA, feeding DCA also decreased most BAs in mouse livers, which may be partially due to suppression of hepatic Cyp7a1, 8b1, and 27a1.

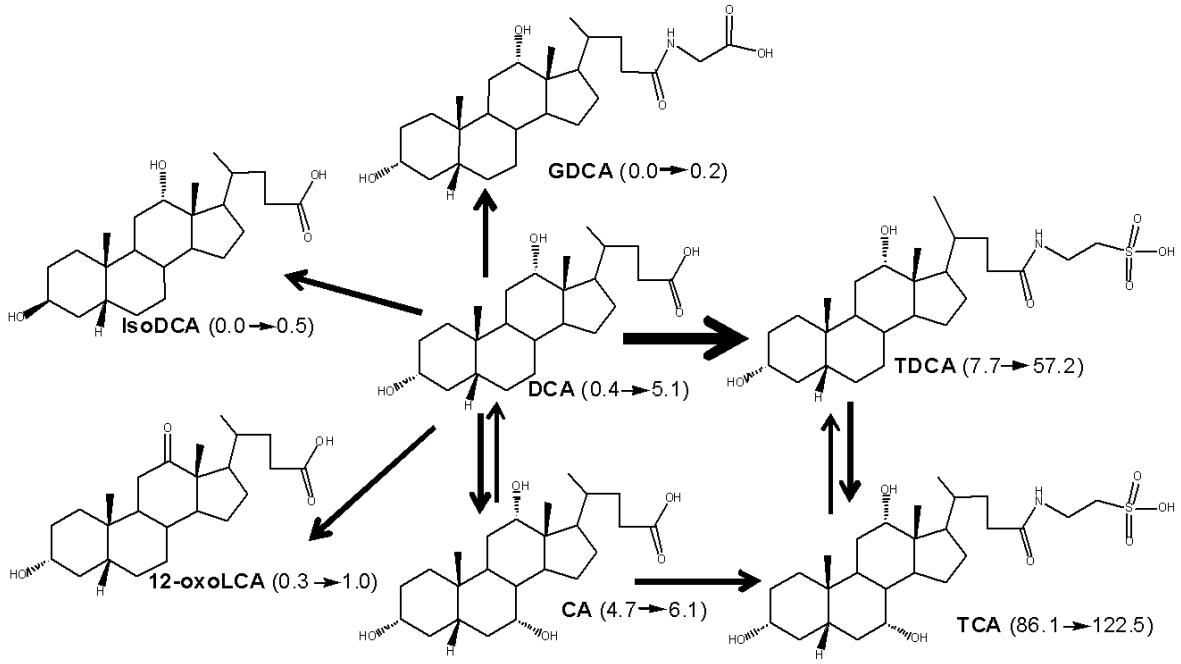

Figure 3-22. Proposed metabolic pathways for DCA in mice. The dark arrows indicate the major metabolic pathway. The number in the parenthesis indicates the average concentration of individual BAs in mouse livers. For example, DCA (0.4→5.1) means that DCA was increased from 0.4 to 5.1 nmol/g in livers of male mice fed DCA.

A scheme for CDCA biotransformation in mice is proposed in figure 3-23. The CDCA fed is metabolized to LCA and UDCA by intestinal bacteria. The majority of these BAs are conjugated with taurine in mouse liver. During CDCA feeding, mouse liver can hydroxylate CDCA at the 6β-position to form αMCA, which can be further dehydroxlated in the intestine to form MDCA. Wang et al. (2003) reported that feeding CDCA increased TβMCA in mouse bile. In the present study, feeding CDCA increased TαMCA, but not TβMCA. This may be due to the difference of BA analytical methods, because it is difficult to separate αMCA from βMCA on a HPLC column. Incubation of CDCA with human hepatic microsomes suggested that 3-dehydroCDCA and HCA are major metabolites of CDCA,

whereas 7-oxoLCA and CA are minor metabolites of CDCA (Deo and Bandiera, 2008). Our study suggests HCA is a minor metabolite of CDCA in mice, whereas liver CA was decreased by CDCA feeding. Two major peaks with the same mass spectra as 3-dehydroCDCA were found in livers of mice fed CDCA, whereas they were almost undetectable in livers of control mice (Figure 3-20). The mRNA expression of Cyp7a1 and Cyp8b1, two enzymes involved in the classic pathway of BA synthesis, were markedly suppressed by feeding CDCA. This may partially contribute to the decreased TCA, CA, TDCA, and DCA in mouse livers after CDCA feeding.

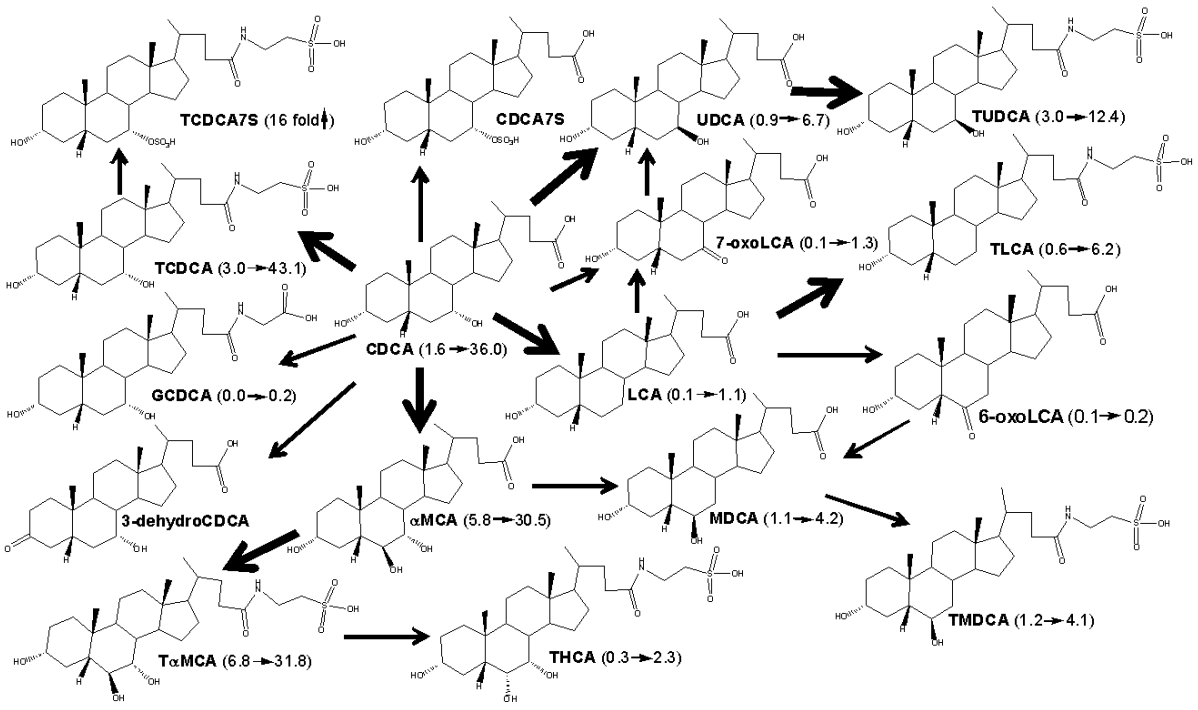

Figure 3-23. Proposed metabolic pathways for CDCA in mice. The dark arrows indicate the major metabolic pathway. The number in the parenthesis indicates the average concentration of individual BAs in mouse livers. For example, CDCA (1.6→36.0) means that CDCA was increased from 1.6 to 36.0 nmol/g in livers of male mice fed CDCA.

The BA profile in mouse livers after feeding LCA undergoes changes similar to that after CDCA feeding (Figure 3-24). Hydroxylation and sulfation are major pathways to detoxify LCA (Kitada et al., 2003; Hofmann, 2004; Kurata, 1967). LCA can be hydroxylated to form HDCA, MDCA, and CDCA in

human liver microsomes (Xie et al., 2001). Cyp3A has been suggested to mediate LCA hydroxylation in humans, rats, and mice (Staudinger et al., 2001; Makishima et al., 2002; Bodin et al., 2005). In the present study, LCA could be hydroxylated at its 6- or 7-position to produce MDCA, HDCA, or CDCA. The majority of these BAs were conjugated with taurine in mouse liver. Among them, MDCA was increased more than other metabolites, suggesting that the 6β-position of LCA is more readily hydroxylated than the other positions. Consistently, 6-oxoLCA was increased more than 7-oxoLCA after feeding LCA. In rat, MDCA, isoLCA, and dehydroLCA were the major LCA metabolites produced by rat liver microsomes, whereas 6-oxoLCA and UDCA were minor metabolites (Deo and Bandiera, 2008). The present study in mice showed that isoLCA and dehydroLCA are minor LCA metabolites. Similar to feeding CDCA, feedubg LCA increased TαMCA and THCA, but decreased CA in male mouse livers. This may be partially due to the suppression of the classic pathway of BA-synthetic enzymes, namely Cyp7a1 and Cyp8b1, in livers of mice fed LCA.

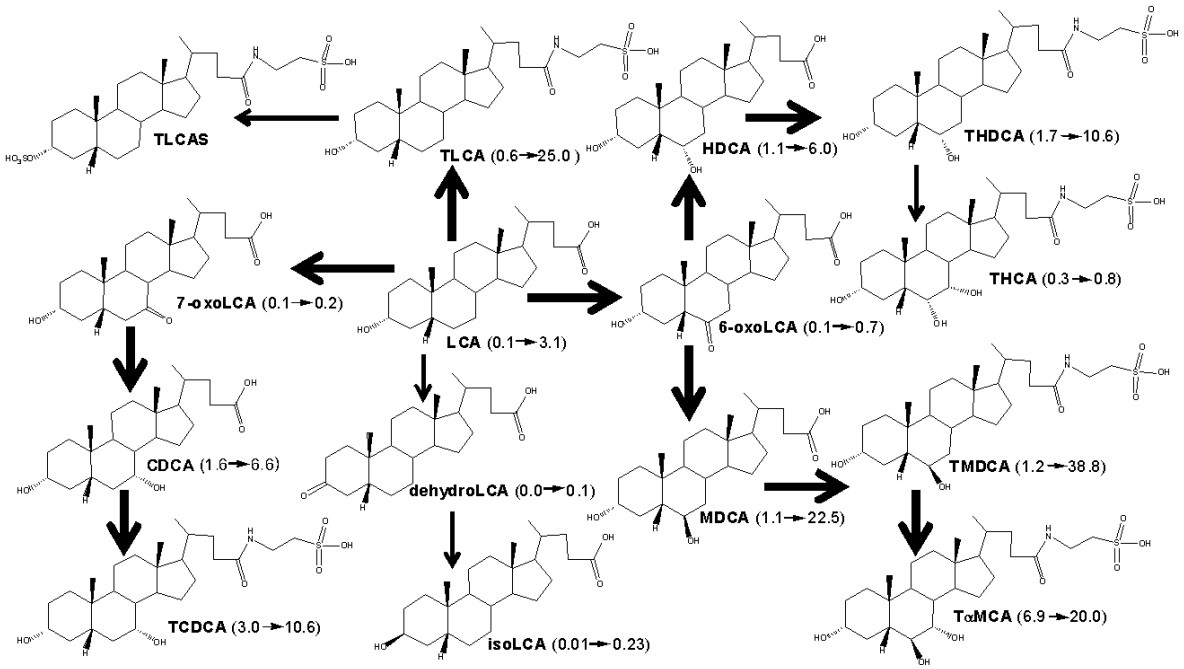

Figure 3-24. Proposed metabolic pathways for LCA in mice. The dark arrows indicate the major metabolic pathway. The number in the parenthesis indicates the average concentration of individual BAs in mouse livers. For example, LCA (0.1→3.1) means that LCA was increased from 0.1 to 3.1 nmol/g in livers of male mice fed LCA.

UDCA is a primary BA in some mammals (e.g. bear and beaver) and is used to treat cholesterol gallstones, primary biliary cirrhosis, and cholestasis of pregnancy (Hofmann and Hagey, 2008; Glantz et al., 2005). The metabolic scheme for UDCA is proposed in figure 3-25. UDCA can be dehydroxylated to LCA by intestinal bacteria. The high dose of UDCA (3%) could saturate the BA-conjugation enzymes, and thus the majority of UDCA and LCA were unconjugated in mouse livers. In mouse liver, LCA can be further hydroxylated at the 6β- and 7α-positions. Feeding UDCA increased liver MDCA more than CDCA, which is consistent with the previous hypothesis that the 6β-position of LCA is more readily hydroxylated than the 7α-position. However, feeidng UDCA had little effect on 6-oxoLCA, but increased 7-oxoLCA. Therefore, 7-oxoLCA may be produced by UDCA, rather than LCA oxidation. Feeding UDCA markedly suppressed TαMCA, TβMCA, TωMCA, TCA, TDCA, and CA, which is consistent with the previous report by Wang et al. (2003) that feeding UDCA decreased TβMCA and TCA in mouse bile. This suppression may be partially due to the marked inhibition of both the classic (Cyp7a1 and Cyp8b1) and alternative (Cyp27a1 and Cyp7b1) pathways of BA synthesis in mice after UDCA feeding.

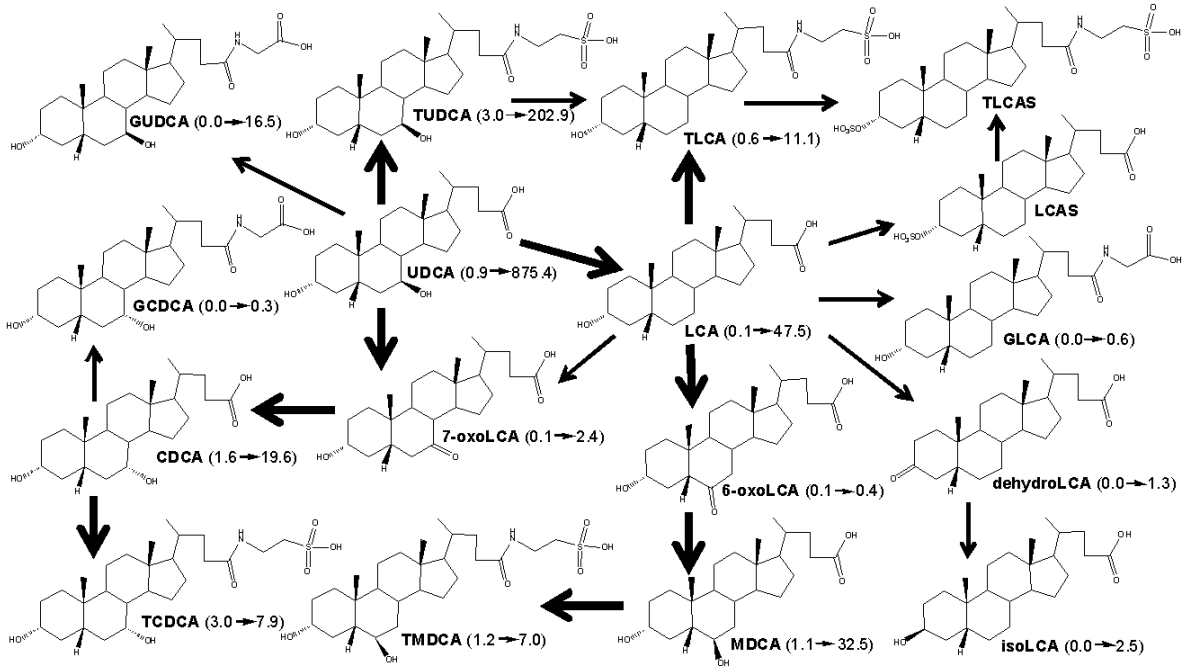

Figure 3-25. Proposed metabolic pathways for UDCA in mice. The dark arrows indicate the major metabolic pathway. The number in the parenthesis indicates the average concentration of individual BAs

in mouse livers. For example, UDCA (0.9→875.4) means that UDCA was increased from 0.9 to 875.4 nmol/g in livers of male mice fed UDCA.

BA-binding resins (e.g. cholestyramine, colestipol, and colesevelam) are used to treat hypercholesterolemia and type 2 diabetes (Aldridge and Ito, 2001). Feeding the resin decreased most BAs in mouse livers. However, feeding the resin tended to increase CDCA and LCA in male mice, and such an increase was statistically significant in female mice. This is consistent with a previous finding in rats that feeding the resin markedly increased CDCA, but decreased βMCA in bile (Imai et al., 1987). Feeding the resin decreased markedly both conjugated and unconjugated BAs in mouse livers. As a feedback, the mRNA expression of liver Cyp7a1 and Cyp8b1 were markedly increased after feeding the resin.

Male mice tend to have higher concentrations of BA metabolites than females during BA feedings (Table 3-1). Feeding CA increased hepatic CA and DCA more in male than female mice. Moreover, 12-oxoLCA was increased only in male mice after CA feeding. Feeding DCA increased TDCA, GDCA, DCA, and 12-oxoLCA more in male than female mice. During CDCA feeding, male mice had higher CDCA, LCA, 6-oxoLCA, and 7-oxoLCA in livers than did females. After LCA feeding, male mice had more TMDCA, TLCA, 7-oxoLCA, 12-oxoLCA, and dehydroLCA than females. Gender differences in BA metabolism may explain the gender-different response of the BA-synthetic enzymes following BA feedings. For example, feeding CA suppressed Cyp7b1 in male but not in female mice, and feeding DCA decreased Cyp7a1 more in male than female mice. The gender difference in hepatic BAs was not prominent during UDCA feeding, except that male mice tended to have higher oxo-BAs than females. During resin feeding, female mice expressed more hepatic Cyp7a1 and Cyp27a1 than male mice. This may be due to lower CA concentrations in livers of female than male mice fed the resin. Because Cyp27a1 initiates the alternative pathway of BA synthesis, the induction of Cyp27a1 may explain why CDCA and LCA were increased in livers of female mice fed the resin.

Table 3-1. Gender difference of hepatic BA and BA synthetic enzymes in mice fed various BA-supplemented diets.

	Hepatic BA		BA-synthetic Enzymes	
	M>F	M<F	M>F	M<F
Cont	αMCA, ωMCA, CDCA, LCA,7-oxoDCA, 7-oxoLCA, 12-oxoLCA		Cyp8b1 Cyp7b1	
1% CA	αMCA, βMCA, ωMCA, CA, MDCA, UDCA, HDCA, isoDCA, CDCA, DCA, 7-oxoDCA, 12-oxoCDCA, 12-oxoLCA	TMDCA	Cyp7b1	Cyp27a1
0.3% DCA	TDCA, GDCA, DCA, GCA, isoDCA, 7-oxoDCA, 12-oxoLCA	TUDCA, UDCA	Cyp7b1	Cyp7a1 Cyp27a1
0.3% CDCA	CDCA, DCA, LCA, 7-oxoDCA, 6-oxoLCA, 7-oxoLCA, 12-oxoLCA		Cyp8b1 Cyp7b1	
0.3% LCA	7-oxoDCA, 6-oxoLCA, 12-oxoLCA		Cyp7b1	
3% UDCA	7-oxoDCA		Cyp7b1	Cyp8b1
2% Resin	CA, 7-oxoDCA	TαMCA, TβMCA, TωMCA, THCA, TCDCA, TMDCA, TUDCA, THDCA, TLCA, HDCA, LCA,	Cyp7b1	Cyp7a1 Cyp27a1

Compared to feeding CDCA and LCA, feeding CA and DCA have more prominent effects on liver proliferation and fibrosis in livers of mice. For example, feeding CA or DCA markedly increased the mRNA expression of Mki67, Pcna, Tgf-β, Col1a1, Top2α, CD1, and Gadd45β, which were not or only slightly increased by feeding CDCA or LCA. As protective mechanisms, the liver may decrease BA synthesis as well as BA uptake, and increase BA efflux to prevent BA accumulation. Consistently, the inhibition of Cyp8b1 (BA synthesis) and Ntcp (BA uptake), as well as the induction of Bsep (BA efflux)

are more prominent in livers of mice fed CA or CDCA than those mice fed CDCA or LCA. Such difference is not due to the total BA concentrations in mouse livers, because feeding CA, DCA, CDCA, and LCA had little effect on the concentrations of total BAs in mouse livers. Instead, it may due to the altered BA composition in the liver. The concentrations of total unconjugated BAs in livers were decreased by feeding CA or DCA, but not altered by feeding CDCA or LCA. In addition, feeding a high dose of the therapeutic BA, namely UDCA, may also cause liver proliferation and fibrosis in mice, manifested by the marked induction of Pcna, c-Myc, and Gadd45β in livers of mice fed UDCA. This may be due to the extreme high concentration of UDCA metabolites, especially the high concentrations of unconjugated UDCA and LCA in livers of mice fed UDCA. Further studies are necessary to clarify the mechanisms of BA-feeding induced liver proliferation and fibrosis.

In summary, the present study establishes an improved simple and sensitive UPLC-MS/MS method for the simultaneous analysis of hydroxy-oxo BAs, as well as BA-sulfates and BA-glucuronides in mouse livers. This method was validated and applied to investigate the BA metabolism in mice fed CA, CDCA, DCA, LCA, UDCA, or resin. Accordingly, the metabolic pathways of each BA *in vivo* are proposed, and can be used to interpret BA-mediated gene regulation and hepatotoxicity.

CHAPTER 4

CHARACTERIZATION OF BILE ACID HOMEOSTASIS IN OATP1A1-NULL MICE

Specific Aim and Hypothesis

Chapter 4 will address specific aim 2 and will evaluate the hypothesis that **Oatp1a1 is important for transporting unconjugated bile acids**. Our previous study (Csanaky et al., 2010) demonstrated that Oatp1b2 mediates the hepatic uptake of unconjugated bile acids, such as CA. In this study, we will use similar methodology to investigate the role of Oatp1a1 in bile acid transport. The purpose of this study is to **determine whether knockout of Oatp1a1 will alter bile acid metabolism in mice.**

I. Introduction

OATP/Oatps mediate the Na^+-independent hepatocellular uptake of BAs and other organic compounds. In mice, Oatp1a1, 1a4, and 1b2 are predominantly expressed in liver and thought to account for the bulk of Na^+-independent BA-uptake into the liver under normal physiological conditions. Oatp1a1 and 1a4 have different distributions in the liver lobule of rodents. Rat Oatp1a1 has a homogeneous lobular distribution, whereas Oatp1a4 is predominantly expressed around the central vein in the liver (Reichel et al., 1999; Kakyo et al., 1999). Such differences are also observed for human OATP1B1 and 1B3, with OATP1B1 being expressed throughout the liver lobe, whereas OATP1B3 is highly expressed around the central vein (Konig et al., 2000a; 2000b). Because the major uptake of BAs occurs in periportal hepatocytes (zone 1), Oatp1a1 is implicated in the uptake of BAs under normal conditions, whereas Oatp1a4 may assume a more important role in situations where Oatp1a1 does not remove most of BAs (Aiso et al., 2000). Oatp1b2 (human orthologs are OATP1B1 and 1B3) is expressed almost exclusively in liver and is considered the major liver-specific uptake transporter for drugs and other

xenobiotics (Cheng et al., 2005). Oatp1b2 has been shown to be important for the hepatic uptake of unconjugated BAs by studies in Oatp1b2-null mice (Csanaky et al., 2010).

Secondary BAs, such as DCA, are implicated in the pathogenesis of some disorders. For example, elevated DCA is associated with increased risk of breast and colorectal cancer (Costarelli and Sanders, 2002; Rial et al., 2009). DCA induces cell proliferation in a human colon cancer cell line (Zeng et al., 2010). DCA can also induce the autophagic pathway in non-cancer colon epithelial cells and contribute to cell survival (Payne et al., 2009). In addition to its tumor promoting activity, DCA can also cause hepatotoxicity. Compared to the same dose of CA and LCA, DCA is the most hepatoxic, and the only BA that induces lipid peroxidation in livers of rats (Delzenne et al., 1992). In addition to its ability to produce hepatotoxicity, DCA has been shown to be useful for drug delivery. For example, oral administration of poly (lactide-co-glycolide) (PLGA) nanoparticles in DCA emulsion significantly increased their bioavailability (Samstein et al., 2007).

In a preliminary study, both male and female C57BL/6 mice were fed diets supplemented with various concentrations of DCA. When fed 1% DCA, all male mice died after 4 days, whereas all female mice survived even after 2 weeks. This indicates that male mice are more susceptible to DCA toxicity than female mice. The mRNA and protein expression of BA-uptake transporters show gender divergence in mouse livers. The Na^+-dependent BA-uptake transporter Ntcp is higher in livers of female than male mice (Cheng et al., 2007). Oatp1a1 is male-predominant, whereas Oatp1a4 is female-predominant in mouse livers (Cheng et al., 2006). In contrast, Oatp1b2 is similarly expressed in male and female mouse livers. Therefore, it is possible that the higher hepatotoxicity of DCA in male mice is due to the male-predominant Oatp1a1, which may transport more DCA into livers of male mice.

Mouse Oatp1a1 has a similar substrate specificity as rat Oatp1a1, and its substrates include hormones such as aldosterone and cortisol; peptides such as glutathione and deltorphin; drugs such as statins; as well as various BAs (Hagenbuch et al., 2000; 2003). Taurocholic acid (TCA) has been shown

to be a substrate of mouse Oatp1a1 with a *K*m of approximately 12 μM when expressed in Xenopus oocytes (Hagenbuch et al., 2000). Although mouse Oatp1a1 has been shown to transport BAs *in vitro*, little is known about the *in vivo* role of Oatp1a1 in BA transport and metabolism.

Therefore, in this study, the concentrations of individual BAs in serum, liver, and bile were compared between WT and Oatp1a1-null mice. The gender-divergent expression of Oatp1a1 was considered in the efforts to identify the endogenous BA substrates for Oatp1a1. In addition, DCA feeding and pharmacokinetic studies were conducted in WT and Oatp1a1-null mice to investigate the role of Oatp1a1 in the disposition of DCA.

II. Results

2.1. Generation and Identification of Oatp1a1-null Mice

Oatp1a1-null mice, which were originally generated by Deltagen (San Carloss, CA), were obtained from Bristol Myers Squibb (Princeton, NJ). Briefly, a 6.93 kb IRES-lacZ reporter and neomycin resistance cassette (IRES-lacZ-neo) was subcloned into a 3.8 kb fragment isolated from a mouse genomic phage library, such that 142 base pairs (from base 219 to base 360; exon 2) coding for the protein were replaced by IRES-LacZ-neo (Figure 4-1a). The IRES-lacZ-neo cassette was flanked by 0.8 kb of mouse genomic DNA at its 5′ end and 3.0 kb of mouse genomic DNA at its 3′ end. The targeting vector was linearized and electroporated into 129/OlaHsd mouse embryonic stem (ES) cells. ES cells were selected for G418 resistance, and colonies carrying the homologously integrated neo DNA were identified by PCR amplification using a 5′ neo-specific primer paired with a primer located outside the targeting homology arms on the 5′ side. The homologous recombination event was confirmed on the 3′ side using a 3′ neo-specific primer paired with a primer located outside the targeting homology arm on the 3′ side. Colonies that gave rise to the correct size PCR product were confirmed by Southern blot analysis using a probe adjacent to the 5′ region of homology. Male chimeric mice were generated by injection of the targeted

ES cells into C57Bl/6J blastocysts. Chimeric mice were bred with C57Bl/6J mice to produce F1 heterozygotes. Germ-line transmission was confirmed by PCR analysis. Initial germ-line heterozygotes were also tested for the homologous recombination event using the primers described above (located outside of the targeting construct). Following confirmation of the targeting event in animals, subsequent genotyping tracked transmission of the targeting construct. F1-heterozygous males and females were mated to produce F2 wild-type (WT), heterozygous- and homozygous-null mutant animals. Mice were backcrossed with C57BL/6J mice for at least five generations. A small segment of null mouse tails was sent to Jackson Lab (Bar Harbor, ME) for congenic genotyping, showing >99% congenicity with the C57BL/6 strain.

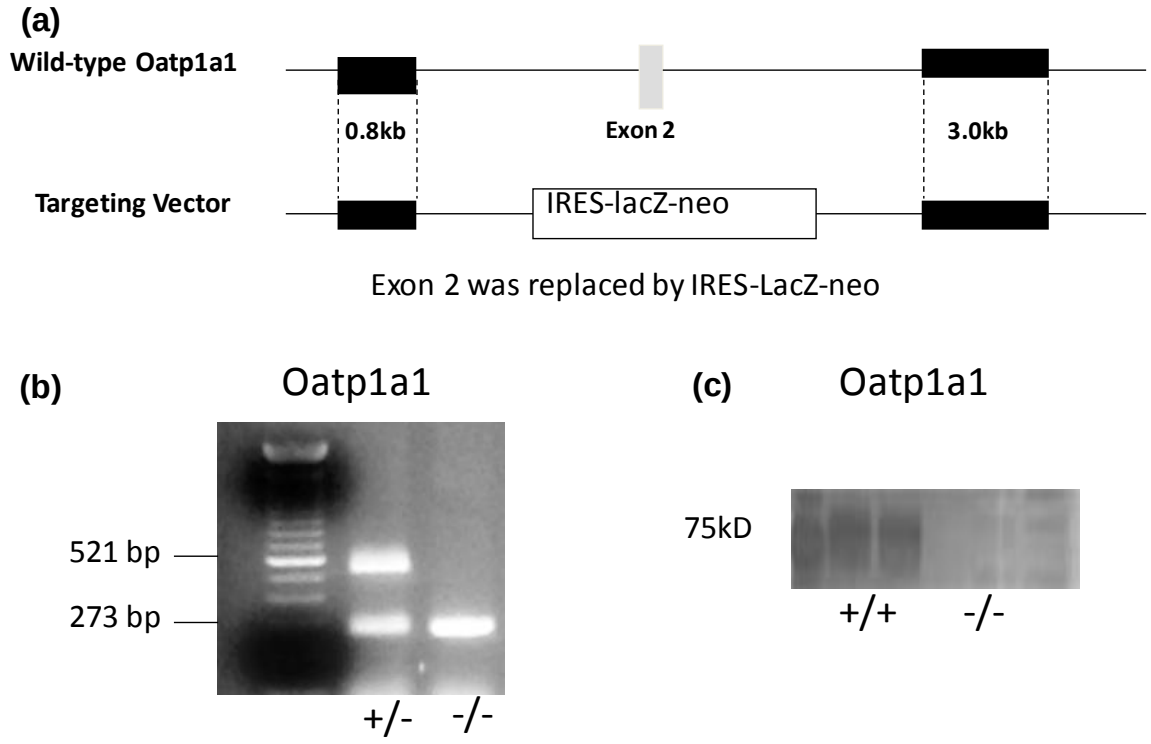

Figure 4-1. Generation and confirmation of Oatp1a1-null mice. (a) Targeted disruption strategy to delete the Oatp1a1 gene; (b) Lack of 512 bp in PCR analysis confirms the absence of Oatp1a1 functional allele; (c) Hepatic Oatp1a1 protein was not detectable by western immunoblotting.

Figure 4-1b shows representative PCR analysis of heterozygous and homozygous genotypes for the Oatp1a1-null mice. No amplification of WT allele (521 base pair product) confirmed the null genotype. The Oatp1a1 proteins were also undetected in liver of homozygote nulls compared to WT C57BL/6N mice (Figure 4-1c). Oatp1a1-null mice developed normally and homozygous nulls bred efficiently. The relative liver/body weight ratio remained unchanged in both genders (data not shown). Compared to WT mice, the free cholesterol level was decreased about 30% in serum of male but not female Oatp1a1-null mice (Table 4-1). Knockout of Oatp1a1 had little effect on serum triglyceride, glucose, and bilirubin levels. No histopathologic changes were observed in liver, kidney or small intestine of young adult Oatp1a1-null mice (data not shown).

Table 4-1. Blood chemistry in C57BL/6 and Oatp1a1-null mice.

	C57BL/6 male	Oatp1a1-null male	C57BL/6 female	Oatp1a1-null female
Free Cholesterol (mg/dL)	16.44±1.22	11.36±1.75*	7.29±0.83	7.80±1.05
Triglyceride (mg/dL)	59.57±7.42	61.28±2.82	45.67±5.63	42.55±4.85
Glucose (mg/dL)	213.90±18.54	276.68±38.08	244.49±15.09	267.06±12.83
Bilirubin total (mg/dL)	0.21±0.02	0.27±0.03	0.17±0.02	0.20±0.03
Bilirubin conjugated (mg/dL)	0.13±0.05	0.17±0.02	0.11±0.01	0.10±0.03
Bilirubin unconjugated (mg/dL)	0.08±0.02	0.11±0.01	0.06±0.02	0.09±0.01

*,statistically significant difference between WT and Oatp1a1-null groups ($p<0.05$).

2.2. Hepatic mRNA Expression of Transporters

To investigate the role of Oatp1a1 in BA homeostasis, it is necessary to determine whether knockout of Oatp1a1 will alter other hepatic transporters, which are involved in BA and cholesterol disposition. Ntcp, Oatp1a1, Oatp1a4, Oatp1b2, and Oatp2b1 are the major BA-uptake transporters in mouse livers (Figure 4-2a). Knockout of Oatp1a1 had little effect on the mRNA expression of Ntcp, Oatp1a4, Oatp1b2, and Oatp2b1, except that Oatp1a4 tended to be increased in Oatp1a1-null mice.

Oatp1a1 mRNA was almost undetectable in Oatp1a1-null mice, further suggesting that Oatp1a1 has been disrupted in Oatp1a1-null mice. Bsep and Mrp2 mediate the BA efflux from hepatocytes into bile canaliculi, whereas Mrp3, Mrp4, and Ostα/β are basolateral BA-efflux transporters which efflux BAs from liver back to the blood (Figure 4-2b). Knockout of Oatp1a1 had little effect on BA-efflux transporters, except that it decreased Ostα (32%) in male mouse livers (Figure 4-2b). This decrease may not be biologically significant because Ostα is only minimally expressed in mouse livers. The mRNA expression of cholesterol transporters in male WT and Oatp1a1-null mice are shown in figure 4-2c. Knockout of Oatp1a1 decreased the mRNA expression of cholesterol-efflux transporter Abca1 about 23%, but had no effect on Abcg5/8 and Mdr2 in livers of male mice. Taken together, knockout of Oatp1a1 had little effect on BA transporters in livers of mice.

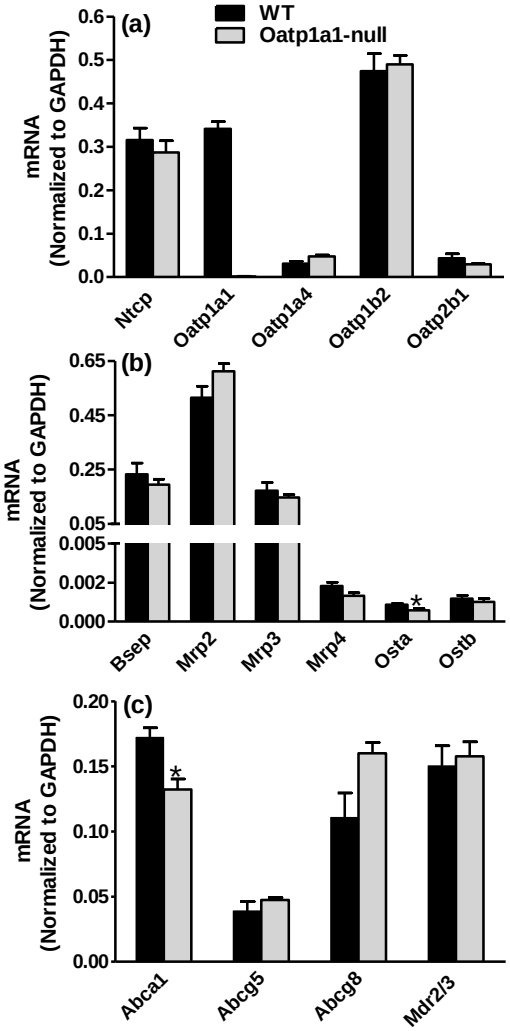

Figure 4-2. mRNA expression of hepatic transporters. Total RNA from livers of male WT and Oatp1a1-null mice (n=5/group) was analyzed by mutiplex suspension array. The mRNA of each gene was normalized to GAPDH. All data are expressed as mean ± S.E. of five mice in each group. *, statistically significant difference between WT and Oatp1a1-null mice ($p<0.05$).

2.3. Concentrations of BAs in Serum of WT and Oatp1a1-null Mice

Because Oatp1a1 is a hepatic uptake transporter, knockout of Oatp1a1 may increase the concentrations of some BAs, which are possibly endogenous substrates for Oatp1a1. Figure 4-3 shows the concentrations of individual BAs in serum of male WT and Oatp1a1-null mice. Compared to WT mice, the concentration of TMCA (TαMCA+TβMCA) decreased about 60% in serum of Oatp1a1-null mice (Figure 4-3a). Knockout of Oatp1a1 tended to, but not significantly, decrease TCA concentration in serum of mice. Knockout of Oatp1a1 had little effect on the concentrations of TMDCA, TUDCA, THDCA, or TCDCA, whereas it markedly increased TDCA (1050%) in serum of mice. The concentrations of unconjugated BAs are shown in figure 4-3b. Knockout of Oatp1a1 increased both ω/αMCA and DCA about 105% in serum of mice. In contrast, knockout of Oatp1a1 had no effect on other unconjugated BAs, such as βMCA, CA, UDCA, HDCA, and CDCA. Taken together, the alterations of BA concentrations in serum of Oatp1a1-null mice suggest that Oatp1a1 may play an important role in the homeostasis of DCA and MCAs.

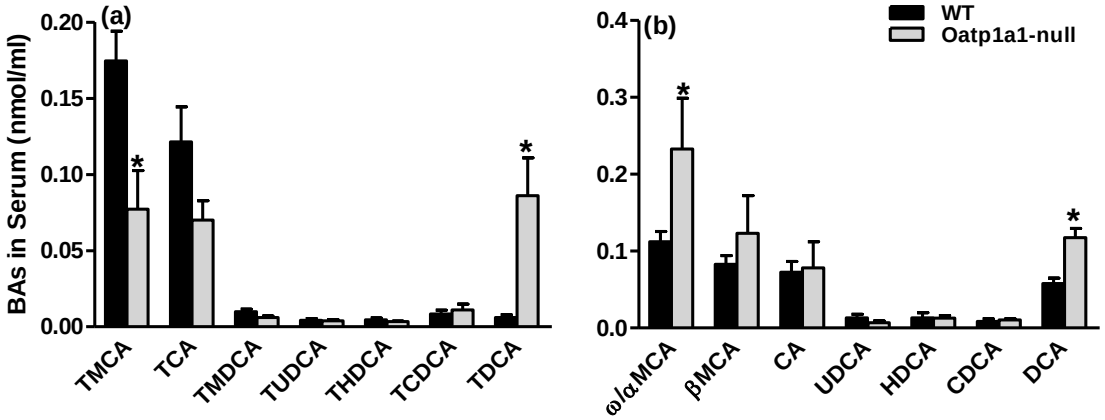

Figure 4-3. BA concentrations in serum of WT and Oatp1a1-null male mice. The concentrations of conjugated (a) and unconjugated (b) BAs in serum of male WT and Oatp1a1-null mice (n=5/group) were analyzed by UPLC-MS/MS. All data are expressed as mean ± S.E. of five mice in each group. *, statistically significant difference between WT and Oatp1a1-null mice ($p<0.05$).

2.4. Liver and Body Weights of WT and Oatp1a1-null Mice Fed 0.3% DCA.

Because knockout of Oatp1a1 increased both TDCA and DCA in serum of mice, it was hypothesized that DCA may be an important endogenous substrate for Oatp1a1. Both male WT and Oatp1a1-null mice were fed a diet supplemented with 0.3% DCA (w/w) for 7 days to determine whether knockout of Oatp1a1 prevented the hepatic uptake of DCA from blood into liver. All mice survived after feeding 0.3% DCA for 7 days, whereas they died within 4 days after feeding 1% DCA. Feeding 0.3% DCA increased the liver/body weight ratio about 51% in Oatp1a1-null but not WT mice (Figure 4-4).

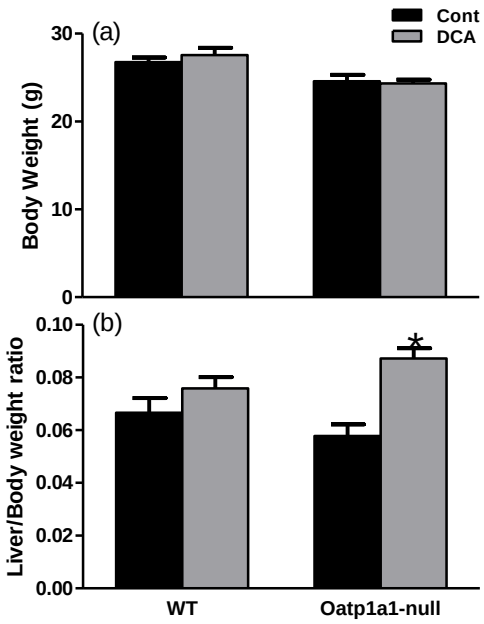

Figure 4-4. Body (a) and relative liver weight (b) of WT and Oatp1a1-null mice fed a 0.3% DCA diet. *, statistically significant difference between control and DCA-fed mice ($p<0.05$).

2.5. Concentrations of DCA Metabolites in Serum of WT and Oatp1a1-null Mice Fed 0.3% DCA.

The concentration of DCA and DCA metabolites were quantified in serum of mice after feeding DCA for 7 days. As shown in figure 4-5a, the concentration of DCA in serum of control Oatp1a1-null mice was about 150% higher than that in control WT mice. Feeding DCA increased serum DCA concentration about 3.8 nmol/ml in WT mice, whereas it increased about 126 nmol/ml in Oatp1a1-null mice. Therefore, after feeding DCA, serum DCA concentration in Oatp1a1-null mice was about 32-fold higher than that in WT mice. After feeding DCA, the DCA metabolites in mice include TDCA, GDCA, TCA, GCA, and CA (Zhang and Klaassen, 2010). Consistently, the concentrations of serum TDCA, GDCA, TCA, GCA, and CA in Oatp1a1-null mice were about 98%, 1090%, 65%, 265%, and 4900%, respectively, higher than those in WT mice (Figure 4-5b). Taken together, Oatp1a1 appears to mediate the hepatic uptake of DCA, because knockout of Oatp1a1 increased the concentrations of DCA and its metabolites in serum of mice after feeding DCA.

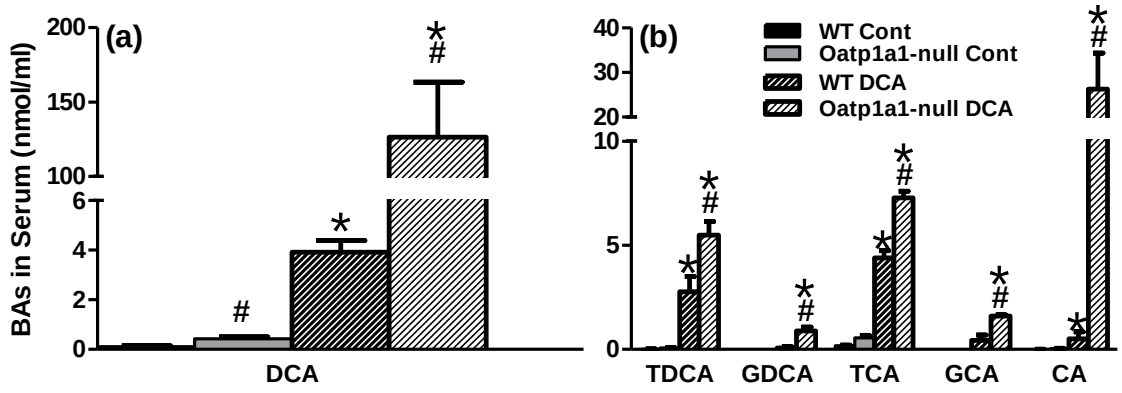

Figure 4-5. Concentrations of DCA and DCA metabolites in serum of WT and Oatp1a1-null mice after feeding DCA for 7 days. The concentrations of DCA (a) and DCA metabolites (b) in serum of male WT and Oatp1a1-null mice (n=5/group) were analyzed by UPLC-MS/MS. All data are expressed as mean ± S.E. of five mice in each group. *, statistically significant difference between WT and Oatp1a1-null mice ($p<0.05$).

2.6. Concentrations of DCA Metabolites in Livers and Gallbladders of WT and Oatp1a1-null Mice Fed 0.3% DCA.

To further determine whether knockout of Oatp1a1 prevented the hepatic uptake of DCA, the concentrations of DCA and DCA metabolites in livers of WT and Oatp1a1-null mice were quantified after feeding DCA. As shown in figure 4-6a, feeding DCA increased DCA concentration in livers of both WT (3.3 nmol/g; 1060%) and Oatp1a1-null (122 nmol/g; 39,300%) mice. The concentrations of DCA metabolites, such as TDCA (40%), GCA (4340%), GDCA (9060%), and CA (780%) were also higher in livers of Oatp1a1-null mice than that in livers of WT mice after feeding DCA (Figure 4-6b). In contrast, TCA concentration was increased in livers of WT (180 nmol/g) but not Oatp1a1-null mice after feeding DCA.

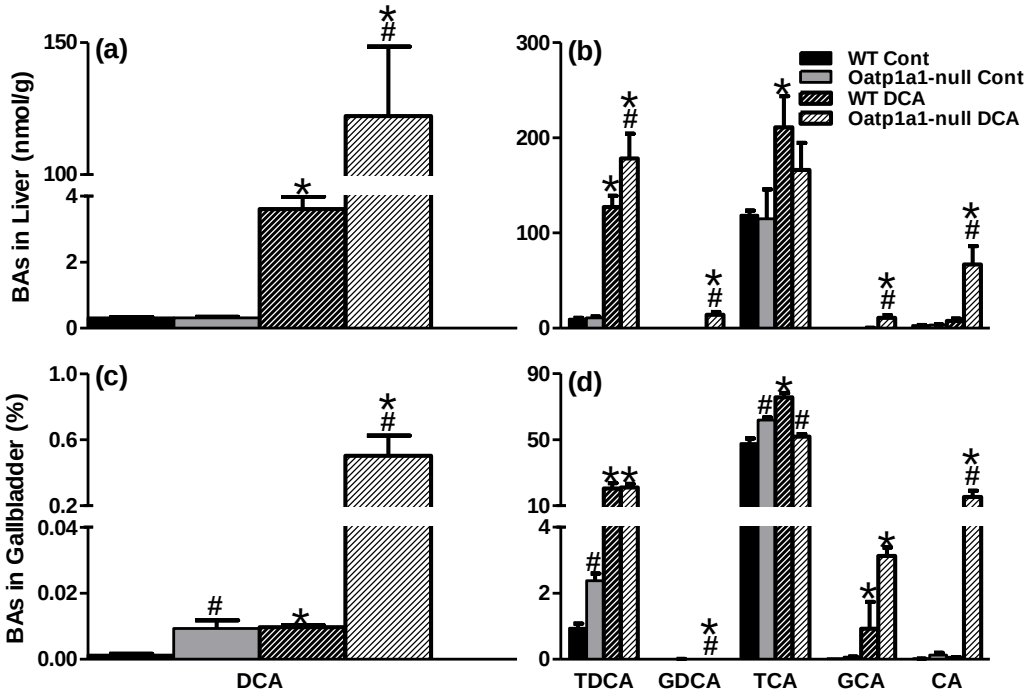

Figure 4-6. Concentrations of DCA and DCA metabolites in livers and gallbladders of WT and Oatp1a1-null mice after feeding DCA for 7 days. The concentrations of DCA and DCA metabolites in livers (a&b) and gallbladders (c&d) of male WT and Oatp1a1-null mice (n=5/group) were analyzed by UPLC-MS/MS. All data are expressed as mean ± S.E. for five mice in each group. *, statistically significant difference between WT and Oatp1a1-null mice ($p<0.05$).

Feeding DCA increased DCA in gallbladder bile about 600% in WT mice, and increased it about 5300% in Oatp1a1-null mice (Figure 4-6c). Feeding DCA also increased GCA (240%), GDCA (660%), and CA (35,100%) in gallbladder bile of Oatp1a1-null more than in WT mice (Figure 4-6d). Similar to the liver, after feeding DCA, TCA in gallbladder bile of Oatp1a1-null mice was lower (40%) than WT mice. In contrast, TDCA was increased in gallbladder bile of WT and Oatp1a1-null mice similarly after feeding DCA. Taken together, the concentrations of DCA in both livers and gallbladders of Oatp1a1-null mice were more than 30-fold higher than that in WT mice after feeding DCA for 7 days, suggesting that knockout of Oatp1a1 did not prevent hepatic uptake of DCA.

2.7. Concentrations of Other Individual BAs in Serum, Livers, and Gallbladders of WT and Oatp1a1-null Mice Fed 0.3% DCA.

In addition to DCA and its metabolites, feeding DCA also altered the concentrations of other BAs in WT and Oatp1a1-null mice. Feeding DCA increased serum TαMCA more in Oatp1a1-null (3 nmol/ml) than in WT (0.2 nmol/ml) mice (Figure 4-7a). Feeding DCA increased serum ωMCA (38 nmol/ml), αMCA (0.5 nmol/ml), and βMCA (1.4 nmol/ml) in Oatp1a1-null mice, but not in WT mice (Figure 4-7b). In contrast, feeding DCA increased serum TUDCA (0.01 nmol/ml) and TCDCA (0.03 nmol/ml) in WT mice, but not in Oatp1a1-null mice (Figure 4-7c). In conclusion, after feeding DCA, Oatp1a1-null mice had higher concentrations of TαMCA, αMCA, βMCA, and ωMCA in serum than WT mice.

Feeding DCA decreased liver TβMCA and TωMCA in both WT (-18.2 and -16.4 nmol/g) and Oatp1a1-null (-19.1 and -21.3 nmol/g) mice, whereas it increased liver TαMCA in Oatp1a1-null (27.8 nmol/g) mice but not in WT mice (Figure 4-7d). Feeding DCA increased ωMCA about 5.7 nmol/g in livers of WT mice, whereas it increased ωMCA about 97.2 nmol/g in livers of Oatp1a1-null mice. Feeding DCA decreased αMCA (-1.6 nmol/g) and βMCA (-17 nmol/g) in WT but not Oatp1a1-null mice (Figure 4-7e). Feeding DCA decreased TCDCA and TUDCA in livers of both Oatp1a1-null (1.2 and 1.1

nmol/g, respectively) and WT (0.8 and 1.1 nmol/g, respectively) mice. In conclusion, after feeding DCA, the livers of Oatp1a1-null mice had higher concentrations of TαMCA, αMCA, βMCA and ωMCA, but lower TβMCA, TCDCA and TUDCA in livers than WT mice.

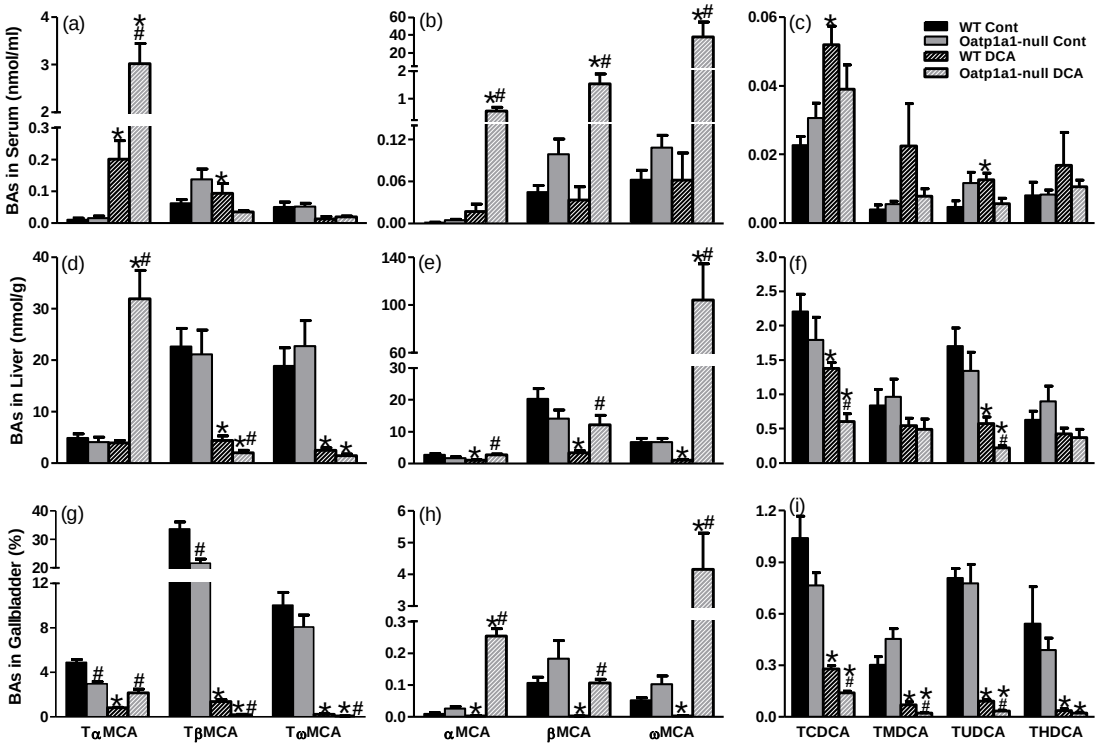

Figure 4-7. Concentrations of other BAs in serum, livers, and gallbladder bile of WT and Oatp1a1-null mice fed a 0.3% DCA diet. BA concentrations were analyzed by UPLC-MS/MS. All data are expressed as mean ± S.E. of five mice in each group. *, statistically significant difference between control and DCA-fed mice ($p<0.05$). #, statistically significant difference between DCA-fed WT and DCA-fed Oatp1a1-null mice ($p<0.05$).

As shown in figure 4-7g, feeding DCA decreased the fraction of TβMCA and TωMCA in the gallbladder bile of both WT (96% and 98%, respectively) and Oatp1a1-null (99% and 99%, respectively) mice. In contrast, feeding DCA decreased TαMCA in gallbladder bile of WT (83%) but not in Oatp1a1-null mice. After feeding DCA, gallbladder αMCA and ωMCA were decreased in WT mice (72% and 94%, respectively), but were increased in Oatp1a1-null mice (920% and 3970%, respectively) (Figure 4-

7h). In contrast, feeding DCA decreased gallbladder βMCA about 98% in WT mice, but not in Oatp1a1-null mice. Feeding DCA decreased TCDCA, TMDCA, TUDCA, and THDCA in both WT (73%, 76%, 88%, and 93%, respectively) and Oatp1a1-null (82%, 96%, 96%, and 95%, respectively) mice (Figure 4-7i). In conclusion, after feeding DCA, Oatp1a1-null mice had higher concentrations of αMCA, βMCA, and ωMCA, but lower concentrations of TβMCA, TωMCA, TCDCA TMDCA, and TUDCA in gallbladder bile than WT mice.

2.8. Total BA Concentrations in Serum, Livers, and Gallbladders of WT and Oatp1a1-null Mice Fed 0.3% DCA.

As shown in figure 4-8a, after feeding DCA, the concentrations of total conjugated BAs, total unconjugated BAs, and total BAs were increased somewhat in serum of WT mice (8, 4, and 12 nmol/ml, respectively), but markedly in Oatp1a1-null mice (17, 167, and 184 nmol/ml, respectively). Feeding DCA increased the concentrations of total conjugated BAs in livers similarly in WT (175 nmol/g) and Oatp1a1-null mice (179 nmol/g) (Figure 4-8b). In contrast, after feeding DCA, total unconjugated BAs were decreased about 23 nmol/g in livers of WT mice, but were increased about 264 nmol/g in livers of Oatp1a1-null mice. Collectively, after feeding DCA, total BAs in livers were increased about 152 nmol/g in WT mcie, but were increased much more in Oatp1a1-null mice (about 443 nmol/g). Feeding DCA tended to increase the amount of total conjugated BAs and total BAs in the gallbladder bile of both the WT (1617 and 1215 nmol, respectively) and Oatp1a1-null (1946 and 2564 nmol, respectively) mice (Figure 4-8c). Feeding DCA increased the amounts of total unconjugated BAs in the gallbladder bile of Oatp1a1-null mice (about 618 nmol), but not in WT mice. Taken together, after DCA feeding, Oatp1a1-null mice had similar concentrations of conjugated BAs, but higher concentrations of unconjugated BAs in their serum, livers, and gallbladders than WT mice.

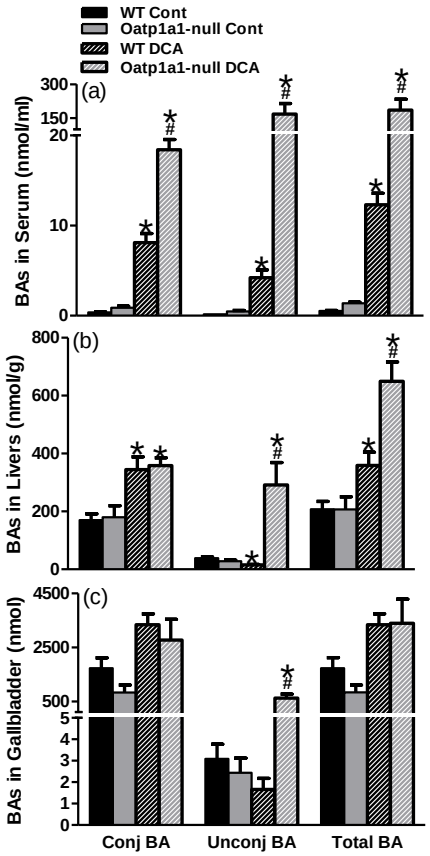

Figure 4-8. Total BA concentrations in serum, livers, and gallbladder bile of WT and Oatp1a1-null mice fed a 0.3% DCA diet. BA concentrations were analyzed by UPLC-MS/MS. All data are expressed as mean ± S.E. of five mice in each group. *, statistically significant difference between control and DCA-fed mice ($p<0.05$). #, statistically significant difference between DCA-fed WT and DCA-fed Oatp1a1-null mice ($p<0.05$).

2.9. Liver Functions of WT and Oatp1a1-null Mice Fed 0.3% DCA.

Because DCA and its metabolites as well as the total BAs were markedly increased in livers of WT and Oatp1a1-null mice after feeding DCA, blood chemistry and DCA hepatotoxicity were determined in WT and Oatp1a1-null mice. Feeding DCA increased serum ALT about 400% in WT mice, and about 200% in Oatp1a1-null mice (Figure 4-9a). Although serum ALT in WT mice is higher than Oatp1a1-null mice after feeding DCA, the low levels of serum ALT (<50 u/L) indicate that feeding DCA

only results in trivial damage to mouse livers. Serum ALP of WT and Oatp1a1-null mice were not affected by feeding DCA (Figure 4-9b). In contrast, serum TG (100%) and conjugated bilirubin (100%) were increased in Oatp1a1-null but not WT mice (Figure 4-9c and d).

In addition to blood chemistry, histological analysis was also conducted to investigate DCA hepatotoxicity in WT and Oatp1a1-null mice (Figure 4-10). After feeding DCA, WT mice had no significant morphological changes in either their livers (Figure 4-10b) or intestinal tract (data not shown). No significant morphological changes were observed in the intestinal tract of Oatp1a1-null mice (data not shown). However, Oatp1a1-null mouse livers after DCA feeding showed mild enlargement of hepatocytes as well as increased mitotic and apoptotic activities (Figure 4-10d).

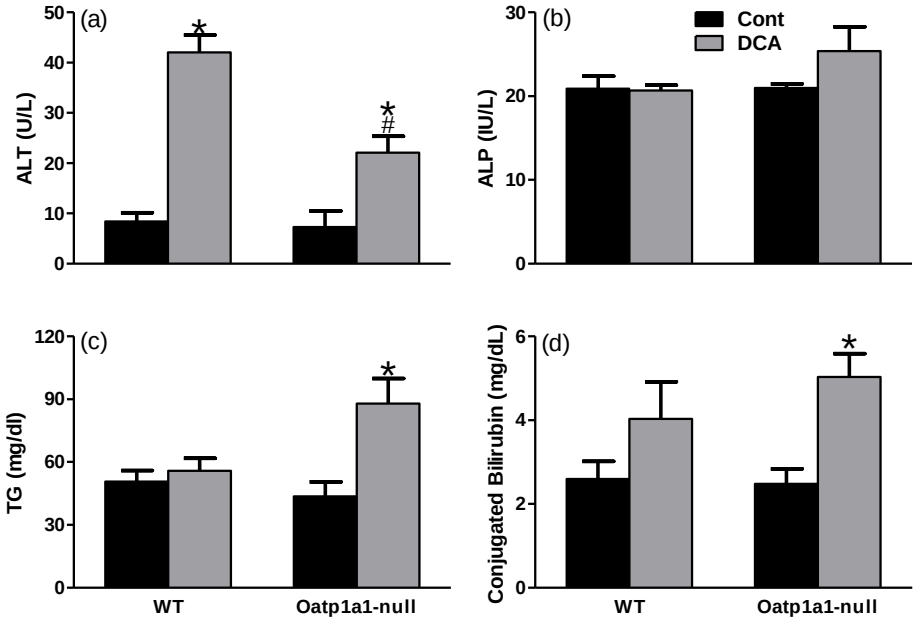

Figure 4-9. Blood chemistry of WT and Oatp1a1-null mice fed a 0.3% DCA diet. Serum ALT (a), ALP (b), triglyceride (c), and conjugated bilirubin (d) from control and DCA-fed mice (n = 5/group) were analyzed with analytical kits (Pointe Scientific, Canton, MI). All data are expressed as mean ± S.E. of five mice in each group. *, statistically significant difference between control and DCA-fed mice ($p<0.05$). #, statistically significant difference between DCA-fed WT and DCA-fed Oatp1a1-null mice ($p<0.05$).

Because the histological analysis indicates enhanced mitotic and apoptotic activities in livers of Oatp1a1-null mice after feeding DCA, the mRNA expression of genes involved in mitosis and apoptosis were determined in livers of WT and Oatp1a1-null mice (Figure 4-11). After feeding DCA, mRNA of Mki67, Pcna, Top2α, CD1, Col1a1, Tgf-β and Gadd45β were increased in livers of both WT and Oatp1a1-null mice. After feeding DCA, compared to WT mice, the livers of Oatp1a1-null mice had higher mRNA expression of Mki67 (105%), Top2α (61%), CD1 (180%), Col1a1 (87%) and Gadd45β (700%). Taken together, although serum ALT levels indicate that feeding DCA caused little liver damage to WT and Oatp1a1-null mice, feeding DCA increased hepatocyte apoptosis and mitosis as well as serum levels of TG and conjugated bilirubin in Oatp1a1-null mice, but not prominently in WT mice.

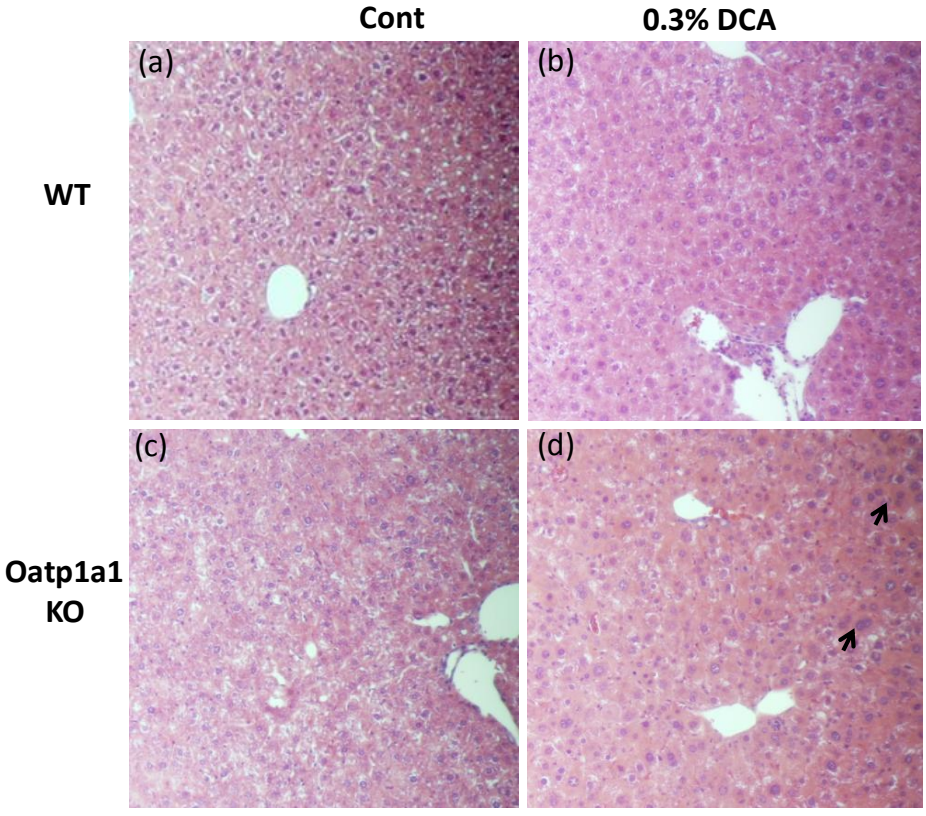

Figure 4-10. Histological analysis of liver sections from WT and Oatp1a1-null mice fed a 0.3% DCA diet. Liver sections (5μm) were stained with hematoxylin-eosin. The hepatocellular damage observed in hematoxylin-eosin-stained liver sections was analyzed by a board-certisfied pathologist (Fan Fang, MD, PhD, Kansas University Hospital, Kansas City, KS).

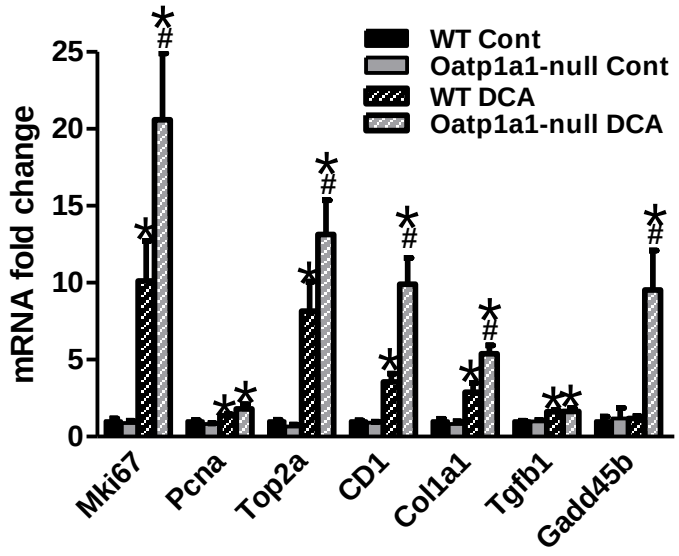

Figure 4-11. mRNA of genes involved in cell proliferation and apoptosis from livers of WT and Oatp1a1-null mice fed a 0.3% DCA diet. Total RNA from livers of male WT and Oatp1a1-null mice (n=5/group) was analyzed by mutiplex suspension array. The mRNA of each gene was normalized to GAPDH and presented as fold change related to the control group. All data are expressed as mean ± S.E. of five mice in each group. *, statistically significant difference between control and DCA-fed mice ($p<0.05$). #, statistically significant difference between DCA-fed WT and DCA-fed Oatp1a1-null mice ($p<0.05$).

2.10. mRNA of Hepatic Transporters and BA Synthetic Enzymes in WT and Oatp1a1-null Mice after Feeding 0.3% DCA.

As protective and adaptive mechanisms, the liver may alter the expression of transporters and BA-synthetic enzymes to prevent BA accumulation. Feeding DCA decreased Ntcp mRNA in livers of both WT (26%) and Oatp1a1-null (31%) mice (Figure 4-12a). Oatp1a4 mRNA was not altered in WT mice, but increased about 249% in Oatp1a1-null mice after feeding DCA. This suggests that Oatp1a4 might be a BA-efflux transporter, which is also increased during extrahepatic cholestasis (Slitt et al., 2006). In contrast, feeding DCA had little effect on Oatp1b2 in livers of either WT or Oatp1a1-null mice.

After feeding DCA, Oct1 mRNA was slightly decreased in both WT (13%) and Oatp1a1-null (19%) mice, whereas Oat2 mRNA was decreased only in Oatp1a1-null mice (79%). Therefore, after feeding DCA, Oatp1a1-null mice had higher mRNA expression of Oatp1a4, but lower mRNA expression of Oatp1b2, Oct1 and Oat2 in livers than WT mice.

After feeding DCA, Bsep mRNA was increased in both WT (36%) and Oatp1a1-null (93%) mice (Figure 4-11b). Feeding DCA decreased Ostα mRNA about 55% in livers of WT mice, but increased Ostα mRNA about 195% in livers of Oatp1a1-null mice. In contrast, feeding DCA increased Ostβ mRNA in livers of both WT (390%) and Oatp1a1-null (1890%) mice. After feeding DCA, the mRNA expression of Mrp2 and Mdr2 were increased in Oatp1a1-null mice (57% and 70%), but not in WT mice. As shown in figure 4-11c, feeding DCA increased Abcg5 and Abcg8 mRNA in both WT (144% and 101%, respectively) and Oatp1a1-null mice (249% and 171%, respectively). In conclusion, after feeding DCA, Oatp1a1-null had higher mRNA expression of Bsep, Ostα, Ostβ, Mrp2, Mrp3, Mdr2, Abcg5 and Abcg8 in livers than WT mice.

Feeding DCA markedly suppressed Cyp7a1 mRNA in both WT (86%) and Oatp1a1-null (97%) mice (Figure 4-11d). In addition, feeding DCA also decreased Cyp8b1 and Cyp27a1 mRNA in both WT (97% and 21%, respectively) and Oatp1a1-null mice (99% and 36%, respectively). In contrast, feeding DCA decreased Cyp7b1 mRNA in Oatp1a1-null (-85%), but not WT mice. In conclusion, after feeding DCA, Oatp1a1-null mice had lower mRNA expression of Cyp7a1, Cyp8b1, Cyp27a1, and Cyp7b1 in livers than WT mice.

Taken together, after feeding DCA, Oatp1a1-null mice expressed lower hepatic uptake transporters (Oatp1b2, Oct1, and Oat2), higher hepatic efflux transporters (Bsep, Ostα, Ostβ, Mrp2, Mrp3, Mdr2, Abcg5 and Abcg8), and lower BA-synthetic enzymes (Cyp7a1, Cyp8b1, Cyp27a1, and Cyp7b1), which together may prevent the hepatic accumulation of BAs.

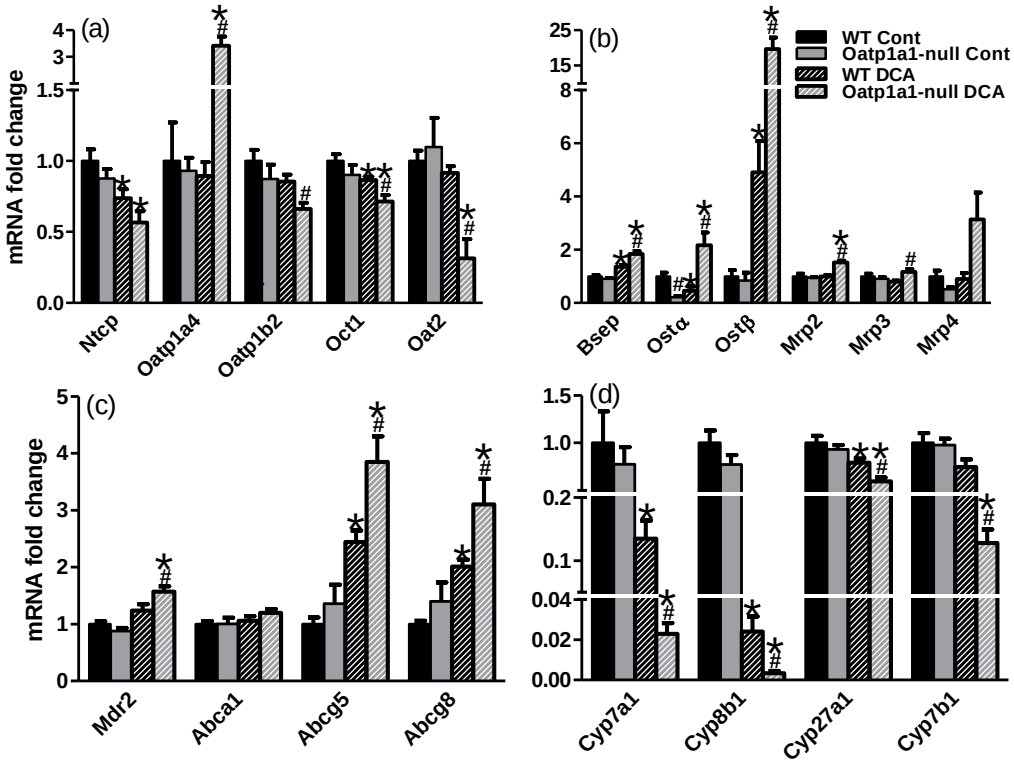

Figure 4-12. mRNA of hepatic transporters and BA-synthetic enzymes from WT and Oatp1a1-null mice fed a 0.3% DCA diet. Total RNA from livers of male WT and Oatp1a1-null mice (n=5/group) was analyzed by mutiplex suspension array. The mRNA of each gene was normalized to GAPDH and presented as fold change related to the control group. All data are expressed as mean ± S.E. of five mice in each group. *, statistically significant difference between control and DCA-fed mice ($p<0.05$). #, statistically significant difference between DCA-fed WT and DCA-fed Oatp1a1-null mice ($p<0.05$).

2.11. Plasma Elimination of DCA in WT and Oatp1a1-null Mice.

Because the data from feeding DCA suggests that knockout of Oatp1a1 does not prevent the hepatic uptake and hepatotoxicity of DCA, a kinetics study of i.v. injected DCA in WT and Oatp1a1-null mice was performed to further determine the role of Oatp1a1 in the disposition of DCA. Figure 4-13 illustrates the plasma elimination of an intravenous dose of DCA (50 μmol/kg). This dose was chosen

because it did not cause hemolysis or signs of cardiac or respiratory toxicity in preliminary experiments. The plasma disappearance curves indicate that the elimination of DCA can be described by a two-compartment open model of elimination. The major pharmacokinetic parameters were calculated and listed in table 4-2.

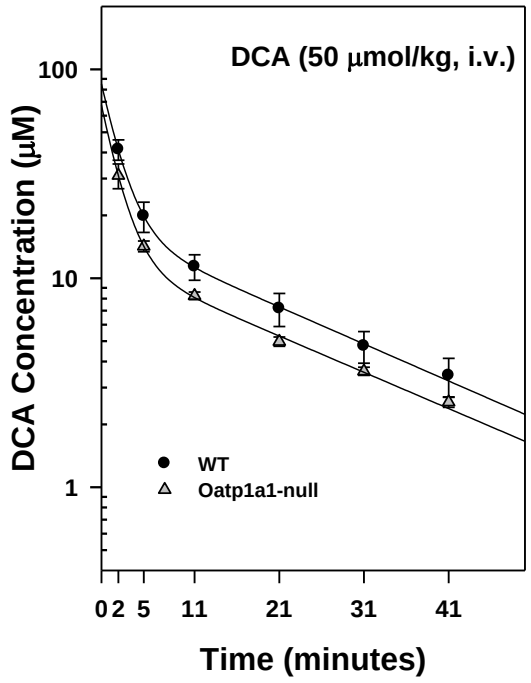

Figure 4-13. Plasma distribution of DCA in WT and Oatp1a1-null mice. DCA was administered intravenously to WT and Oatp1a1-null mice (50 μmol/kg, n=6/group). Blood was collected at 0, 2, 5, 11, 21, 31, and 41 minutes after dosing. DCA concentrations in serum were quantified by UPLC-MS/MS.

After DCA administration, the DCA surprisingly tended to decrease faster from the plasma in Oatp1a1-null than WT mice (Figure 4-13). The half-life times of DCA for distribution and elimination were similar in WT and Oatp1a1-null mice (Table 4-2). No significant difference was observed for the central volume of distribution of DCA between WT and Oatp1a1-null mice. In contrast, Oatp1a1-null mice had higher apparent (46%) and peripheral (44%) volumes of distribution, as well as clearance (33%) than WT mice. Taken together, knockout of Oatp1a1 did not decrease the plasma elimination of DCA in

mice. Instead, knockout of Oatp1a1 slightly increased the peripheral volume of distribution and clearance of DCA in mice

Table 4-2. Pharmacokinetic parameters of DCA administered i.v. to WT and Oatp1a1-null mice (50 µmol/kg).

		DCA	
		WT	**Oatp1a1-null**
$T_{1/2\ distr}$	(min)	1.40 ± 0.25	1.72 ± 0.45
$T_{1/2\ el}$	(min)	16.93 ± 0.74	18.73 ± 1.07
Vd_{cent}	(L/kg)	0.53 ± 0.10	0.87 ± 0.22
$Vd_{app.}$	(L/kg)	2.23 ± 0.17	**3.25 ± 0.32***
Vd_{perif}	(L/kg)	3.14 ± 0.28	**4.51 ± 0.38***
Cl	(L/min/kg)	0.09 ± 0.01	**0.12 ± 0.01***

Each value represents the mean ± SE of five to six mice.
* Significant difference ($P < 0.05$) from the respective value of the wild-type mice.

2.12. Concentrations of DCA and DCA Metabolites in Ileum and Colon Tissues of WT and Oatp1a1-null Mice Fed 0.3% DCA.

To determine whether knockout of Oatp1a1 increased the intestinal absorption of DCA, the concentrations of DCA and its metabolites were quantified in ileum and colon tissues of WT and Oatp1a1-null mice. Feeding DCA increased the concentration of DCA about 33 nmol/g in ileum tissue of WT mice, and about 84 nmol/g in Oatp1a1-null mice (Figure 4-14a). In addition, feeding DCA increased TDCA concentration about 170 nmol/g in ileum tissue of WT mice, and about 450 nmol/g in Oatp1a1-null mice (Figure 4-14b). Feeding DCA had no effect on CA concentration in ileum tissue of WT and Oatp1a1-null mice. Feeding DCA increased TCA concentration about 450 nmol/g in ileum tissue of WT mice, but not signifcantly in Oatp1a1-null mice. In contrast, feeding DCA increased GCA and GDCA concentrations about 74 and 31 nmol/g, respectively, in ileum tissue of Oatp1a1-null mice, but not in WT mice.

As shown in figure 4-14c, feeding DCA increased DCA concentration about 80 nmol/g in colon tissue of WT mice, and about 180 nmol/g in Oatp1a1-null mice. Feeding DCA had little effect on TDCA concentration in colon tissue of WT and Oatp1a1-null mice, whereas it increased GDCA concentration about 0.6 nmol/g in colon tissue of Oatp1a1-null but not WT mice (Figure 4-14d). Similar to ileum tissue, feeding DCA increased TCA concentrations about 20 nmol/g in colon tissue of WT but not Oatp1a1-null mice. Feeding DCA increased GCA concentration about 0.8 nmol/g in colon tissue of Oatp1a1-null but not WT mice. In contrast, feeding DCA increased CA concentration about 20 nmol/g in colon tissue of both WT and Oatp1a1-null mice.

Taken together, after feeding DCA, Oatp1a1-null mice had higher concentrations of DCA in both ileum and colon tissues than WT mice, suggesting that knockout of Oatp1a1 increases the intestinal absorption of DCA in mice.

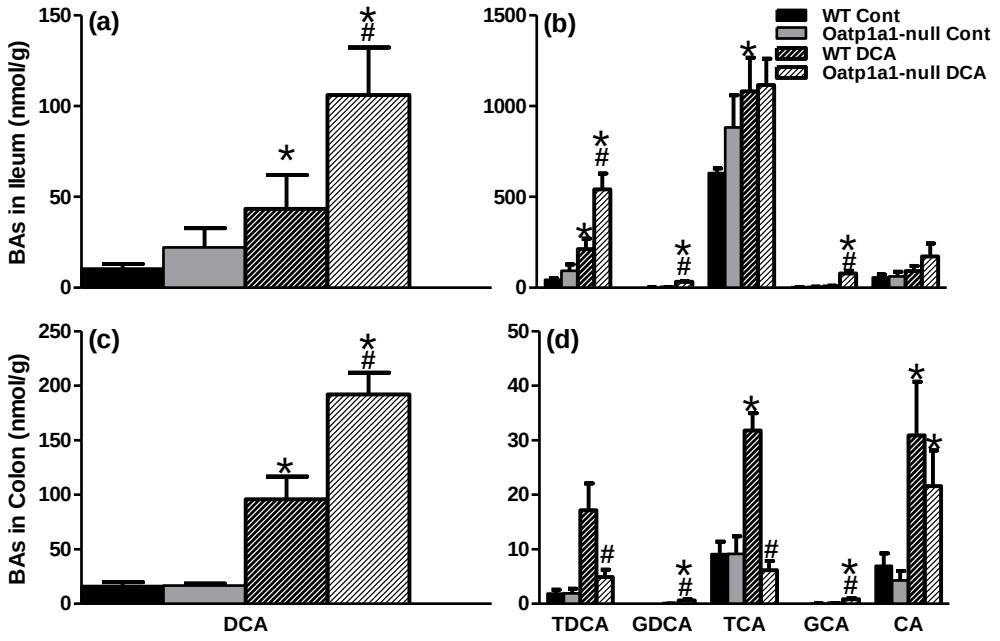

Figure 4-14. Concentrations of DCA and DCA metabolites in ileum and colon tissue of WT and Oatp1a1-null mice after feeding DCA for 7 days. The concentrations of DCA and DCA metabolites in ilea (a&b) and colons (c&d) of male WT and Oatp1a1-null mice (n=5/group) were analyzed by UPLC-MS/MS. All data are expressed as mean ± S.E. of five mice in each group. *, statistically significant difference between WT and Oatp1a1-null mice ($p<0.05$).

2.13. mRNA of BA- and Cholesterol-transporters in Ilea of WT and Oatp1a1-null Mice.

To determine whether the enhanced intestinal absorption of DCA in Oatp1a1-null mice is via the intestinal BA-transporters, the mRNA expression of major BA- and cholesterol-transporters in ilea of WT and Oatp1a1-null mice were quantified. Knockout of Oatp1a1 did not affect the major BA transporters, namely Asbt, Ostα and Ostβ in mouse ileums (Figure 4-15a). Compared to WT mice, Mrp3 mRNA was increased about 33%, whereas Mrp2 mRNA was decreased about 34% in ilea of male Oatp1a1-null mice. Figure 4-15b shows the mRNA expression of cholesterol transporters. Cholesterol efflux transporter Abca1 mRNA was increased about 30%, whereas Abcg5/8 mRNA was not altered in ileums of male mice after knockout of Oatp1a1. Taken together, knockout of Oatp1a1 had little effect on ileal BA transporters, in particular Asbt and Ostα/β.

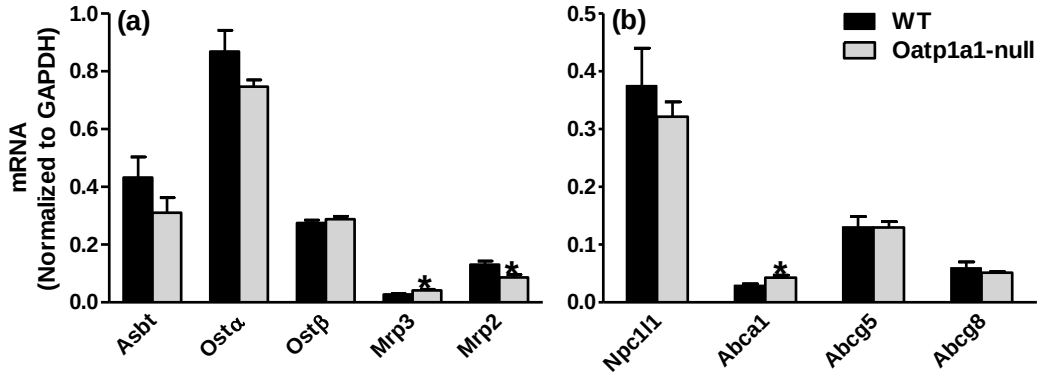

Figure 4-15. mRNA of BA- and cholesterol-transporters in ilea of WT and Oatp1a1-null mice. Total RNA from ileums of WT and Oatp1a1-null mice (n=5/group) was analyzed by mutiplex suspension array. The mRNA of each gene was normalized to GAPDH. All data are expressed as mean ± S.E. of five mice in each group. *, statistically significant difference between WT and Oatp1a1-null mice ($p<0.05$).

2.14. Intestinal Permeability in WT and Oatp1a1-null Mice

As a secondary BA, DCA has been thought to be reabsorbed free the intestine by passively diffusion. To determine whether knockout of Oatp1a1 alters intestinal permeability, the urinary excretion

of lactulose and mannitol was determined in both WT and Oatp1a1-null mice gavaged with lactulose and mannitol. The urinary excretion of mannitol in Oatp1a1-null mice was about 2.5-fold higher than that in WT mice (Figure 4-15). In addition, the urinary excretion of lactulose in Oatp1a1-null mice tended to be, but was not significantly higher than that in WT mice. Therefore, knockout of Oatp1a1 increased the intestinal permeability of mice.

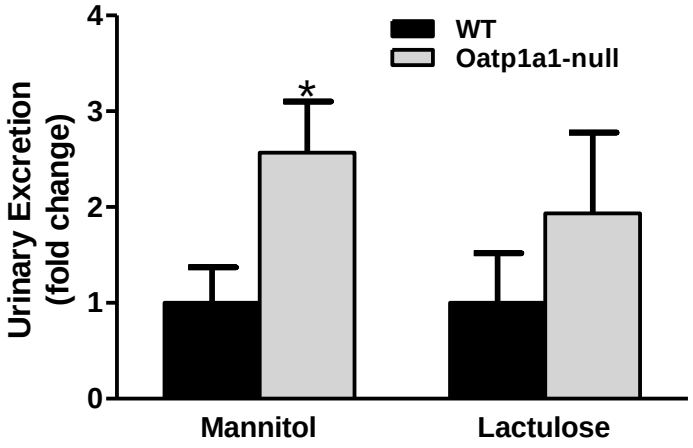

Figure 4-16. Intestinal permeability in WT and Oatp1a1-null mice. Mice (n=4/group) were gavaged with 13.3 mg lactulose and 10.1 mg mannitol, and urine was collected for 20 hr. The concentration of mannitol and lactulose were quantified by UPLC-MS/MS and presented as fold change related to WT mice. *, statistically significant difference between WT and Oatp1a1-null mice ($p<0.05$).

2.15. Gender Difference of DCA Concentrations in Serum and Livers of Oatp1a1-null mice Fed 0.3% DCA.

Because Oatp1a1 is expressed higher in male than female mice, the DCA concentration in serum and livers of both male and female mice after feeding DCA was qauntified to determine whether knockout of Oatp1a1 caused a more prominent effect in male than female mice. After feeding DCA, the serum concentration of DCA was increased about 126 nmol/ml in male Oatp1a1-null mice, but only about 5 nmol/ml in female Oatp1a1-null mice (Figure 4-17a). In addition, feeding DCA increased the liver concentration of DCA about 122 nmol/g in male Oatp1a1-null mice, but only about 8 nmol/g in female

Oatp1a1-null mice (Figure 4-17b). Therefore, feeding DCA had more prominent effects in male than female Oatp1a1-null mice.

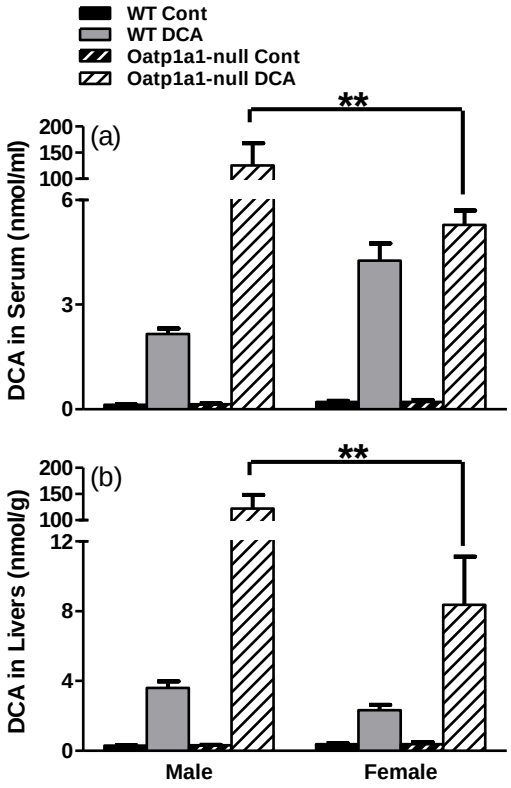

Figure 4-17. Gender difference of DCA concentrations in serum and livers of WT and Oatp1a1-null mice fed a 0.3% DCA diet. DCA concentrations were analyzed by UPLC-MS/MS. All data are expressed as mean ± S.E. of five mice in each group. ** indicates statistically significant difference between male and female Oatp1a1-null mice after feeding DCA ($p<0.05$).

2.16. Principle Component Analysis (PCA) of Serum and Liver BAs in both Genders of WT and Oatp1a1-null Mice Fed 0.3% DCA.

The quantitative data of serum and liver BAs obtained by the UPLC-MS from four groups per gender (WT Cont, WT DCA, Oatp1a1-null Cont, and Oatp1a1-null DCA) were analyzed by PCA (Figure 4-18). Based on serum BAs, male WT control group could be separated from male Oatp1a1-null control group (Figure 4-18a), whereas female WT and female Oatp1a1-null control groups were aggregated

together (Figure 4-18b). After feeding DCA, the distance between male WT and Oatp1a1-null group was much farther than that between female WT and Oatp1a1-null group, suggesting that feeding DCA had a more prominent effect on serum BAs of male than those of female Oatp1a1-null mice. Unlike serum, male WT and Oatp1a1-null control groups could not be discriminated based on liver BA concentrations (Figure 4-18c and d). Similar to serum, feeding DCA also had a more prominent effect on liver BAs of male than female Oatp1a1-null mice.

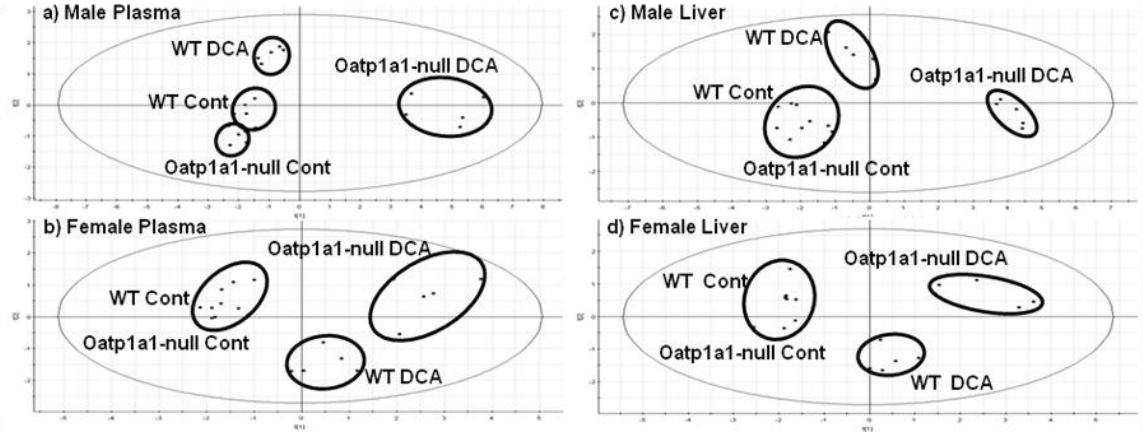

Figure 4-18. Principle component analysis of serum and liver BAs in WT and Oatp1a1-null mice fed a 0.3% DCA diet. A two-component PCA model was constructed to characterize serum and liver BA metabolism among eight groups. (a) PCA map of serum BAs from male WT and male Oatp1a1-null mice with or without feeding DCA; (b) PCA map of serum BAs from female WT and female Oatp1a1-null mice with or without feeding DCA; (c) PCA map of liver BAs from male WT and male Oatp1a1-null mice with or without feeding DCA; (d) PCA map of liver BAs from female WT and female Oatp1a1-null mice with or without feeding DCA.

2.17. Gender Differences in mRNA Expression of Hepatic Genes in WT and Oatp1a1-null mice Fed 0.3% DCA.

Gender-differences in BA metabolism of Oatp1a1-null mice may result in gender-different mRNA expression of some genes in the liver after feeding DCA (Figure 4-18). After feeding DCA, the

mRNA expression of BA efflux transporters Ostα (350%), Ostβ (150%), and Bsep (30%) were all much higher in male than female Oatp1a1-null mice. After feeding DCA, male Oatp1a1-null mice had higher Mki67 (120%), Gadd45β (200%), and Top2α (90%) than female Oatp1a1-null mice. In addition, feeding DCA increased the mRNA expression of some other genes, such as Oatp1a4, CD1, and Pcna in livers of male but not female Oatp1a1-null mice.

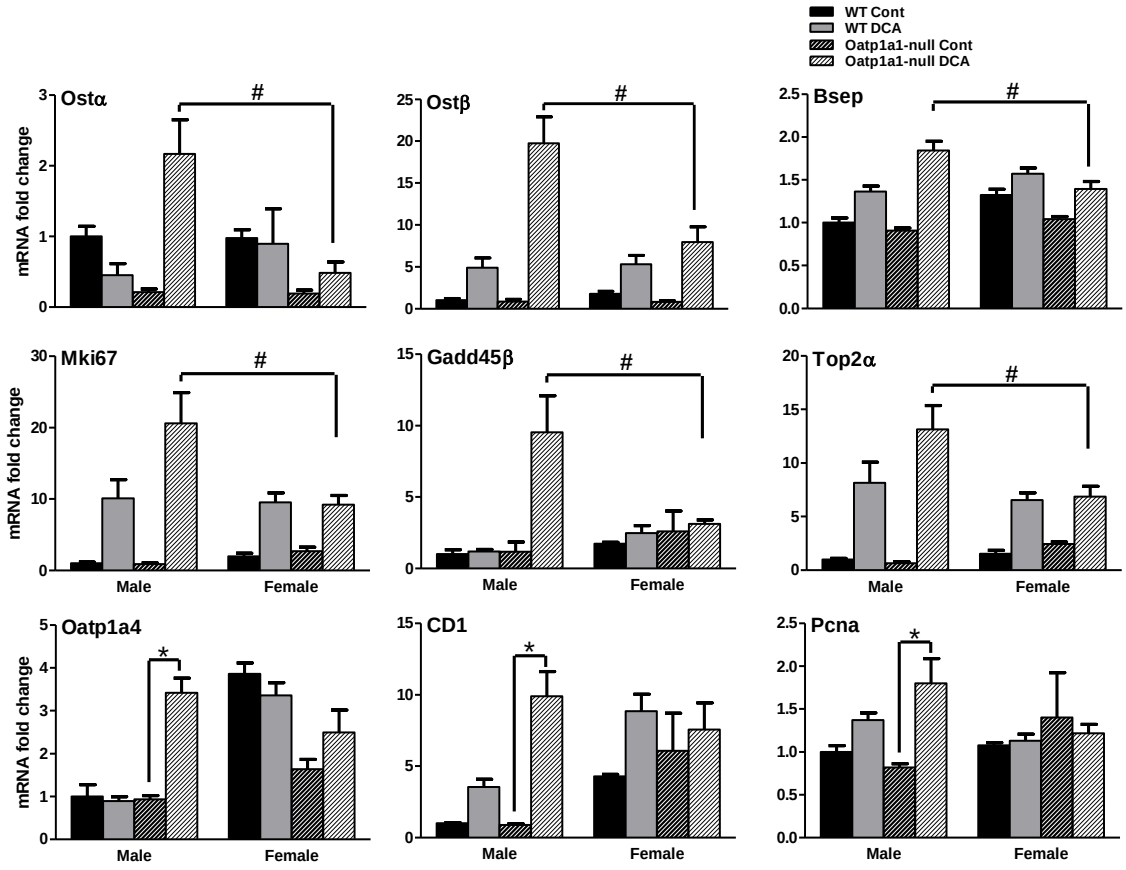

Figure 4-19. Gender different mRNA expression of hepatic genes of WT and Oatp1a1-null mice fed a 0.3% DCA diet. Total RNA from livers of male WT and Oatp1a1-null mice (n=5/group) was analyzed by mutiplex suspension array. The mRNA of each gene was normalized to GAPDH and presented as fold change related to the control group. All data are expressed as mean ± S.E. of five mice in each group. #, statistically significant difference between male and female Oatp1a1-null mice fed DCA ($p<0.05$). *, statistically significant increase between male control and DCA-fed Oatp1a1-null mice ($p<0.05$).

III. Discussion

Mouse Oatp1a1 is highly expressed in liver and kidney, but almost undetectable in the intestinal tract (Cheng et al., 2005). Mouse Oatp1a1 has been shown *in vitro* to transport BAs, such as TCA (Hagenbuch et al., 2000). Therefore, it was expected that concentrations of some BAs would be higher in serum of Oatp1a1-null mice. Surprisingly, the total BA concentration in serum was decreased in Oatp1a1-null mice due to the decreased concentrations of TMCA and TCA. This indicates that Oatp1a1 may play a role other than hepatic uptake in the enterohepatic circulation of BAs.

A preliminary study showed that DCA caused more hepatotoxicity in male than female mice. Ntcp, Oatp1a1, 1a4, and 1b2 are thought to be the major BA uptake transporters in mouse livers. Among them, Oatp1b2 is similarly expressed in livers of male and female mice (Cheng et al., 2005). Female mice have higher Ntcp and Oatp1a4 mRNA than male mice, and thus possibly take up more BAs into livers than male mice. Therefore, Ntcp and Oatp1a4 are possibly not the reason why female mice are more resistant to DCA toxicity than male mice. In contrast, Oatp1a1 is male-predominantly expressed in livers of mice. In addition, knockout of Oatp1a1 increases the concentrations of DCA and TDCA in serum of mice. Therefore, it is reasonable that male mice are more susceptible to DCA feeding because the higher expression of Oatp1a1 in male mice might transport more DCA into their livers than do female mice.

As expected, DCA concentrations in serum of Oatp1a1-null mice were more than 30-fold higher than in WT mice after feeding DCA. However, this is not due to diminished hepatic uptake of DCA by knockout of Oatp1a1, because the concentrations of DCA in livers of Oatp1a1-null mice were also 30-fold higher than in WT mice after feeding DCA. In addition, after feeding DCA, Oatp1a1-null mice had about 50-fold more DCA in their gallbladders than WT mice, indicating that the abnormal increase of DCA in serum of Oatp1a1-null mice after feeding DCA is not due to a block in liver efflux. Furthermore, after feeding DCA, the concentrations of DCA metabolites, such as TDCA, GCA, GDCA, and CA in

serum, livers, and gallbladders were all higher in Oatp1a1-null mice than in WT mice. Intravenously injection of a high dose of DCA showed that Oatp1a1-null mice had a similar volume of distribution and clearance as WT mice. Taken together, knockout of Oatp1a1 does not prevent hepatic uptake of DCA in mice.

Knockout of Oatp1a1 increases the hepatotoxicity of DCA in mice. After feeding a non-lethal dose of DCA (0.3%, w/w), serum ALT was increased slightly higher in WT than Oatp1a1-null mice. However, the low ALT values (<100 U/L) indicated that feeding DCA did not cause severe liver damage in either WT or Oatp1a1-null mice. Feeding DCA increased the liver/body weight ratio, serum TG, and serum conjugated bilirubin in Oatp1a1-null mice, but not in WT mice. Histological analysis showed that Oatp1a1-null mouse livers increased mitotic and apoptotic activities, whereas WT mouse livers had no significant morphologic changes after feeding DCA. Consistently, Oatp1a1-null mouse livers had higher mRNA of proliferation markers, such as Mki67, Top2α, CD1, Col1a1, and Gadd45β after feeding DCA than WT mice. Therefore, feeding DCA causes more hepatotoxicity in Oatp1a1-null than WT mice. Therefore, feeding DCA enhances proliferation in livers of mice, which is more prominent in Oatp1a1-null than WT mice.

Livers have various defensive mechanisms to detoxify DCA and maintain BA homeostasis. First, livers can decrease BA-uptake transporters to reduce BA uptake. For example, Ntcp was suppressed in both WT and Oatp1a1-null mice after feeding DCA. Second, livers can increase BA-efflux transporters to pump out more BAs. For example, Oatp1a1-null mice have higher hepatic Bsep, Ostα/β, and Mrp2 than WT mice after feeding DCA. Third, livers can decrease BA-synthetic enzymes to suppress BA synthesis. After feeding DCA, Oatp1a1-null mice had lower Cyp7a1, 8b1, 27a1, and 7b1 in livers than WT mice. Finally, livers can convert DCA to more hydrophilic and thus less toxic metabolites. DCA can be conjugated with taurine and glycine to form less toxic TDCA and GDCA. In addition, DCA can be "repaired" in the liver by being hydroxylated back to CA, which is further conjugated with taurine or glycine. Consistent with higher DCA concentrations, Oatp1a1-null mice also have higher concentrations

of DCA metabolites in livers than WT mice after feeding DCA. Interestingly, after feeding DCA, concentrations of almost all MCAs were decreased in livers of WT mice, whereas concentrations of TαMCA and ωMCA were markedly increased in livers of Oatp1a1-null mice. This suggests that TαMCA and ωMCA might be DCA metabolites in Oatp1a1-null mice. With all these adaptive mechanisms, livers have the ability to maintain the total BA concentrations in mice after feeding DCA. For example, although feeding DCA increases the concentrations of DCA and its metabolites in livers of WT mice, concentrations of other BAs were decreased in livers of WT mice. Therefore, WT mice only had slightly increased total BA concentration in livers, and this resulted in little hepatoxicity after feeding DCA. In contrast, knockout of Oatp1a1 markedly increased unconjugated BAs, in particular unconjugated DCA, in mouse livers, and thus increased hepatotoxicity after feeding DCA.

Feeding DCA has more prominent effects in male than female Oatp1a1-null mice, probably because Oatp1a1 is a male-predominant transporter in mice. Metabonomics of serum can separate male WT control mice from male Oatp1a1-null control mice, but it cannot discriminate between female WT and Oatp1a1-null control mice. After feeding DCA, male Oatp1a1-null mice had 30-fold more DCA in serum and livers than male WT mice, whereas female Oatp1a1-null mice had similar levels of DCA as female WT mice. In addition, on the PCA map of BA concentrations in both serum and liver, the distance between female WT and Oatp1a1-null DCA-fed groups is less than that between male WT and Oatp1a1-null DCA-fed groups. Therefore, knockout of Oatp1a1 has more dramatic effects on BA metabolism of male than female mice. Consistently, the mRNA expression of Ostα/β, Bsep, Mki67, Gadd45β, and Top2α were increased more in livers of male than female Oatp1a1-null mice. The mRNA expression of some other genes, such as Oatp1a4, CD1, and Pcna, were increased in livers of male Oatp1a1-null mice, but not in female Oatp1a1-null mice. Taken together, there is a strong relationship between the expression of Oatp1a1 and the disposition of DCA in mice.

Knockout of Oatp1a1 increased the intestinal absorption of DCA in mice. DCA is mainly formed by intestinal bacteria in the cecum and colon, and is thought to be reabsorbed into enterocytes by passive

diffusion (Hofmann and Hagey, 2008). Knockout of Oatp1a1 has little effect on the BA transporters in intestine, namely Asbt and Ostα/β. However, knockout of Oatp1a1 increases the intestinal permeability of mice. This suggests that the abnormal increase of DCA in serum and livers of Oatp1a1-null mice after feeding DCA is due to the passive, rather than active intestinal absorption of DCA. Compared to the 30-fold higher DCA in serum and livers of Oatp1a1-null male mice, they only had a 2-fold higher DCA concentration in ileum and colon tissues than WT mice, indicating that the majority of DCA is probably reabsorbed in the cecum, which contains the majority of intestinal bacteria. Further studies are required to investigate the intestinal uptake of DCA as well as the intestinal bacteria changes after feeding DCA.

To conclude, the present study shows a critical role of Oatp1a1 in DCA metabolism of mice. DCA does not appear to be a substrate of Oatp1a1, because knockout of Oatp1a1 does not prevent hepatic uptake and hepatotoxicity of DCA. Instead, knockout of Oatp1a1 increases the intestinal permeability and thus increases intestinal absorption of DCA. Therefore, future studies will address the role of Oatp1a1 in regulation of intestinal BAs and bacteria in mice.

CHAPTER 5

CHARACTERIZATION OF INTESTINAL BACTERIA AND BILE ACIDS IN OATP1A1-NULL MICE

Specific Aim and Hypothesis

Chapter 5 will address questions emerging from our effort to evaluate the hypothesis in chapter 4. We have shown that Oatp1a1 does not mediate the hepatic uptake of DCA, but plays an important role in regulation of intestinal permeability. Therefore, **the purpose of this study is to determine whether knockout of Oatp1a1 alters the intestinal environment in mice**.

I. Introduction

Bile acids (BAs) that are synthesized from cholesterol in hepatocytes are known as primary BAs. The two primary BAs synthesized in human liver are CA and CDCA. Rodent livers can hydroxylate CDCA at the 6β-position to form α-muricholic acid (αMCA), which can be further converted to βMCA by epimerization of the 7α-OH to 7β-OH (Botham and Boyd, 1983). Thus, in addition to CA and CDCA, α- and β-MCA are also primary BAs in rodents. BAs are further conjugated with taurine or glycine before excretion into bile. The conjugation of BAs with taurine or glycine lowers the pKa (which is about 5) to around 4 (Fini and Roda, 1987), which results in almost full ionization of conjugated BAs at physiological pH. The negatively charged conjugated-BAs are impermeable to the apical membrane of cholangiocytes and enterocytes as well as the paracellular junctions between these cells. Therefore, this impermeability is a key factor in promoting the high intraluminal concentration of conjugated BAs in the biliary tract and small intestine (Hofmann and Hagey, 2008).

Conjugated BAs are secreted actively into the canaliculi and are concentrated in the gallbladder during inter-digestive periods. Following a meal, release of cholecystokinin from endocrine cells of the intestinal mucosa results in contraction of the gallbladder to deliver gallbladder bile into the duodenum (Hofmann, 1999). BAs are then efficiently absorbed by both active and passive mechanisms in the intestine, returned to the liver, and resecreted into the canaliculi, which together is known as the enterohepatic circulation of BAs.

Secondary BAs are formed from primary BAs by intestinal bacterial enzymes. In small intestine, BAs mainly undergo deconjugation and hydroxyl group oxidation by the relatively low numbers and diversity of bacteria. Although the majority of BAs (95%) are efficiently absorbed in the ileum, approximately 5% of BAs (400-800 mg in human) escape the enterohepatic circulation daily and become the substrate for large numbers of microbes in the large intestine (Turley et al., 1988). The modifications of BAs in large intestine consist of deconjugation, desulfation, 7-dehydroxylation, dehydrogenation, epimerization of 3-, 7-, and 12-hydroxy groups, as well as isomerization of the A/B ring junction (Ridlon et al., 2006). The most common secondary BAs in humans are DCA and LCA, formed by bacterial 7-dehydroxylation of CA and CDCA, respectively.

Bacteroidetes and Firmicutes are the two predominant bacterial divisions, which make up >99% of the identified phylogenetic types in human intestinal microbiota (Ley et al., 2008). More than 95% of the Firmicutes are members of the *Clostridia* class. BA deconjugation is mediated by bile salt hydrolases (BSH), which have been cloned from *Bacteroides fragilis, Bacteroides vulgates, Clostridium perfringens, Lactobacillus plantarum, Lactobacillus johnsonii, Bifidobacterium Longum, Bifidobacterium bifidum, Bifidobacterium adolescentis,* and *Listeria monocytogenes*. Hydroxysteroid dehydrogenases (HSDH), which mediate the oxidation and epimerization of the 3-, 7-, and 12-hydroxy groups of BAs in the GI tract, have been cloned from *Clostridum perfringens, Clostridium* sp., *Clostridium absonum, Clostridium sordellii, Clostridium innocuum, Clostridium scindens, Clostridium bifermentans, Clostridium limosum, Clostridium leptum, Clostridium* group P strain, *Clostridium paraputrificum, Bacteroides fragilis,*

Bacteroides thetaiotaomicron, Peptostreptococcus productus, Escherichia coli, Eggerthella lenta, and *Eubacterium aerofaciens* (Ridlon et al., 2006).

Mouse Oatp1a1 exhibits a similar substrate specificity as rat Oatp1a1, and its substrates include hormones, such as aldosterone and cortisol; peptides, such as glutathione and deltorphin; drugs, such as statins; as well as various BAs (Hagenbuch et al., 2000; 2003). Our previous study showed that knockout of Oatp1a1 increases the concentration of DCA in serum of mice (Chapter 4). In addition, knockout of Oatp1a1 does not prevent the hepatic uptake of DCA. It is not known whether the increase of DCA in the serum of Oatp1a1-null mice is due to intestinal absorption or bacterial modifications. Therefore, the purpose of this study is to determine whether knockout of Oatp1a1 alters the intestinal BAs and bacteria in mice.

II. Results

2.1. BA-synthetic Enzymes in Livers of WT and Oatp1a1-null Mice

Our previous study showed that knockout of Oatp1a1 has little effect on BA-transporters in either liver or intestine of mice. In this study, we quantified the mRNA expression of BA-synthetic enzymes in livers of both WT and Oatp1a1-null mice to determine whether knockout of Oatp1a1 affects BA synthesis in liver. Cyp7a1 is the rate-limiting enzyme of the classic pathway of BA synthesis. Surprisingly, knockout of Oatp1a1 mRNA decreased Cyp7a1 about 60% in mice (Figure 5-1). Cyp8b1 is the critical enzyme (12α-hydroxylase) for CA biosynthesis. Knockout of Oatp1a1 had no effect on Cyp8b1 mRNA in livers of mice. In addition, knockout of Oatp1a1 also had no effect on Cyp27a1 mRNA, which is involved in both the classic and alternative pathways of BA biosynthesis. Cyp7b1 is a critical enzyme for the alternative pathway of BA biosynthesis. Knockout of Oatp1a1 decreased Cyp7b1 mRNA about 30% in livers of mice. Taken together, knockout of Oatp1a1 suppressed the mRNA expression of Cyp7a1 and

Cyp7b1 in livers of mice, indicating a role of Oatp1a1 in maintaining the mRNA expression of hepatic BA-synthetic enzymes.

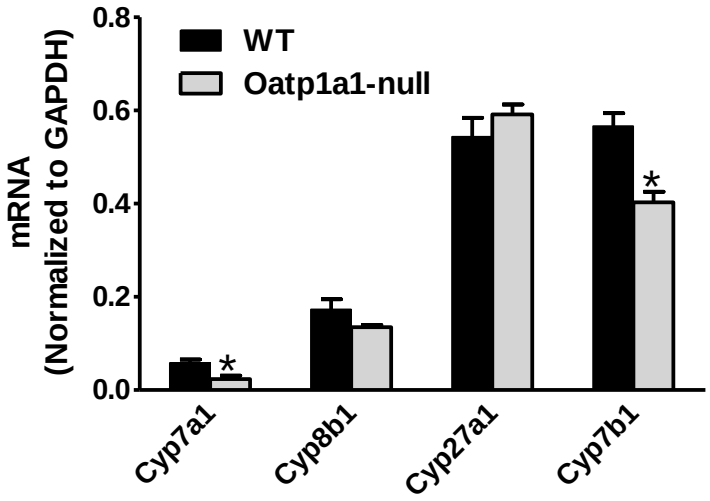

Figure 5-1. Hepatic mRNA expression of BA-synthetic enzymes. Total RNA from livers of male WT and Oatp1a1-null mice (n=5/group) was analyzed by mutiplex suspension array. The mRNA of each gene was normalized to GAPDH. All data are expressed as mean ± S.E. of five mice in each group. *, statistically significant difference between WT and Oatp1a1-null mice ($p<0.05$).

2.2. BA Concentrations in Livers and Bile of WT and Oatp1a1-null Mice

The concentrations of individual BAs were quantified to determine whether suppression of hepatic Cyp7a1 and Cyp7b1 in Oatp1a1-null mice is due to enhanced BA concentrations in the liver. As shown in figure 5-2a, knockout of Oatp1a1 had little effect on the concentrations of unconjugated BAs in livers of mice. Knockout of Oatp1a1 also had little effect on most conjugated BAs, except that it increased the concentration of TDCA about 200% in livers of mice. The increase in TDCA may contribute to the suppression of Cyp7a1 and Cyp7b1 mRNA in livers of Oatp1a1-null mice. Our previous study showed that the increase of TDCA was also observed in the serum of Oatp1a1-null mice. Therefore,

the increase of TDCA in both serum and livers of Oatp1a1-null mice suggests that Oatp1a1 may be not important in the hepatic uptake of TDCA in mice.

The increase of TDCA in livers of Oatp1a1-null mice does not appear to be due to a decrease in biliary excretion, because knockout of Oatp1a1 had no effects on the concentrations of BAs in bile of mice (Figure 5-2c and d). In addition, knockout of Oatp1a1 did not alter bile flow (data not shown). Taken together, knockout of Oatp1a1 increased TDCA concentrations in both serum and livers of mice, which is not due to a decrease in the billiary excretion of BAs.

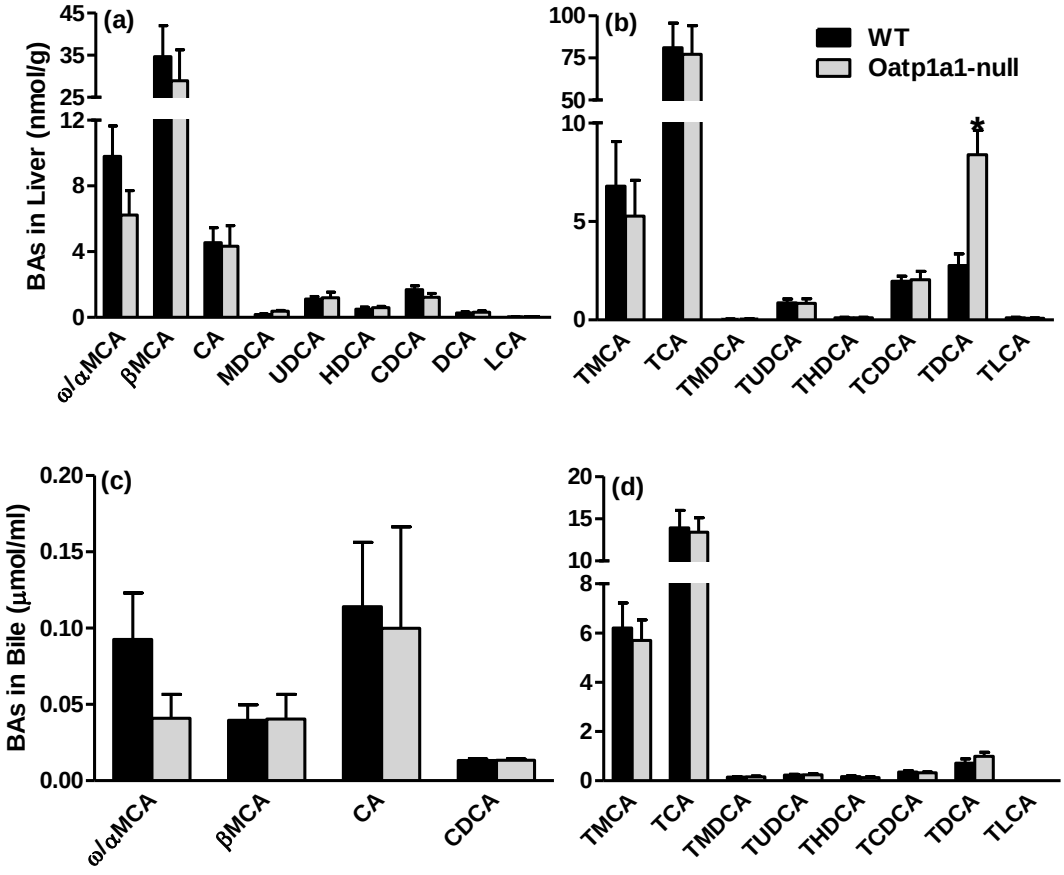

Figure 5-2. BA concentrations in livers and bile of WT and Oatp1a1-null mice. The concentrations of unconjugated and conjugated BAs in livers (a&b) and bile (c&d) of male WT and Oatp1a1-null mice (n=5/group) were analyzed by UPLC-MS/MS. All data are expressed as mean ± S.E. of five mice in each group. *, statistically significant difference between WT and Oatp1a1-null mice ($p<0.05$).

2.3. Concentrations of Primary BAs in Feces of WT and Oatp1a1-null Mice

Because DCA is produced solely by bacteria in the intestine, the increase of TDCA in serum and livers of Oatp1a1-null mice suggests that knockout of Oatp1a1 may alter the BA composition in the intestine, which can be determined by quantification of BA concentrations in mouse feces. More than 90% of primary BAs (CA, CDCA, αMCA, and βMCA) in mice are conjugated with taurine in liver, concentrated in bile, and deconjugated by bacterial enzymes in the intestine. As shown in figure 5-3a, knockout of Oatp1a1 markedly decreased the concentrations of TCA (80%), TCDCA (60%), TαMCA (80%), and TβMCA (90%) in feces of mice. In addition, knockout of Oatp1a1 also decreased GCA (30%) and GCDCA (50%) in feces of mice (Figure 5-3b). This suggests more BA-deconjugation enzyme activity in Oatp1a1-null mice. Figure 5-3c shows the concentrations of unconjugated primary BAs in feces of mice. Knockout of Oatp1a1 decreased CA about 65%, but had no effect on CDCA in feces of mice. This suggests that more deconjugated-CA in the intestine are further metabolized by bacterial enzymes in Oatp1a1-null mice than in WT mice. Knockout of Oatp1a1 increased αMCA about 95%, but decreased βMCA about 30% in feces of mice. The increase of αMCA may be due to enhanced deconjugation of TαMCA in the intestine of Oatp1a1-null mice, whereas the decrease of βMCA may indicate that more deconjugated-βMCA are further metabolized by bacterial enzymes in the intestine of Oatp1a1-null mice than in WT mice.

BA sulfates can be desulfated by bacterial enzymes in the intestine (Huijghebaert et al., 1984). TCA7S, CA7S, TCDCA7S, and CDCA7S are the major BA-sulfates in feces of mice (Figure 5-3d). Knockout of Oatp1a1 markedly decreased the concentrations of TCA7S (99%), TCDCA7S (99%), CA7S (40%), and CDCA7S (80%) in feces of mice. Taken together, the deconjugation and desulfation of BAs in the intestine of Oatp1a1-null mice are more active than in WT mice. In addition, the unconjugated BAs from the deconjugation are more extensively metabolized in Oatp1a1-null mice than in WT mice.

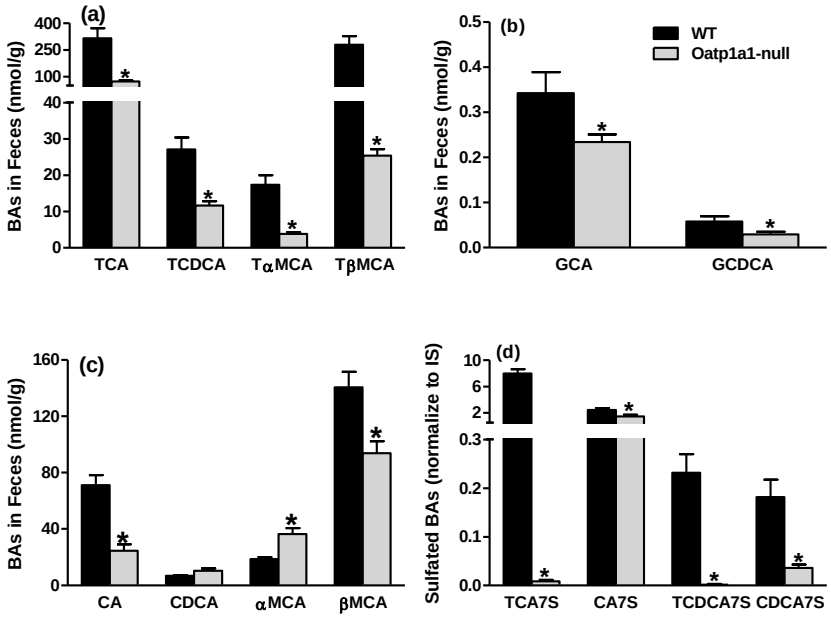

Figure 5-3. Concentrations of primary BAs in feces of WT and Oatp1a1-null mice. Feces were collected from WT and Oatp1a1-null mice for 24 hr and dried under vacuum. The concentrations of taurine-conjugated (a), glycine-conjugated (b), unconjugated (c) and sulfated BAs (d) in dried feces of male WT and Oatp1a1-null mice (n=5/group) were analyzed by UPLC-MS/MS. All data are expressed as mean ± S.E. of five mice in each group. *, statistically significant difference between WT and Oatp1a1-null mice ($p<0.05$).

2.4. 7-Dehydroxylation of BAs in Feces of WT and Oatp1a1-null Mice

Bacteria-mediated 7-dehydroxylation is another major modification of BAs in the intestine. It is well known that DCA and LCA are products of the 7-dehydroxylation of CA and CDCA, respectively. In mice, MDCA is thought to be produced by the 7-dehydroxylation of βMCA, whereas HDCA is produced by further epimerization of MDCA (Eyssen et al., 1999). Knockout of Oatp1a1 tended to, but not significantly, increase TDCA, whereas it significantly increased GDCA 420% in feces of mice (Figure 5-4a). In addition, knockout of Oatp1a1 increased DCA about 1300% in feces of mice (Figure 5-4b). This suggests that knockout of Oatp1a1 increases the 7-dehydroxylation of TCA, GCA, and CA in mice. Knockout of Oatp1a1 had little effect on TLCA, but markedly increased LCA (1900%) in feces of mice

(Figure 5-4a and b), suggesting that 7-dehydroxylation of CDCA is more prominent than 7-dehydroxylation of TCDCA in Oatp1a1-null mice. Furthermore, knockout of Oatp1a1 markedly increased TMDCA (170%) and MDCA (130%), as well as THDCA (80%) and HDCA (1700%) in feces of mice. This suggests that 7-dehydroxylation of TβMCA and βMCA is also enhanced in the intestine of Oatp1a1-null mice. Taken together, knockout of Oatp1a1 increases the activity of 7-dehydroxylation in the intestine of mice.

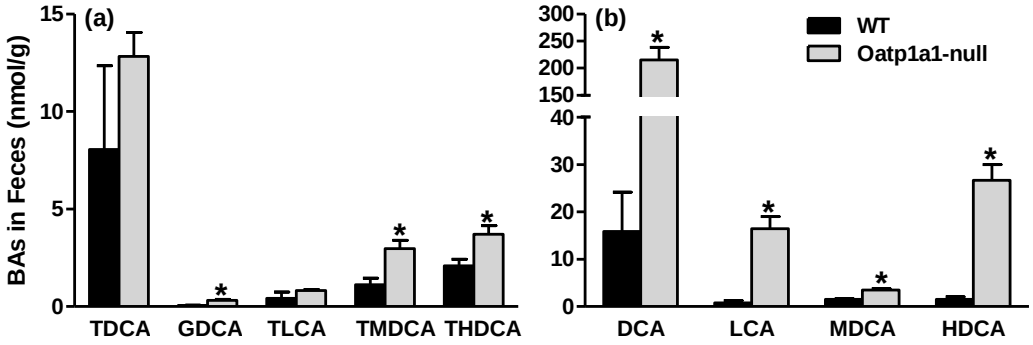

Figure 5-4. Concentrations of BAs produced from 7-dehydroxylation in feces of WT and Oatp1a1-null mice. Feces were collected from WT and Oatp1a1-null mice for 24 hr and dried under vacuum. The concentrations of conjugated (a) and unconjugated (b) BAs in dried feces of male WT and Oatp1a1-null mice (n=5/group) were analyzed by UPLC-MS/MS. All data are expressed as mean ± S.E. of five mice in each group. *, statistically significant difference between WT and Oatp1a1-null mice ($p<0.05$).

2.5. 3-Epimerization and Oxidation of BAs in Feces of WT and Oatp1a1-null Mice

IsoDCA and isoLCA are produced from the 3α/β-epimerization of DCA and LCA, respectively. The concentrations of isoDCA (1300%) and isoLCA (1900%) were increased markedly in feces of Oatp1a1-null mice, suggesting that knockout of Oatp1a1 enhances the 3-epimerization of DCA and LCA in the intestine of mice (Figure 5-5). In addition, the concentrations of oxo-BAs, such as dehydroLCA (4300%), 6-oxoLCA (700%), 7-oxoLCA (70%), and 12-oxoLCA (1300%) were also increased markedly

in feces of Oatp1a1-null mice, suggesting that knockout of Oatp1a1 increases the oxidation of BAs in the intestine of mice. The concentration of 12-oxoLCA is much higher than other oxo-LCAs, suggesting that 12-oxoLCA might be produced from the oxidation of DCA, which is much higher than LCA in feces of mice. Taken together, knockout of Oatp1a1 promotes the 3-epimerization and oxidation of BAs in the intestine of mice.

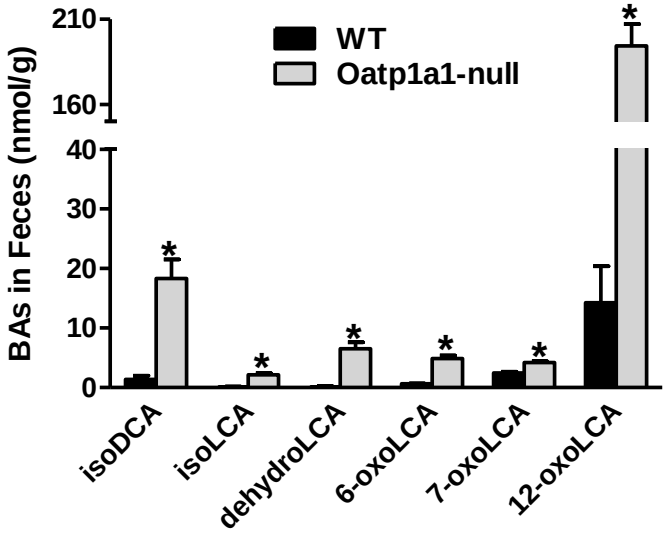

Figure 5-5. Concentrations of BAs produced from 3-epimerization and oxidation in feces of WT and Oatp1a1-null mice. Feces were collected from WT and Oatp1a1-null mice for 24 hr and dried under vacuum. The concentrations of BAs in dried feces of male WT and Oatp1a1-null mice were analyzed by UPLC-MS/MS. All data are expressed as mean ± S.E. of five mice in each group. *, statistically significant difference between WT and Oatp1a1-null mice ($p<0.05$).

2.6. 7-Epimerization of BAs in Feces of WT and Oatp1a1-null Mice

During the quantification of BA concentrations in feces, an unknown peak **A**, which had the same molecular weights of parent and daughter ions as TMCA and TCA, was found to be the predominant taurine-conjugated trihydroxy-BA in feces of male mice (Figure 5-6a). This peak **A** was almost undetectable in small intestine contents (data not shown), but was detected in the cecum and large intestine contents, indicating this unknown BA was mainly produced in the cecum and large intestine.

Interestingly, peak **A** was lower in female WT mice (Figure 5-6b), and was almost undetectable in both male and female Oatp1a1-null mice (Fig 5-6c and d). Thus, the concentration of this unknown peak A correlates well with the expression of Oatp1a1, which is higher in male than female mice. By comparing the LC-retention time and mass spectrum with the standard, this unknown BA was identified as tauro-ursocholic acid (TUCA), which may be produced by 7-epimerization of TCA (Figure 5-7).

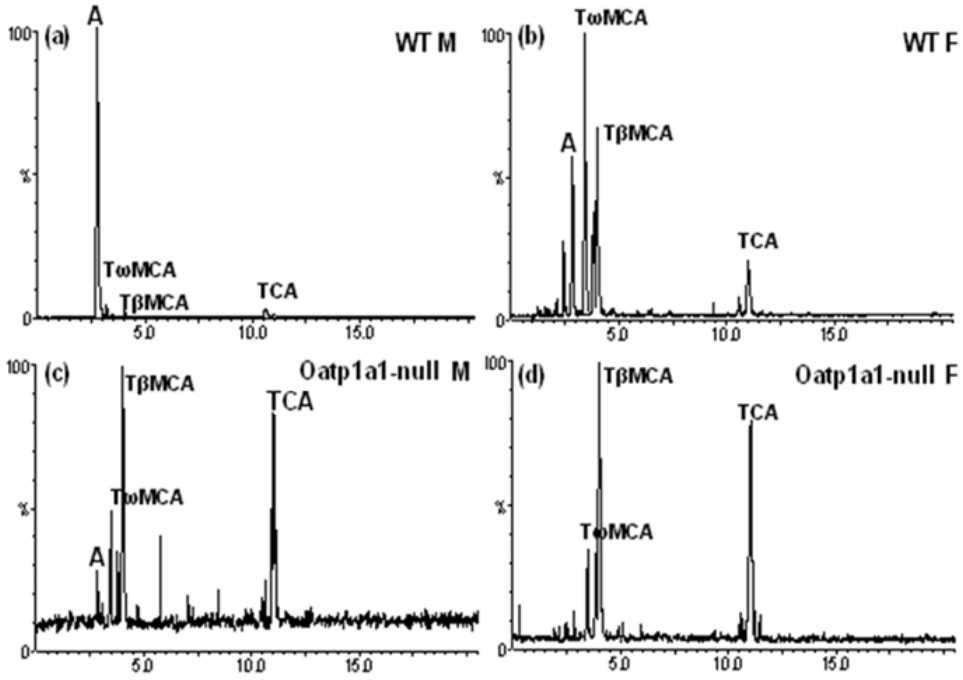

Figure 5-6. An unknown BA in feces of WT and Oatp1a1-null mice. An unknown peak A was found in the chromatogram window of taurine-conjugated trihydroxy BAs. Peak A was predominant in feces of male WT mice, but almost undetectable in feces of female WT mice, as well as Oatp1a1-null mice.

The decrease of TUCA suggests that knockout of Oatp1a1 decreases the bacteria-mediated 7-epimerization in the intestine of mice. It is known that UDCA is produced from 7-epimerization of CDCA by bacterial enzymes in the intestine (Lepercq et al., 2004). In this study, the concentrations of both TUDCA (75%) and UDCA (60%) decreased markedly in feces of Oatp1a1-null mice (Figure 5-8). Therefore, knockout of Oatp1a1 suppresses the 7-epimerization of BAs in the intestine of mice.

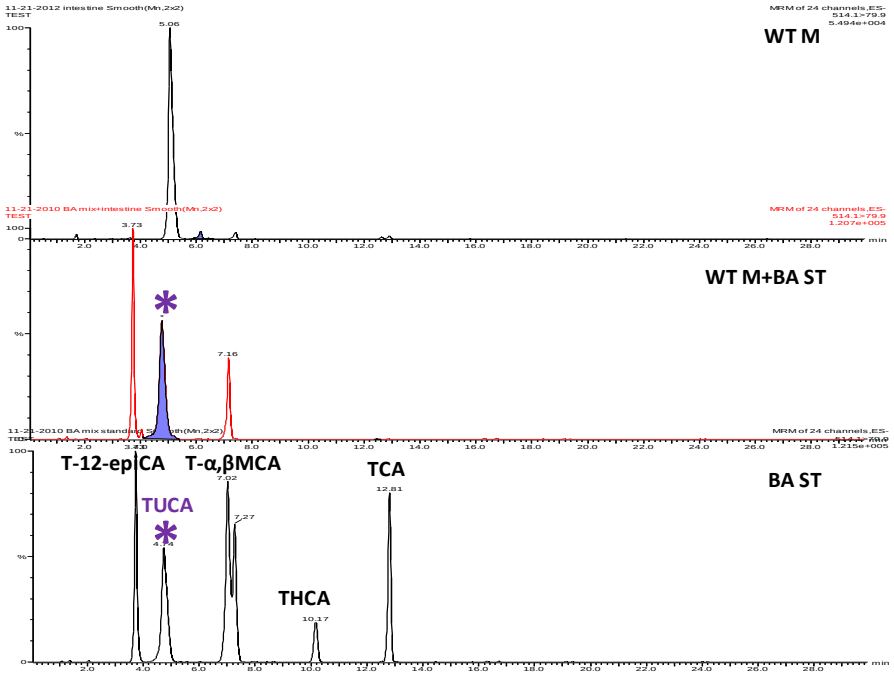

Figure 5-7. Identification of the unknown peak A in feces of mice. The chromatograph windows from fecal sample, fecal sample mixed with BA standards, and BA standards were compared. This peak has the same retention time as the standard TUCA.

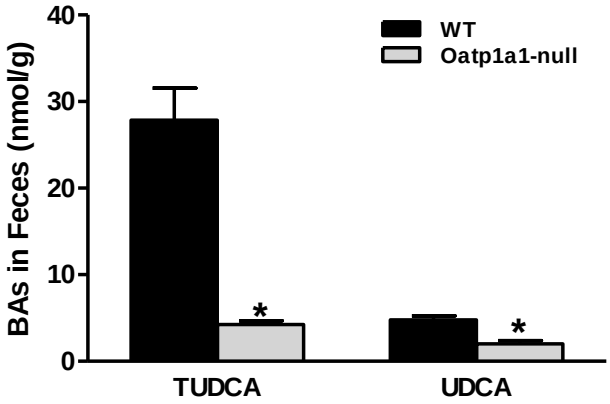

Figure 5-8. Concentrations of TUDCA and UDCA in feces of WT and Oatp1a1-null mice. Feces were collected from WT and Oatp1a1-null mice for 24 hr and dried under vacuum. The concentrations of TUDCA and UDCA in dried feces of male WT and Oatp1a1-null mice (n=5/group) were analyzed by UPLC-MS/MS. All data are expressed as mean ± S.E. for five mice in each group. *, statistically significant difference between WT and Oatp1a1-null mice ($p<0.05$).

2.7. Concentrations of Total BAs in Feces of WT and Oatp1a1-null Mice

The concentration of total BAs in feces was calculated by adding together the concentrations of all individual BAs. As shown in figure 5-9, the concentration of total conjugated BAs was decreased about 80%, whereas the concentration of total unconjugated BAs was increased about 70% in feces of Oatp1a1-null mice. As a result, the concentration of total fecal BAs in Oatp1a1-null mice tended to be, but not significantly lower than that in WT mice. In addition, the weight of feces, which were collected for 24 hr, was not significantly different between WT and Oatp1a1-null mice (data not shown). Thus, despite the different BA composition in feces, the total amount of BA excretion in feces is similar between WT and Oatp1a1-null mice.

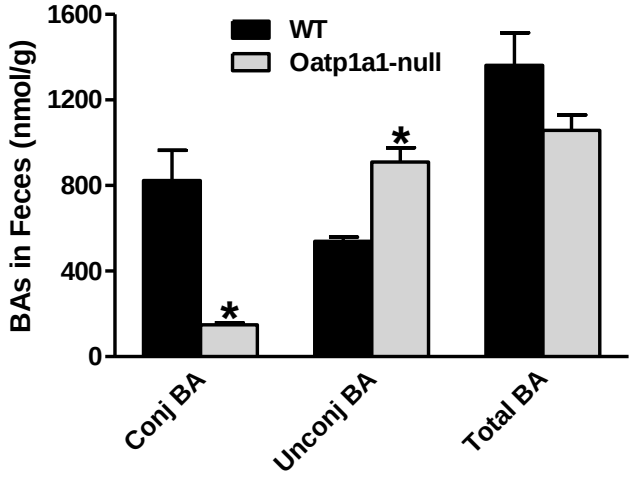

Figure 5-9. Concentrations of total conjugated BAs, total unconjugated BAs, and total BAs in feces of WT and Oatp1a1-null mice. Feces were collected from WT and Oatp1a1-null mice for 24 hr and dried under vacuum. The concentrations of total BAs were calculated by adding the concentrations of all BAs together. All data are expressed as mean ± S.E. for five mice in each group. *, statistically significant difference between WT and Oatp1a1-null mice ($p<0.05$).

2.8. Bacteria in the Small Intestinal Luminal Contents of WT and Oatp1a1-null Mice

Because knockout of Oatp1a1 markedly alters the fecal BAs that are made by bacterial enzymes, the bacteria in the intestinal contents of both WT and Oatp1a1-null mice were quantified. Figure 5-10 illustrates the bacteria in the small intestinal contents. Knockout of Oatp1a1 significantly increased *C. absonum* (85%), *C. perfringens* (350%), *C. scindens* (100%), *C. methylpentosum* (110%), and *C.* sp. ASF502 (ii) (220%) in the small intestine of mice (Figure 5-10a). *C. absonum* expresses both 7α- and 7β-HSDHs, and is shown to form UCA from CA and UDCA from CDCA, but does not transform DCA in whole cell cultures (Macdonald and Roach, 1981; Macdonald et al., 1981). *C. perfringens* express both BSH (Gopal-Srivastava and Hylemon, 1988) as well as 3α- and 12α-HSDHs (Macdonald et al., 1976). *C. scindens* express both 3α- and 7α-HSDHs, and show high BA 7α-dehydroxylation activity (Kitahara et al., 2000). Therefore, the increase in *C. absonum*, *C. perfringens*, and *C. scindens* suggests that BA epimerization, deconjugation, and 7α-dehydroxylation are enhanced in the small intestine of Oatp1a1-null mice.

In addition to Clostridia, knockout of Oatp1a1 also significantly increased several members of Lactobacilli (Figure 5-10b), such as *La. acidophilus* (190%), *La. reuteri* (200%), and *La.* sp. ASF519 (90%). The increase of *La. acidophilus* and *La.reuteri*, which express BSHs (Corzo and Gilliland, 1999; Martoni et al., 2008), suggests enhanced activity of BA deconjugation in the small intestine of Oatp1a1-null mice.

Almost all the Bacteroides members, including *Ba. acidifaciens*, *Ba. forsythus* (i and ii), *Ba. vulgatus*, *Ba.* sp. ASF519, and *Ba. distasonis* (i, ii, iii, iv, and v), were increased about 50-100 fold in the small intestine of Oatp1a1-null mice (Figure 5-10c). The increase of *Ba. vulgatus* and *Ba. distasonis*, which shows BSH and 7β-dehydroxylation acitivty, respectively (Kawamoto et al., 1989; Takamine and Imamura, 1985), suggests that BA deconjugation and 7β-dehydroxylation are increased in the small intestine of Oatp1a1-null mice.

Furthermore, as shown in figure 5-10d, knockout of Oatp1a1 also significantly increased other bacteria, including 1-8 fold increase in *Lactococcus lactis*, *Klebsiella granulomatis*, *Streptococcus gordnii*, *Eubacterium desmolans*, *Ralstonia* sp., *Eubacterium limosum*, *Acetibibrio cellulosolvens*, and *Ruminococcus gnavus*, as well as 20-100 fold increase in *Prevotella* sp. (i, and ii), *Porphyromonas* sp. (i), *Desulfovibrio* sp., and *Porphyromonas* sp. (ii).

Taken together, knockout of Oatp1a1 increased the total bacteria about 10-fold in the small intestine of mice. In addition, the bacterial species that increased by knockout of Oatp1a1 suggest that the activity of BA deconjugation, dehydroxylation, and epimerization are enhanced in the small intestine of Oatp1a1-null mice.

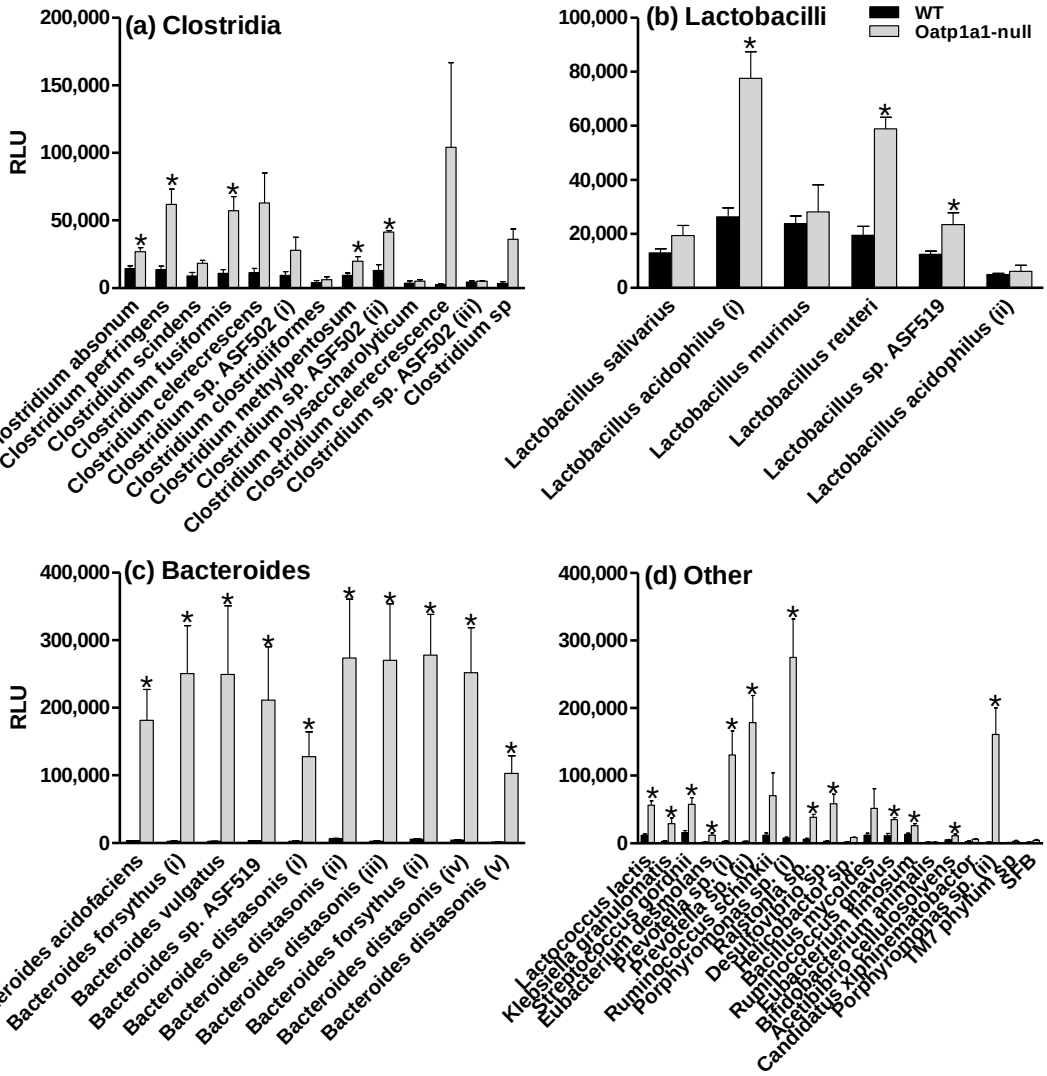

Figure 5-10. Small intestinal bacteria in WT and Oatp1a1-null mice. Clostridia (a), Lactobacilli (b), Bacteroides (c), and other bacteria (d) in the small intestinal contents of WT and Oatp1a1-null mice were quantified by branched DNA assay (Panomics/Affymetrix, Fremont, CA). All data are expressed as mean ± S.E. of five mice in each group. *, statistically significant difference between WT and Oatp1a1-null mice ($p<0.05$).

2.9. BA Composition in the Small Intestinal Luminal Contents of WT and Oatp1a1-null Mice

Because the BA concentrations in bile are similar between WT and Oatp1a1-null mice, the changes in the BA composition of the small intestinal contents reflect alterations in the small intestinal bacteria. As shown in figure 5-11a, conjugated BAs were the predominant BAs in the small intestinal contents of WT mice. Among them, TMCA and TCA were the two major conjugated BAs in the small intestinal contents of WT mice. Knockout of Oatp1a1 markedly decreased TMCA (60%) and TUDCA (81%) in the small intestinal contents of mice, suggesting enhanced BA-deconjugation activity in the small intestine of Oatp1a1-null mice (Figure 5-11b). The major unconjugated BAs in small intestinal contents of WT mice were ωMCA, βMCA, and CA (Figure 5-11a). Knockout of Oatp1a1 markedly increased CA (330%), MDCA (1150%), UDCA (170%), HDCA (220%), CDCA (130%), and DCA (1000%) in the small intestinal contents of mice (Figure 5-11b), suggesting enhanced activities of BA deconjugation (CA and CDCA), 7-dehydroxylation (MDCA and DCA), 7-epimerization (UDCA), and 6-epimerization (HDCA) in the small intestine of Oatp1a1-null mice. As a result, the composition of conjugated BAs in the small intestinal contents is about 85% in WT mice, but decreases to 52% in Oatp1a1-null mice.

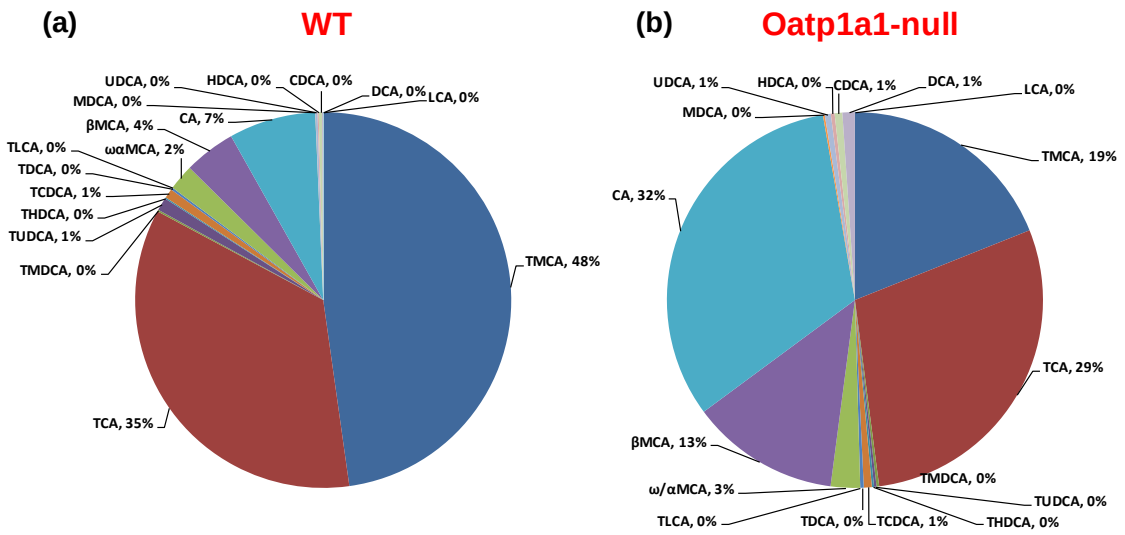

Figure 5-11. BA composition in the small intestinal luminal contents of WT and Oatp1a1-null mice. BA concentrations in the small intestinal luminal contents of male WT and Oatp1a1-null mice (n=5/group) were analyzed by UPLC-MS/MS. BA compositions were calculated for WT (a) and Oatp1a1-null mice (b).

2.10. Bacteria in the Large Intestinal Luminal Contents of WT and Oatp1a1-null Mice

Figure 5-12 illustrates the bacteria in the large intestinal luminal contents of WT and Oatp1a1-null mice. Knockout of Oatp1a1 significantly decreased almost all Clostridia, including *C. absonum* (30%), *C. perfringens* (30%), *C. sindens* (50%), *C. fusiformis* (30%), *C. celerecrescens* (30%), *C.* sp. ASF502 (i, ii and iii) (45%), *C. clostridiiformes* (65%), *C. polysaccharolyticum* (50%), and *C. celerecrescence* (40%), except for *C. methylpentosum* and *C.* sp. in the large intestinal contents of mice. The decrease of *C. absonum*, which mediates 7-epimerization, may explain the decrease of UDCA in feces of Oatp1a1-null mice. In addition to Clostridia, knockout of Oatp1a1 also decreased the *La. acidophilus* (13%) and *La. murinus* (40%) in the large intestine of mice. In contrast to Clostridia and Lactobacilli, knockout of Oatp1a1 markedly increased Bacteroides, including *Ba. acidofaciens* (105%), *Ba. forsythus* (ii and ii) (250%), *Ba.* sp. ASF519 (540%), *Ba. distasonis* (i, ii, and iv) (300-400%), and *Ba.*

distasonis (iii and v) (78-88 fold). Furthermore, knockout of Oatp1a1 decreased *Streptococcus gordnii* (25%), *Ruminococcus schinkii* (40%), *Ruminococcus gnavus* (35%), but increased *Prevotella* sp. (i, and ii) (200%), *Porphyromonas* sp. (i) (170%), *Porphyromonas* sp. (ii) (90 fold), and *Helicobactor* sp. (600%).

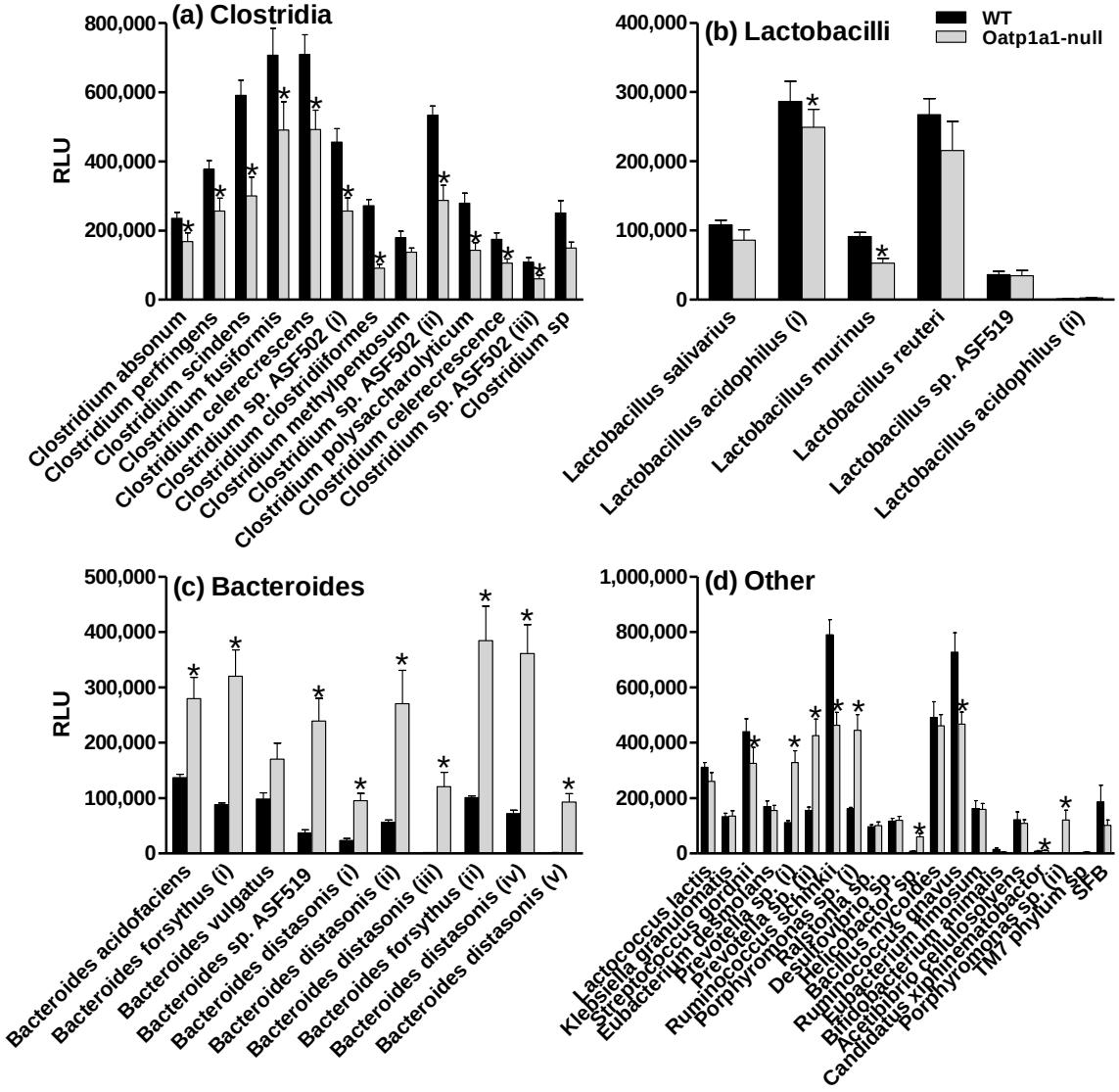

Figure 5-12. Large intestinal bacteria in WT and Oatp1a1-null mice. Clostridia (a), Lactobacilli (b), Bacteroides (c), and other bacteria (d) in the large intestinal luminal contents of WT and Oatp1a1-null mice were quantified by branched DNA assay (Panomics/Affymetrix, Fremont, CA). All data are

expressed as mean ± S.E. of five mice in each group. *, statistically significant difference between WT and Oatp1a1-null mice ($p<0.05$).

Taken together, knockout of Oatp1a1 decreased Clostridia and Lactobacilli, but increased Bacteroides in the large intestine of mice. As a result, the total bacteria increased about 97% in Oatp1a1-null mice, mainly due to the increase in Bacteroides. Because the percentage of the increase in Bacteroides (280%) is higher than the percentage of the decrease in Clostridia and Lactobacilli (35%), the large intestine of Oatp1a1-null mice may have higher activity of BA deconjugation, epimerization, and oxidation than that of WT mice. In addition, because the majority of UDCA is produced in the large intestine, the decrease of *C. absonum* in the large intestine of Oatp1a1-null mice may explain why knockout of Oatp1a1 decreased both TUDCA and UDCA in the feces of mice, although *C. absonum* is increased in the small intestine of Oatp1a1-null mice resulting in an increase of both TUDCA and UDCA in the small intestinal contents.

2.11. Composition of BAs in the Large Intestinal Luminal Contents of WT and Oatp1a1-null Mice

In contrast to the small intestinal contents, the major BAs in the large intestinal contents of WT mice were unconjugated BAs (Figure 5-13a). Knockout of Oatp1a1 decreased TMCA (70%), TUDCA (70%), and TCDCA (50%), resulting in a 50% decrease of the total conjugated BAs in the large intestinal contents of mice (Figure 5-13b). In contrast, knockout of Oatp1a1 increased TDCA about 280% in the large intestinal contents of mice. Compared to WT mice, βMCA (40%) and UDCA (69%) were decreased, whereas CDCA (210%), MDCA (320%), HDCA (150%), DCA (310%), and LCA (320%) were increased in the large intestinal contents of Oatp1a1-null mice. Taken together, the overall activities of BA deconjugation, dehydroxylation, and epimerization are enhanced in the large intestinal contents of Oatp1a1-null mice.

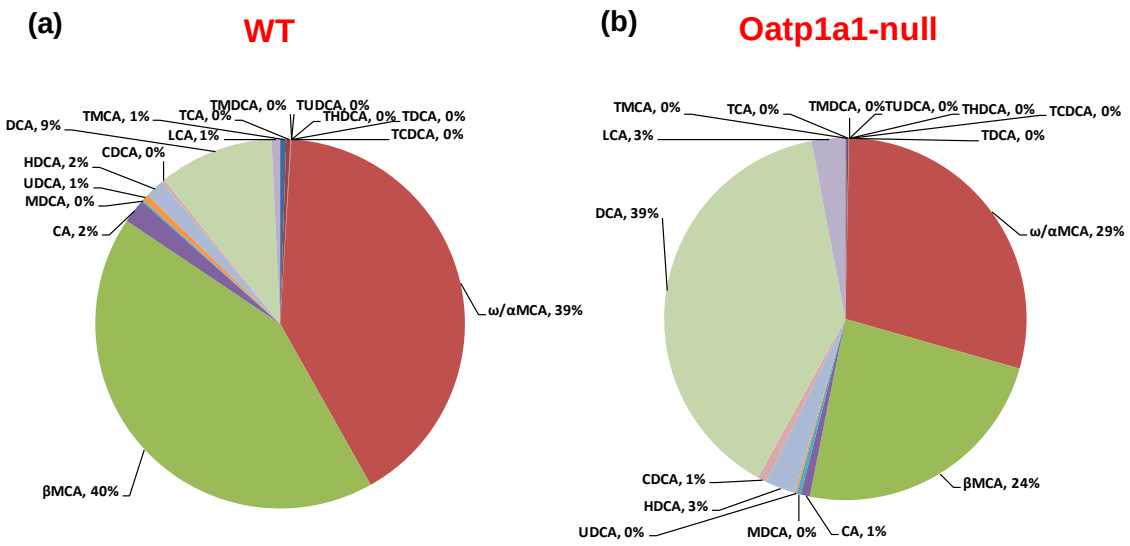

Figure 5-13. BA composition in the large intestinal luminal contents of WT and Oatp1a1-null mice. BA concentrations in the large intestinal luminal contents of male WT and Oatp1a1-null mice (n=5/group) were analyzed by UPLC-MS/MS. BA compositions were calculated for WT (a) and Oatp1a1-null mice (b).

2.12. Urinary Metabolomic Profiling of WT and Oatp1a1-null Mice

The mammalian intestinal microbiota interact extensively with the host through metabolic exchange and co-metabolism of substrates. The importance of such metabolome-metabolome interactions has been implicated by comparing the metabolomic profiling between conventional and germ-free animals (Wikoff et al., 2009). Because the intestinal bacteria altered in Oatp1a1-null mice are not limited to those bacteria involved in BA metabolism, we conducted urinary metabolomic analysis in WT and Oatp1a1-null mice to determine whether the urinary metabolomic profile of Oatp1a1-null mice will reflect changes of intestinal bacteria, as well as transport activity in mice. In this study, TOFMS was operated in both the positive and negative modes with electrospray ionization. The unsupervised PCA analysis score plot of the urine (Figure 5-14a and c) revealed two clusters, corresponding to the WT and

Oatp1a1-null mice. The S-plots generated from OPLC-DA display the ion contribution to the group separation in the urine (Figure 5-14b and d).

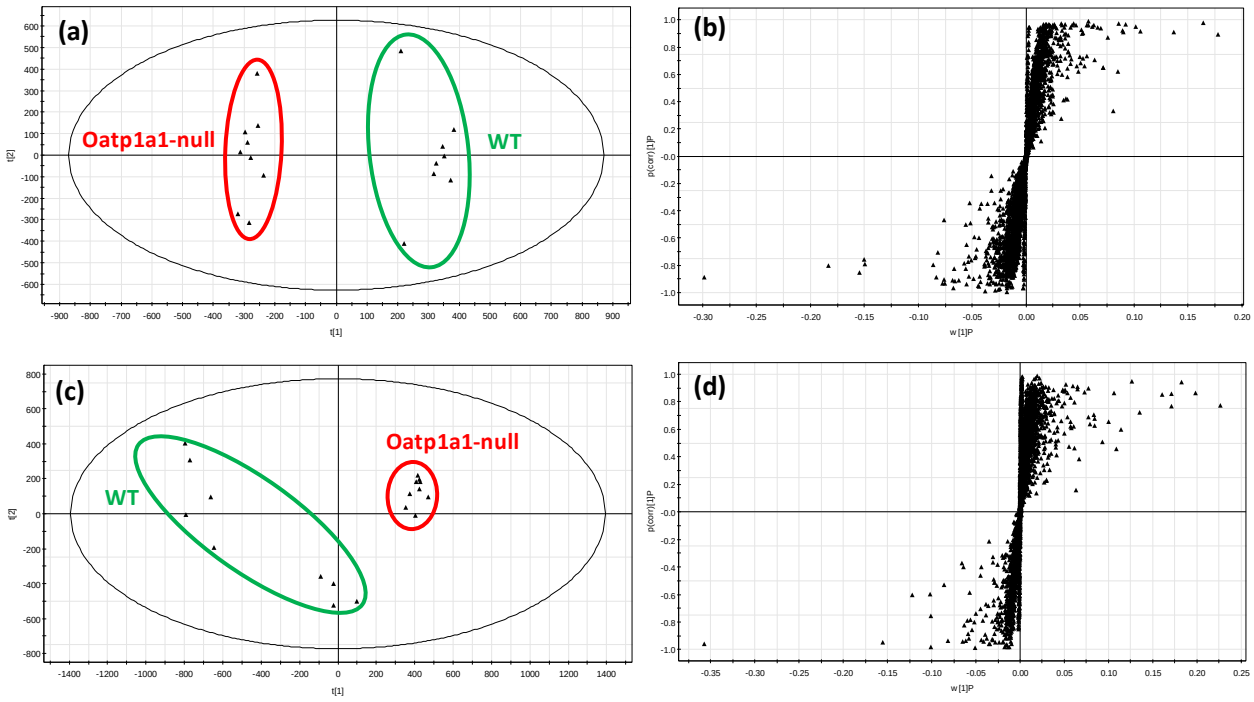

Figure 5-14. Metabolomic analysis of WT and Oatp1a1-null mouse urine. Urine of two-month-old male WT and Oatp1a1-null mice (n=9) were collected for analysis. (a) Separation of WT and Oatp1a1-null mouse urine in a PCA score plot with operation of TOFMS in the positive mode. The t[1] and t[2] values represent the score of each sample in principal component 1 and 2, respectively. (b) Loading *S*-plot generated by OPLS-DA analysis of metabolome in urine of Oatp1a1-null mice with the operation of TOFMS in the positive mode. The *X*-axis is a measure of the relative abundance of ions and the *Y*-axis is a measure of the correlation of each ion to the model. These loading plots represent the relationship between variables (ions) in relation to the first and second components present in the PCA score plot. (c) Separation of WT and Oatp1a1-null mouse urine in a PCA score plot with operation of TOFMS in the negative mode. (d) Loading *S*-plot generated by OPLS-DA analysis of the metabolome in urine of Oatp1a1-null mice with the TOFMS in the negative mode. Based on the MS/MS fragmentations, we identified lower concentrations of glucuronidated indole-3-carboxylic acid (indole-3-carboxylic acid-G), glucuronidated-daidzein (daidzein-G), and glucuronidated-*O*-desmethylangolensin (*O*-desmethylangolensin-G), as well as higher concentration of hippuric acid in the urine of Oatp1a1-null mice than in WT mice (Figure 5-15).

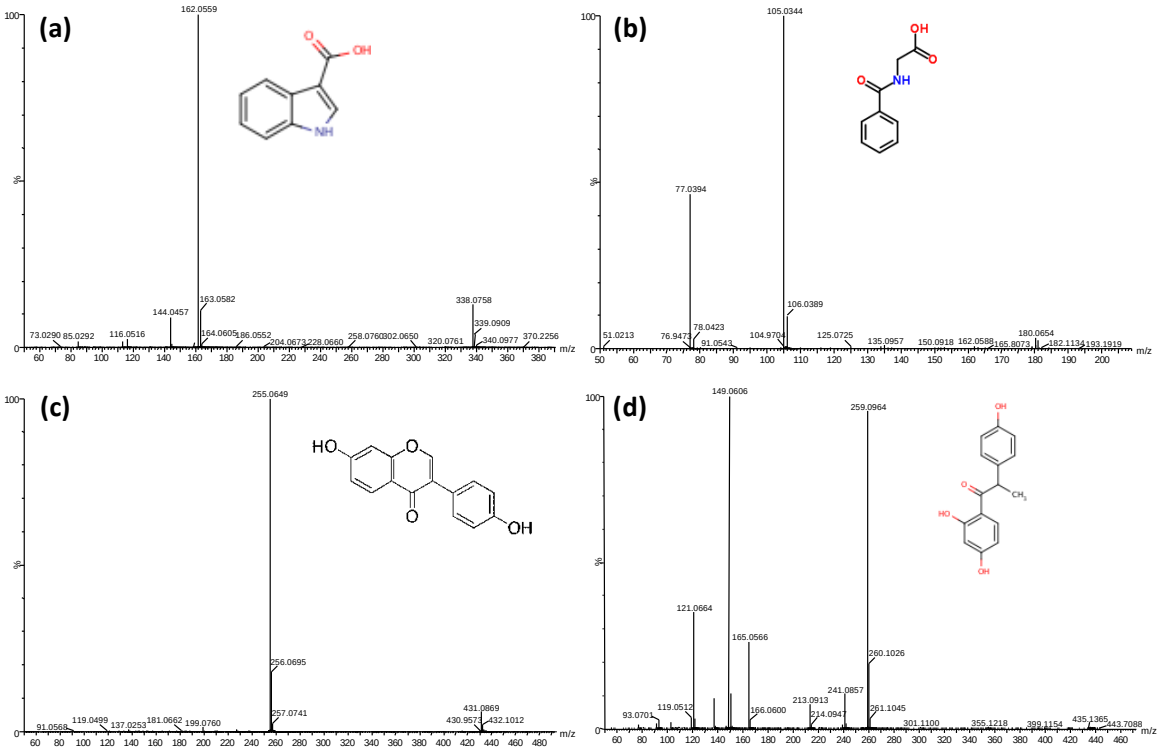

Figure 5-15. Identification of (a) glucuronidated-indole-3-carboxylic acid, (b) hippuric acid, (c) glucuronidated-daidzein, and (d) glucuronidated-*O*-desmethylangolensin in urine of WT and Oatp1a1-null mice. Structural elucidations were performed based on accurate mass measurement (mass errors less than 10 ppm) and MS/MS fragmentations. MS/MS fragmentation was conducted with collision energy ramping from 10 eV.

The standards, indole-3-carboxylic acid-G and daidzein-G were enzymatically synthesized from indole-3-carboxylic acid and daidzein, respectively. By comparison of the retention time in the same MS/MS chromatograph window, we confirmed indole-3-carboxylic acid-G and hippuric acid in the urine samples (Figure 5-16a and b). The enzymatic reaction of daidzein resulted in three daidzein glucuronides, suggesting that daidzein can be glucuronidated at different positions. There was one peak with the same retention time as one of daidzein-Gs in the urine samples (Figure 5-16c). In addition, there were four peaks with the same molecular weight as daidzein in the urine samples, one of which was confirmed as daidzein by the authentic standard (Figure 5-16d).

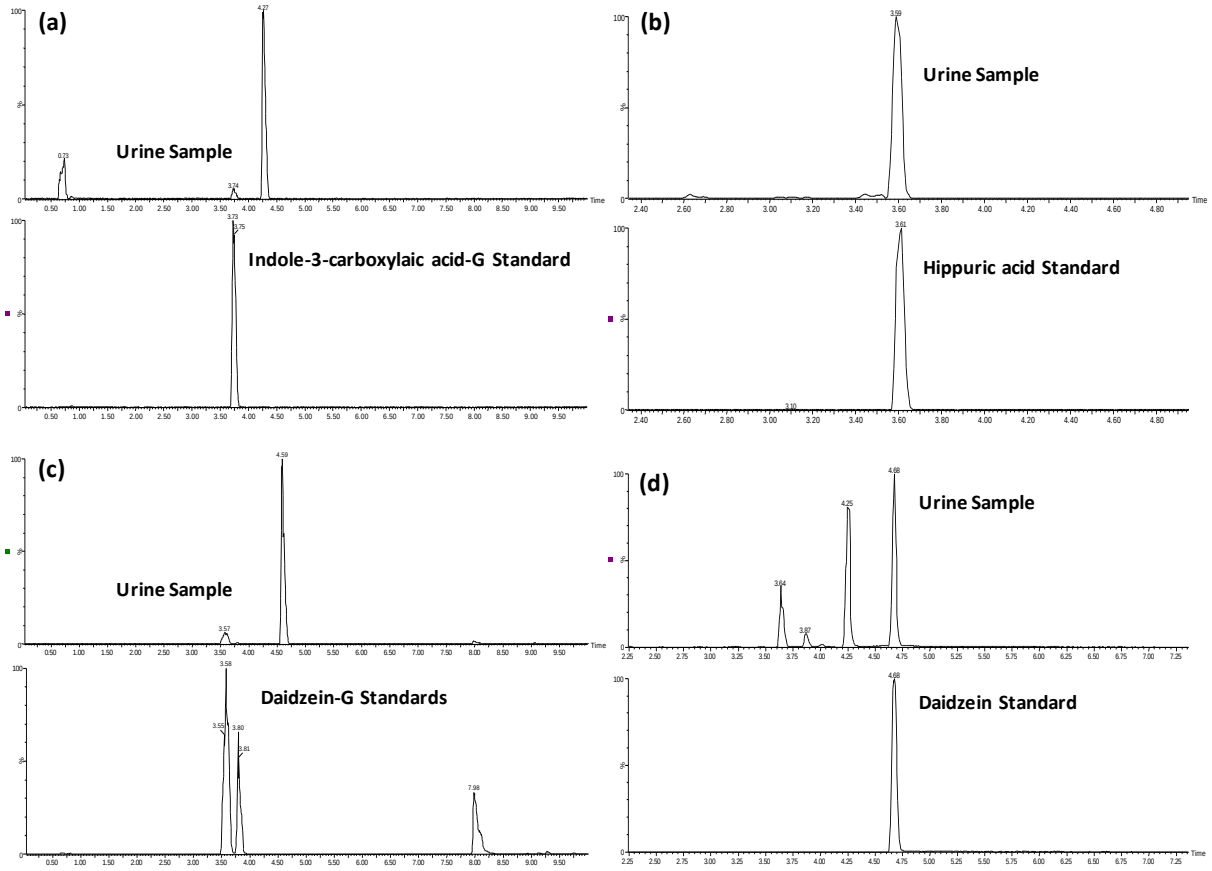

Figure 5-16. Confirmation (a) glucuronidated-indole-3-carboxylic acid, (b) hippuric acid, (c) glucuronidated-daidzein, and (d) daidzein in the urine samples by comparison their retention time with authentic standards.

Taken together, metabolomic analysis revealed that knockout of Oatp1a1 decreased indole-3-carboxylic acid-G, daidzein-G, as well as *O*-desmethylangolensin-G, but increased hippuric acid in the urine of mice. The intestinal bacteria are known to play important roles in the production or breakdown of these metabolites (Patrick et al., 1976; Schoefer et al., 2002; Wikoff et al., 2009). Therefore, the increase or decrease of these metabolites further provides evidence on the alterations of intestinal bacteria in Oatp1a1-null mice.

2.13. Urinary Excretion of Riboflavin in WT and Oatp1a1-null Mice.

During the metabolomic analysis of urine, we identified and confirmed riboflavin, which was higher in the urine of Oatp1a1-null mice than in WT mice (Figure 5-17a and b). Riboflavin can be synthesized by intestinal lactic acid bacteria (Burkholder et al., 1942). The lactic acid bacteria include the genera Lactobacillus, Lactococcus, Leuconostoc, Pediococcus, and Streptococcus (Daly et al., 1996). Riboflavin can be synthesized by Lactococcus lactis (Burgess et al., 2004). The intestinal absorption of riboflavin has been suggested to be mediated by a riboflavin transporter (RFT), which is highly expressed in the small intestine of humans and rats (Yonezawa et al., 2008; Fujimura et al., 2010). This suggests that the majority of riboflavin is absorbed in the small intestine. Therefore, the increase of lactic acid bacteria, such as Lactococcus lactis, in the small intestine of Oatp1a1-null mice may increase the biosynthesis and intestinal absorption of riboflavin, and thus result in an increase in the urinary excretion of riboflavin in Oatp1a1-null mice.

To further determine whether knockout of Oatp1a1 alters the disposition of riboflavin, mice were injected i.p. either riboflavin (RF) or flavin mononucleotide (FMN), and urine was collected for 24 hr to quantify the concentrations of RF and FMN. More than 97% of FMN was converted to RF in mice treated with FMN (Figure 5-17c). Knockout of Oatp1a1 increased the urinary excretion of RF about 82% and 74% in mice after RF and FMN injection, respectively. This suggests that knockout of Oatp1a1 may decrease the hepatic uptake or the renal reabsorption of riboflavin in mice, because Oatp1a1 is highly expressed at the basolateral membrane of hepatocytes and the apical membrane of kidney. Therefore, further studies are necessary to evaluate the role of Oatp1a1 in the disposition of riboflavin.

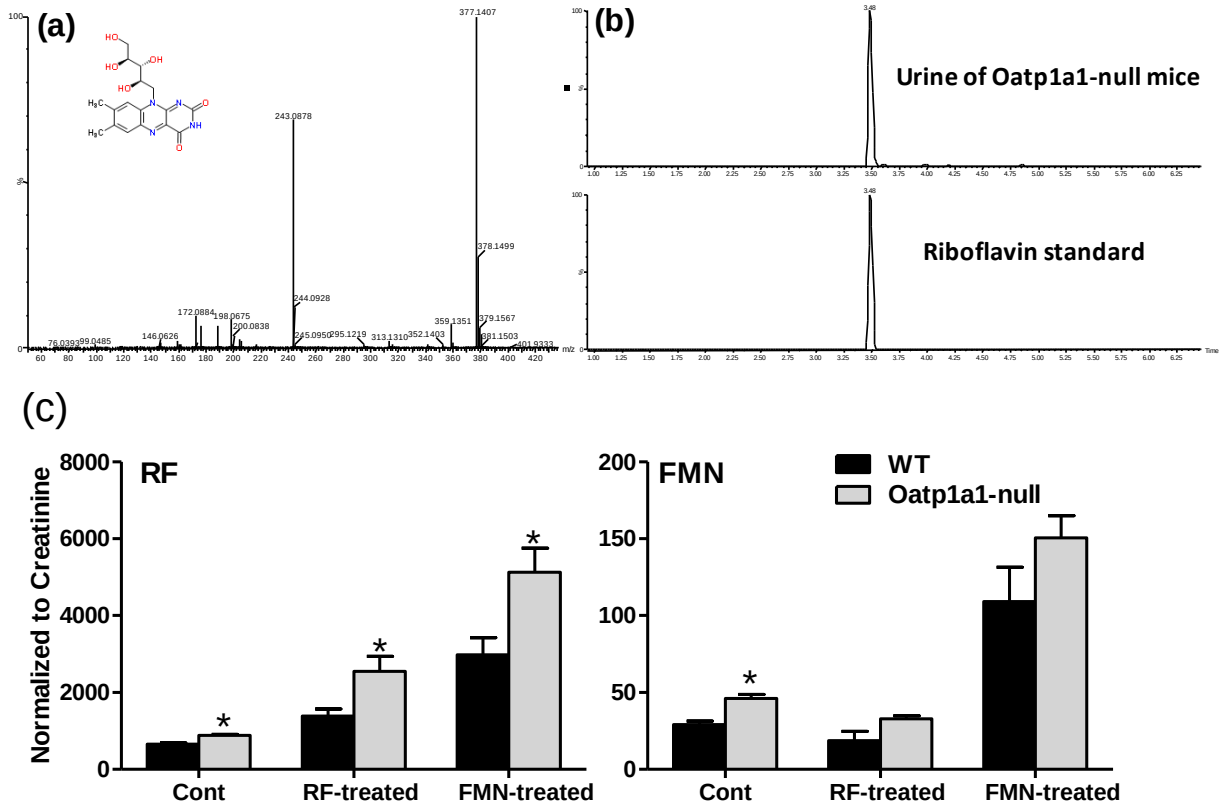

Figure 5-17. Urinary excretion of riboflavin in WT and Oatp1a1-null mice. Riboflavin was identified (a) and confirmed by authentic standard (b) in the urine of Oatp1a1-null mice. The concentration of RF (c, left) and FMN (c, right) was quantified by UPLC-MS/MS in the 24 hr urine collected from WT and Oatp1a1-null mice after i.p. injection of RF and FMN, and normalized by urinary creatinine. All data are expressed as mean ± S.E. of five mice in each group. *, statistically significant difference between WT and Oatp1a1-null mice ($p<0.05$).

III. Discussion

As a transporter, mouse Oatp1a1 is implicated to be important in the hepatic uptake and renal reabsorption of endogenous compounds and xenobiotics, due to its high expression at the basolateral membrane of hepatocytes and the apical side of renal tubules. Oatp1a1 has been shown to transport BAs, such as TCA *in vitro* (Hagenbuch et al., 2000). In our previous study, we showed that Oatp1b2, a liver-specific Oatp in mice, is important for transporting unconjugated BAs (Csanaky et al., 2010). In addition, knockout of Oatp1a1 has little effect on other BA transporters in livers and intestines of mice. Thus, we hypothesized that BA concentrations will increase in the serum but decrease in livers of Oatp1a1-null mice. Surprisingly, the concentration of total BAs in serum was less in Oatp1a1-null mice, mainly due to a decrease in TMCA and TCA. Although TDCA and DCA are increased in the serum of Oatp1a1-null mice, it does not appear to be due to disruption of hepatic uptake, because TDCA is also increased in livers of Oatp1a1-null mice. As further evidence, kinetics of an exogenous dose of DCA indicated that knockout of Oatp1a1 did not slow the plasma elimination of DCA in mice. Knockout of Oatp1a/1b (Oatp1a1, 1a4, b2, and 1a6) increased markedly the concentration of total BAs, in particular unconjugated BAs, in serum of mice (Steeg et al., 2010). The elevated concentration of unconjugated BAs in Oatp1a/1b-null mice is similar to that in serum of Oatp1b2-null mice, in which the concentration of unconjugated BAs, but not conjugated BAs, increased significantly (Csanaky et al., 2010). This suggests that the increase of BAs in Oatp1a/1b-null mice is due to the knockout of Oatp1b2, but not Oatp1a1. Taken together, Oatp1a1 may not be important in the hepatic uptake of BAs, but play a critical role in the regulation of intestinal bacteria.

Knockout of Oatp1a1 markedly alters the composition and amount of intestinal bacteria, and thus alters the intestinal BA metabolism. The concentration of individual BAs in the bile, and the bile flow rate are the same in WT and Oatp1a1-null mice, suggesting that knockout of Oatp1a1 does not alter the BAs entering the intestine. Knockout of Oatp1a1 increased the total bacteria about 10 fold in the small intestine of mice, and the bacterial species that increased suggest that the activity of BA deconjugation,

dehydroxylation, and epimerization are enhanced in the small intestine of Oatp1a1-null mice. This is consistent with the alterated BA composition in the small intestinal contents of Oatp1a1-null mice, in which conjugated BAs, such as TMCA and TUDCA, are decreased, whereas unconjugated BAs, such as CA, MDCA, HDCA, CDCA, and DCA, are increased. Knockout of Oatp1a1 decreased Clostridia and Lactobacilli, but increased Bacteroides in the large intestine of mice. However, the percent increase in Bacteroides (280%) is higher than the percent decrease in Clostridia and Lactobacilli (35%), suggesting that the large intestine of Oatp1a1-null mice have higher activity of BA deconjugation, epimerization, and oxidation than WT mice. Therefore, conjugated BAs, such as TMCA, TCA, and TCDCA are further decreased, whereas unconjugated BAs, such as CDCA, DCA, and LCA, are further increased in the large intestinal contents of Oatp1a1-null mice. The alterations of BA composition in the intestine are reflected by the BA concentrations in feces, where the conjugated primary BAs (taurine-, glycine-, and sulfate-conjugated BAs) are markedly decreased, but secondary BAs that are produced by 7-dehydroxylation, oxidation, and epimerization, are markedly increased in Oatp1a1-null mice. TUCA, which is high in the large intestine but almost undetectable in the small intestine, suggests that BA 7-epimerization occurs predominantly in the large intestine of mice. The decrease of TUCA in Oatp1a1-null mice may be due to the decrease of *C. absonum* in large intestine, which may also explain the decrease of TUDCA and UDCA in the large intestine of Oatp1a1-null mice. Although *C. absonum* is increased in the small intestine of Oatp1a1-null mice, the concentration of UDCA is decreased in the feces because most of UDCA is produced in the large intestine. Interestingly, despite the marked changes in BA composition, the total BA excretion in feces is similar between WT and Oatp1a1-null mice. This is consistent with the similar billiary excretion of BAs into the intestine between these two mouse strains. Taken together, the alterations of intestinal bacteria in Oatp1a1-null mice result in marked changes in BA composition in intestine and feces, but have little effect on the total fecal BA excretion, due to the same billiary input of BAs between WT and Oatp1a1-null mice.

FXR has been shown to play a critical role in preventing bacterial overgrowth and maintaining the integrity of the intestinal epithelium. For example, administration of GW4064, a FXR agonist, blocks bacterial overgrowth and translocation in ilea and ceca of BDL mice (Inagaki et al., 2006). In the present study, knockout of Oatp1a1 has little effect on FXR mRNA expression, but tends to decrease Fgf15 mRNA expression in ilea of mice. In addition, knockout of Oatp1a1 decreases the concentrations of conjugated BAs in ilea and thus decreases the influx of BAs into enterocytes. Therefore, it is possible that knockout of Oatp1a1 deactivates FXR in ilea of mice, and thus results in bacterial overgrowth and enhanced intestinal permeability. Further studies are required to understand whether and how knockout of Oatp1a1 deactivates FXR in ilea of mice.

The results from the present study suggest a critical role of Oatp1a1 in mouse nutrition and obesity. Because knockout of Oatp1a1 changes the intestinal BA composition and bacteria, the intestinal absorption and metabolism of cholesterol, lipids, food supplements, and vitamins may be increased or decreased in Oatp1a1-null mice. These alterations were revealed by metabolomic analysis of mouse serum and urine. The increase of hippuric acid and the decrease of indole-3-carboxylic acid further reveals alterations of intestinal bacteria in Oatp1a1-null mice, because intestinal bacteria play important roles in their production and metabolism (Wikoff et al., 2009). Some of the most altered metabolites in urine of Oatp1a1-null mice are isoflavones, such as daidzein, and vitamins, such as riboflavin. Both daidzein and its bacteria-mediated metabolite, namely *O*-desmethylangolensin, are decreased in the urine of Oatp1a1-null mice, suggesting a critical role of Oatp1a1 in the disposition of daidzein. Daidzein has been shown to have beneficial effect on obesity, hypertension, cholesterol, and glucose levels in animals and humans (Bhathena et al., 2002, Manzoni et al., 2005; Furumoto et al., 2010). Therefore, Oatp1a1-null mice may be susceptible to low-daidzein and high-fat diets. In a preliminary study, we observed that triglyceride concentrations in livers were markedly higher in Oatp1a1-null mice than in WT mice, when feeding a Teklad #2108C diet, which contains lower isoflavones but higher fat than the Tekalad #8604 diet (data not shown). It is established that riboflavin participates in a diversity of redox reactions central

to human metabolism, and that riboflavin deficiency has been linked to abnormal gastrointestinal development, neurodegeneration, cardiovascular diseases, and cancer (Powers, 2003). Riboflavin is increased in urine of Oatp1a1-null mice, which may be due to an increase in riboflavin biosynthesis from lactic acid bacteria, such as *Lactococcus lactis*, which are increased in the small intestine of Oatp1a1-null mice. However, urinary excretion of riboflavin indicated that Oatp1a1 may also play an important role in the hepatic uptake or the renal reabsorption of riboflavin in mice. Therefore, further studies are required to determine whether the effects of Oatp1a1 on the disposition of isoflavones and vitamins are direct or indirect.

Furthermore, the present study on mouse Oatp1a1 provides valuable information for future studies in mouse obesity and aging. Cheng et al. (2008) showed that Oatp1a1 mRNA and protein expression in livers of ob/ob mice were diminished to <5% and <15%, respectively, of that in WT mice. In contrast, Oatp1a4 and 1b2 were not altered in the livers of ob/ob mice. This suggests that Oatp1a1 may play a unique and essential role in obesity. Compared to lean mice, ob/ob mice have a 50% reduction in the abundance of Bacteroidetes, and a proportional increase in Firmicutes in the contents of ceca (Ley et al., 2005). In contrast, compared to WT mice, Oatp1a1-null mice have a 200% increase of Bacteroidetes, and a 30% reduction of Firmicutes in the large intestine. This suggests that the suppression of Oatp1a1 in ob/ob mice may be an adaptive response for mice to maintain the homeostasis of intestinal bacteria. In addition to the suppression of Oatp1a1 in ob/ob mice, hepatic Oatp1a1 can also be suppressed by high-fat diet in rats (Fisher et al., 2009). Thus, further research is required to clarify the regulation of Oatp1a1 and the metabolism of BAs in ob/ob mice. Zhang et al. (2010) showed that Oatp1a1 in livers of mice is decreased by aging and energy restriction. This may be due to the physiological decline in growth hormone during aging or due to the feminization of gene expression in mice with caloric restriction (Tollet-Egnell et al., 2001; Estep et al., 2009), because Oatp1a1 is induced by male-pattern growth hormones and androgens (Cheng et al., 2006). However, it remains unclear how the

suppression of Oatp1a1 during aging and energy restriction contributes to the homeostasis of nutrition and obesity.

In summary, mouse Oatp1a1 does not appear to be important in the hepatic uptake of BAs, but plays an important role in maintaining the homeostasis of intestinal bacteria. This suggests that Oatp1a1 may have implications in nutrition, obesity, energy restriction, and aging. It remains unclear how knockout of Oatp1a1 alters the intestinal bacteria in mice. Given the ability to transport various endogenous compounds, such as hormones, eicosanoids and peptides (Hagenbuch and Meier, 2003), as well as fatty acid analogues, such as perfluorinated carboxylates (Weaver et al., 2010), it is possible that knockout of Oatp1a1 disrupts the disposition of some endogenous substrates, which are important to maintain normal functions of the intestine.

CHAPTER 6

THE CRITICAL ROLE OF MOUSE OATP1A1 IN EXTRAHEPATIC CHOLESTASIS

Specific Aim and Hypothesis

Chapter 6 will address specific aim 3 and evaluate the hypothesis that knockout of Oatp1a1 decreases the liver toxicity in mice during extrahepatic cholestasis. The decrease of Oatp1a1 in mice after bile duct ligation (BDL) has been suggested to be a protective mechanism for the liver to protect against the accumulation of BAs. However, chapter 3 and 4 suggest that Oatp1a1 may be not important for the *in vivo* hepatic uptake of BAs, but may play a role in maintaining the homeostasis of intestinal bacteria in mice. Therefore, the purpose of this study is to determine the *in vivo* role of mouse Oatp1a1 during BDL-induced extrahepatic cholestasis by using Oatp1a1-null mice.

I. Introduction

Cholestasis is a reduction of bile flow, resulting in the hepatic retention of products normally excreted into bile, such as cholesterol and BAs. The progression of cholestasis causes hepatocellular injury, bile-duct proliferation, fibrosis, cirrhosis, and finally liver failure (Sellinger and Boyer, 1990). Cholestasis has been examined in rats by surgical ligation of the common bile duct (Johnstone and Lee, 1976). More recently, as a result of new technologies to generate genetically modified animals, mice have become a popular experimental model for studying extrahepatic cholestasis by BDL.

Adaptive responses in liver during cholestasis include suppression of BA-uptake, induction of BA-efflux, inhibition of BA-synthesis, and acceleration of BA-detoxification (Boyer, 2007; Hofmann, 2007; Copple et al., 2010). For example, BDL has been shown to decrease BA-uptake transporters (such

as Ntcp, Oatp1a1, and Oatp1b2), increase BA-efflux transporters (such as Bsep, Mrp3, Mrp4, and Ostβ), and decrease BA-synthetic enzymes (Cyp7a1) in livers of mice (Slitt et al., 2006; Soroka et al., 2010; Park et al., 2008). Although BDL has been shown to increase the total BA concentrations in both serum and livers of mice (Slitt et al, 2006), little is known about the concentrations of individual BAs in serum and livers of mice after BDL. In addition, previous studies showed non-consistent effects of BDL on BA-transporters and BA-synthetic enzymes in mice, probably because they quantified the mRNA expression of these genes at different and limited time intervals after BDL. Because cholestasis is a chronic progressive disease, it is important to know the time course of the effects of BDL on BA-transporters and BA-synthetic enzymes to understand their roles at different stages of cholestasis. Therefore, the time course of BA concentrations as well as the mRNA expression of BA transporters in livers of WT mice was determined at various times after BDL.

Because Oatp1a1 is decreased markedly in BDL mice (Slitt et al., 2006), we hypothesize that knockout of Oatp1a1 will protect against the liver toxicity by reducing the hepatic uptake of BAs in mice after BDL. To evaluate this hypothesis, an early time point after BDL, when Oatp1a1 has not been decreased prominently in livers of WT mice, and a later time point after BDL, when Oatp1a1 has been decreased markedly in livers of WT mice, will be examined. By comparing the time courses of individual BAs in serum and livers of WT and Oatp1a1-null mice, the role of Oatp1a1 in mice during BDL-induced extrahepatic cholestasis may be revealed, and some BAs may be identified as endogenous substrates for Oatp1a1. Therefore, we also plan to determine whether and how knockout of Oatp1a1 prevents liver toxicity in mice during BDL-induced extrahepatic cholestasis.

II. Results

2.1. Serum BAs in C57BL/6 mice after BDL

Total BA concentrations in mouse serum were quantified at 0 h, 6 h, 12 h, 1 d, 2 d, 3 d, 5 d, 7 d, and 14 d after sham and BDL surgeries (Figure 6-1). During the study, the sham-operated mice maintained their serum BA concentrations in the range of 0.5 to 2.3 nmol/ml. BDL increased unconjugated (1.3→360 mmol/ml) and conjugated (0.5→2100) BAs in mouse serum about 300 and 4000 fold, respectively, within 6 h. Thereafter, unconjugated BAs in serum of BDL mice decreased about 99% between 6 h and 14 d (360→3.2), but were still about 3-fold higher than sham-operated mice at 14 d. In contrast, conjugated BAs in serum of BDL mice decreased about 60% between 6 h and 1 d (2100→869), followed by a tripling between 1 and 5 d, and thereafter was maintained at concentrations (~3000 nmol/ml) about 3000-fold higher than sham-operated mice. Two weeks after surgery, more than 99% of BAs in serum of BDL mice were conjugated, whereas only 60% of BAs in serum of sham-operated mice were conjugated. Mainly due to the increase in conjugated BAs, the total BA concentration in serum of BDL mice increased about 1360 fold at 6 h (1.8→2460 nmol/ml), followed by a 60% decrease (2460→884) from 6 h to 1 d, and increased again from 1 to 5 d to a final concentration of 2890 to 3250 nmol/ml.

The major primary BAs in serum of sham-operated mice were CA (0.1~0.2), TCA (0.1~1.2), α/ωMCA (0.2~0.7), βMCA (0.1~0.2), and TMCA (0.2~1.4 nmol/ml) (Figure 6-2a). After BDL, most primary BAs, except GCDCA, underwent a marked increase at 6 h (CA: 0.2→17, GCA: 0.0→1.1, TCA: 0.1→1070, CDCA: 0.0→0.1, TCDCA: 0.0→7.2, α/ωMCA: 0.7→87.5, βMCA: 0.2→253.7, and TMCA: 0.2→1004), followed by a rapid decrease from 6 h to 1 d. After that, serum CA and CDCA in BDL mice decreased to the level in sham mice, whereas α/ωMCA (0.4~2.5) and βMCA (1.7~39.2) remained at a higher concentration than in sham controls. In contrast, GCA (0.1→0.3), TCA (319→649), TCDCA (4.0→62.8), and TMCA (543→2030) in serum of BDL mice increased markedly from 1 d to 5 d. As a

result, after 1d of BDL, βMCA and TMCA became the predominant unconjugated and conjugated BAs, respectively, in mouse serum.

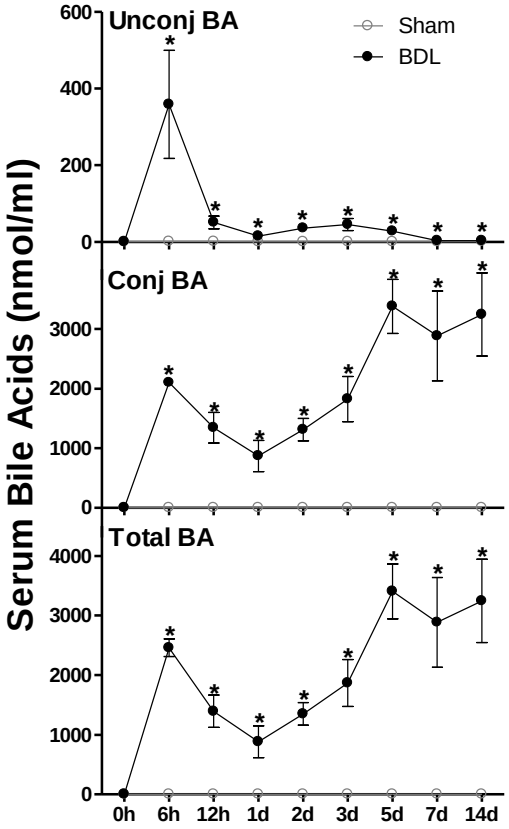

Figure 6-1. Unconjugated, conjugated, and total BA concentrations in serum of sham-operated and BDL mice. All BA data are expressed as mean ±S.E. of six mice in each group. *, Statistically significant difference between sham-operated (open circles) and BDL (closed circles) mice ($p<0.05$).

Figure 6-2b shows the time course of secondary BAs in serum of mice after surgery. The predominant secondary BAs in serum of sham-operated mice were TDCA (0.02~0.05 nmol/ml) and UDCA (0.09~0.13). BDL had little effect on DCA, TDCA, LCA, and UDCA, although it increased TDCA and TLCA at 6 h and 1 d after surgery. Interestingly, BDL increased TUDCA markedly at 6h

(0.0→15.6), followed by a decrease from 6h to 1d (15.6→2.5), and another increase from 1d to 5d (2.5→24.4). Therefore, after BDL, TUDCA became the predominant secondary BA in mouse serum.

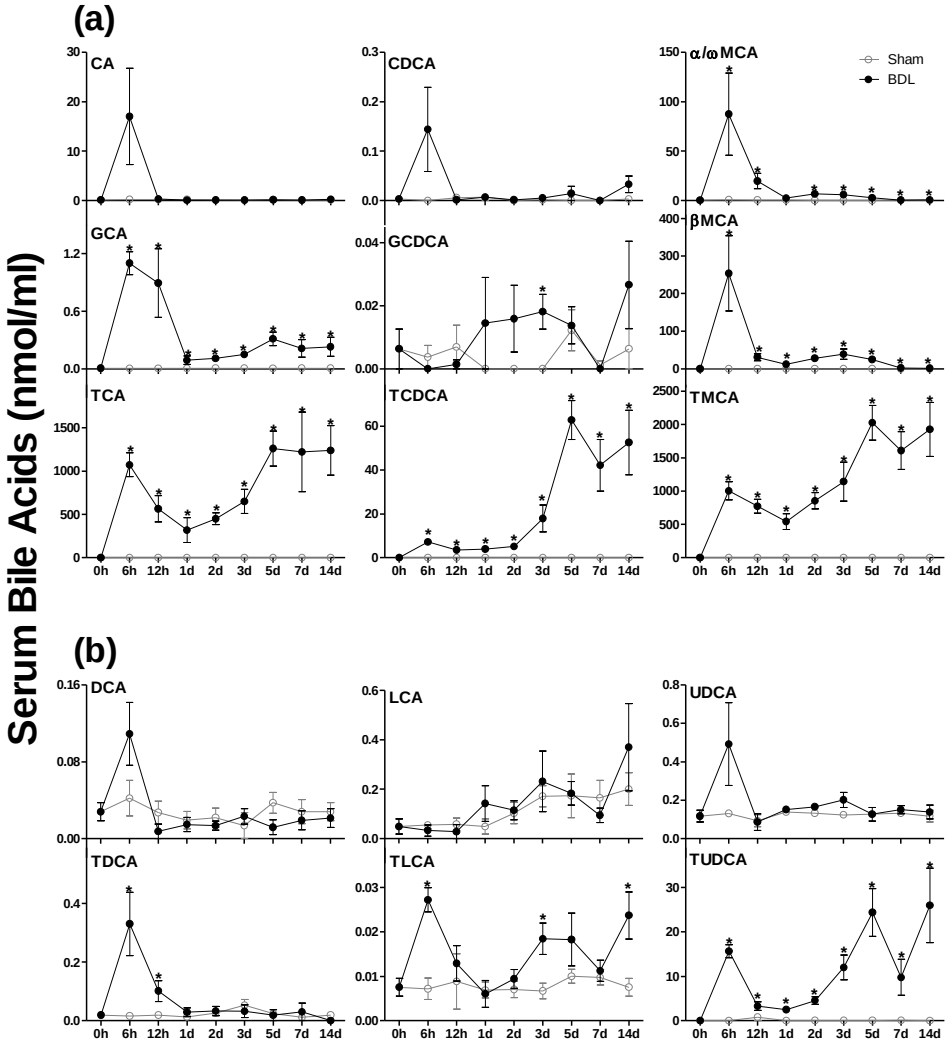

Figure 6-2. Primary BAs (a) and secondary BAs (b) in serum of sham-operated and BDL mice. All BA data are expressed as mean ±S.E. of six mice in each group. *, Statistically significant difference between sham-operated (open circles) and BDL (closed circles) mice ($p<0.05$).

2.2. Concentrations of BAs in Livers of C57BL/6 Mice after BDL

Total BA concentrations in livers of mice after surgery are shown in figure 6-3. Sham-operated mice maintained their liver BAs in a range of 55 to 254 nmol/g, with about 80% of the BAs conjugated.

At 6 h after BDL, unconjugated and conjugated BAs increased about 26 and 27 fold, respectively (unconj BAs: 18.8→509, conj BAs: 71.3→2040 nmol/g). Thereafter, unconjugated BAs decreased more than 90% between 12 h and 14 d (364→25) after BDL, whereas conjugated BAs remained at high concentrations (1216~1781). As a result, the percentage of conjugated BAs in livers of BDL mice increased from 80% at 6 h to 99% at 14 d. Mainly due to the increase in conjugated BAs, the total BA concentration in livers of mice increased about 27 fold at 6 h (90.2→2550) after BDL, decreased 28% from 6 h to 1 d (2550→1830), and thereafter were maintained in a range of 1540 to 1810 nmol/g, which was about 12-fold higher than that in sham-operated mice.

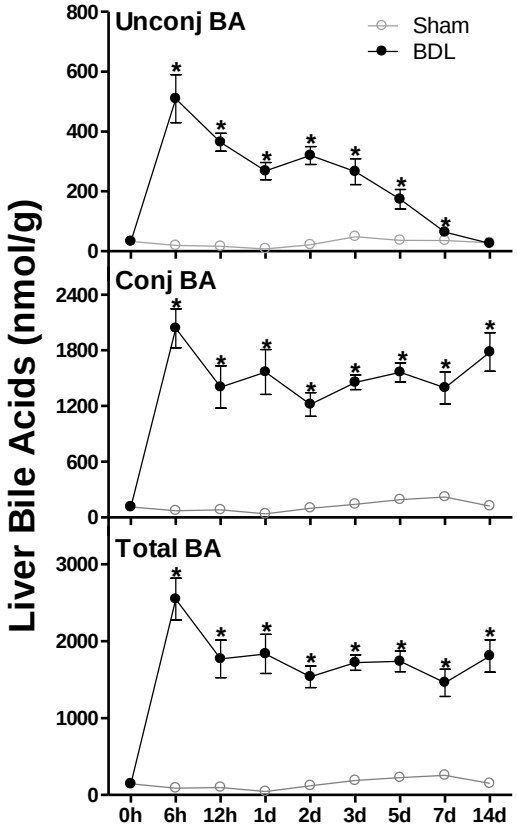

Figure 6-3. Unconjugated, conjugated, and total BA concentrations in livers of sham-operated and BDL mice. All BA data are expressed as mean ±S.E. of six mice in each group. *, Statistically significant difference between sham-operated (open circles) and BDL (closed circles) mice ($p<0.05$).

The major primary BAs in livers of sham-operated mice were TCA and TβMCA (Figure 6-4a). After 6 h of BDL, CA (1.1→10.6), GCA (0.1→1.5), and TCA (50.8→850) increased 9, 14, and 17 fold, respectively. CA and GCA decreased to sham levels within 2 d after BDL, whereas TCA underwent a decrease from 6 h to 1 d, but was maintained at higher concentrations than sham controls thereafter. BDL had little effect on CDCA and GCDCA, whereas BDL gradually increased TCDCA concentrations about 4 fold (2.5→10.5) within two weeks. After BDL, the concentration of αMCA in the liver underwent a 3-fold increase (1.6→6.3) at 6 h, followed by a decrease to concentrations in sham mice at 12 h, and became lower than sham controls after 7 d. In contrast, TαMCA in livers of mice increased about 12 fold (3.1→39.0) at 6 h after BDL, and remained at higher levels (13.6~26.7) than sham controls thereafter. After BDL, βMCA increased about 35 fold (11.4→416) at 6 h, and thereafter decreased gradually to similar concentrations as in livers of sham-operated mice after 7 d. In contrast, TβMCA in livers of BDL mice underwent a 150-fold increase (5.4→812) at 6 h, followed by a 45% decrease from 6 h to 1 d, and increased gradually about 1.5 fold (432→1110) from 1 to 14 d. TCA7S and TCDCA7S were the two predominant BA sulfates in livers of sham-operated mice. After BDL, both TCA7S and TCDCA7S increased about 17 fold during the first 3 days, but thereafter decreased rapidly to similar concentrations as in livers of sham-operated mice. Therefore, sulfation is not a prominent pathway of BA metabolism in livers of BDL mice.

Figure 6-4b illustrates the time course of secondary BAs in livers of mice after surgery. The predominant secondary BAs in livers of sham-operated mice were TωMCA and TDCA. BDL had little effect on DCA concentration in liver, but after 1 d significantly decreased TDCA, LCA, and TLCA. Within 6 h after BDL, UDCA (0.2→1.7), HDCA (0.3→1.8), and MDCA (0.2→1.9) increased about 5-8 fold, whereas TUDCA (0.6→17.0), THDCA (0.2→9.1), and TMDCA (0.1→6.7) increased 27-66 fold in livers of mice. Among these secondary BAs, UDCA, HDCA, THDCA, MDCA, and TMDCA decreased to similar concentrations as observed in sham mice within 1 d, and became lower than sham controls after 5 d. In contrast, TUDCA underwent a 75% decrease between 6 h and 12 h, but remained at higher

concentrations than sham controls thereafter. After BDL, ωMCA increased about 18 fold (3.7→70.6) at 6 h, and decreased rapidly to become lower than that in sham controls after 5 d. In contrast, TωMCA in livers of BDL mice increased about 46 fold (6.3→295) at 6 h, decreased thereafter, but remained about 3-fold higher than sham controls at the end of two weeks. Therefore, the predominant secondary BAs in livers of BDL mice were TUDCA and TωMCA.

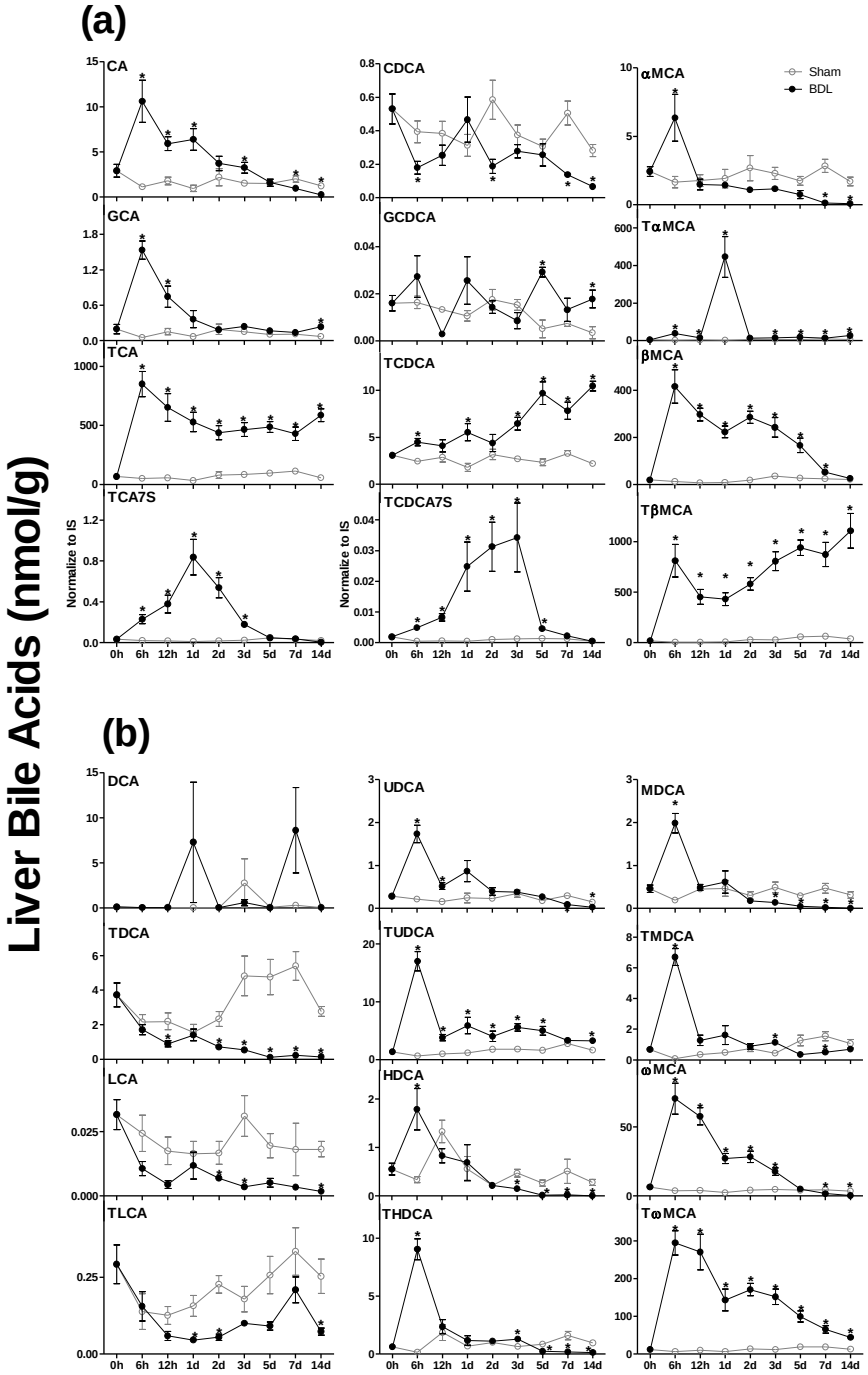

Figure 6-4. Individual primary BAs (a) and secondary BAs (b) in livers of sham-operated and BDL mice. All BA data are expressed as mean ±S.E. of six mice in each group. *, Statistically significant difference between sham-operated (open circles) and BDL (closed circles) mice ($p<0.05$).

2.3. mRNA Expression of BA-Uptake Transporters in C57BL/6 Mice after BDL

The impact of BDL on mRNA expression of BA-uptake transporters, namely Ntcp, Oatp1a1, Oatp1a4, and Oatp1b2 in mouse livers is shown in figure 6-5. Ntcp in BDL mice increased about 54% within 6 h after surgery, followed by a 50% decrease from 6 h to 1 d, and became significantly lower than sham controls after 2 d. After BDL, Oatp1a1 increased about 55% at 6 h, decreased markedly thereafter, and became almost undetectable at the end of two weeks. Oatp1a4 in BDL mice underwent a 62% increase at 6 h, an additional 120% increase at 5 d, and remained at levels higher than sham controls thereafter. Similar to Ntcp, Oatp1b2 in BDL mice increased about 62% at 6 h, followed by a 30% decrease from 6 h to 1 d, and became significantly lower than sham-operated mice thereafter. Therefore, BDL decreased Ntcp, Oatp1a1, and Oatp1b2, whereas it increased Oatp1a4 in livers of mice.

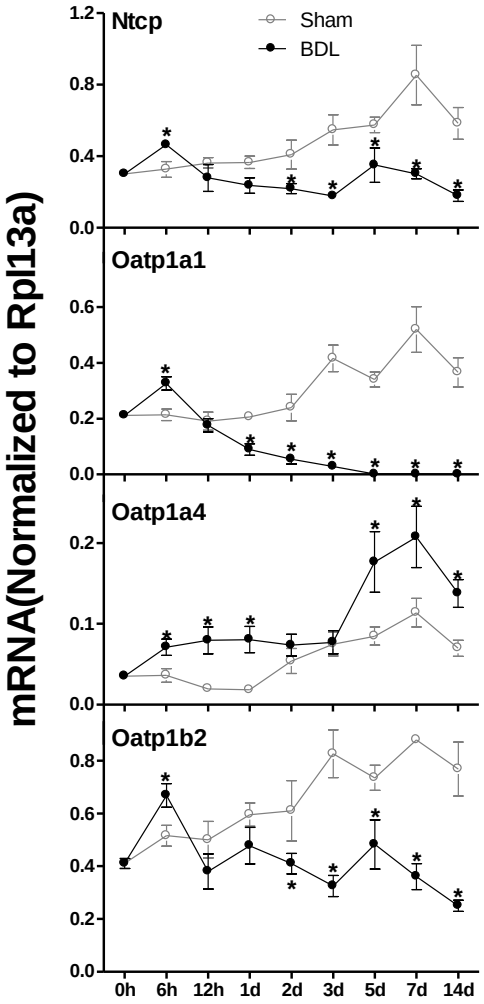

Figure 6-5. mRNA of BA uptake transporters in livers of sham-operated and BDL mice. Total RNA from livers of sham-operated (open circles) and BDL (closed circles) mice were analyzed by multiplex suspension array. The mRNA expression of each gene was normalized to Rpl13a. All data are expressed as mean ±S.E. of six mice in each group. *, Statistically significant difference between sham-operated and BDL mice ($p<0.05$).

2.4. mRNA Expression of BA-Efflux Transporters in C57BL/6 Mice after BDL

BDL had little effect on the canalicular BA-efflux transporters, such as Bsep, Mrp2, and Bcrp (Figure 6-6a). Although Bsep in BDL mice was higher than sham controls at 6h, 12 h, and 1 d, the significance

of this effect is questionable because the difference appears to be mainly due to the decrease of Bsep in sham-operated mice. The impact of BDL on mRNA expression of the basolateral BA-efflux transporters is shown in figure 6-6b. BDL had little effect on Ostα (data not shown), whereas it increased Ostβ about 25 fold 6 h after surgery, and remained high thereafter. BDL had little effect on Mrp3, whereas it increased Mrp4 about 6 fold 2 d after surgery. Therefore, BDL increased the mRNA of the BA-efflux transporters Ostβ and Mrp4 in livers of mice.

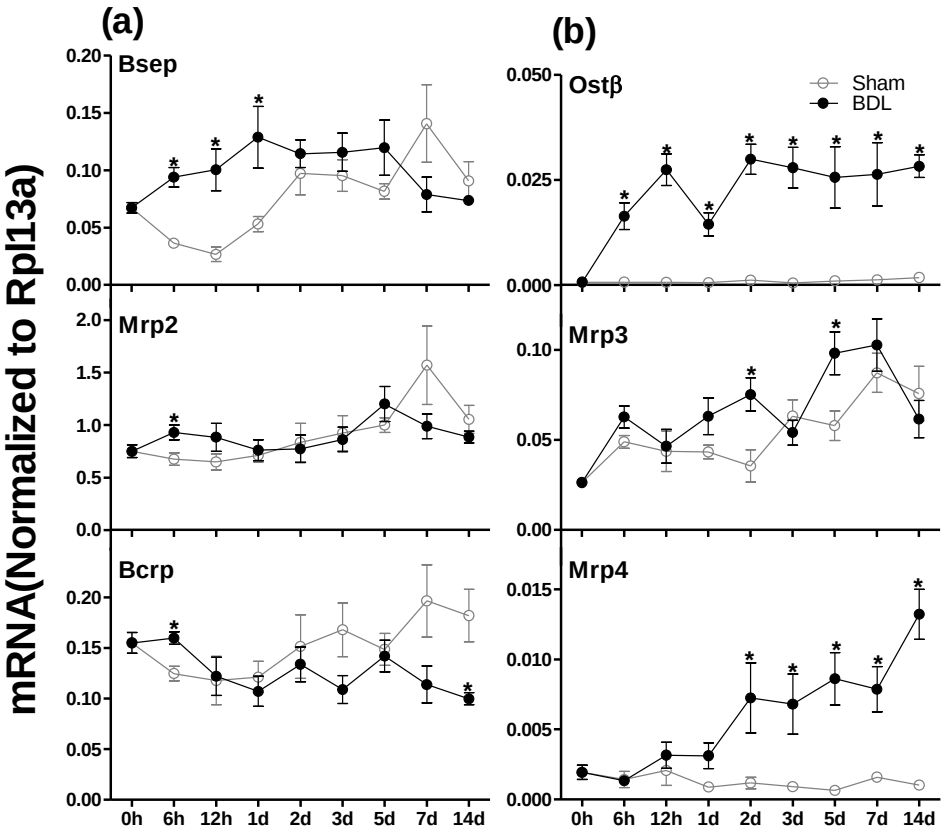

Figure 6-6. mRNA expression of canalicular (a) and basolateral (b) BA efflux transporters in livers of sham-operated and BDL mice. Total RNA from livers of sham-operated (open circles) and BDL (closed circles) mice were analyzed by multiplex suspension array. The mRNA expression of each gene was normalized to Rpl13a. All data are expressed as mean ±S.E. of six mice in each group. *, Statistically significant difference between sham-operated and BDL mice ($p<0.05$).

2.5. Liver H&E Staining of WT and Oatp1a1-null Mice after BDL

A time course of BDL in WT and Oatp1a1-null mice was examined. Surprisingly, all Oatp1a1-null mice died within 3 days after BDL, whereas most WT mice survived at least one week. Because Oatp1a1-null mice became very sick 2 days after BDL, we investigated the role of Oatp1a1 in livers of mice one day after BDL. Histopathological analysis indicated that the livers of Oatp1a1-null mice had large areas of necrosis, whereas no obvious differences were observed between WT-sham and WT-BDL mice (Figure 6-7). Thus, one-day BDL resulted in more severe liver toxicity in Oatp1a1-null mice than in WT mice.

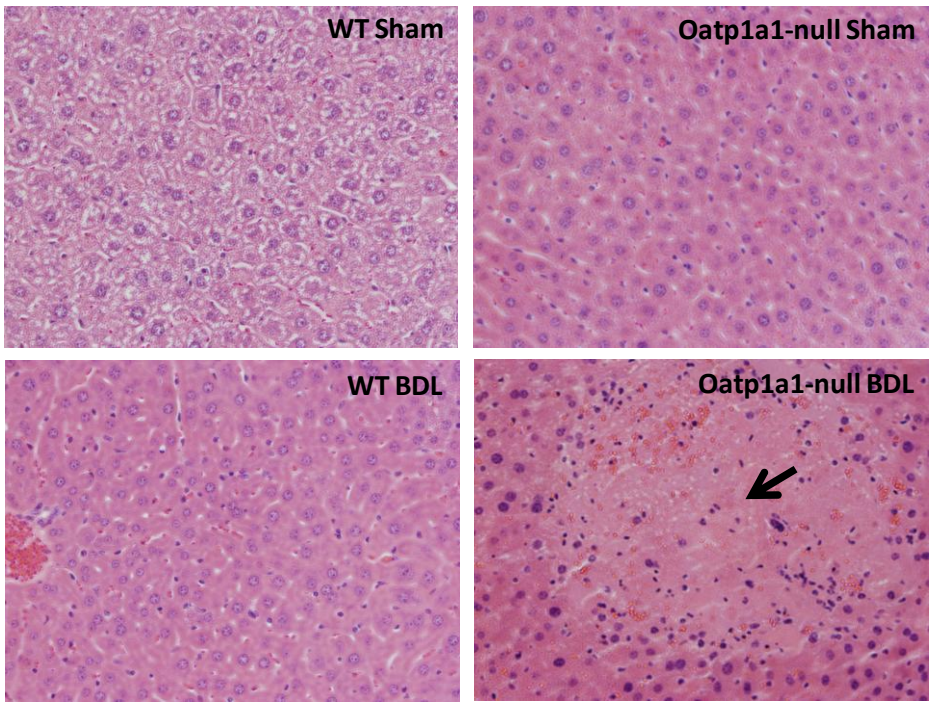

Figure 6-7. Histopathological analysis of liver sections from WT and Oatp1a1-null mice 1 day after BDL. Liver sections (5µm) were stained with hematoxylin-eosin**.**

2.6. Serum ALT, ALP, and Total Bilirubin in WT and Oatp1a1-null Mice 1 day after BDL

Serum ALT, ALP, and total bilirubin are markers of liver toxicity. After BDL, serum ALT, ALP, and total bilirubin were increased markedly in both WT and Oatp1a1-null mice. However, no significant differences were observed between WT and Oatp1a1-null mice (Figure 6-8). Therefore, serum ALT, ALP, and bilirubin may not reflect the difference of liver toxicity between WT and Oatp1a1-null mice during early stage of cholestasis.

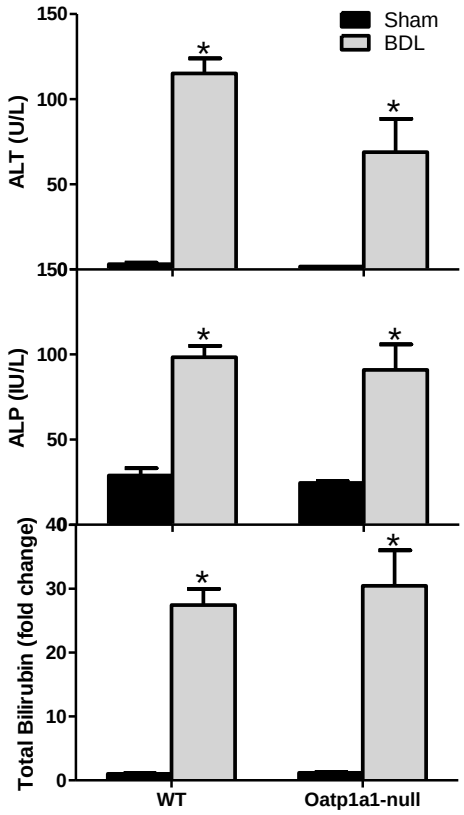

Figure 6-8. Blood chemistry of WT and Oatp1a1-null mice 1 day after BDL. Serum ALT, ALP, and total bilirubin from sham and BDL mice (n = 5/group) were analyzed with analytical kits (Pointe Scientific, Canton, MI). All data are expressed as mean ± S.E.of five mice in each group. *, statistically significant difference between sham and BDL mice ($p<0.05$).

2.7. BA Profiling in Serum and Livers of WT and Oatp1a1-null Mice 1 day after BDL

In contrast to serum ALT, ALP, and total bilirubin, serum BA profiles were markedly different between WT and Oatp1a1-null mice after BDL. After BDL, the most striking differences between WT and Oatp1a1-null mice were observed in the chromatograph window for tauro-dihydroxy BAs in serum and livers. As shown in figure 6-9a, a number of major peaks were detected in the chromatograph window for tauro-dihydroxy BAs in the serum of WT-BDL mice. Five peaks were markedly increased in serum of the Oatp1a1-null BDL mice. Two peaks, which were almost undetectable in serum of WT BDL mice, were markedly increased in serum of Oatp1a1-null BDL mice. Similar changes in the BA profiles were observed in livers of WT and Oatp1a1-null mice after BDL (Figure 6-9b). By comparing the retention time and mass spectrum, these two peaks were identified as T-12-epiDCA and TDCA, respectively (Figure 6-9c). Taken together, Oatp1a1-null mice had higher secondary taurine-conjugated dihydroxy BAs, in particular, T-12-epiDCA (12-epimerization of TDCA) and TDCA, in both serum and livers than WT mice 1 day after BDL, suggesting a possible contribution of secondary BAs to the liver toxicity in Oatp1a1-null BDL mice.

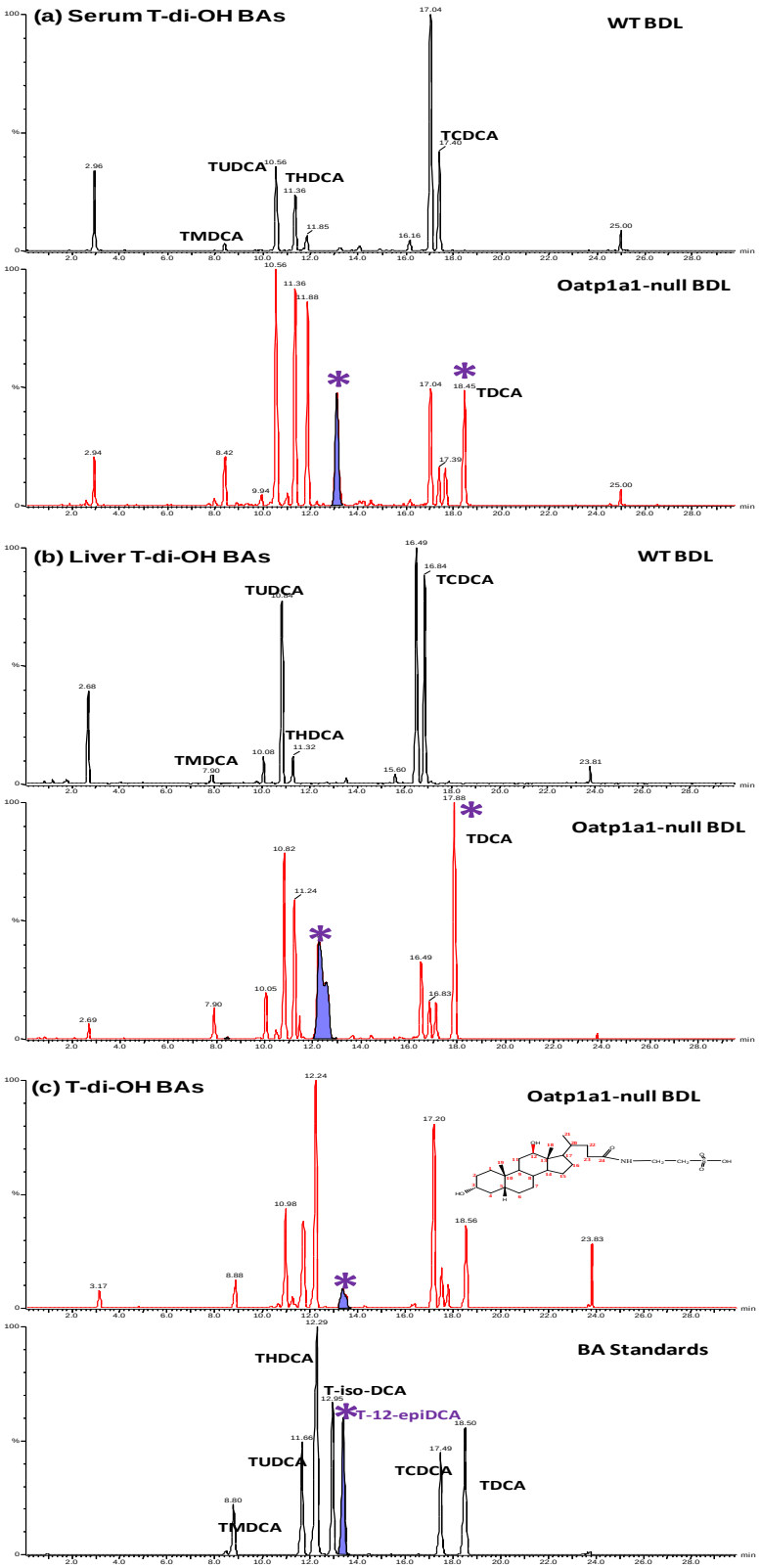
(a) Serum T-di-OH BAs
WT BDL
TUDCA
THDCA
TMDCA
TCDCA
Oatp1a1-null BDL
TDCA
(b) Liver T-di-OH BAs
WT BDL
TUDCA
THDCA
TMDCA
TCDCA
Oatp1a1-null BDL
TDCA
(c) T-di-OH BAs
Oatp1a1-null BDL
BA Standards
THDCA
T-iso-DCA
T-12-epiDCA
TUDCA
TCDCA
TDCA
TMDCA

Figure 6-9. BA profiling in serum and livers of WT and Oatp1a1-null mice 1 day after BDL. The chromatograph windows of tauro-dihydroxy BAs for (a) serum and (b) livers showed marked differences between WT and Oatp1a1-null mice 1 day after BDL. (c) T-12-epiDCA was identified by the retention time and mass spectrum of authentic standards.

2.8. Total BAs in Serum and Livers of WT and Oatp1a1-null Mice 1 day after BDL

Due to the recent availability of some additional BA standards for the present BDL study on Oatp1a1-null mice, some concentrations of BAs are different than those previously reported in this chapter for C57BL/6 mice. Figure 6-10a shows the concentrations of unconjugated BAs, conjugated BAs, and total BAs in serum of WT and Oatp1a1-null mice after BDL. Similar to the previous BDL study in C57BL/6 mice, the concentrations of both unconjugated (0.2→65.7 nmol/ml) and conjugated BAs (0.9→1017 nmol/ml) in serum of WT mice were increased about 300 and 1060 fold, respectively, within 1 day after BDL (Figure 6-10a). Similarly, the concentrations of both unconjugated (0.7→103.7 nmol/ml) and conjugated BAs (0.9→1140 nmol/ml) in serum of Oatp1a1-null BDL mice were also increased 140 and 1250 fold, respectively, within 1 day after BDL. Mainly due to the increase of conjugated BAs, the concentrations of total BAs in serum of WT and Oatp1a1-null mice were increased about 910 and 750 fold, respectively, within 1 day after BDL. Taken together, serum total BAs were not significantly different between WT and Oatp1a1-null mice after BDL, although the concentration of serum unconjugated BAs (103.7 nmol/ml) in Oatp1a1-null BDL mice tended to be higher than that in WT BDL mice (65 nmol/ml).

Figure 6-10b illustrates the concentrations of unconjugated BAs, conjugated BAs, and total BAs in livers of WT and Oatp1a1-null mice 1 day after BDL. Although the concentration of unconjugated BAs in serum tended to be higher in Oatp1a1-null mice than in WT mice after BDL, it does not appear to be due to decreased hepatic uptake of BAs in Oatp1a1-null mice, because the concentration of unconjugated BAs in livers was increased similarly between WT (48→300 nmol/g) and Oatp1a1-null mice (73→325

nmol/g) after BDL (Figure 6-10b). In contrast, the concentration of conjugated BAs in livers was about 35% higher in Oatp1a1-null mice (170→3123 nmol/g) than WT mice (143→2270 nmol/g) after BDL. Thus, mainly due to increased conjugation of BAs, Oatp1a1-null mice (240→3450 nmol/g) also had about 35% higher concentration of total BAs in livers than WT mice (190→2570 nmol/g) after BDL. Taken together, after BDL, Oatp1a1-null mice had higher concentrations of conjugated BAs in livers than WT mice, indicating that knockout of Oatp1a1 does not prevent the accumulation of BAs in livers of mice during BDL-induced cholestasis.

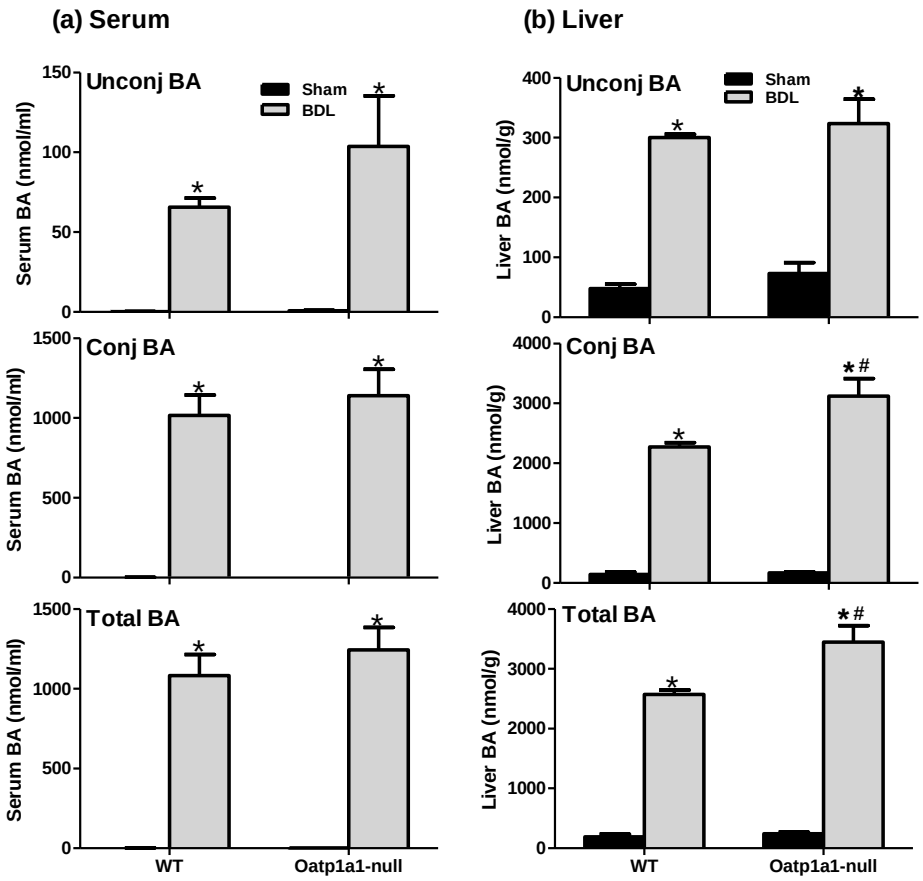

Figure 6-10. Unconjugated, conjugated, and total BA concentrations in serum (a) and livers (b) of WT and Oatp1a1-null mice 1 day after BDL. All BA data are expressed as mean ±S.E. of five mice in each group. *, Statistically significant difference between sham-operated and BDL mice ($p<0.05$). #. Statistically significant difference between WT and Oatp1a1-null mice after BDL.

2.9. Primary BAs in Serum and Livers of WT and Oatp1a1-null Mice 1 day after BDL

After BDL, Oatp1a1-null mice had similar concentrations of total BAs in serum, and had 35% higher concentration of total BAs (majorly conjugated BAs) in livers than WT mice. The difference in total BA concentrations is unlikely to explain the dramatic difference in liver toxicity between WT and Oatp1a1-null mice after BDL. Thus, the concentrations of individual BAs in serum and livers of WT and Oatp1a1-null mice after BDL were quantified and compared. Figure 6-11 illustrates the concentrations of primary BAs in serum and livers of WT and Oatp1a1-null mice after BDL. BDL markedly increased TCA (0.4→670 nmol/ml) and CA (0.0→0.9) in serum of WT mice (Figure 6-11a). Similarly, BDL also increased TCA (65→1300 nmol/g) and CA (1.2→4.7 nmol/g) in livers of WT mice (Figure 6-11b). This suggests that TCA and CA were effluxed to blood from the liver in mice after BDL. After BDL, Oatp1a1-null mice had similar TCA (0.5→830 nmol/ml), but about 5-fold higher concentrations of CA (0.1→5.2 nmol/ml) in serum than WT mice. BDL of Oatp1a1-null mice markedly increased TCA (113→2200 nmol/g), but had little effect on CA in livers. As a result, after BDL, Oatp1a1-null mice had about 70% higher TCA in livers than WT mice. Thus, knockout of Oatp1a1 increased serum CA and liver TCA in mice after BDL.

BDL in WT mice markedly increased TCDCA (0.0→1.5 nmol/ml), but had little effect on CDCA in serum (Figure 6-11a). In contrast, BDL in WT mice had little effect on TCDCA, but decreased CDCA (0.3→0.1 nmol/g) in livers (Figure 6-11b). Similarly, BDL in Oatp1a1-null mice also increased TCDCA (0.0→0.8 nmol/ml) in serum, but decreased CDCA (0.6→0.1 nmol/g) in livers. As a result, after BDL, TCDCA was about 50% lower in serum, and tended to be lower in livers of Oatp1a1-null mice than WT mice. Thus, knockout of Oatp1a1 decreased TCDCA in both serum and livers.

BDL of WT mice increased TβMCA and βMCA in both serum (0.2→193 and 0.0→28 nmol/ml, respectively) and livers (46→570 and 27→180 nmol/g, respectively). After BDL, Oatp1a1-null mice had

similar concentrations of TβMCA and βMCA in serum and livers as WT mice, although βMCA tended to be higher in serum of Oatp1a1-null mice (0.1→52 nmol/ml) than in WT mice.

Taken together, 1 day after BDL, TCA is the highest conjugated primary BA, whereas βMCA is the highest unconjugated primary BA in both serum and livers of mice. Knockout of Oatp1a1 decreased TCDCA, but increased CA in serum of BDL mice. In addition, knockout of Oatp1a1 increases TCA in livers of BDL mice.

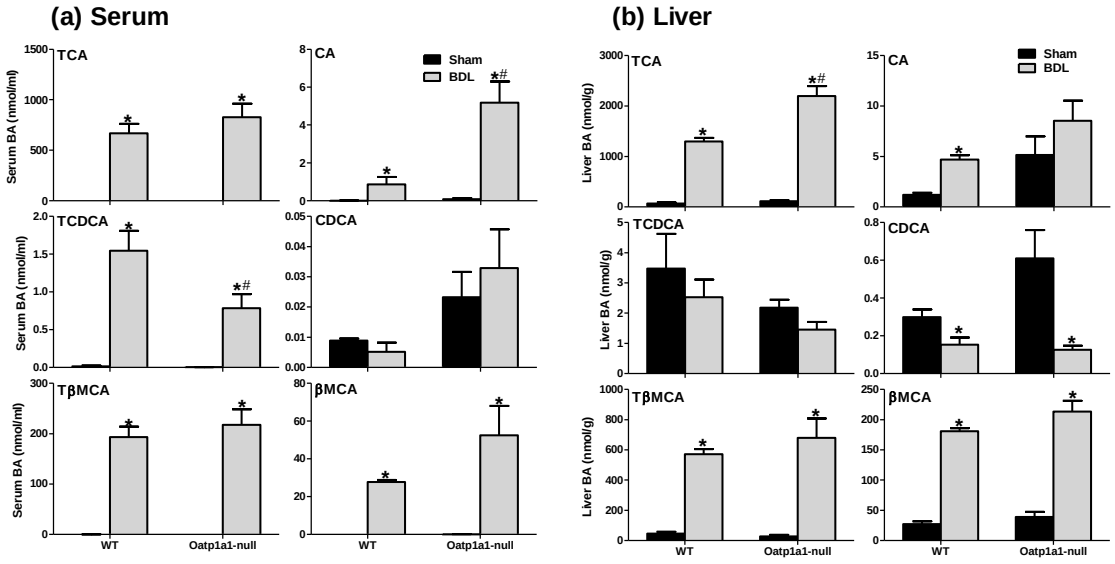

Figure 6-11. Individual primary BAs in serum (a) and livers (b) of WT and Oatp1a1-null mice 1 day after BDL. All BA data are expressed as mean ±S.E. of five mice in each group. *, Statistically significant difference between sham-operated and BDL mice ($p<0.05$). #. Statistically significant difference between WT and Oatp1a1-null mice after BDL.

2.10. Secondary BAs in Serum and Livers of WT and Oatp1a1-null Mice 1 day after BDL

Figure 6-12 shows the concentrations of secondary BAs in WT and Oatp1a1-null mice. Similar to the BDL time-response study, BDL in WT mice had little effect on TDCA and DCA in serum (Figure 6-12a), but decreased TDCA (1.5→ 0.1 nmol/g) and DCA (0.1→0.0 nmol/g) in livers (Figure 6-12b). In

contrast, BDL of Oatp1a1-null mice markedly increased TDCA (0.1→2.7 nmol/ml) and DCA (0.1→0.3 nmol/ml) in serum. BDL of Oatp1a1-null mice had little effect on TDCA, but decreased DCA (0.3→0.1 nmol/g) in livers. Thus, after BDL, Oatp1a1-null mice had about 30-fold higher TDCA in both serum and livers than WT mice. In addition, Oatp1a1-null mice also had 7-fold higher DCA in serum and 2-fold higher DCA in livers than WT mice after BDL.

Similar to TDCA and DCA, TLCA and LCA were not altered in serum, but were significantly decreased in livers of WT mice after BDL. BDL also decreased TLCA and LCA in livers of Oatp1a1-null mice. In contrast, BDL significantly increased serum TLCA in Oatp1a1-null mice. Thus, Oatp1a1-null mice had about 8-fold higher concentration of TLCA in serum than WT mice after BDL.

BDL in WT mice increased TMDCA and MDCA in serum, but decreased than in livers. In contrast, BDL in Oatp1a1-null mice increased TMDCA in both serum and livers. In addition, BDL of Oatp1a1-null mice increased MDCA in serum but not in livers. Thus, after BDL, Oatp1a1-null mice had about 12-14 fold higher TMDCA and MDCA in both serum and livers than WT mice.

BDL of WT and Oatp1a1-null mice resulted in similar changes in TUDCA and THDCA as well as UDCA and HDCA in serum and livers. BDL of WT mice increased TUDCA and THDCA in serum but not in liver. BDL of WT mice had little effect on UDCA and HDCA in serum, but decreased them in livers. In contrast, BDL of Oatp1a1-null mice markedly increased TUDCA and THDCA in serum and livers. BDL of Oatp1a1-null mice increased UDCA and HDCA in serum, but not in livers. Thus, after BDL, Oatp1a1-null mice had 3-4 fold higher TUDCA and 4-6 fold higher THDCA as well as 5-7 fold higher UDCA and 7-10 fold higher HDCA in serum and livers than in WT mice.

BDL of WT mice increased TωMCA (0.3→150 mg/ml and 22→395 nmol/g, respectivley) and ωMCA (0.1→28 nmol/ml and 8→56 nmol/g, respectively) in both serum and livers. Similarly, BDL of Oatp1a1-null mice also increased TωMCA (0.1→79 mg/ml and 13→220 nmol/g, respectivley) and ωMCA (0.1→35 nmol/ml and 11→47 nmol/g, respectively) in both serum and livers. Thus, after BDL,

Oatp1a1-null mice had about a 50% lower concentration of TωMCA, but a similar concentration of ωMCA in serum and livers as WT mice.

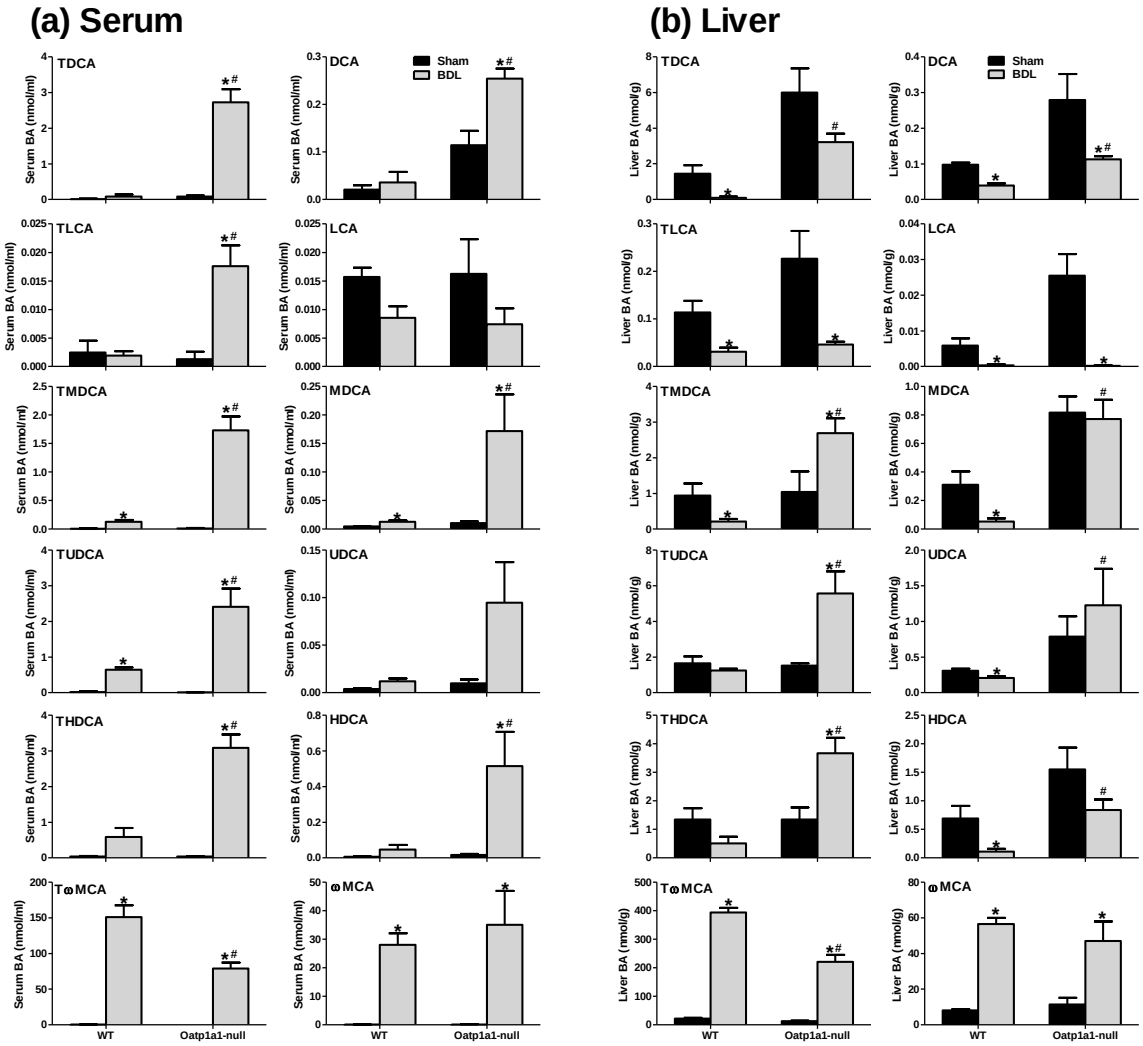

Figure 6-12. Individual secondary BAs in serum (a) and livers (b) of WT and Oatp1a1-null mice 1 day after BDL. All BA data are expressed as mean ±S.E. of five mice in each group. *, Statistically significant difference between sham-operated and BDL mice ($p<0.05$). #. Statistically significant difference between WT and Oatp1a1-null mice after BDL.

Figure 6-13 illustrates the concentrations of another three secondary BAs in WT and Oatp1a1-null mice. 7-OxoDCA and 12-oxoCDCA are the two major oxo-BAs in serum and livers of mice. BDL had little effect on 7-oxoDCA in serum and livers of WT mice, but significantly increased it in serum and livers of Oatp1a1-null mice. In contrast, BDL increased 12-oxoCDCA similarly in serum and livers of WT and Oatp1a1-null mice. In addition, BDL markedly increased T-12-epoDCA, which was almost undetectable in serum and livers of WT mice, in serum and livers of Oatp1a1-null mice. Thus, Oatp1a1-null mice had higher 7-oxoDCA (3- and 6-fold, respectively) and T-12-epiDCA (75- and 510-fold, respectively) in serum and livers than WT mice after BDL.

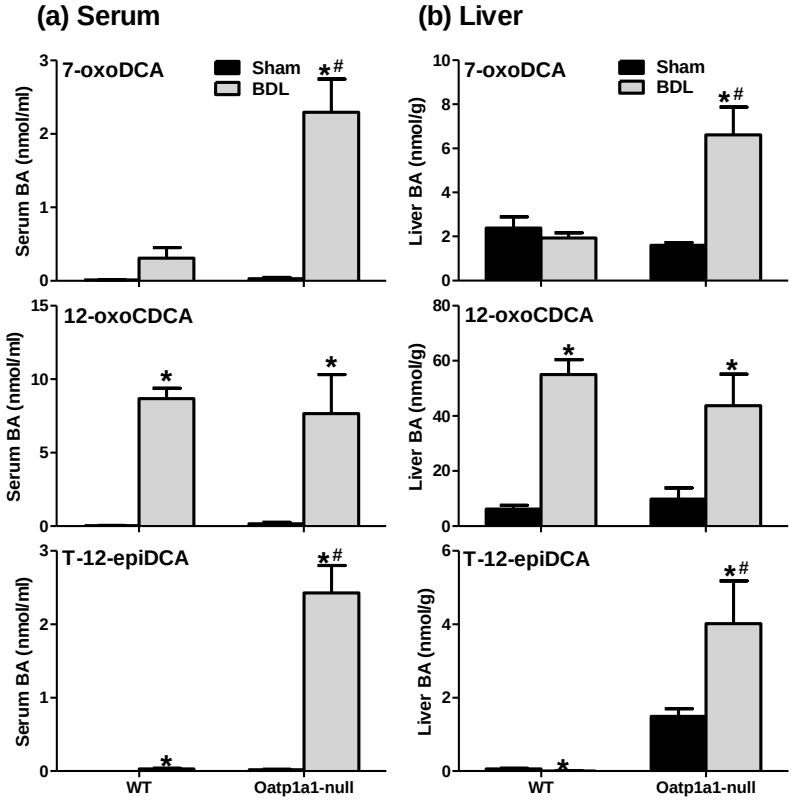

Figure 6-13. 7-OxoDCA, 12-oxoCDCA, and T-12-epiDCA in serum (a) and livers (b) of WT and Oatp1a1-null mice 1 day after BDL. All BA data are expressed as mean ±S.E. of five mice in each group. *, Statistically significant difference between sham-operated and BDL mice ($p<0.05$). #. Statistically significant difference between WT and Oatp1a1-null mice after BDL.

2.11. BA-conjugation Enzymes in WT and Oatp1a1-null Mice 1 Day after BDL

Unconjugated BAs are first activated with coenzyme A by Fatp5, which is located at the basolateral membrane of hepatocytes (Mihalik et al., 2002). Next, Baat, which is predominantly present in peroxisomes of hepatocytes, conjugates the CoA-activated BAs with taurine or glycine (Pellicoro et al., 2007). Because Oatp1a1-null BDL mice have higher concentrations of conjugated BAs than WT BDL mice, the mRNA expression of Fatp5 and Baat in livers were quantified. As shown in figure 6-14, BDL decreased Fatp5 about 30%, but increased Baat about 80% in livers of WT mice. In contrast, BDL had little effect on Fatp5 or Baat in livers of Oatp1a1-null mice. Thus, Oatp1a1-null BDL mice had similar Fatp5 but lower Baat than WT BDL mice, suggesting that the increased concentration of conjugated BAs in livers of Oatp1a1-null BDL mice is not due to elevated hepatic BA-conjugation.

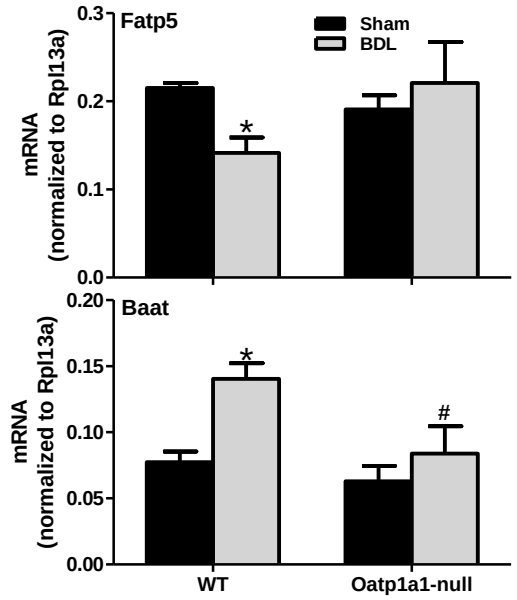

Figure 6-14. mRNA expression of BA-conjugation enzymes in livers of WT and Oatp1a1-null mice 1 day after BDL. Total RNA from livers of sham-operated and BDL mice were analyzed by multiplex suspension array. The mRNA expression of each gene was normalized to Rpl13a. All data are expressed as mean ±S.E. of five mice in each group. *, Statistically significant difference between sham-operated and BDL mice ($p<0.05$).

2.12. BA-uptake Transporters in Livers of WT and Oatp1a1-null Mice 1 day after BDL

It is possible that knockout of Oatp1a1 increased other BA-uptake transporters and thus increased the conjugated BAs in livers of mice after BDL. Thus, the mRNA expression of BA-uptake transporters, namely Ntcp, Oatp1a1, Oatp1a4, and Oatp1b2 were quantified in livers of WT and Oatp1a1-null mice after BDL. As shown in figure 6-15, BDL in WT mice tended to, but did not significantly decrease Ntcp, Oatp1a1, and Oatp1b2. Furthermore, BDL in WT mice increased Oatp1a4 mRNA about 5-fold. This is consistent with the BDL time-response study (Figure 6-5). In contrast, BDL of Oatp1a1-null mice had little effect on the mRNA expression of Ntcp, Oatp1a4, and Oatp1b2. As a result, Oatp1a1-null BDL mice had about 60% lower Oatp1a4 mRNA than WT BDL mice. This suggests that Oatp1a1 may be important for the induction of Oatp1a4 during BDL, which has been suggested to be a protective mechanism for livers of mice during BDL-induced cholestasis. Taken together, the increase of conjugated BAs in livers of Oatp1a1-null mice after BDL does not appear to be due to an increase in BA-uptake transporters.

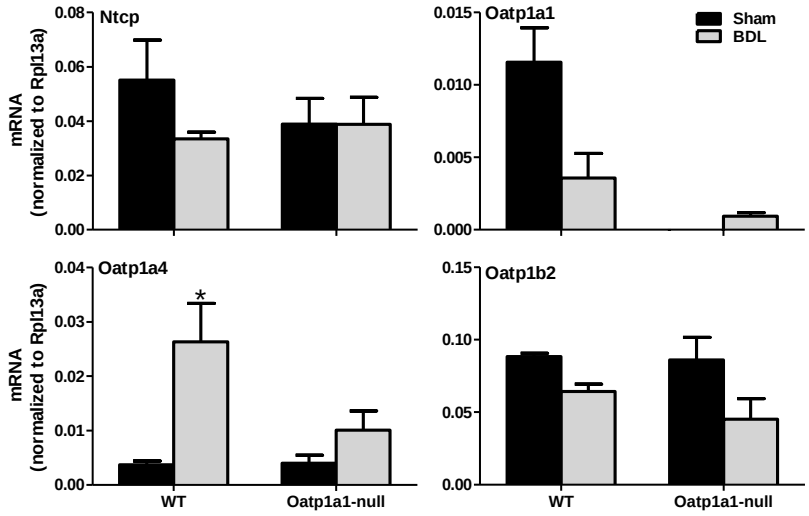

Figure 6-15. mRNA expression of BA-uptake transporters in livers of WT and Oatp1a1-null mice 1 day after BDL. Total RNA from livers of sham-operated and BDL mice were analyzed by multiplex suspension array. The mRNA levels were normalized to Rpl13a. All data are expressed as mean ±S.E. of

five mice in each group. *, Statistically significant difference between sham-operated and BDL mice ($p<0.05$).

2.13. BA-efflux Transporters in Livers of WT and Oatp1a1-null Mice 1 Day after BDL

It is also possible that knockout of Oatp1a1 inhibits hepatic BA-efflux transporters and thus increases the concentration of conjugated BAs in livers of mice after BDL. Figure 6-16 shows the mRNA expression of BA-efflux transporters in livers of WT and Oatp1a1-null mice after BDL. Bsep and Mrp2 are canalicular BA-efflux transporters that efflux BAs from liver to bile. BDL of WT mice increased Bsep mRNA about 88%, but had no effect on Mrp2 mRNA. In contrast, BDL of Oatp1a1-null mice had little effect on Bsep or Mrp2 mRNA. As a result, livers of Oatp1a1-null BDL mice had about 70% lower Bsep mRNA and 50% lower Mrp2 mRNA than WT BDL mice. Mrp3 and Mrp4 are two basolateral BA-efflux transporters, which efflux BAs from liver to blood. BDL of WT mice increased Mrp3 mRNA about 120%, but had little effect on Mrp4 mRNA. In contrast, BDL of Oatp1a1-null mice had little effect on Mrp3 and Mrp4 mRNA, although it tended to increase Mrp3 mRNA. Ostα/β is a heterodimer protein that is highly expressed in the basalateral membrane of enterocytes and responsible for the BA-efflux from intestine back to blood. Unlike in intestine, Ostα/β is minimally expressed in mouse liver. BDL of WT mice increased Ostα/β mRNA about 4-fold in livers. BDL of Oatp1a1-null mice had little effect on Ostα mRNA, but increased Ostβ mRNA about 3-fold in livers. As a result, Oatp1a1-null BDL mice had similar mRNA expression of Ostα/β as WT BDL mice. Taken together, after BDL, Oatp1a1-null mice had lower mRNA expression of Bsep and Mrp2, but had similar mRNA expression of Mrp3/4 and Ostα/β in livers than WT mice. The lower mRNA expression of Bsep and Mrp2 may not explain the increased conjugated BAs in livers of Oatp1a1-null BDL mice, because BDL has already blocked the excretion of BAs from the liver to the common bile duct. In addition, the conjugated secondary BAs were also increased in serum of Oatp1a1-null mice after BDL.

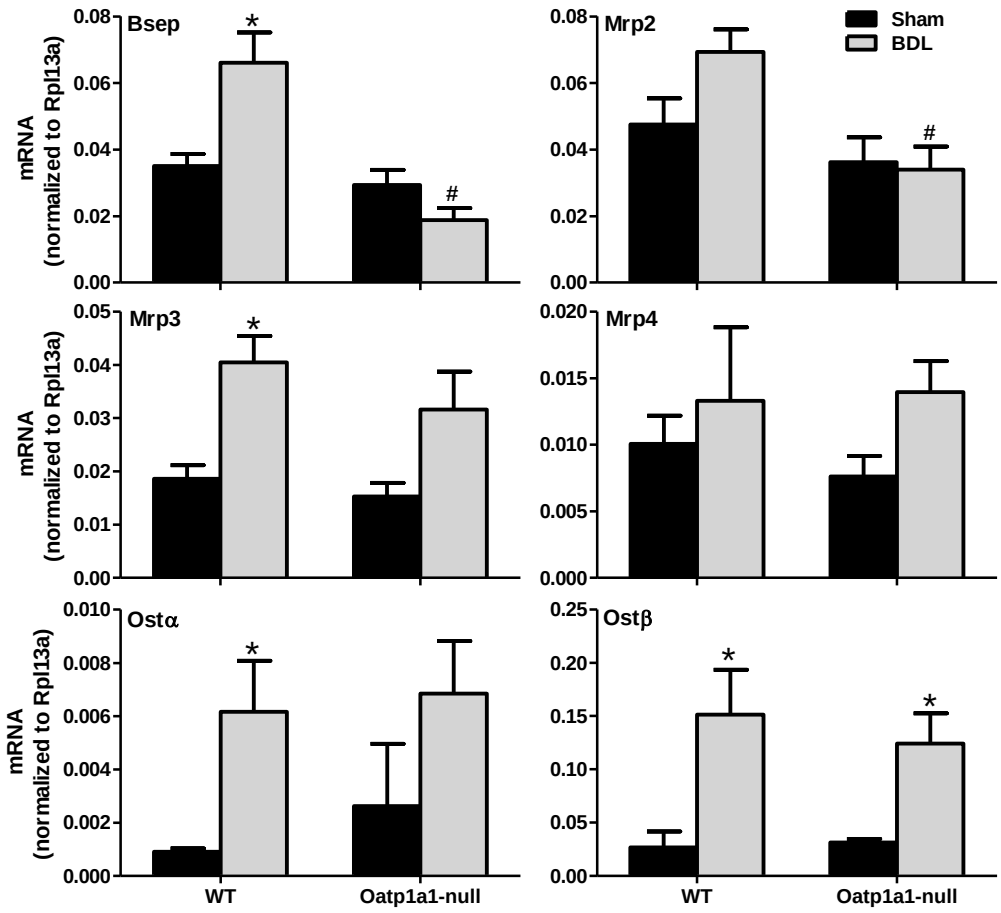

Figure 6-16. mRNA expression of BA-efflux transporters in livers of WT and Oatp1a1-null mice 1 day after BDL. Total RNA from livers of sham-operated and BDL mice were analyzed by multiplex suspension array. The mRNA expression of each gene was normalized to Rpl13a. All data are expressed as mean ±S.E. of five mice in each group. *, Statistically significant difference between sham-operated and BDL mice ($p<0.05$). #. Statistically significant difference between WT and Oatp1a1-null mice after BDL.

2.14. BA-transporters in Ileum of WT and Oatp1a1-null Mice 1 Day after BDL

The mRNA expression of BA transporters were quantified in ilea of WT and Oatp1a1-null mice after BDL. Asbt is the major BA-uptake transporter for conjugated BAs in the ileum. BDL had no effect

on Asbt mRNA in WT mice, but tended to increase Asbt mRNA in Oatp1a1-null mice (Figure 6-17). Mrp3 is one basolateral transporter which has been suggested to play a role in the BA efflux from the intestine to blood. BDL had little effect on Mrp3 mRNA in ilea of WT and Oatp1a1-null mice. However, Mrp3 mRNA tended to be higher in both sham and BDL Oatp1a1-null mice than in WT mice. Ostα/β are major BA-efflux transporters in ileum. BDL had little effect on Ostα mRNA in WT or Oatp1a1-null mice. In contrast, BDL increased Ostβ mRNA about 120% in Oatp1a1-null mice but not in WT mice. Taken together, BDL appears to increase the BA-uptake and efflux transporters in ilea of Oatp1a1-null mice, and thus may increase the conjugated secondary BAs in serum and livers of Oatp1a1-null mice.

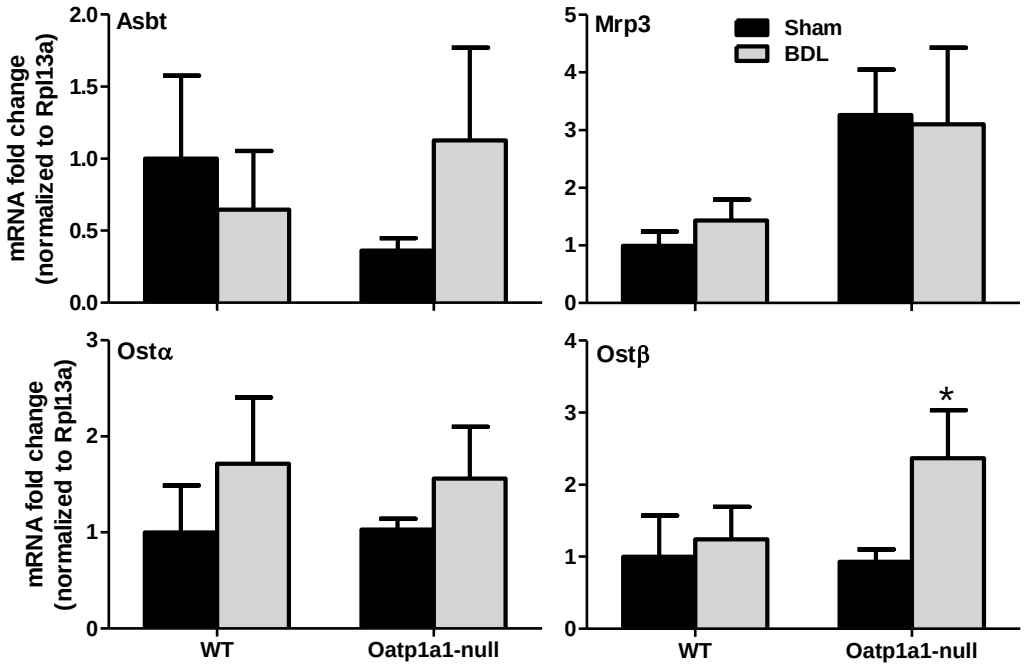

Figure 6-17. mRNA expression of BA-transporters in ilea of WT and Oatp1a1-null mice 1 day after BDL. Total RNA from ilea of sham-operated and BDL mice were analyzed by multiplex suspension array. The mRNA expression of each gene was normalized to Rpl13a. All data are expressed as mean ±S.E. of five mice in each group. *, Statistically significant difference between sham-operated and BDL mice ($p<0.05$).

2.15. BA-synthetic enzymes in WT and Oatp1a1-null Mice 1 Day after BDL

The mRNA expression of hepatic BA-synthetic enzymes was quantified to determine whether the increase of conjugated BAs in Oatp1a1-null mice after BDL is due to more BA-synthesis. Cyp7a1 and 8b1 are two critical enzymes in the classic pathway of BA synthesis. BDL of WT mice tended to decrease Cyp7a1 mRNA (about 95%), and significantly decreased Cyp8b1 mRNA (about 85%) (Figure 6-18). Similarly, BDL of Oatp1a1-null mice also decreased Cyp7a1 mRNA (about 95%) and Cyp8b1 mRNA (about 75%). Cyp27a1 and Cyp7b1 are involved in the alternative pathway of BA synthesis. BDL had little effect on Cyp27a1 mRNA in both WT and Oatp1a1-null mice. In contrast, BDL markedly decreased Cyp7b1 mRNA (about 82%) in WT mice but not in Oatp1a1-null mice. Taken together, Oatp1a1-null BDL mice had similar mRNA expression of BA-synthetic enzymes as WT BDL mice. Therefore, the increase of conjugated BAs in Oatp1a1-null mice after BDL does not appear to be due to BA-synthesis.

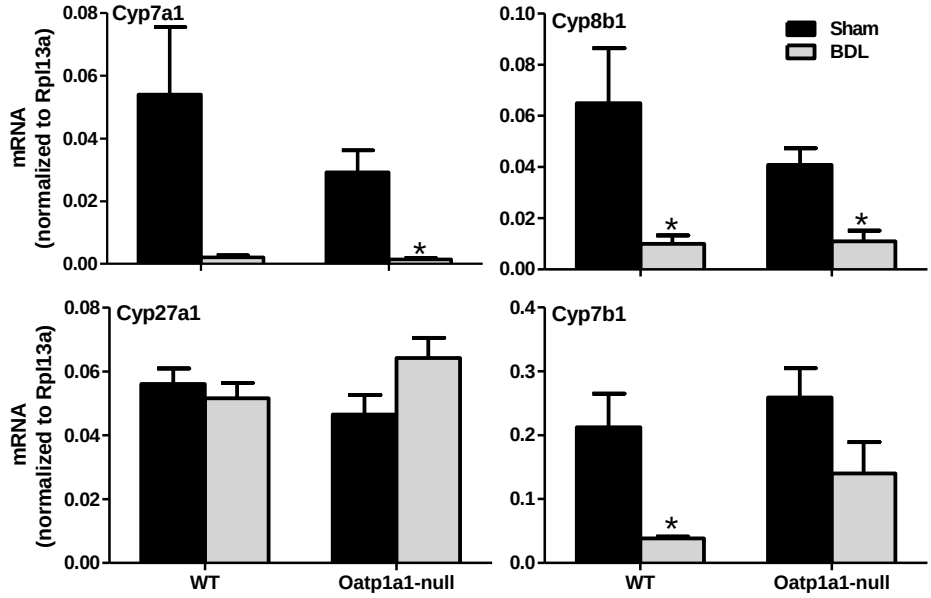

Figure 6-18. mRNA expression of BA-synthetic enzymes in livers of WT and Oatp1a1-null mice 1 day after BDL. Total RNA from livers of sham-operated and BDL mice were analyzed by multiplex

suspension array. The mRNA expression of each gene was normalized to Rpl13a. All data are expressed as mean ±S.E. of five mice in each group. *, Statistically significant difference between sham-operated and BDL mice ($p<0.05$).

2.16. Nuclear Receptors in WT and Oatp1a1-null Mice 1 Day after BDL

To investigate the mechanism of Cyp7a1 suppression in BDL mice, the mRNA expression of FXR, LXR, SHP, and LRH-1, which have been shown to regulate Cyp7a1, were quantified in livers of WT and Oatp1a1-null mice after BDL (Figure 6-19). BDL tended to increase FXR mRNA in livers of WT mice, but had no effect on FXR mRNA in livers of Oatp1a1-null mice. Although BDL had little effect on LXR mRNA in either WT or Oatp1a1-null mice, LXR mRNA was lower in Oatp1a1-null BDL mice than in WT BDL mice. BDL increased SHP mRNA about 3.5-fold in livers of WT mice, but not significantly in Oatp1a1-null mice. As a result, Oatp1a1-null BDL mice had about 50% lower SHP mRNA than WT BDL mice. Furthermore, BDL had little effect on LRH-1 mRNA in livers of both WT and Oatp1a1-null mice. Taken together, it appears that the FXR-SHP pathway is activated in livers of WT BDL mice, but not in livers of Oatp1a1-null BDL mice. Therefore, the activation of FXR-SHP does not appear to be the reason why Cyp7a1 was suppressed in Oatp1a1-null mice after BDL.

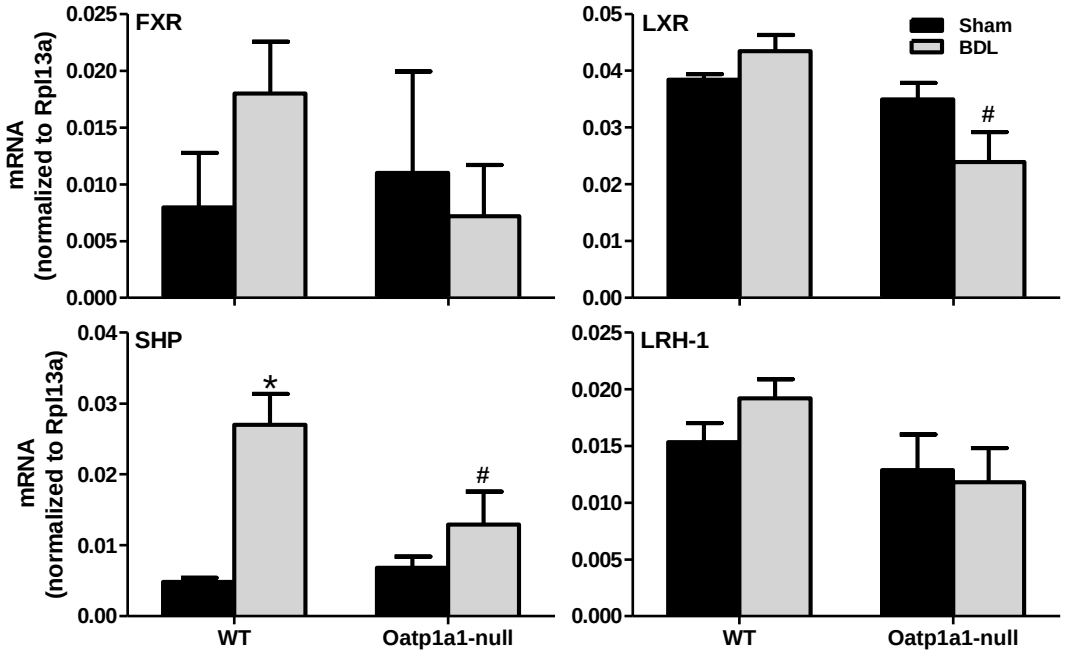

Figure 6-19. mRNA expression of FXR, LXR, SHP, and LRH-1 in livers of WT and Oatp1a1-null mice 1 day after BDL. Total RNA from livers of sham-operated and BDL mice were analyzed by multiplex suspension array. The mRNA expression of each gene was normalized to Rpl13a. All data are expressed as mean ±S.E. of five mice in each group. *, Statistically significant difference between sham-operated and BDL mice ($p<0.05$). #, Statistically significant difference between WT and Oatp1a1-null mice after BDL.

2.17. Fgf15-Fgfr4 Pathway in WT and Oatp1a1-null Mice 1 Day after BDL

To further investigate the regulation of Cyp7a1, the mRNA expression of Fgfr4 in livers and Fgf15 in ilea were quantified in WT and Oatp1a1-null mice after BDL. As shown in figure 6-20, BDL had little effect on either Fgfr4 or Fgf15 mRNA in WT and Oatp1a1-null mice, suggesting that the inhibition of Cyp7a1 in mice 1 day after BDL does not appear to be due to intestinal Fgf15.

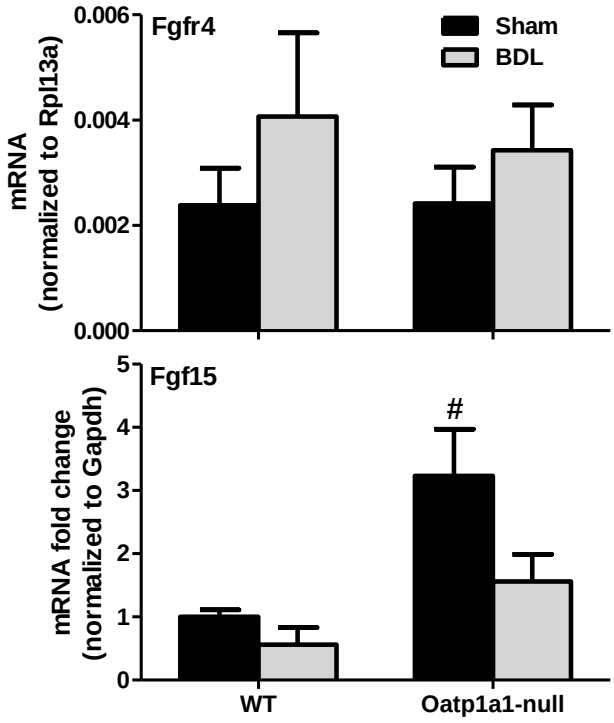

Figure 6-20. mRNA expression of Fgfr4 in livers and Fgf15 in ilea of WT and Oatp1a1-null mice 1 day after BDL. Total RNA from ilea of sham-operated and BDL mice were analyzed by multiplex suspension array. The mRNA expression of each gene was normalized to Rpl13a. All data are expressed as mean ±S.E. of five mice in each group. #, Statistically significant difference between WT and Oatp1a1-null mice after BDL.

2.18. PXR, CAR, PPARα, and Nrf2 Target Genes in WT and Oatp1a1-null Mice 1 Day after BDL

Activations of PXR, CAR, PPARα, and Nrf2 are possible adaptive responses of mice to protect against liver toxicity during cholestasis. Cyp3a11 is a target gene of PXR. BDL increased Cyp3a11 mRNA about 4.5-fold in livers of WT mice, but not in Oatp1a1-null mice (Figure 6-21). As a result, Cyp3a11 mRNA in Oatp1a1-null BDL mice was 70% lower than in WT BDL mice. Cyp2b10 is a target gene of CAR. BDL increased Cyp2b10 mRNA in livers of both WT (about 14-fold) and Oatp1a1-null

mice (about 8-fold). Cyp4a14 is a target gene of PPARα. BDL increased Cyp4a14 mRNA about 2.5-fold in livers of WT mice, but not in Oatp1a1-null mice. Nqo1 is a target gene of Nrf2. BDL increased Nqo1 mRNA about 3-fold in livers of WT mice but not significantly in Oatp1a1-null mice. As a result, Nqo1 mRNA in Oatp1a1-null BDL mice was about 45% lower than in WT BDL mice. Thus, it appears that BDL activated PXR, CAR, PPARα, and Nrf2 in livers of WT mice. However, the activation of these nuclear receptors was either deficient (PXR, PPARα and Nrf2) or lower (CAR) in livers of Oatp1a1-null BDL mice than in WT BDL mice.

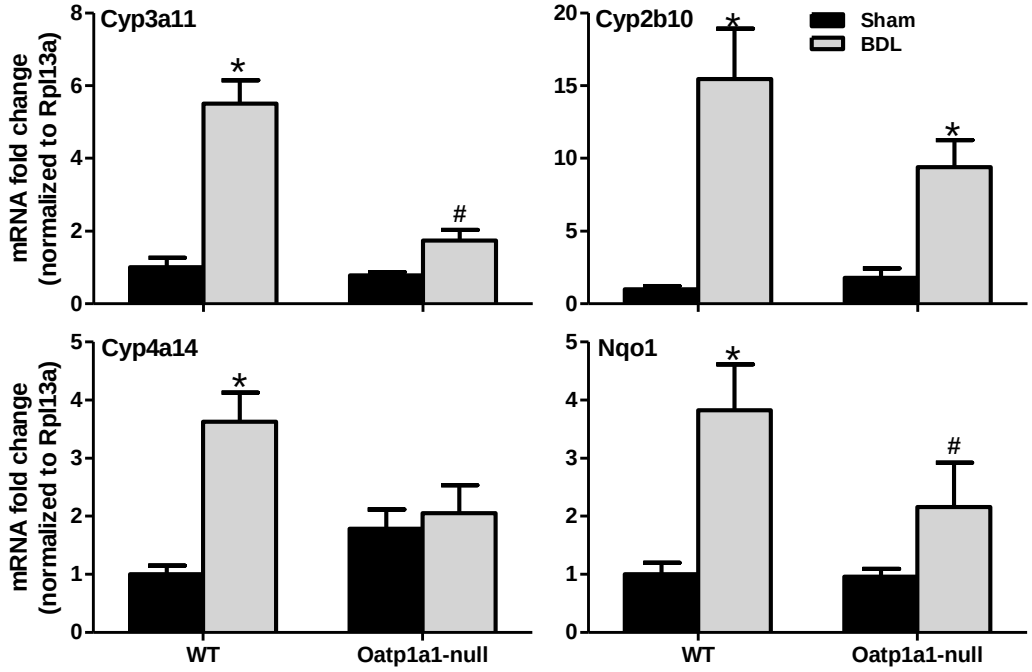

Figure 6-21. mRNA expression of Cyp3a11, Cyp2b10, Cyp4a14, and Nqo1 in livers of WT and Oatp1a1-null mice 1 day after BDL. Total RNA from livers of sham-operated and BDL mice were analyzed by multiplex suspension array. The mRNA expression of each gene was normalized to Rpl13a. All data are expressed as mean ±S.E. for five mice in each group. *, Statistically significant difference between sham-operated and BDL mice ($p<0.05$). #, Statistically significant difference between WT and Oatp1a1-null mice after BDL.

2.19. Liver Inflammation in WT and Oatp1a1-null Mice 1 Day after BDL

Because the previous study (Chapter 5) showed that knockout of Oatp1a1 increased intestinal bacteria in mice, it is possible that the liver toxicity in Oatp1a1-null mice 1 day after BDL is caused by bacteria-mediated inflammation. Therefore, the mRNA expression of three inflammation markers, namely TNFα, IL-6, and TGF-β1 were quantified in livers of WT and Oatp1a1-null mice after BDL. As shown in figure 6-22, BDL tended to, but not significantly increase TNFα mRNA in livers of both WT and Oatp1a1-null mice. BDL increased IL-6 mRNA significantly in WT mice (about 120%), but not significantly in Oatp1a1-null mice. BDL had no effect on TGF-β1 mRNA in WT mice, but significantly increased TGF-β1 mRNA about 45% in Oatp1a1-null mice. As a result, Oatp1a1-null BDL mice had similar mRNA expression of TNFα, IL-6, and TGF-β1 in livers as WT BDL mice, which does not explain the difference of liver toxicity between WT and Oatp1a1-null mice after BDL.

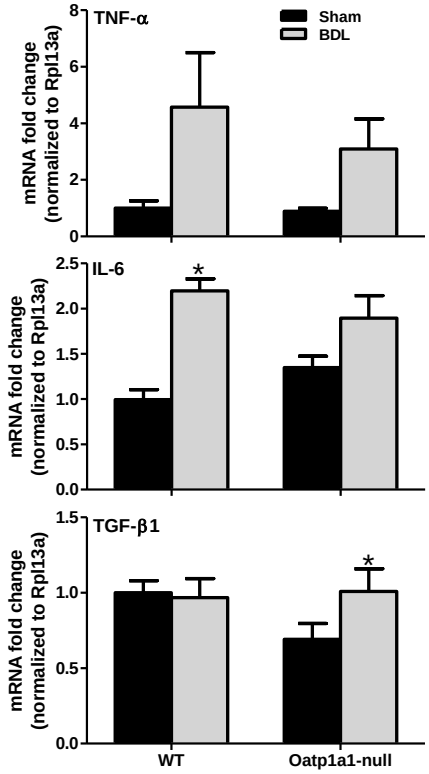

Figure 6-22. mRNA expression of TNFα, IL-6, and Tgf-β1 in livers of WT and Oatp1a1-null mice 1 day after BDL. Total RNA from livers of sham-operated and BDL mice were analyzed by multiplex suspension array. The mRNA expression of each gene was normalized to Rpl13a. All data are expressed as mean ±S.E. of five mice in each group. *, Statistically significant difference between sham-operated and BDL mice ($p<0.05$). #, Statistically significant difference between WT and Oatp1a1 after BDL.

2.20. Liver Histological Analysis in Antibobiotic-treated WT and Oatp1a1-null Mice after BDL

After BDL, the secondary BAs, which are produced by intestinal bacteria, were increased markedly in Oatp1a1-null mice. To determine the effect of secondary BAs in liver toxicity, WT and Oatp1a1-null mice were treated with antibiotics for 10 days before BDL. In a preliminary experiment, antibiotics-treated Oatp1a1-null mice were shown to be very sick within 3 days of BDL. Thus, 1-day BDL was conducted on antibiotic-treated WT and Oatp1a1-null mice. Liver histological analysis showed that 1-day of BDL resulted in large area of necrosis in livers of antibiotic-treated Oatp1a1-null mice, but not in antibiotic-treated WT mice (Figure 6-23), indicating that antibiotic-treatment did not prevent liver toxicity in Oatp1a1-null mice after BDL.

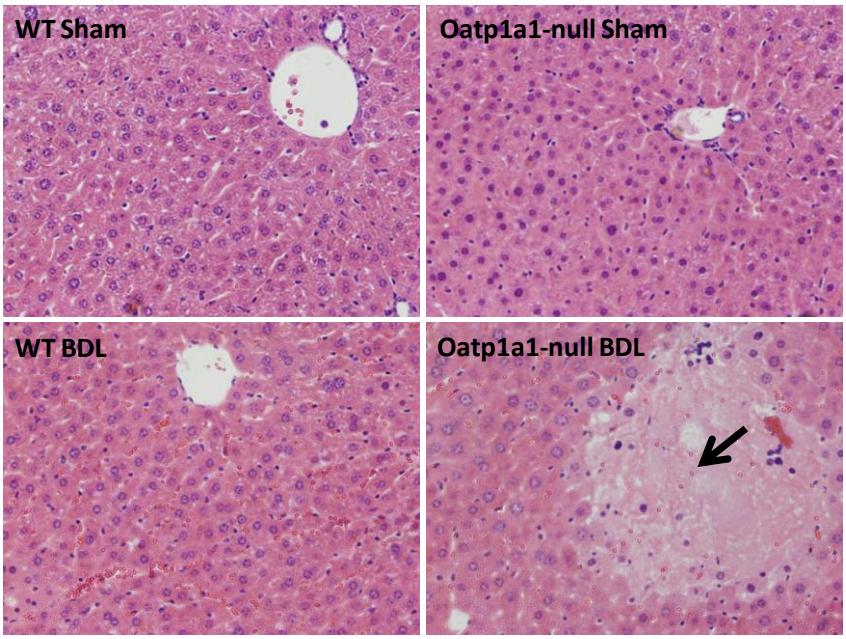

Figure 6-23. Histological analysis of liver sections from antibiotic-treated WT and Oatp1a1-null mice 1 day after BDL. Liver sections (5μm) were stained with hematoxylin-eosin.

2.21. Serum BAs in Antibiotic-treated WT and Oatp1a1-null Mice after BDL

The concentration of total BAs was quantified in serum of WT and Oatp1a1-null mice after BDL to determine the effect of antibiotics on BA metabolism (Figure 6-24). Antibiotics markedly altered the BA profiles, even in Oatp1a1-null sham mice. Compared to WT sham mice, Oatp1a1-null sham mice had similar concentrations of unconjugted BAs, but had about 15-fold higher concentrations of conjugated BAs in serum. As a result, Oatp1a1-null sham mice had about 15-fold higher concentration of total BAs in serum than did WT sham mice.

After BDL, both unconjugated and conjugated BAs were markedly increased in serum of WT and Oatp1a1-null mice. Oatp1a1-null BDL mice had about 4-fold higher unconjugated BAs and 23-fold higher conjugated BAs in serum than WT BDL mice. As a result, the concentration of total BAs in serum of Oatp1a1-null BDL mice was about 5-fold higher than that in WT BDL mice.

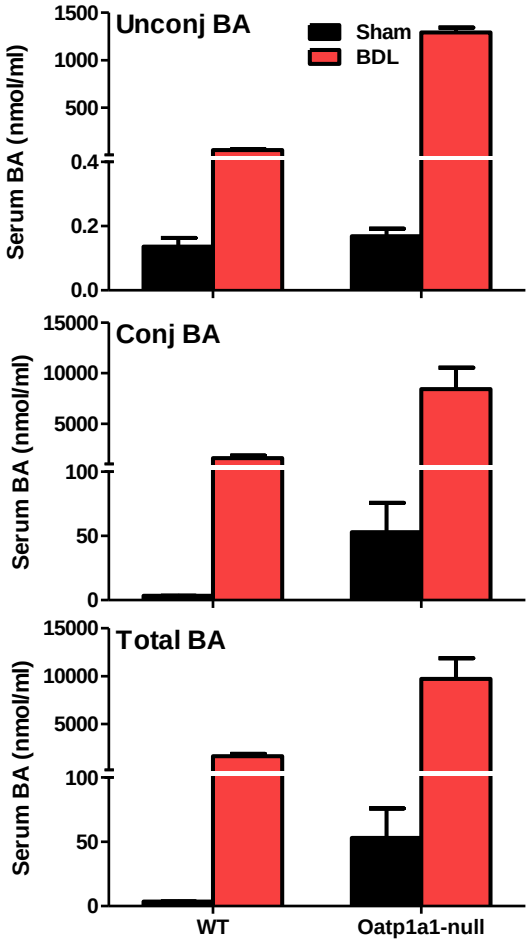

Figure 6-24. Concentrations of unconjugated BAs, conjugated BAs, and total BAs in serum of antibiotic-treated WT and Oatp1a1 mice 1 day after BDL. All BA data are expressed as mean ±S.E. of 2-4 mice in each group.

2.22. Individual BAs in Serum of Antibiotic-treated WT and Oatp1a1-null Mice after BDL

The concentrations of individual BAs in serum were quantified to determine which BAs were altered in WT and Oatp1a1-null mice after BDL. After antibiotic treatment, Oatp1a1-null sham mice had higher βMCA (about 2-fold), but similar ωMCA, CA, MDCA, UDCA, HDCA, CDCA, DCA, and LCA in serum than WT sham mice (Figure 6-25a). In contrast, after antibiotic treatment, Oatp1a1-null sham

mice had higher TωMCA (7-fold), TβMCA (13-fold), TCA (17-fold), TMDCA (28-fold), TUDCA (9-fold), THDCA (6-fold), TCDCA (69-fold), and TDCA (2-fold) in serum than WT sham mice (Figure 6-25b).

After antibiotic treatment, Oatp1a1-null BDL mice had higher ωMCA (9-fold), βMCA (24-fold), CA (24-fold), MDCA (49-fold), UDCA (172-fold), HDCA (64-fold), CDCA (13-fold), and DCA (11-fold) in serum than WT BDL mice (Figure 6-25a). In addition, Oatp1a1-null BDL mice also had higher TωMCA (4-fold), TβMCA (5-fold), TCA (4-fold), TMDCA (5-fold), TUDCA (8-fold), THDCA (3-fold), TCDCA (9-fold), TDCA (7-fold), and TLCA (8-fold) in serum than WT BDL mice (Figure 6-26b).

Taken together, knockout of Oatp1a1 increased serum conjugated BAs in mice after antibiotic treatment. After BDL, both unconjugated and conjugated BAs were increased in serum of Oatp1a1-null mice with antibiotic treatment.

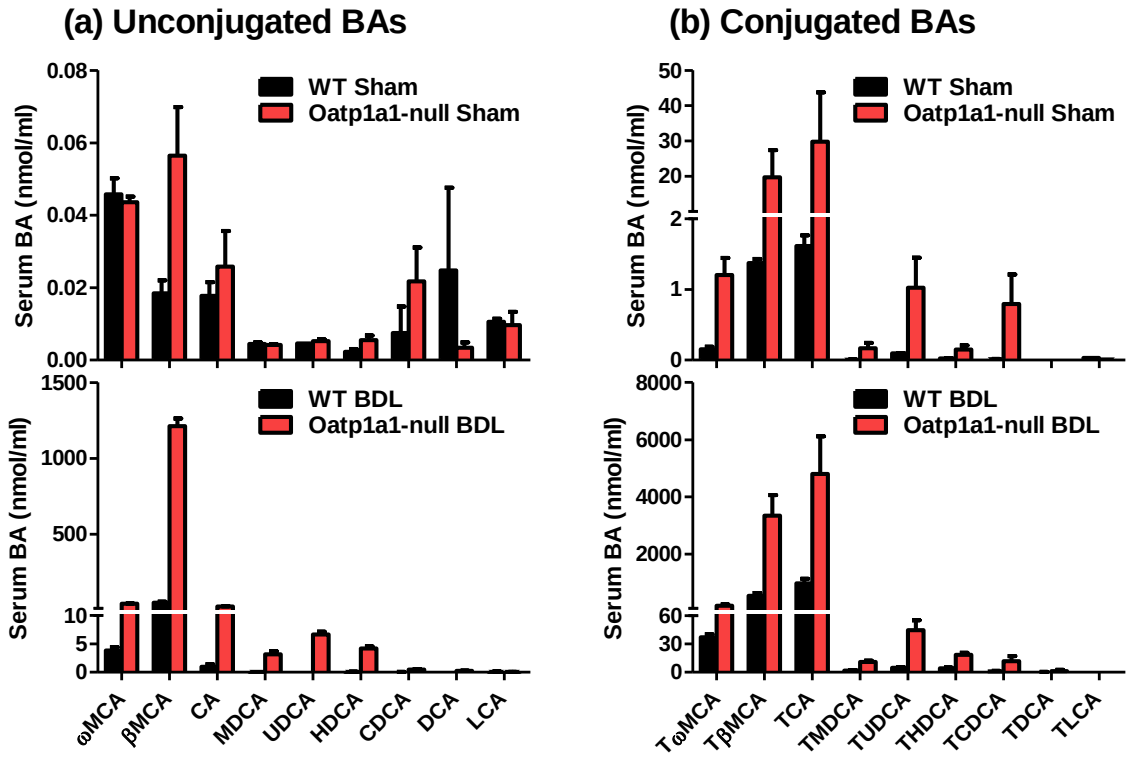

Figure 6-25. Concentrations of individual unconjugated (a) and conjugated BAs (b) in serum of antibiotic-treated WT and Oatp1a1 mice 1 day after BDL. All BA data are expressed as mean ±S.E. of 2-4 mice in each group.

2.23. Total BAs in Livers of Antibiotic-treated WT and Oatp1a1-null Mice after BDL

Figure 6-26 shows the concentrations of unconjugated BAs, conjugated BAs, and total BAs in livers of WT and Oatp1a1-null mice. Compared to WT sham mice, Oatp1a1-null sham mice tended to have lower concentrations of unconjugated BAs (decrease about 50%) and conjugated BAs (decrease about 20%) in livers. As a result, Oatp1a1-null sham mice had about 25% lower concentrations of total BAs in livers than WT sham mice. After BDL, unconjugated and conjugated BAs were increased similarly in livers of both WT and Oatp1a1-null mice. Oatp1a1-null BDL mice had similar concentrations of unconjugated and conjugated BAs in livers as WT BDL mice. Therefore, the concentrations of total BAs in livers were similar between WT BDL and Oatp1a1-null BDL mice.

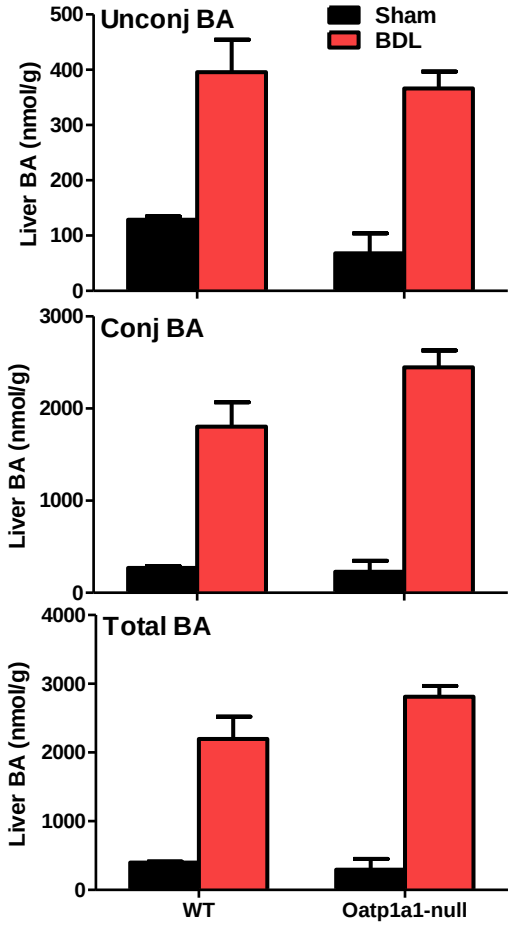

Figure 6-26. Concentrations of unconjugated BAs, conjugated BAs, and total BAs in livers of antibiotic-treated WT and Oatp1a1 mice 1 day after BDL. All BA data are expressed as mean ±S.E. of 2-4 mice in each group.

2.24. Individual BAs in Livers of Antibiotic-treated WT and Oatp1a1-null Mice after BDL

Figure 6-27 shows the concentrations of individual BAs in livers of WT and Oatp1a1-null mice. After antibiotic treatment, Oatp1a1-null sham mice tended to have lower ωMCA, βMCA, CA, MDCA, UDCA, HDCA, and CDCA in livers than WT sham mice. In contrast, the concentrations of individual conjugated BAs were similar between WT and Oatp1a1-null mice after BDL.

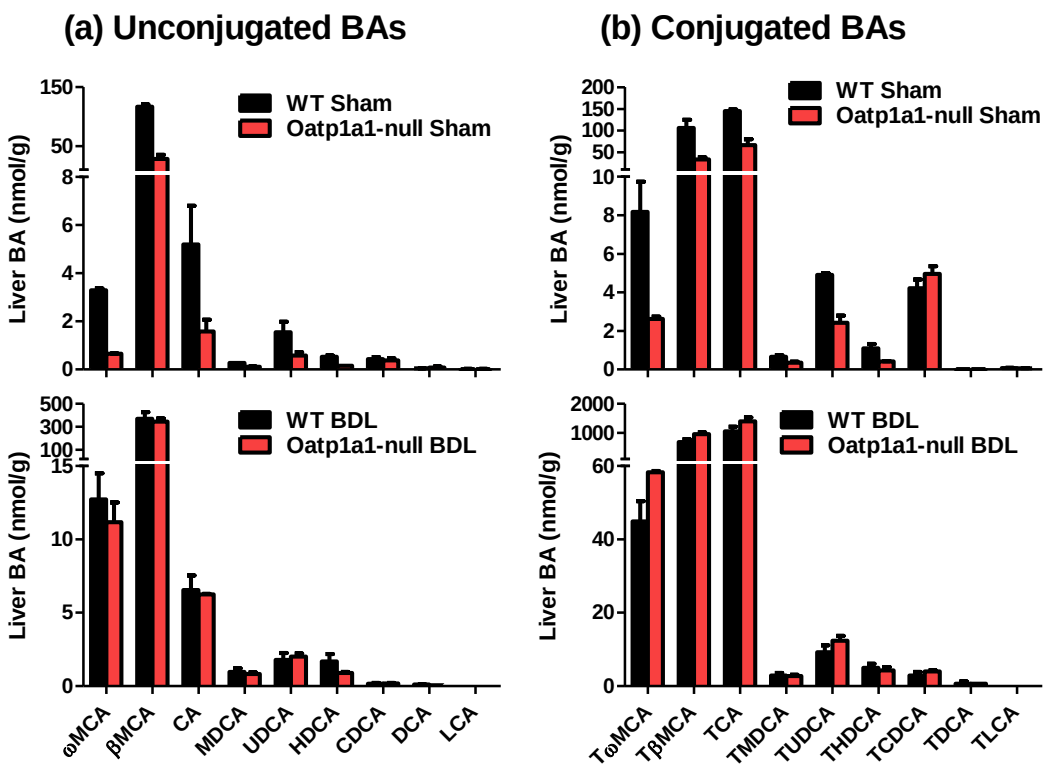

Figure 6-27. Concentrations of individual unconjugated (a) and conjugated BAs (b) in livers of antibiotic-treated WT and Oatp1a1 mice 1 day after BDL. All BA data are expressed as mean ±S.E. of two-four mice in each group.

2.25. BA Transporters in Ilea of Antibiotic-treated WT and Oatp1a1-null Mice after BDL

The mRNA expression of BA transporters was quantified in the ilea of WT and Oatp1a1-null mice after BDL to determine the effect of antibiotics on intestinal BA transport (Figure 6-28). After antibiotic treatment, knockout of Oatp1a1 increased Asbt (12-fold), Mrp3 (2-fold), and Ostα/β (3-fold) in ilea of sham mice. This may explain why knockout of Oatp1a1 increased the serum conjugated BAs in sham mice after antibiotic treatment. Interestingly, BDL had little effect on BA-transporters in ilea of WT and Oatp1a1-null mice pretreated with antibiotics.

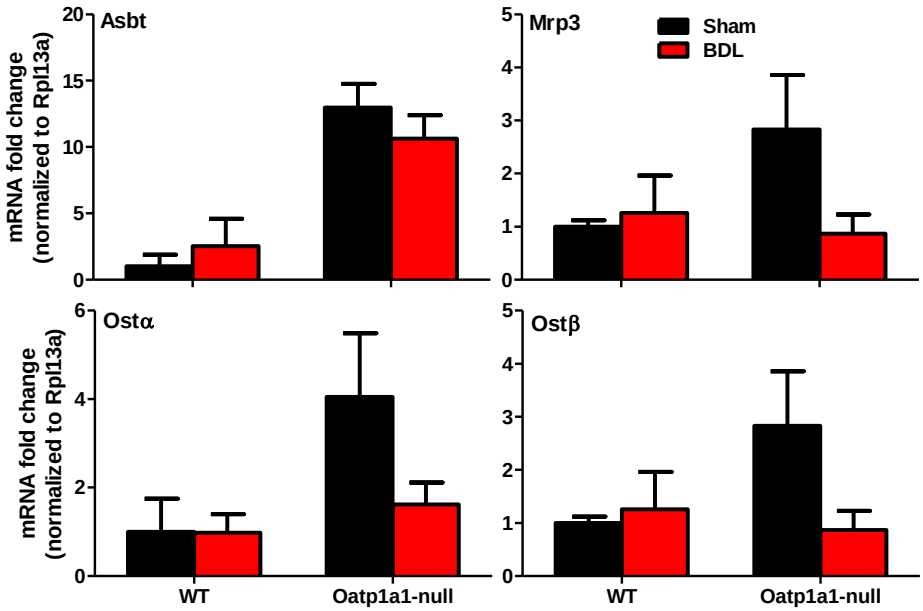

Figure 6-28. mRNA expression of BA-transporters in ilea of WT and Oatp1a1-null mice 1 day after BDL. Total RNA from ilea of sham-operated and BDL mice were analyzed by multiplex suspension array. The mRNA expression of each gene was normalized to Gapdh. All data are expressed as mean ±S.E. of 2-4 mice in each group. *, Statistically significant difference between sham-operated and BDL mice ($p<0.05$). #. Statistically significant difference between WT and Oatp1a1-null mice after BDL.

III. Discussion

In general, the cholestatic liver favors the synthesis of more hydrophilic and thus less toxic BAs. During cholestasis, human livers favor the synthesis of CA, which is more hydrophilic than CDCA. For example, GCA is lower than GCDCA in serum of healthy humans, but GCA becomes the prevailing BA in serum of patients with drug-induced cholestasis (Burkard et al., 2005). In addition, CA becomes the prevailing BA in livers of patients with chronic cholestasis, and is about 8-fold higher than in healthy controls (Fischer et al., 1996). In contrast to humans, rodent livers hydroxylate CDCA extensively at the 6β-position to form αMCA, which can be further converted to βMCA by epimerization of the 7α-OH to the 7β-OH (Botham and Boyd, 1983). MCAs are more hydrophilic than CA and CDCA. This may explain why βMCA becomes the predominant BA in livers of BDL rats (Mahowald et al., 1957; Greim et al., 1972; Kinugasa et al., 1981).

The present study indicates that livers of BDL mice have three mechanisms to make BAs more hydrophilic and thus less toxic. First, livers of BDL mice increased both the 6β-hydroxylation and 7-epimerization of BAs. As a result, TβMCA concentration increased in both serum and livers of BDL mice and became the predominant BA within 1 d after BDL. In addtion, TUDCA, a 7-epimerization product of TCDCA, also increased markedly in serum and livers of BDL mice. Second, livers of BDL mice increased the conjugation of BAs with taurine. In livers of BDL mice, CA and βMCA continued to decrease between 6 h and 14 d, whereas TCA and TβMCA remained at high levels. Their relative concentrations suggest that more than 99% of newly synthesized BAs (CA and βMCA) are conjugated with taurine in livers of BDL mice. As a result, more than 99% of BAs were conjugated BAs in livers of mice 14 d after BDL. In contrast, only 80% of BAs were conjugated BAs in livers of sham-operated mice. Third, livers of BDL mice increased BA sulfation. TCA7S and TCDCA7S increased markedly in livers of BDL mice between 6h and 5 d, but decreased thereafter. The decrease in TCA7S and TCDCA7S after 5 d of BDL may be due to inhibition of sulfotransferases by high concentrations of BAs, such as TUDCA, because a previous study showed that feeding UDCA markedly suppressed sulfation of CA and CDCA in

mice (Zhang and Klaassen, 2010). Therefore, BA sulfation does not appear to be an important pathway to detoxify BAs during obstructive cholestasis in mice. Taken together, BAs in livers of BDL mice are more hydrophilic than sham controls, mainly due to increased 6β-hydroxylation and conjugation of BAs with taurine.

After BDL, the liver becomes the primary source of serum BAs. Kinugasa et al. (1981) reported that the urinary excretion of BAs in BDL rats increased markedly after surgery, whereas the fecal excretion of BAs decreased. This suggests that BAs in BDL rats efflux from the liver, enter into the circulation, and are excreted into urine. In the present study, the total BA concentrations in sham-operated mice were about 30- to 100-fold higher in liver (46~250 nmol/g) than in serum (1.6~3.2 nmol/ml). After BDL, the total BA concentrations in serum (880~3400 nmol/ml) were close to that in liver (1540~2550 nmol/g). More than 90% of BAs in the serum of BDL mice were conjugated primary BAs (TCA, TCDCA, and TMCA), indicating that BAs in serum of BDL mice are refluxed from the livers, but not the intestine. This reflux of BAs from liver to blood occured rapidly after BDL, which resulted in a 1300-fold increase of BAs in mouse serum within 6 h. Because the liver does not synthesize DCA and LCA, the concentrations of TDCA and TLCA decreased in livers of BDL mice, and were lower than sham controls 1 d after BDL. Taurine-conjugated primary BAs (TCA, TCDCA, and TMCA), but not unconjugated primary BAs (CA, CDCA, or MCA), increased markedly in serum of BDL mice, indicating that primary BAs are conjugated with taurine in hepatocytes before they are effluxed back into the blood. In conclusion, serum BAs in BDL mice are refluxed from the livers, and may serve as a biomarker for cholestatic progression.

The present study shows that Oatp1a1-null mice are more susceptible to BDL than WT mice. One-day BDL was chosen in the present study, because Oatp1a1-null mice became very sick after 2 days of BDL. BDL decreases the mRNA expression of BA-uptake transporters Ntcp, Oatp1a1, and Oatp1b2 at late time intervals, but increases Oatp1a4 mRNA in livers of mice, which is consistent with a previous study (Slitt et al., 2006). The decrease of these BA transporters has been hypothesized to prevent further

BA-accumulation in livers of mice after BDL. However, little research has been performed to evaluate this hypothesis due to the lack of knockout mice. Surprisingly, even within 1 day after BDL, Oatp1a1-null mice had severe liver toxicity. The enhanced liver toxicity in Oatp1a1-null mice after BDL appears to be due to the increase of secondary BAs in serum and livers. Knockout of Oatp1a1 markedly increased conjugated secondary BAs, such as TDCA, TLCA, TMDCA, TUDCA, and THDCA in serum of mice after BDL. In contrast, knockout of Oatp1a1 only slightly increased the unconjugated secondary BAs, such as DCA, MDCA, and HDCA. In addition, knockout of Oatp1a1 had little effect on the mRNA expression of BA conjugation enzymes, namely Fatp5 and Baat, in livers of mice after BDL. This suggests that these secondary BAs, which are increased in Oatp1a1-null BDL mice, were mainly from the small intestine, but not from the large intestine, where the majority conjugated BAs will be deconjugated. The increase of conjugated secondary BAs in serum of Oatp1a1-null BDL mice seems to be due to the enhanced intestinal absorption, because knockout of Oatp1a1 tended to increase the BA transporters, such as Asbt and Ostβ, in ilea of mice after BDL. As a result of the enhanced intestinal absorption, the conjugated secondary BAs such as TDCA, TMDCA, TUDCA, and THDCA were also higher in livers of Oatp1a1-null BDL mice than in WT BDL mice. It is interestingly to find that knockout of Oatp1a1 also increased TCA in livers, but not serum of mice after BDL. Actually, almost all the CA-derived secondary BAs, such as TDCA, T-12-epiDCA, and 7-oxoDCA, which were almost undetectable in WT mice after BDL, were markedly increased in Oatp1a1-null mice after BDL. As shown in the BDL study on the time course of BA concentrations in C57BL/6 mice, TCA in livers of BDL mice were markedly increased at 6 h, and thereafter decreased from 6h to 1d after surgery. Thus, it is possible that knockout of Oatp1a1 fails to decrease or detoxify TCA from 6h to 1d in livers of mice after BDL. Taken together, knockout of Oatp1a1 appears to decrease the liver BA detoxification, increase secondary BAs, and therefore increase the liver toxicity in mice after BDL. Interestingly, after BDL, the intestine contents in Oatp1a1-null mice were much drier than in WT mice, suggesting that BDL may dehydrate the intestine of Oatp1a1-null mice

(data not shown). Further studies are required to determine the effects of BDL on the intestinal contents of Oatp1a1-null mice.

It appears that BDL actiaves the FXR-SHP pathway in livers of WT mice, but not in Oatp1a1-null mice. The mechanisms of Cyp7a1 regulation are still not fully understood during obstructive cholestasis. FXR plays a key role in regulating Cyp7a1, via SHP in liver and Fgf15 in intestine (Goodwin et al., 2000; Inagaki et al., 2005). However, knockout of SHP did not prevent the repression of Cyp7a1 in within 2 d or 5 d after BDL, suggesting that Cyp7a1 in BDL mice may be regulated in a SHP-independent pathway (Park et al., 2008). In the present study, Cyp7a1 and Cyp8b1 were decreased markedly in livers of both WT and Oatp1a1-null mice 1 day after BDL. FXR tended to increase in livers of WT mice after BDL. In addition, the increase of SHP and Bsep, as well as the decrease of Ntcp, suggest that FXR is activated in livers of WT mice after BDL. In a previous study, 4 d after BDL, ileal Fgf15 was decreased, whereas hepatic Cyp7a1 was increased in mice, suggesting a critical role of Fgf15 in Cyp7a1 regualtion during cholestasis (Inagaki et al., 2005). In the present study, BDL had little effect on intestinal Fgf15 and liver Fgfr4 in both WT and Oatp1a1-null mice, suggesting that Ffg15-Fgfr4 pathway is not activated in mice 1 day after BDL. Thus, the suppression of Cyp7a1 and Cyp8b1 in livers of WT BDL mice may be due to the activation of FXR pathway. In contrast to WT mice, the suppression of Cyp7a1 and Cyp8b1 in livers of Oatp1a1-null BDL mice appears not to be due to activation of either FXR-SHP or Fgf15-Fgfr4 pathway, because BDL in Oatp1a1-null mice had little effect on the target genes involved in these two pathways. In a previous study (Chapter 5), Cyp7a1 was lower in livers of Oatp1a1-null mice than in WT mice. In the present study, Cyp7a1 tended to be lower in livers of Oatp1a1-null sham mice than in WT sham mice. This suggests that Oatp1a1, similar as Oatp1b2 (Csanaky et al., 2010), is important to maintain the expression of Cyp7a1 in livers of mice. Thus, it is possible that BDL further strengthens the suppression of Cyp7a1 in livers of Oatp1a1-null mice. During cholestatic liver injury, hepatic non-parenchymal cells release proinflammatory cytokines (IL-1β, TNFα) and growth factors (TGFβ), which have been shown to inhibit Cyp7A1 in human hepatocytes (De Fabiani et al., 2001; Li et al., 2006, 2007).

Thus, it is also possible that these cytokines may contribute to the suppression of Cyp7a1 in Oatp1a1-null mice, because the overgrowth of bacteria in the intestine of Oatp1a1-null mice may increase the inflammation in the liver (as shown in chapter 5). However, the present study shows that the mRNA expression of TNFα, IL-6, and TGF-β1 were similar in WT and Oatp1a1-null mice after BDL. Therefore, further studies are required to clarify the mechanism of Cyp7a1 regulation in Oatp1a1-null mice after BDL.

PXR, CAR, PPARα, and Nfr2 are all key nuclear receptors that participate in the adaptive response to cholestatic injury (Guo et al, 2003; Stedman et al., 2005; Thomas et al., 2005; Okada et al., 2009). PXR and CAR play important roles in BA-detoxifying enzymes in mice, such as the regulation of Mrp4 (Wagner et al., 2005). In addition, PPARa and Nrf2 have also been shown to regulate BA-detoxyfying enzymes, such as Mrps and Ugts (Barbier et al., 2003; Maher et al., 2008; Okada et al., 2009). Unlike other studies, the present study shows that BDL had little effect on Mrp4 in either WT or Oatp1a1-null mice, which may be due to the early stage (within 1 d) of BDL in mice, because Mrp4 was found to be only induced after 2 days of BDL in C57BL/6 mice (data not shown). Thus, Mrp transporters may be not an ideal marker for activation of nuclear receptors during the early stage of BDL-induced cholestasis. In the present study, BDL markedly increased Cyp3a11, Cyp2b10, Cyp4a14, and Nqo1 in WT mice 1 day after surgery, suggesting that PXR, CAR, PPARα, and Nrf2 are activated in WT mice after BDL. In contrast, in livers of Oatp1a1-null BDL mice, activation of these nuclear receptors was either not apparent (PXR, PPARα and Nrf2) or lower (CAR) than WT BDL mice. Taken together, Oatp1a1-null mice have an impaired cytoprotective response in BDL-induced obstructive cholestasis.

Antibiotic treatment does not prevent liver toxicity in Oatp1a1-null mice after BDL. Endotoxin has been shown to potentiate hepatocyte apoptosis and necrosis during obstructive cholestasis (Sewnath et al., 2000; Yorganci et al., 2004). Knockout of Oatp1a1 markedly increased the secondary BAs in serum and livers of mice after BDL. In addition, knockout of Oatp1a1 increased the intestinal bacteria in mice (as shown in Chapter 5). Therefore, it is possible that the overgrowth of intestinal bacteria may increase

secondary BAs and endotoxins, and thus enhance the liver toxicity in Oatp1a1-null mice after BDL. Surprisingly, antibiotic treatment in the present study tended to increase BDL-induced liver toxicity in Oatp1a1-null mice. After antibiotic treatment, the secondary BAs were decreased in both WT and Oatp1a1-null mice, and were not increased in Oatp1a1-null mice after BDL. This suggests that the liver toxicity in antibiotic-treated Oatp1a1-null mice after BDL is not due to an increase of secondary BAs. Interestingly, antibiotics treatment markedly increased TβMCA, βMCA, and TCA in serum of Oatp1a1-null mice. In addition, antibiotics treatment also increased TωMCA, TUDCA, and THDCA in serum of Oatp1a1-null mice, suggesting that the increase of these three secondary BAs is mainly due to the increase of their primary BA, namely TβMCA. After BDL, not only conjugated BAs but also unconjugated BAs, were markedly increased in antibiotic-treated Oatp1a1-null mice. This may be due to enhanced intestinal absorption, because antibiotic treatment increases the mRNA expression of Asbt, Mrp3, and Ostα/β in ilea of Oatp1a1-null mice. Taken together, antibiotics treatment appears to increase the intestinal absorption of BAs in Oatp1a1-null mice, and thus increase liver toxicity.

In summary, the findings in this study demonstrate that: (1) BDL increases the hydrophilic BAs, but decreases secondary BAs in livers of WT mice; (2) Compared to Ntcp and Oatp1b2, the suppression of Oatp1a1 in mouse liver is more prominent during the progression of BDL-induced cholestasis; (3) Knockout of Oatp1a1 increases liver toxicity in mice 1 day after BDL, which may be due to the increase of secondary BAs in livers of Oatp1a1-null mice; (4) Knockout of Oatp1a1 results in an impaired cytoprotective response in mice during BDL-induced cholestasis; (5) Antibiotic treatment appears to increase intestinal BA absorption and thus increase BDL-induced liver toxicity in Oatp1a1-null mice. Taken together, Oatp1a1 plays a unique and essential protective role in the adaptive response to obstructive cholestasis liver injury.

CHAPTER 7

SUMMARY AND DISCUSSION OF DISSERTATION

Organic anion transporting polypeptides (human: OATPs; all other species: Oatps; gene symbol: *SLCO/Slco*) are sodium-independent transport systems that mediate the transmembrane transport of a wide range of amphipathic endogenous and exogenous organic compounds (Hagenbuch and Meier, 2003; Hagenbuch and Meier, 2004). The first Oatp was cloned in rat by Jacquemin and colleagues in 1994 (Jacquemin *et al.*, 1994). Since then, the superfamily of OATP/Oatps has expanded to include 9 human, 13 rat, and 15 mouse Oatps (Hagenbuch and Meier, 2003). OATP/Oatps are thought to be 12-transmembrane spanning "multi-specific" transporters, capable of transporting structurally diverse substrates, including conjugated hormones, leukotriene C_4, bile acids, thyroid hormones, prostaglandins, digoxin, ouabain, fexofenadine, ochratoxin A, pravastatin, phalloidin, and potentially many other chemicals. Malfunction of OATPs may lead to decreased drug efficacy, and/or increased toxicity. Thus, for better human health, it is important to understand the *in vivo* roles of these transporters.

Mouse Oatp1a1, 1a4, and 1b2 as well as human OATP1A2, 1B1 and 1B3 are highly expressed in liver (Hagenbuch et al., 2000; Ogura et al., 2000; Ogura et al., 2001; Li et al., 2002). Whereas mouse Oatp1b2 is orthologous to human OATP1B1 and OATP1B3, Oatp1a1 and 1a4 have no human orthologs as defined by sequence similarity. However, Oatp1a1 and 1a4 functions are preserved in humans. For example, Oatp1a1 and Oatp1a4 have been shown to share a wide range of substrates as do human OATP1B1 and 1B3 (Hagenbuch and Meier, 2003). Although Oatp1b2 is a homolog of human OATP1B1, Chen et al. (2008) showed that Oatp1b2 plays important roles in the hepatic uptake of only two (rifampicin and lovastatin) out of total six model compounds (cerivastatin, lovastatin, pravastatin, simvastatin, rifampicin, and rifamycin SV), which have been shown to interact with human OATP1B1. Thus, it is possible that other Oatps, such as Oatp1a1 and Oatp1a4, may mediate the hepatic uptake of the

other four model compounds. Furthermore, understanding the *in vivo* role of Oatp1a1 and Oatp1a4 is necessary for extrapolation of data from laboratory animals to humans. In the development of drugs and other chemicals, such as pesticides, pharmacokinetic and toxicity studies in rats and mice are necessary before humans can be exposed to these chemicals. This necessitates the understanding of both similarities and differences among species. Therefore, it is paramount to understand all aspects of OATP/Oatp expression, regulation, and function not only in humans, but also in rats and mice.

OATP/Oatps are thought to mediate the Na^+-independent hepatocellular uptake of BAs. In mice, Oatp1a1, 1a4, and 1b2 are thought to account for the bulk of Na-independent BA uptake into the liver during normal physiological conditions. Oatp1b2 (human orthologs are OATP1B1 and 1B3) is expressed almost exclusively in the liver and is considered the major liver-specific uptake transporter for drugs and other xenobiotics (Cheng et al., 2005). Oatp1b2 has been shown to be important for the hepatic uptake of unconjugated BAs by studies in Oatp1b2-null mice (Csanaky et al., 2010). In contrast, Oatp1a1 and 1a4 have different distributions in liver lobule. Rat Oatp1a1 has a homogeneous lobular distribution, whereas Oatp1a4 is predominantly expressed in perivenous hepatocytes (Reichel et al., 1999; Kakyo et al., 1999). Such differences are also observed for human OATP1B1 and 1B3, with OATP1B1 expressed throughout the liver lobule whereas OATP1B3 highly expressed around the central vein (Konig et al., 2000a; 2000b). Because most of the uptake of BAs occurs in periportal hepatocytes, Oatp1a1 is implicated in the uptake of BAs under normal conditions, whereas Oatp1a4 may assume a more important role in situations when Oatp1a1 does not remove most of the BAs (Aiso et al., 2000).

As mentioned in the introduction, the overall goal of this dissertation has focused on characterization of the *in vivo* role of mouse Oatp1a1 in BA homeostasis by using Oatp1a1-null mice. Because a method to quantify BAs is a prerequisite to investigate BA homeostasis in mice, we needed to establish a valid and sensitive LC-MS/MS method. Because Oatp1b2 has been shown to mediate the hepatic uptake of unconjugated BAs, we hypothesized that Oatp1a1 also plays a role in transporting unconjugated BAs. Because Oatp1a1 is decreased in mice during BDL-induced cholestasis, we

hypothesized that inhibition of Oatp1a1 prevents the hepatic uptake of BAs and thus protects against liver toxicity in mice during obstructive cholestasis. To achieve this overall goal, three specific aims were examined in the present dissertation.

In **the first specific aim**, a simple and sensitive UPLC-MS/MS method was established and validated for the simultaneous analysis of various BAs, and applied to investigate liver BA content in C57BL/6 mice fed 1% cholic acid (CA), 0.3% deoxycholic acid (DCA), 0.3% chenodeoxycholic acid (CDCA), 0.3% lithocholic acid (LCA), 3% ursodeoxycholic acid (UDCA), or 2% cholestyramine (resin). The design of this study is based on three considerations. First, this study will provide valuable guidance and information for BA feeding experiments in rodents. Second, several BA metabolic pathways, which are minor during normal conditions, can be manifested by feeding BAs in mice. Finally, this study will provide valuable information regarding the species difference between humans and mice. Overall, the purpose of this study is to understand the BA metabolic pathways in mice by using a newly developed BA-quantification method, and thus provide tools and knowledge for the future study of Oatp1a1-null mice.

Mouse livers have a remarkable ability to maintain BA homeostasis during BA feedings. This is due to various BA biotransformations in mouse liver and intestine. When the primary BAs (CA or CDCA) are fed, they enter the intestine and can be metabolized to their secondary BAs (DCA or LCA) by intestinal bacteria. Both primary and secondary BAs are absorbed from intestine to the liver, where the majority of them are conjugated with taurine. Therefore, feeding CA and CDCA markedly increased hepatic TDCA and TLCA, respectively. In addition, when the secondary BAs (DCA or LCA) are fed, they can be re-hydroxylated to their primary BAs (CA or CDCA) in the liver, a process known as BA "repair". For example, feeding LCA markedly increased CDCA and TCDCA, and feeding DCA increased TCA and CA in the liver. Only a small fraction of the fed BAs were conjugated with glycine in mouse liver, because mouse BA CoA:amino acid N-acyltransferase is specific for taurine (Falany et al., 1997). In addition, this BA conjugation enzyme can be saturated with high-dose of BA feeding. For

example, in mice fed a very high-dose of UDCA (3%), the majority of UDCA and LCA remained unconjugated in the liver.

BA sulfation and glucuronidation have been thought to be important pathways to detoxify and eliminate BAs (Trottier et al., 2006; Alnouti, 2009). In the present study, both CA and CDCA are found to be sulfated at the 7-OH position in mouse livers. This sulfation is likely specific to the 7α-OH position, because DCA or UDCA feeding did not increase DCA or UDCA sulfates (data not shown). Sulfation is an important detoxification pathway of LCA in human, chimpanzee, and rodents (Hofmann, 2004). In the present study, LCAS could only be detected in female mice fed UDCA, whereas TLCAS could be detected in female mice fed LCA or UDCA. One possible reason for this different LCA sulfation between UDCA and LCA feeding is that feeding the high dose of UDCA markedly increased both LCA and TLCA, whereas feeding LCA only increased TLCA. The female-predominant sulfation of LCA is also likely due to Sult2a, which is predominantly expressed in female mouse livers but essentially absent from male mouse livers (Alnouti and Klaassen, 2008). Unlike sulfation of LCA, sulfation of CA and CDCA is male-predominant in mouse liver. CA and CDCA feeding can suppress each other's sulfation, indicating that CA and CDCA are sulfated by the same enzyme. This enzyme activity is likely inhibited by high concentrations of UDCA, because UDCA feeding markedly suppressed both CA and CDCA sulfation. The present study shows that BA glucuronidation is a minor BA metabolic pathway in mice. BA glucuronidation could be only detected in mouse livers after UDCA feeding, which is not surprising because the massive dose of UDCA (3%) may have overloaded the capacity of enzymes conjugating BA with amino acids (taurine or glycine).

The BA profiles are similar when feeding CA or DCA. IsoDCA is a possible product by DCA epimerization by intestinal bacteria, and 12-oxoLCA is a possible product of DCA oxidation in mouse livers. Both of these are minor metabolites during CA and DCA feeding. A previous study showed that incubation of CA with human hepatic microsomes produced 3-dehydroCA as the only metabolite (Deo and Bandiera, 2008a). In the present study, 3-dehydroCA was not detected in livers of mice fed CA.

Interestingly, both CA and DCA feeding decreased most BAs in livers, especially the muricholic acids (>70%). This is consistent with a previous report that the percent of TβMCA in bile was markedly decreased in mice fed CA and DCA for 7 days (Wang et al., 2003). Such decreases may be due to marked suppresion of Cyp7a1, 27a1, and 8b1 after feeding CA and DCA.

BA profiles in mouse livers are similar when feeding CDCA or LCA. The metabolites of CDCA and LCA indicate that livers of mice have a rich capacity to hydroxylate the BA steroid nucleus at the 6β- and 7α-positions. During CDCA feeding, mouse livers can hydroxylate CDCA at the 6β-position to form αMCA, which can be further dehydroxlated by intestinal bacteria to form MDCA. Wang et al. (2003) reported that CDCA feeding increased TβMCA in mouse bile. In the present study, either CDCA or LCA feeding increased TαMCA, but not TβMCA. This may be due to the difference in BA-quantification methods, as it is difficult to separate αMCA from βMCA by HPLC. Incubation of CDCA with human hepatic microsomes suggests that 3-dehydroCDCA and HCA were major metabolites of CDCA, whereas 7-oxoLCA and CA were minor metabolites of CDCA (Deo and Bandiera, 2008a). Our study suggests that HCA is a minor metabolite of CDCA in mice, whereas CA was decreased by feeding CDCA. Two major peaks with the same mass spectra as 3-dehydroCDCA were found in livers of mice fed CDCA, whereas they were almost undetectable in control mouse livers. Feeding CDCA markedly suppressed the classic pathway of BA synthetic enzymes Cyp7a1 and Cyp8b1, which may be the reason why TCA, CA, TDCA, and DCA were all decreased. Hydroxylation is also a major pathway to detoxify LCA (Kurata, 1967; Kitada et al., 2003; Hofmann, 2004). In the present study, LCA was hydroxylated at its 6- or 7-position to produce MDCA, UDCA, HDCA, and CDCA. Among them, MDCA was increased more than the other metabolites, suggesting that the 6β-position of LCA is more readily hydroxylated than other positions. Consistently, 6-oxoLCA was increased more than 7-oxoLCA after feeding LCA. DehydroLCA is a minor metabolite of LCA in mouse liver. TCDCA and CDCA are major metabolites of LCA, and they may suppress Cyp7a1 and Cyp8b1. This may explain why feeding LCA also markedly decreased CA in livers of male mice.

BAs and BA sequestrants have been used therapeutically for several decades (Hofmann and Hagey, 2008). UDCA is a primary BA in some mammals (e.g. bear, beaver, and nutria) and has been used to treat cholesterol gallstones, primary biliary cirrhosis (PBC), and cholestasis of pregnancy (Glantz et al., 2005; Hofmann and Hagey, 2008). BA binding resins (e.g. cholestyramine, colestipol, and colesevelam) are used to treat hypercholesterolemia and type 2 diabetes (Aldridge and Ito, 2001). The present study shows that UDCA fed to mice can be dehydroxylated to form LCA in mouse intestine. The high-dose of UDCA (3%) may saturate the BA-conjugation enzymes and thus the majority of UDCA and LCA remain unconjugated in livers of mice. During UDCA feeding, the major metabolite of LCA can be further hydroxylated at the 6β- or 7α-positions. Feeding UDCA increased hepatic MDCA more than CDCA, which is consistent with the previous hypothesis that the 6β-position of LCA is more readily hydroxylated than the 7α-position. However, feeding UDCA had little effect on 6-oxoLCA, but increased 7-oxoLCA. Therefore, 7-oxoLCA may be produced from UDCA but not LCA. Feeding UDCA markedly suppressed TαMCA, TβMCA, TωMCA, TCA, TDCA, and CA, which is consistent with the previous report by Wang et al. (2003) that UDCA feeding decreased TβMCA and TCA in bile of mice. This suppression may be due to marked inhibition of both the classic (Cyp7a1 and 8b1) and alternative (Cyp27a1 and 7b1) pathways of BA synthesis in mice after feeding UDCA. Feeding the resin decreased most BAs in mouse livers. However, it tended to increase CDCA and LCA in male mice, and such an increase was statistically significant in female mice. This is consistent with a previous finding in rats that feeding a resin markedly increased CDCA, but decreased βMCA (Imai et al., 1987). Feeding the resin markedly decreased both conjugated and unconjugated BAs in mouse livers. As a feedback, the mRNA expression of Cyp7a1 and Cyp8b1 were markedly increased after feeding the resin.

Male mice tend to have higher concentrations of BA metabolites than females during BA feeding. Feeding CA increased hepatic CA and DCA more in male than in female mice. Moreover, 12-oxoLCA was increased only in male mice after CA feeding. Feeding DCA increased TDCA, GDCA, DCA, and 12-oxoLCA more in male than female mice. During CDCA feeding, male mice had higher hepatic

CDCA, LCA, 6-oxoLCA, and 7-oxoLCA than female mice. After LCA feeding, male mice had more TMDCA, TLCA, 7-oxoLCA, 12-oxoLCA, and dehydroLCA than female mice. Gender differences in BA metabolism may explain the gender-different response of BA synthetic enzymes following BA feedings. For example, feeding CA suppressed Cyp7b1 mRNA in male but not female mice, and feeding DCA decreased Cyp7a1 mRNA more in male than female mice. The gender difference in hepatic BAs is not prominent during UDCA feeding, except that male mice tend to have higher oxo-BAs than females. During the resin feeding, female mice expressed more hepatic Cyp7a1 and Cyp27a1 than male mice. This may be due to lower CA concentrations in female than male mice after feeding the resin. Because Cyp27a1 initiates the alternative pathway of BA synthesis, the induction of Cyp27a1 may explain why CDCA and LCA were increased in livers of female, but not male mice fed the resin.

In **the second specific aim**, we evaluated the hypothesis that Oatp1a1 is important for transporting unconjugated BAs. Mouse Oatp1a1 is highly expressed in liver and kidney, but almost undetectable in the intestinal tract (Cheng et al., 2005). Mouse Oatp1a1 has been shown to transport BAs, such as TCA *in vitro* (Hagenbuch et al., 2000). Therefore, it is expected that concentrations of some BAs will increase in serum of Oatp1a1-null mice. Surprisingly, the total BA concentration in serum was decreased in Oatp1a1-null mice due to decreased concentrations of TMCA and TCA. This indicates that Oatp1a1 may play a role other than hepatic uptake in the enterohepatic circulation of BAs.

A preliminary study showed that DCA caused more toxicity in male than female mice. Ntcp, Oatp1a1, 1a4, and 1b2 are thought to be the major BA uptake transporters in mouse livers. Among them, Oatp1b2 is similarly expressed in livers of male and female mice (Cheng et al., 2005). Female mice have higher Ntcp and Oatp1a4, and thus possibly take up more BAs into livers than male mice. Therefore, Ntcp and Oatp1a4 do not appear to be the reason why female mice are more resistant to DCA toxicity than male mice. In contrast, Oatp1a1 is predominantly expressed in livers of male mice. In addition, knockout of Oatp1a1 increases the concentrations of DCA and TDCA in serum of mice. Therefore, it is reasonable that male mice are more susceptible to DCA feeding because the higher expression of Oatp1a1

in male mice results in more DCA in their livers than in female mice. As expected, serum DCA concentrations in Oatp1a1-null mice were 30-fold higher than in WT mice after feeding DCA. However, this is not due to decreased hepatic uptake of DCA by knockout of Oatp1a1, because livers of Oatp1a1-null mice also had 30-fold higher DCA than livers of WT mice after feeding DCA. In addition, after feeding DCA, Oatp1a1-null mice had 50-fold higher concentrations of DCA in their gallbladders than WT mice, indicating that the abnormal increase of DCA in Oatp1a1-null mice after feeding DCA is not due to decreased liver efflux. Finally, intravenous injection of DCA indicated that Oatp1a1-null mice did not have a slower clearance of DCA than WT mice. Taken together, knockout of Oatp1a1 does not prevent hepatic uptake of DCA in mice.

Livers have various defense mechanisms to detoxify DCA and maintain BA homeostasis. First, livers decrease BA-uptake transporters to reduce BA-uptake. For example, Ntcp was suppressed in both WT and Oatp1a1-null mice after feeding DCA. Second, livers increase BA-efflux transporters to pump out more BAs. For example, Oatp1a1-null mice have higher hepatic Bsep, Ostα/β, and Mrp2 than WT mice after feeding DCA. Third, livers decrease BA-synthetic enzymes to suppress BA synthesis. After feeding DCA, Oatp1a1-null mice had lower Cyp7a1, 8b1, 27a1, and 7b1 in livers than WT mice. Finally, livers can convert DCA to more hydrophilic and thus less toxic metabolites. DCA can be conjugated with taurine and glycine to form less toxic TDCA and GDCA. In addition, DCA can be "repaired" by the liver to form CA, which is further conjugated with taurine and glycine. Consistent with higher DCA concentrations, Oatp1a1-null mice also have higher concentrations of DCA metabolites in livers than WT mice after feeding DCA. Interestingly, after feeding DCA, concentrations of almost all MCAs were decreased in livers of WT mice, whereas concentrations of TαMCA and ωMCA were markedly increased in livers of Oatp1a1-null mice. This suggests that TαMCA and ωMCA might be DCA metabolites in Oatp1a1-null mice. With all these adaptive mechanisms, livers have the ability to maintain the total BA concentrations in mice after feeding DCA. For example, although feeding DCA increases the concentrations of DCA and its metabolites in livers of WT mice, concentrations of other BAs were

decreased in livers of WT mice. Thus, WT mice only had slightly increased total BA concentrations in livers, and thus resulted in little hepatotoxicity after feeding DCA. In contrast, knockout of Oatp1a1 markedly increased unconjugated BAs in livers, and thus increased hepatotoxicity after feeding DCA.

Because Oatp1a1 is predominantly expressed in male mice, feeding DCA had a more prominent effect in male than female Oatp1a1-null mice. Serum BA metabonomics can separate male WT control mice from male Oatp1a1-null control mice, but it could not discriminate between female WT and Oatp1a1-null control mice. After feeding DCA, male Oatp1a1-null mice had 30-fold higher DCA in serum and livers than male WT mice, whereas female Oatp1a1-null mice had similar concentrations of DCA as female WT mice. In addition, in the principle component analysis (PCA) map of both serum and liver BAs, the distance between female WT and Oatp1a1-null DCA-fed mice is less than that between male WT and Oatp1a1-null DCA-fed mice. Therefore, knockout of Oatp1a1 has more effects on BA metabolism in male than female mice. Consistently, hepatic genes such as Ostα/β, Bsep, Mki67, Gadd45β, and Top2α were increased more in male than female Oatp1a1-null mice. Some hepatic genes, such as Oatp1a4, CD1, and Pcna, were increased only in male but not female Oatp1a1-null mice. Taken together, there is a strong relationship between the expression of hepatic Oatp1a1 and the disposition of DCA in mice.

Knockout of Oatp1a1 markedly alters the composition and amount of intestinal bacteria, and thus alters DCA metabolism in the intestine. The concentrations of individual BAs in bile, and bile flow are the same in WT and Oatp1a1-null mice, suggesting that knockout of Oatp1a1 does not alter the amount of BAs entering the intestine. Knockout of Oatp1a1 increased the total bacteria about 10 fold in the small intestine of mice. The bacterial species that increased suggest that BA deconjugation, dehydroxylation, and epimerization are enhanced in the small intestine of Oatp1a1-null mice. This is consistent with the alteration in BA composition in the small intestinal contents of Oatp1a1-null mice, in which conjugated BAs, such as TMCA and TUDCA are decreased, whereas unconjugated BAs, such as CA, MDCA, HDCA, CDCA, and DCA are increased. Knockout of Oatp1a1 decreased Clostridia and Lactobacilli, but

increased Bacteroides in the large intestine of mice. However, the percent increase in Bacteroides (280%) is higher than the percent decrease in Clostridia and Lactobacilli (35%), suggesting that the large intestine of Oatp1a1-null mice may also have higher activity of BA deconjugation, epimerization, and oxidation than WT mice. Therefore, conjugated BAs, such as TMCA, TCA, and TCDCA are further decreased, whereas unconjugated BAs, such as CDCA, DCA, and LCA are further increased in the large intestinal contents of Oatp1a1-null mice. The alterations of BA composition in the intestine are also reflected by the BA concentration in feces, where the conjugated primary BAs (taurine-, glycine-, and sulfate-conjugated BAs) are markedly decreased, but secondary BAs that are produced by 7-dehydroxylation, oxidation, and epimerization, are markedly increased in Oatp1a1-null mice. TUCA was found at high concentrations in the large intestine but almost undetectable in the small intestine, which suggests that BA 7-epimerization occurs predominantly in the large intestine of mice. The decrease of TUCA in Oatp1a1-null mice may be due to the decrease of large intestinal *C. absonum*, which may also explain the decrease of TUDCA and UDCA in the large intestine of Oatp1a1-null mice. Although *C. absonum* is increased in the small intestine of Oatp1a1-null mice, the concentration of UDCA is decreased in the feces because most of UDCA is produced in the large intestine. Interestingly, despite the marked changes in BA composition, the total BA excretion in feces is similar between WT and Oatp1a1-null mice. This is consistent with the similar billiary input of BAs into the intestine between these two mouse strains. Taken together, the alterations of intestinal bacteria in Oatp1a1-null mice result in marked changes of BA composition in the intestine and feces, but have no effect on the total fecal BA excretion, due to the same billiary input of BAs between WT and Oatp1a1-null mice.

The results from the present study suggest a role of Oatp1a1 in mouse nutrition and obesity. Because knockout of Oatp1a1 changes the intestinal BA composition and bacteria, the intestinal absorption and metabolism of cholesterol, lipids, food supplements, and vitamins may be either increased or decreased in Oatp1a1-null mice. These alterations were revealed by the metabolomic analysis of mouse serum and urine. The increase of hippuric acid and the decrease of indole-3-carboxylic acid

further reveal the alterations of intestinal bacteria in Oatp1a1-null mice, because intestinal bacteria play important roles in their production and metabolism (Wikoff et al., 2009). Some of the most altered urine metabolites in Oatp1a1-null mice were isoflavones, such as daidzein, and vitamins, such as riboflavin. Both daidzein and its bacteria-mediated metabolite, namely *O*-desmethylangolensin, are decreased in the urine of Oatp1a1-null mice, suggesting a critical role of Oatp1a1 in the disposition of daidzein. Daidzein has been shown to have beneficial effect on obesity, hypertension, cholesterol, and glucose levels in animals and humans (Bhathena et al., 2002, Saito, 1991; Manzoni et al., 2005; Furumoto et al., 2010). Therefore, Oatp1a1-null mice may be susceptible to low-daidzein and high-fat diets. In a preliminary study, we observed that the hepatic triglyceride concentrations were markedly higher in Oatp1a1-null mice than in WT mice, when feeding a Teklad #2108C diet, which contains lower isoflavones but higher fat than the Tekalad #8604 diet (data not shown). It is well established that riboflavin participates in a diversity of redox reactions central to human metabolism, and riboflavin deficiency has been linked to abnormal gastrointestinal development, neurodegeneration, cardiovascular diseases, and cancer (Powers, 2003). Riboflavin is increased in urine of Oatp1a1-null mice, which may be due to an increase in riboflavin biosynthesis from lactic acid bacteria, such as *Lactococcus lactis*, which are more abundant in the small intestine of Oatp1a1-null mice. However, preliminary studies show that Oatp1a1 may also play important roles in the hepatic uptake or the renal reabsorption of riboflavin in mice. Further studies are required to determine whether the effects of Oatp1a1 on the disposition of isoflavones and vitamins are direct or indirect.

In **the third specific aim**, we evaluated the hypothesis that knockout of Oatp1a1 decreases the liver toxicity in mice during extrahepatic cholestasis. BDL decreased BA-uptake transporters Ntcp, Oatp1a1, and Oatp1b2 after 1 day in livers of mice. Inhibition of these BA transporters has been hypothesized to prevent further BA-accumulation in livers of mice after BDL. However, little has been done to evaluate this hypothesis due to the lack of knockout mice. The purpose of this study was to determine the *in vivo* role of mouse Oatp1a1 during BDL-induced extrahepatic cholestasis by using

Oatp1a1-null mice. The present study showed that Oatp1a1-null mice are more susceptible to BDL than WT mice. Because Oatp1a1-null mice became very sick after 2 days of BDL, one-day BDL was used in the present study. Surprisingly, even at 1 day after BDL, Oatp1a1-null mice had severe liver toxicity. The enhanced liver toxicity in Oatp1a1-null mice after BDL appears to be due to the increase of secondary BAs in serum and livers. Knockout of Oatp1a1 markedly increased conjugated secondary BAs, such as TDCA, TLCA, TMDCA, TUDCA, and THDCA in serum of mice after BDL. This seems to be due to enhanced intestinal absorption, because knockout of Oatp1a1 tended to increase the intestinal BA transporters, such as Asbt and Ostβ in mice after BDL. In addition, the intestinal contents of Oatp1a1-null became very dry 1 day after BDL. This suggests BDL dehydrates the intestine of Oatp1a1-null mice, which is possibly due to the enhanced intestinal absorption of BAs. It is interestingly to note that knockout of Oatp1a1 also increased TCA in livers, but not in serum of mice after BDL. Actually, almost all the CA-derived secondary BAs, such as TDCA, T-12-epiDCA, and 7-oxoDCA, which were almost undetectable in WT mice after BDL, were markedly increased in Oatp1a1-null mice after BDL. As shown in the time-response study after BDL, TCA in livers of WT BDL mice were markedly increased at 6 h, and thereafter decreased from 6 h to 1 d after surgery. Thus, it is possible that knockout of Oatp1a1 fails to decrease or detoxify TCA from 6 h to 1 d in livers of mice after BDL. Taken together, knockout of Oatp1a1 appears to decrease BA detoxification in liver, increase the intestinal absorption of secondary BAs, and therefore increase liver toxicity in mice after BDL.

FXR, PXR, CAR, PPARα, and Nfr2 are all key nuclear receptors that participate in the adaptive response to cholestatic injury (Guo et al, 2003; Stedman et al., 2005; Thomas et al., 2005; Okada et al., 2009). In the present study, Cyp7a1 and Cyp8b1 were decreased markedly in livers of both WT and Oatp1a1-null mice 1 day after BDL. An increase of SHP and Bsep, as well as a decrease of Ntcp, suggest that FXR is activated in livers of WT mice after BDL. In contrast, BDL had little effect on intestinal Fgf15 and liver Fgfr4 in WT mice, suggesting that Ffg15-Fgfr4 pathway is not activated in WT mice 1 day after BDL. Thus, the suppression of Cyp7a1 and Cyp8b1 in livers of WT BDL mice may be due to

the activation of the FXR pathway. In contrast to WT mice, suppression of Cyp7a1 and Cyp8b1 in livers of Oatp1a1-null BDL mice does not appear to be due to activation of either FXR-SHP or Fgf15-Fgfr4 pathway, because BDL in Oatp1a1-null mice had little effect on target genes involved in these two pathways. CAR and PXR play important roles in BA-detoxifying enzymes in mice, such as the regulation of Mrp4 (Wagner et al., 2005; Assem et al., 2004). In addition, PPARα and Nrf2 have also been shown to regulate BA-detoxyfying enzymes, such as Mrps and Ugts (Barbier et al., 2003; Maher et al., 2008; Okada et al., 2009). In the present study, BDL increased Cyp2b10, Cyp3a11, Cyp4a14, and Nqo1 in WT mice 1 day after surgery, suggesting that CAR, PXR, PPARα, and Nrf2 are activated in WT mice after BDL. In contrast, activation of these nuclear receptors was either not apparent (PXR, PPARα and Nrf2) or lower (CAR) in livers of Oatp1a1-null BDL mice. Taken together, Oatp1a1-null mice have an impaired cytoprotective response in BDL-induced obstructive cholestasis.

Antibiotic treatment does not prevent liver toxicity in Oatp1a1-null mice after BDL. Endotoxin has been shown to potentiate hepatocyte apoptosis and necrosis during obstructive cholestasis (Sewnath et al., 2000; Yorganci et al., 2004). Knockout of Oatp1a1 increased the intestinal bacteria in mice. In addition, knockout of Oatp1a1 markedly increased secondary BAs in serum and livers of mice after BDL. Therefore, it is possible that the overgrowth of intestinal bacteria may increase secondary BAs and endotoxins, and thus enhance the liver toxicity in Oatp1a1-null mice after BDL. Surprisingly, antibiotic treatment in the present study tended to potentiate the liver toxicity in Oatp1a1-null mice after BDL. BDL did not increase the secondary BAs in antibiotic-treated Oatp1a1-null mice. This suggests that the liver toxicity in antibiotic-treated Oatp1a1-null mice after BDL is not due to the increase of secondary BAs. Interestingly, antibiotic treatment markedly increased TβMCA, βMCA, and TCA in serum of Oatp1a1-null mice. After BDL, not only conjugated BAs, but also unconjugated BAs, were markedly increased in antibiotic-treated Oatp1a1-null mice. This may be due to the enhanced intestinal absorption, because antibiotic treatment increases the mRNA expression of Asbt, Mrp3, and Ostα/β in ilea of

Oatp1a1-null mice. Therefore, antibiotic treatment does not appear to be an ideal method to investigate the effect of intestinal bacteria on liver toxicity in Oatp1a1-null mice.

Overall, **this dissertation demonstrates that:** (1) A simple and sensitive UPLC-MS/MS method was established for the simultaneous analysis of various BAs and was applied to investigate the BA metabolism in mice fed CA, CDCA, DCA, LCA, UDCA, or resin; (2) Oatp1a1 does not mediate the hepatic uptake of DCA, but plays a critical role in the intestinal metabolism of DCA; (3) Knockout of Oatp1a1 increases intestinal bacteria and thus alters the urinary metabolomics in mice; (4) Knockout of Oatp1a1 increases liver toxicity in mice after BDL, which may be due to the increase of secondary BAs in both serum and livers of mice; (5) Antibiotic treatment appears to increase the intestinal BA absorption, and thus increase BDL-induced liver toxicity in Oatp1a1-null mice. Taken together, Oatp1a1 plays a unique and essential role in the homeostasis of intestinal bacteria, homeostasis of BA metabolism, as well as the adaptive response to liver injury during obstructive cholestasis.

REFERENCE LIST

Abe T, Kakyo M, Tokui T, Nakagomi R, Nishio T, Nakai D, Nomura H, Unno M, Suzuki M, Naitoh T, Matsuno S and Yawo H (1999) Identification of a novel gene family encoding human liver-specific organic anion transporter LST-1. J Biol Chem 274:17159-17163.

Aiso M, Takikawa H and Yamanaka M (2000) Biliary excretion of bile acids and organic anions in zone 1- and zone 3-injured rats. Liver 20:38-44.

Aldridge MA and Ito MK (2001) Colesevelam hydrochloride: a novel bile acid-binding resin. Ann Pharmacother 35:898-907.

Alme B, Bremmelgaard A, Sjovall J and Thomassen P (1977) Analysis of metabolic profiles of bile acids in urine using a lipophilic anion exchanger and computerized gas-liquid chromatorgaphy-mass spectrometry. J Lipid Res 18:339-362.

Alnouti Y (2009) Bile acid sulfation: a pathway of bile acid elimination and detoxification. Toxicol Sci 108:225-246.

Alnouti Y, Csanaky IL and Klaassen CD (2008) Quantitative-profiling of bile acids and their conjugates in mouse liver, bile, plasma, and urine using LC-MS/MS. J Chromatogr B Analyt Technol Biomed Life Sci 873:209-217.

Alnouti Y and Klaassen CD (2006) Tissue distribution and ontogeny of sulfotransferase enzymes in mice. Toxicol Sci 93:242-255.

Alpini G, Glaser SS, Ueno Y, Rodgers R, Phinizy JL, Francis H, Baiocchi L, Holcomb LA, Caligiuri A and LeSage GD (1999) Bile acid feeding induces cholangiocyte proliferation and secretion: evidence for bile acid-regulated ductal secretion. Gastroenterology 116:179-186.

Amuro Y, Endo T, Higashino K, Uchida K and Yamamura Y (1981) Serum, fecal and urinary bile acids in patients with mild and advanced liver cirrhosis. Gastroenterol Jpn 16:506-513.

Backhed F, Ley RE, Sonnenburg JL, Peterson DA and Gordon JI (2005) Host-bacterial mutualism in the human intestine. Science 307:1915-1920.

Barbier O, Duran-Sandoval D, Pineda-Torra I, Kosykh V, Fruchart JC and Staels B (2003) Peroxisome proliferator-activated receptor alpha induces hepatic expression of the human bile acid glucuronidating UDP-glucuronosyltransferase 2B4 enzyme. J Biol Chem 278:32852-32860.

Bennion LJ, Drobny E, Knowler WC, Ginsberg RL, Garnick MB, Adler RD and Duane WC (1978) Sex differences in the size of bile acid pools. Metabolism 27:961-969.

Bhathena SJ and Velasquez MT (2002) Beneficial role of dietary phytoestrogens in obesity and diabetes. Am J Clin Nutr 76:1191-1201.

Bodin K, Lindbom U and Diczfalusy U (2005) Novel pathways of bile acid metabolism involving CYP3A4. Biochim Biophys Acta 1687:84-93.

Bonnot O, Fraidakis MJ, Lucanto R, Chauvin D, Kelley N, Plaza M, Dubourg O, Lyon-Caen O, Sedel F and Cohen D (2010) Cerebrotendinous xanthomatosis presenting with severe externalized disorder: improvement after one year of treatment with chenodeoxycholic Acid. CNS Spectr 15:231-236.

Botham KM and Boyd GS (1983) The metabolism of chenodeoxycholic acid to beta-muricholic acid in rat liver. Eur J Biochem 134:191-196.

Boyer JL (2007) New perspectives for the treatment of cholestasis: lessons from basic science applied clinically. J Hepatol 46:365-371.

Briz O, Serrano MA, MacIas RI, Gonzalez-Gallego J and Marin JJ (2003) Role of organic anion-transporting polypeptides, OATP-A, OATP-C and OATP-8, in the human placenta-maternal liver tandem excretory pathway for foetal bilirubin. Biochem J 371:897-905.

Burgess C, O'Connell-Motherway M, Sybesma W, Hugenholtz J and van Sinderen D (2004) Riboflavin production in Lactococcus lactis: potential for in situ production of vitamin-enriched foods. Appl Environ Microbiol 70:5769-5777.

Burkard I, von Eckardstein A and Rentsch KM (2005) Differentiated quantification of human bile acids in serum by high-performance liquid chromatography-tandem mass spectrometry. J Chromatogr B Analyt Technol Biomed Life Sci 826:147-159.

Burkholder PR and McVeigh I (1942) Synthesis of Vitamins by Intestinal Bacteria. Proc Natl Acad Sci U S A 28:285-289.

Cantafora A, Alvaro D, Attili AF, Di Biase A, Anza M, Mantovani A and Angelico M (1986) Hepatic 3 alpha-dehydrogenation and 7 alpha-hydroxylation of deoxycholic acid in the guinea-pig. Comp Biochem Physiol B 85:805-810.

Chen C, Stock JL, Liu X, Shi J, Van Deusen JW, DiMattia DA, Dullea RG and de Morais SM (2008) Utility of a novel Oatp1b2 knockout mouse model for evaluating the role of Oatp1b2 in the hepatic uptake of model compounds. Drug Metab Dispos 36:1840-1845.

Cheng Q, Aleksunes LM, Manautou JE, Cherrington NJ, Scheffer GL, Yamasaki H and Slitt AL (2008) Drug-metabolizing enzyme and transporter expression in a mouse model of diabetes and obesity. Mol Pharm 5:77-91.

Cheng X, Buckley D and Klaassen CD (2007) Regulation of hepatic bile acid transporters Ntcp and Bsep expression. Biochem Pharmacol 74:1665-1676.

Cheng X, Maher J, Chen C and Klaassen CD (2005) Tissue distribution and ontogeny of mouse organic anion transporting polypeptides (Oatps). Drug Metab Dispos 33:1062-1073.

Cheng X, Maher J, Dieter MZ and Klaassen CD (2005) Regulation of mouse organic anion-transporting polypeptides (Oatps) in liver by prototypical microsomal enzyme inducers that activate distinct transcription factor pathways. Drug Metab Dispos 33:1276-1282.

Cheng X, Maher J, Lu H and Klaassen CD (2006) Endocrine regulation of gender-divergent mouse organic anion-transporting polypeptide (Oatp) expression. Mol Pharmacol 70:1291-1297.

Chiang JY (2002) Bile acid regulation of gene expression: roles of nuclear hormone receptors. Endocr Rev 23:443-463.

Cook AM and Denger K (2002) Dissimilation of the C2 sulfonates. Arch Microbiol 179:1-6.

Copple BL, Jaeschke H and Klaassen CD (2010) Oxidative stress and the pathogenesis of cholestasis. Semin Liver Dis 30:195-204.

Corzo G and Gilliland SE (1999) Bile salt hydrolase activity of three strains of Lactobacillus acidophilus. J Dairy Sci 82:472-480.

Costarelli V and Sanders TA (2002) Plasma bile acids and risk of breast cancer. IARC Sci Publ 156:305-306.

Csanaky IL, Lu H, Zhang Y, Ogura K, Choudhuri S and Klaassen CD (2010) Organic anion-transporting polypeptide 1b2 (Oatp1b2) is important for the hepatic uptake of unconjugated bile acids: Studies in Oatp1b2-null mice. Hepatology.

Daly C, Fitzgerald GF and Davis R (1996) Biotechnology of lactic acid bacteria with special reference to bacteriophage resistance. Antonie Van Leeuwenhoek 70:99-110.

Davis PJ, Gustafson ME and Rosazza JP (1976) Formation of indole-3-carboxylic acid by Chromobacterium violaceum. J Bacteriol 126:544-546.

Dawson PA, Hubbert M, Haywood J, Craddock AL, Zerangue N, Christian WV and Ballatori N (2005) The heteromeric organic solute transporter alpha-beta, Ostalpha-Ostbeta, is an ileal basolateral bile acid transporter. J Biol Chem 280:6960-6968.

Delzenne NM, Calderon PB, Taper HS and Roberfroid MB (1992) Comparative hepatotoxicity of cholic acid, deoxycholic acid and lithocholic acid in the rat: in vivo and in vitro studies. Toxicol Lett 61:291-304.

Deo AK and Bandiera SM (2008) Identification of human hepatic cytochrome p450 enzymes involved in the biotransformation of cholic and chenodeoxycholic acid. Drug Metab Dispos 36:1983-1991.

Duane WC (2009) Bile acids: developments new and very old. J Lipid Res 50:1507-1508.

Dubos R, Schaedler RW, Costello R and Hoet P (1965) Indigenous, normal, and autochthonous flora of the gastrointestinal tract. J Exp Med 122:67-76.

Estep PW, 3rd, Warner JB and Bulyk ML (2009) Short-term calorie restriction in male mice feminizes gene expression and alters key regulators of conserved aging regulatory pathways. PLoS One 4:e5242.

Eyssen HJ, De Pauw G and Van Eldere J (1999) Formation of hyodeoxycholic acid from muricholic acid and hyocholic acid by an unidentified gram-positive rod termed HDCA-1 isolated from rat intestinal microflora. Appl Environ Microbiol 65:3158-3163.

Eyssen HJ, Parmentier GG and Mertens JA (1976) Sulfate bile acids in germ-free and conventional mice. Eur J Biochem 66:507-514.

Falany CN, Fortinberry H, Leiter EH and Barnes S (1997) Cloning, expression, and chromosomal localization of mouse liver bile acid CoA:amino acid N-acyltransferase. J Lipid Res 38:1139-1148.

Fini A and Roda A (1987) Chemical properties of bile acids. IV. Acidity constants of glycine-conjugated bile acids. J Lipid Res 28:755-759.

Fiorucci S, Rizzo G, Antonelli E, Renga B, Mencarelli A, Riccardi L, Morelli A, Pruzanski M and Pellicciari R (2005) Cross-talk between farnesoid-X-receptor (FXR) and peroxisome proliferator-activated receptor gamma contributes to the antifibrotic activity of FXR ligands in rodent models of liver cirrhosis. J Pharmacol Exp Ther 315:58-68.

Fischer S, Beuers U, Spengler U, Zwiebel FM and Koebe HG (1996) Hepatic levels of bile acids in end-stage chronic cholestatic liver disease. Clin Chim Acta 251:173-186.

Fisher CD, Lickteig AJ, Augustine LM, Oude Elferink RP, Besselsen DG, Erickson RP and Cherrington NJ (2009) Experimental non-alcoholic fatty liver disease results in decreased hepatic uptake transporter expression and function in rats. Eur J Pharmacol 613:119-127.

Fisher MM, Price VM, Magnusson RJ and Yousef IM (1974) Bile acid metabolism in mammals. VII. Studies on sex differences in deoxycholic acid metabolism in isolated perfused rat liver. Lipids 9:786-794.

Fujimura M, Yamamoto S, Murata T, Yasujima T, Inoue K, Ohta KY and Yuasa H (2010) Functional characteristics of the human ortholog of riboflavin transporter 2 and riboflavin-responsive expression of its rat ortholog in the small intestine indicate its involvement in riboflavin absorption. J Nutr 140:1722-1727.

Furumoto H (2010) [Relationship between food mixing ability and oral health-related quality of life in partially edentulous patients]. Kokubyo Gakkai Zasshi 77:7-13.

Gerloff T, Stieger B, Hagenbuch B, Madon J, Landmann L, Roth J, Hofmann AF and Meier PJ (1998) The sister of P-glycoprotein represents the canalicular bile salt export pump of mammalian liver. J Biol Chem 273:10046-10050.

Gill SR, Pop M, Deboy RT, Eckburg PB, Turnbaugh PJ, Samuel BS, Gordon JI, Relman DA, Fraser-Liggett CM and Nelson KE (2006) Metagenomic analysis of the human distal gut microbiome. Science 312:1355-1359.

Glantz A, Marschall HU, Lammert F and Mattsson LA (2005) Intrahepatic cholestasis of pregnancy: a randomized controlled trial comparing dexamethasone and ursodeoxycholic acid. Hepatology 42:1399-1405.

Goodwin B and Kliewer SA (2002) Nuclear receptors. I. Nuclear receptors and bile acid homeostasis. Am J Physiol Gastrointest Liver Physiol 282:G926-931.

Gopal-Srivastava R and Hylemon PB (1988) Purification and characterization of bile salt hydrolase from Clostridium perfringens. J Lipid Res 29:1079-1085.

Goris H, de Boer F and van der Waaij D (1986) Oral administration of antibiotics and intestinal flora associated endotoxin in mice. Scand J Infect Dis 18:55-63.

Goto J, Kato H and Nambara T (1978) Separation of sulfated bile acids by high-performance liquid chromatography. Lipids 13:908-909.

Greim H, Trulzsch D, Roboz J, Dressler K, Czygan P, Hutterer F, Schaffner F and Popper H (1972) Mechanism of cholestasis. 5. Bile acids in normal rat livers and in those after bile duct ligation. Gastroenterology 63:837-845.

Gu JJ, Hofmann AF, Ton-Nu HT, Schteingart CD and Mysels KJ (1992) Solubility of calcium salts of unconjugated and conjugated natural bile acids. J Lipid Res 33:635-646.

Guo GL, Lambert G, Negishi M, Ward JM, Brewer HB, Jr., Kliewer SA, Gonzalez FJ and Sinal CJ (2003) Complementary roles of farnesoid X receptor, pregnane X receptor, and constitutive androstane receptor in protection against bile acid toxicity. J Biol Chem 278:45062-45071.

Hagenbuch B, Adler ID and Schmid TE (2000) Molecular cloning and functional characterization of the mouse organic-anion-transporting polypeptide 1 (Oatp1) and mapping of the gene to chromosome X. Biochem J 345:115-120.

Hagenbuch B and Gui C (2008) Xenobiotic transporters of the human organic anion transporting polypeptides (OATP) family. Xenobiotica 38:778-801.

Hagenbuch B and Meier PJ (2003) The superfamily of organic anion transporting polypeptides. Biochim Biophys Acta 1609:1-18.

Hagenbuch B and Meier PJ (2004) Organic anion transporting polypeptides of the OATP/ SLC21 family: phylogenetic classification as OATP/ SLCO superfamily, new nomenclature and molecular/functional properties. Pflugers Arch 447:653-665.

Hagio M, Matsumoto M, Fukushima M, Hara H and Ishizuka S (2009) Improved analysis of bile acids in tissues and intestinal contents of rats using LC/ESI-MS. J Lipid Res 50:173-180.

Hofmann AF (1994) Maximal bile acid biosynthesis in humans. Gastroenterology 106:273-274.

Hofmann AF (1999) Bile Acids: The Good, the Bad, and the Ugly. News Physiol Sci 14:24-29.

Hofmann AF (2004) Detoxification of lithocholic acid, a toxic bile acid: relevance to drug hepatotoxicity. Drug Metab Rev 36:703-722.

Hofmann AF (2007) Why bile acid glucuronidation is a minor pathway for conjugation of endogenous bile acids in man. Hepatology 45:1083-1084; author reply 1084-1085.

Hofmann AF and Hagey LR (2008) Bile acids: chemistry, pathochemistry, biology, pathobiology, and therapeutics. Cell Mol Life Sci 65:2461-2483.

Hofmann AF, Loening-Baucke V, Lavine JE, Hagey LR, Steinbach JH, Packard CA, Griffin TL and Chatfield DA (2008) Altered bile acid metabolism in childhood functional constipation: inactivation of secretory bile acids by sulfation in a subset of patients. J Pediatr Gastroenterol Nutr 47:598-606.

Hofmann AF, Sjovall J, Kurz G, Radominska A, Schteingart CD, Tint GS, Vlahcevic ZR and Setchell KD (1992) A proposed nomenclature for bile acids. J Lipid Res 33:599-604.

Imai Y, Kawata S, Inada M, Miyoshi S, Minami Y, Matsuzawa Y, Uchida K and Tarui S (1987) Effect of cholestyramine on bile acid metabolism in conventional rats. Lipids 22:513-516.

Inagaki T, Choi M, Moschetta A, Peng L, Cummins CL, McDonald JG, Luo G, Jones SA, Goodwin B, Richardson JA, Gerard RD, Repa JJ, Mangelsdorf DJ and Kliewer SA (2005) Fibroblast growth factor 15 functions as an enterohepatic signal to regulate bile acid homeostasis. Cell Metab 2:217-225.

Ismair MG, Stieger B, Cattori V, Hagenbuch B, Fried M, Meier PJ and Kullak-Ublick GA (2001) Hepatic uptake of cholecystokinin octapeptide by organic anion-transporting polypeptides OATP4 and OATP8 of rat and human liver. Gastroenterology 121:1185-1190.

Jacquemin E, Hagenbuch B, Stieger B, Wolkoff AW and Meier PJ (1994) Expression cloning of a rat liver Na(+)-independent organic anion transporter. Proc Natl Acad Sci U S A 91:133-137.

Jansen PL, Strautnieks SS, Jacquemin E, Hadchouel M, Sokal EM, Hooiveld GJ, Koning JH, De Jager-Krikken A, Kuipers F, Stellaard F, Bijleveld CM, Gouw A, Van Goor H, Thompson RJ and Muller M (1999) Hepatocanalicular bile salt export pump deficiency in patients with progressive familial intrahepatic cholestasis. Gastroenterology 117:1370-1379.

Johnstone JM and Lee EG (1976) A quantitative assessment of the structural changes the rat's liver following obstruction of the common bile duct. Br J Exp Pathol 57:85-94.

Jung D, Hagenbuch B, Fried M, Meier PJ and Kullak-Ublick GA (2004) Role of liver-enriched transcription factors and nuclear receptors in regulating the human, mouse, and rat NTCP gene. Am J Physiol Gastrointest Liver Physiol 286:G752-761.

Kakyo M, Sakagami H, Nishio T, Nakai D, Nakagomi R, Tokui T, Naitoh T, Matsuno S, Abe T and Yawo H (1999) Immunohistochemical distribution and functional characterization of an organic anion transporting polypeptide 2 (oatp2). FEBS Lett 445:343-346.

Kawamoto K, Horibe I and Uchida K (1989) Purification and characterization of a new hydrolase for conjugated bile acids, chenodeoxycholyltaurine hydrolase, from Bacteroides vulgatus. J Biochem 106:1049-1053.

Kinugasa T, Uchida K, Kadowaki M, Takase H, Nomura Y and Saito Y (1981) Effect of bile duct ligation on bile acid metabolism in rats. J Lipid Res 22:201-207.

Kitada H, Miyata M, Nakamura T, Tozawa A, Honma W, Shimada M, Nagata K, Sinal CJ, Guo GL, Gonzalez FJ and Yamazoe Y (2003) Protective role of hydroxysteroid sulfotransferase in lithocholic acid-induced liver toxicity. J Biol Chem 278:17838-17844.

Kitahara M, Takamine F, Imamura T and Benno Y (2000) Assignment of Eubacterium sp. VPI 12708 and related strains with high bile acid 7alpha-dehydroxylating activity to Clostridium scindens and proposal of Clostridium hylemonae sp. nov., isolated from human faeces. Int J Syst Evol Microbiol 50 Pt 3:971-978.

Klaassen CD (1971) Gas-liquid-chromatographic determination of bile acids in bile. Clin Chim Acta 35:225-229.

Klaassen CD, Liu L and Dunn RT, 2nd (1998) Regulation of sulfotransferase mRNA expression in male and female rats of various ages. Chem Biol Interact 109:299-313.

Konig J, Cui Y, Nies AT and Keppler D (2000a) Localization and genomic organization of a new hepatocellular organic anion transporting polypeptide. J Biol Chem 275:23161-23168.

Konig J, Cui Y, Nies AT and Keppler D (2000b) A novel human organic anion transporting polypeptide localized to the basolateral hepatocyte membrane. Am J Physiol Gastrointest Liver Physiol 278:G156-164.

Kullak-Ublick GA, Ismair MG, Stieger B, Landmann L, Huber R, Pizzagalli F, Fattinger K, Meier PJ and Hagenbuch B (2001) Organic anion-transporting polypeptide B (OATP-B) and its functional comparison with three other OATPs of human liver. Gastroenterology 120:525-533.

Kurata Y (1967) Stero-bile acids and bile alcohols. CII. Metabolism of lithocholic acid in a mouse and a dog. Hiroshima J Med Sci 16:281-285.

Lee W, Glaeser H, Smith LH, Roberts RL, Moeckel GW, Gervasini G, Leake BF and Kim RB (2005) Polymorphisms in human organic anion-transporting polypeptide 1A2 (OATP1A2): implications for altered drug disposition and central nervous system drug entry. J Biol Chem 280:9610-9617.

Lepage G, Fontaine A and Roy CC (1978) Vulnerability of keto bile acids to alkaline hydrolysis. J Lipid Res 19:505-509.

Lepercq P, Gerard P, Beguet F, Raibaud P, Grill JP, Relano P, Cayuela C and Juste C (2004) Epimerization of chenodeoxycholic acid to ursodeoxycholic acid by Clostridium baratii isolated from human feces. FEMS Microbiol Lett 235:65-72.

Ley RE, Backhed F, Turnbaugh P, Lozupone CA, Knight RD and Gordon JI (2005) Obesity alters gut microbial ecology. Proc Natl Acad Sci U S A 102:11070-11075.

Ley RE, Lozupone CA, Hamady M, Knight R and Gordon JI (2008) Worlds within worlds: evolution of the vertebrate gut microbiota. Nat Rev Microbiol 6:776-788.

Li N, Hartley DP, Cherrington NJ and Klaassen CD (2002) Tissue expression, ontogeny, and inducibility of rat organic anion transporting polypeptide 4. J Pharmacol Exp Ther 301:551-560.

Lu H, Choudhuri S, Ogura K, Csanaky IL, Lei X, Cheng X, Song PZ and Klaassen CD (2008) Characterization of organic anion transporting polypeptide 1b2-null mice: essential role in hepatic uptake/toxicity of phalloidin and microcystin-LR. Toxicol Sci 103:35-45.

Macdonald IA and Hutchison DM (1982) Epimerization versus dehydroxylation of the 7 alpha-hydroxyl-group of primary bile acids: competitive studies with Clostridium absonum and 7 alpha-dehydroxylating bacteria (Eubacterium sp.). J Steroid Biochem 17:295-303.

Macdonald IA, Hutchison DM and Forrest TP (1981) Formation of urso- and ursodeoxy-cholic acids from primary bile acids by Clostridium absonum. J Lipid Res 22:458-466.

Macdonald IA, Meier EC, Mahony DE and Costain GA (1976) 3alpha-, 7alpha- and 12alpha-hydroxysteroid dehydrogenase activities from Clostridium perfringens. Biochim Biophys Acta 450:142-153.

MacDonald IA and Roach PD (1981) Bile induction of 7 alpha- and 7 beta-hydroxysteroid dehydrogenases in Clostridium absonum. Biochim Biophys Acta 665:262-269.

Maher JM, Aleksunes LM, Dieter MZ, Tanaka Y, Peters JM, Manautou JE and Klaassen CD (2008) Nrf2- and PPAR alpha-mediated regulation of hepatic Mrp transporters after exposure to perfluorooctanoic acid and perfluorodecanoic acid. Toxicol Sci 106:319-328.

Mahowald TA, Matschiner JT, Hsia SL, Doisy EA, Jr., Elliott WH and Doisy EA (1957) Bile acids. III. Acid I; the principal bile acid in urine of surgically jaundiced rats. J Biol Chem 225:795-802.

Makishima M, Lu TT, Xie W, Whitfield GK, Domoto H, Evans RM, Haussler MR and Mangelsdorf DJ (2002) Vitamin D receptor as an intestinal bile acid sensor. Science 296:1313-1316.

Manzoni MS, Rossi EA, Carlos IZ, Vendramini RC, Duarte AC and Damaso AR (2005) Fermented soy product supplemented with isoflavones affected fat depots in juvenile rats. Nutrition 21:1018-1024.

Martoni C, Bhathena J, Urbanska AM and Prakash S (2008) Microencapsulated bile salt hydrolase producing Lactobacillus reuteri for oral targeted delivery in the gastrointestinal tract. Appl Microbiol Biotechnol 81:225-233.

Mihalik SJ, Steinberg SJ, Pei Z, Park J, Kim DG, Heinzer AK, Dacremont G, Wanders RJ, Cuebas DA, Smith KD and Watkins PA (2002) Participation of two members of the very long-chain acyl-CoA synthetase family in bile acid synthesis and recycling. J Biol Chem 277:24771-24779.

Ogura K, Choudhuri S and Klaassen CD (2000) Full-length cDNA cloning and genomic organization of the mouse liver-specific organic anion transporter-1 (lst-1). Biochem Biophys Res Commun 272:563-570.

Ogura K, Choudhuri S and Klaassen CD (2001) Genomic organization and tissue-specific expression of splice variants of mouse organic anion transporting polypeptide 2. Biochem Biophys Res Commun 281:431-439.

Okada K, Shoda J, Taguchi K, Maher JM, Ishizaki K, Inoue Y, Ohtsuki M, Goto N, Sugimoto H, Utsunomiya H, Oda K, Warabi E, Ishii T and Yamamoto M (2009) Nrf2 counteracts cholestatic liver injury via stimulation of hepatic defense systems. Biochem Biophys Res Commun 389:431-436.

Park YJ, Qatanani M, Chua SS, LaRey JL, Johnson SA, Watanabe M, Moore DD and Lee YK (2008) Loss of orphan receptor small heterodimer partner sensitizes mice to liver injury from obstructive cholestasis. Hepatology 47:1578-1586.

Parks DJ, Blanchard SG, Bledsoe RK, Chandra G, Consler TG, Kliewer SA, Stimmel JB, Willson TM, Zavacki AM, Moore DD and Lehmann JM (1999) Bile acids: natural ligands for an orphan nuclear receptor. Science 284:1365-1368.

Payne CM, Crowley-Skillicorn C, Holubec H, Dvorak K, Bernstein C, Moyer MP, Garewal H and Bernstein H (2009) Deoxycholate, an endogenous cytotoxin/genotoxin, induces the autophagic stress-survival pathway: implications for colon carcinogenesis. J Toxicol 785-907.

Pellicciari R, Gioiello A, Macchiarulo A, Thomas C, Rosatelli E, Natalini B, Sardella R, Pruzanski M, Roda A, Pastorini E, Schoonjans K and Auwerx J (2009) Discovery of 6alpha-ethyl-23(S)-methylcholic acid (S-EMCA, INT-777) as a potent and selective agonist for the TGR5 receptor, a novel target for diabesity. J Med Chem 52:7958-7961.

Pellicoro A, van den Heuvel FA, Geuken M, Moshage H, Jansen PL and Faber KN (2007) Human and rat bile acid-CoA:amino acid N-acyltransferase are liver-specific peroxisomal enzymes: implications for intracellular bile salt transport. Hepatology 45:340-348.

Powers HJ (2003) Riboflavin (vitamin B-2) and health. Am J Clin Nutr 77:1352-1360.

Raedsch R, Lauterburg BH and Hofmann AF (1981) Altered bile acid metabolism in primary biliary cirrhosis. Dig Dis Sci 26:394-401.

Reddy BS, Watanabe K, Weisburger JH and Wynder EL (1977) Promoting effect of bile acids in colon carcinogenesis in germ-free and conventional F344 rats. Cancer Res 37:3238-3242.

Reichel C, Gao B, Van Montfoort J, Cattori V, Rahner C, Hagenbuch B, Stieger B, Kamisako T and Meier PJ (1999) Localization and function of the organic anion-transporting polypeptide Oatp2 in rat liver. Gastroenterology 117:688-695.

Rial NS, Lazennec G, Prasad AR, Krouse RS, Lance P and Gerner EW (2009) Regulation of deoxycholate induction of CXCL8 by the adenomatous polyposis coli gene in colorectal cancer. Int J Cancer 124:2270-2280.

Ridlon JM, Kang DJ and Hylemon PB (2006) Bile salt biotransformations by human intestinal bacteria. J Lipid Res 47:241-259.

Rius M, Hummel-Eisenbeiss J, Hofmann AF and Keppler D (2006) Substrate specificity of human ABCC4 (MRP4)-mediated cotransport of bile acids and reduced glutathione. Am J Physiol Gastrointest Liver Physiol 290:G640-649.

Roberts LR, Kurosawa H, Bronk SF, Fesmier PJ, Agellon LB, Leung WY, Mao F and Gores GJ (1997) Cathepsin B contributes to bile salt-induced apoptosis of rat hepatocytes. Gastroenterology 113:1714-1726.

Salzman NH, de Jong H, Paterson Y, Harmsen HJ, Welling GW and Bos NA (2002) Analysis of 16S libraries of mouse gastrointestinal microflora reveals a large new group of mouse intestinal bacteria. Microbiology 148:3651-3660.

Samstein RM, Perica K, Balderrama F, Look M and Fahmy TM (2008) The use of deoxycholic acid to enhance the oral bioavailability of biodegradable nanoparticles. Biomaterials 29:703-708.

Sato H, Macchiarulo A, Thomas C, Gioiello A, Une M, Hofmann AF, Saladin R, Schoonjans K, Pellicciari R and Auwerx J (2008) Novel potent and selective bile acid derivatives as TGR5 agonists: biological screening, structure-activity relationships, and molecular modeling studies. J Med Chem 51:1831-1841.

Schaedler RW, Dubs R and Costello R (1965) Association of germfree mice with bacteria isolated from normal mice. J Exp Med 122:77-82.

Schoefer L, Mohan R, Braune A, Birringer M and Blaut M (2002) Anaerobic C-ring cleavage of genistein and daidzein by Eubacterium ramulus. FEMS Microbiol Lett 208:197-202.

Schuster VL (2002) Prostaglandin transport. Prostaglandins Other Lipid Mediat 68-69:633-647.

Sellinger M and Boyer JL (1990) Physiology of bile secretion and cholestasis. Prog Liver Dis 9:237-259.

Setchell KD and Worthington J (1982) A rapid method for the quantitative extraction of bile acids and their conjugates from serum using commercially available reverse-phase octadecylsilane bonded silica cartridges. Clin Chim Acta 125:135-144.

Sewnath ME, Levels HH, Oude Elferink R, van Noorden CJ, ten Kate FJ, van Deventer SJ and Gouma DJ (2000) Endotoxin-induced mortality in bile duct-ligated rats after administration of reconstituted high-density lipoprotein. Hepatology 32:1289-1299.

Shefer S, Salen G, Hauser S, Dayal B and Batta AK (1982) Metabolism of iso-bile acids in the rat. J Biol Chem 257:1401-1406.

Singh N, Webb R, Adams R, Evans SA, Al-Mosawi A, Evans M, Roberts AW and Thomas AW (2005) The PPAR-gamma activator, Rosiglitazone, inhibits actin polymerisation in monocytes: involvement of Akt and intracellular calcium. Biochem Biophys Res Commun 333:455-462.

Slitt AL, Allen K, Morrone J, Aleksunes LM, Chen C, Maher JM, Manautou JE, Cherrington NJ and Klaassen CD (2007) Regulation of transporter expression in mouse liver, kidney, and intestine during extrahepatic cholestasis. Biochim Biophys Acta 1768:637-647.

Smith NF, Acharya MR, Desai N, Figg WD and Sparreboom A (2005) Identification of OATP1B3 as a high-affinity hepatocellular transporter of paclitaxel. Cancer Biol Ther 4:815-818.

Song C, Hiipakka RA and Liao S (2000) Selective activation of liver X receptor alpha by 6alpha-hydroxy bile acids and analogs. Steroids 65:423-427.

Soroka CJ, Mennone A, Hagey LR, Ballatori N and Boyer JL (2010) Mouse organic solute transporter alpha deficiency enhances renal excretion of bile acids and attenuates cholestasis. Hepatology 51:181-190.

Staudinger J, Liu Y, Madan A, Habeebu S and Klaassen CD (2001) Coordinate regulation of xenobiotic and bile acid homeostasis by pregnane X receptor. Drug Metab Dispos 29:1467-1472.

Stedman CA, Liddle C, Coulter SA, Sonoda J, Alvarez JG, Moore DD, Evans RM and Downes M (2005) Nuclear receptors constitutive androstane receptor and pregnane X receptor ameliorate cholestatic liver injury. Proc Natl Acad Sci U S A 102:2063-2068.

Stellaard F, Langelaar SA, Kok RM and Jakobs C (1989) Determination of plasma bile acids by capillary gas-liquid chromatography-electron capture negative chemical ionization mass fragmentography. J Lipid Res 30:1647-1652.

Takamine F and Imamura T (1985) 7 beta-dehydroxylation of 3,7-dihydroxy bile acids by a Eubacterium species strain C-25 and stimulation of 7 beta-dehydroxylation by Bacteroides distasonis strain K-5. Microbiol Immunol 29:1247-1252.

Tollet-Egnell P, Flores-Morales A, Stahlberg N, Malek RL, Lee N and Norstedt G (2001) Gene expression profile of the aging process in rat liver: normalizing effects of growth hormone replacement. Mol Endocrinol 15:308-318.

Trottier J, Verreault M, Grepper S, Monte D, Belanger J, Kaeding J, Caron P, Inaba TT and Barbier O (2006) Human UDP-glucuronosyltransferase (UGT)1A3 enzyme conjugates chenodeoxycholic acid in the liver. Hepatology 44:1158-1170.

Tserng KY (1978) A convenient synthesis of 3-keto bile acids by selective oxidation of bile acids with silver carbonate-Celite. J Lipid Res 19:501-504.

Tserng KY, Hachey DL and Klein PD (1977) An improved procedure for the synthesis of glycine and taurine conjugates of bile acids. J Lipid Res 18:404-407.

Tserng KY and Klein PD (1977) Formylated bile acids: improved synthesis, properties, and partial deformylation. Steroids 29:635-648.

Turley SD and Whiting MJ (1988) Regulation of bile acid pool size and plasma lipid levels in the SHR/N-corpulent rat: influence of the level of caloric intake. Metabolism 37:22-27.

van de Steeg E, Wagenaar E, van der Kruijssen CM, Burggraaff JE, de Waart DR, Elferink RP, Kenworthy KE and Schinkel AH (2010) Organic anion transporting polypeptide 1a/1b-knockout mice provide insights into hepatic handling of bilirubin, bile acids, and drugs. J Clin Invest 120:2942-2952.

Vonk RJ, Tuchweber B, Masse D, Perea A, Audet M, Roy CC and Yousef IM (1981) Intrahepatic cholestasis induced by allo monohydroxy bile acid in rats. Gastroenterology 80:242-249.

Wagner M, Halilbasic E, Marschall HU, Zollner G, Fickert P, Langner C, Zatloukal K, Denk H and Trauner M (2005) CAR and PXR agonists stimulate hepatic bile acid and bilirubin detoxification and elimination pathways in mice. Hepatology 42:420-430.

Wang DQ, Tazuma S, Cohen DE and Carey MC (2003) Feeding natural hydrophilic bile acids inhibits intestinal cholesterol absorption: studies in the gallstone-susceptible mouse. Am J Physiol Gastrointest Liver Physiol 285:G494-502.

Wang H, Chen J, Hollister K, Sowers LC and Forman BM (1999) Endogenous bile acids are ligands for the nuclear receptor FXR/BAR. Mol Cell 3:543-553.

Weaver YM, Ehresman DJ, Butenhoff JL and Hagenbuch B (2010) Roles of rat renal organic anion transporters in transporting perfluorinated carboxylates with different chain lengths. Toxicol Sci 113:305-314.

Wikoff WR, Anfora AT, Liu J, Schultz PG, Lesley SA, Peters EC and Siuzdak G (2009) Metabolomics analysis reveals large effects of gut microflora on mammalian blood metabolites. Proc Natl Acad Sci U S A 106:3698-3703.

Wilson PJ and Basit AW (2005) Exploiting gastrointestinal bacteria to target drugs to the colon: an in vitro study using amylose coated tablets. Int J Pharm 300:89-94.

Xiang X, Han Y, Neuvonen M, Pasanen MK, Kalliokoski A, Backman JT, Laitila J, Neuvonen PJ and Niemi M (2009) Effect of SLCO1B1 polymorphism on the plasma concentrations of bile acids and bile acid synthesis marker in humans. Pharmacogenet Genomics 19:447-457.

Xie W, Radominska-Pandya A, Shi Y, Simon CM, Nelson MC, Ong ES, Waxman DJ and Evans RM (2001) An essential role for nuclear receptors SXR/PXR in detoxification of cholestatic bile acids. Proc Natl Acad Sci U S A 98:3375-3380.

Yonezawa A, Masuda S, Katsura T and Inui K (2008) Identification and functional characterization of a novel human and rat riboflavin transporter, RFT1. Am J Physiol Cell Physiol 295:C632-641.

Yorganci K, Baykal A, Kologlu M, Saribas Z, Hascelik G and Sayek I (2004) Endotoxin challenge causes a proinflammatory state in obstructive jaundice. J Invest Surg 17:119-126.

Yousef IM, Magnusson R, Price VM and Fisher MM (1973) Bile acid metabolism in mammals. V. Studies on the sex difference in the response of the isolated perfused rat liver to chenodeoxycholic acid. Can J Physiol Pharmacol 51:418-423.

Zeng H, Botnen JH and Briske-Anderson M (2010) Deoxycholic acid and selenium metabolite methylselenol exert common and distinct effects on cell cycle, apoptosis, and MAP kinase pathway in HCT116 human colon cancer cells. Nutr Cancer 62:85-92.

Zhang YK, Saupe KW and Klaassen CD (2010) Energy restriction does not compensate for the reduced expression of hepatic drug-processing genes in mice with aging. Drug Metab Dispos 38:1122-1131.

APPENDICES

Appendix I: Publications

1. Merrell MD, Jackson JP, Augustine LM, Fisher CD, Slitt AL, Maher JM, Huang W, Moore DD, **Zhang Y**, Klaassen CD, and Cherrington NJ. The Nrf2 activator oltipraz also activates the constitutive androstane receptor, **2008**, Drug Metab Dispos., 36: 1716-1721.
2. **Zhang Y** and Klaassen CD. Effects of feeding bile acids and a bile acid sequestrant on hepatic bile acid composition in mice, **2010**, Journal of Lipid Research, 51: 3230-42.
3. Csanaky IL, Lu H, **Zhang Y,** Ogura K, Choudhuri S, and Klaassen CD, Oatp1b2 is important for the hepatic uptake of unconjugated bile acids as well as maintaining the expression of Cyp7a1 in mice: Studies on the Oatp1b2-null mice, **2010**, Hepatology, 53: 272-81.
4. Gong L, Han YH, Aranibar N, Khandewal P, **Zhang Y**, Lecureux L, Bhaskaran, Klaassen CD, and Lehman-McKeeman LD, Characterization of organic anion transporting polypeptide (Oatp)1a1 and 1a4 null mice reveals altered transport function and urinary metabolomic profiles, **2011** (to be submitted)
5. **Zhang Y**, Csanaky IL, Lehman-McKeeman LD, and Klaassen CD. Knockout of organic anion transporting polypeptide 1a1 increases the toxicity of deoxycholic acid in mice, **2011** (to be submitted)
6. **Zhang Y**, Limaye PB, Lehman-McKeeman LD, and Klaassen CD. Knockout of organic anion transporting polypeptide 1a1 alters the intestinal bacteria and bile acid metabolism in mice, **2011** (to be submitted)
7. **Zhang Y**, Csanaky IL, Lehman-McKeeman LD, and Klaassen CD. Knockout of Oatp1a1 does not prevent liver toxicity in mice during extrahepatic cholestasis, **2011** (to be submitted)
8. **Zhang Y,** Selwyn F, Lehman-McKeema LD, Csanaky IL, and Klaassen CD. Characterization of organic anion transporting polypeptide 1a4 in bile acid homeostasis: Studies in Oatp1a4-null mice, **2011,** (to be submitted).

9. **Zhang Y**, Hong J-Y, Rockwell CE, Copple B, Jaeschke H, and Klaassen CD. Effect of bile duct ligation on bile acid metabolism and liver toxicity in mice, **2011,** (to be submitted)
10. Wu K, **Zhang Y**, and Klaassen CD, Nrf2 activation protects against diquat-induced toxicity, **2011**, (to be submitted).
11. Cheng XG, **Zhang Y**, and Klaassen CD, Hepatocyte-specific deletion of NADPH-cytochrome P450 reductase (Cpr) in mice disturbs bile-acid homeostasis by minimizing the classic route of bile-acid biosynthesis, **2011,** (to be submitted).
12. **Zhang Y** and Klaassen CD. Transcription factor-mediated regulation of carboxylesterases by prototypical microsomal enzyme inducers in mouse liver, **2011**, (to be submitted).
13. Cheng XG, **Zhang Y**, and Klaassen CD. Regulation of mouse carboxylesterases by tissue, age, and gender, **2011**, (to be submitted).
14. **Zhang Y** and Klaassen CD. Hormonal regulation of Cyp4a in C57BL/6 mouse liver and kidney, **2011**, (to be submitted).
15. **Zhang Y**, Guo GL, and Klaassen, CD. Bile acid metabolism in tissue-specific FXR-null mice fed resin, **2011** (in preparation).

Appendix II: Poster Abstracts

1. **Zhang Y** and Klaassen CD. Endocrine regulation of gender-divergent mouse Cyp4a isoforms in liver and kidney, Student Research Forum, University of Kansas Medical Center, 2008.
2. **Zhang Y** and Klaassen CD. Male mice have lower plasma concentration of unconjugated bile acids than female mice because livers of male mice have more Oatp1a1, Central States Society of Toxicology Annual Meeting, 2008.
3. Csanaky IL, Lu H, Choudhuri S, Ogura K, **Zhang Y** and Klaassen CD. Oatp1b2 is important for the hepatic uptake of unconjugated bile acids as well as maintaining the expression of Cyp7a1 in mice: Studies on the Oatp1b2-null mice, The 60th Annual Meeting of American Association for the Study of Liver Diseases, 2009.
4. **Zhang Y** and Klaassen CD. Male-predominant expression of hepatic transporter Oatp1a1 explains the gender difference in plasma levels of unconjugated bile acids in mice, National Society of Toxicology Annual Meeting, 2009.
5. **Zhang Y** and Klaassen CD. The bile acid metabolome in mice, XXI international bile acid meeting-Falk Gastro-conference (Freiburg, Germany), 2010
6. Csanaky IL, Lu H, **Zhang Y** and Klaassen CD. Oatp1b2 is important for the hepatic uptake of unconjugated bile acids as well as maintaining the expression of Cyp7a1 in mice, XXI international bile acid meeting-Falk Gastro-conference (Freiburg, Germany), 2010
7. **Zhang Y** and Klaassen CD. Liver bile acid metabolism in male and female C57BL/6 mice fed bile acid-supplemented diets, National Society of Toxicology Annual Meeting, 2010.
8. Limaye P, **Zhang Y** and Klaassen CD. The intestinal bacteria and bile acid metabolism in mice. KUMC's resident, postdoc, and fellow research day, 2010.
9. Cheng XG, **Zhang Y** and Klaassen CD. Hepatocyte-specific deletion of NADPH-cytochrome P450 reductase (Cpr) in mice disturbs bile-acid homeostasis by minimizing the classical route of bile-acid biosynthesis, National Society of Toxicology Annual Meeting, 2010.

10. Wu K, **Zhang Y** and Klaassen CD. Nrf2 activation protects against diquat-induced toxicity, National Society of Toxicology Annual Meeting, 2010.